Quantification of Seismic Responses to Mining Using Novel Seismic Response Parameters

by

Laura Grace Brown

A thesis submitted in partial fulfillment
of the requirements for the degree of
Doctor of Philosophy (PhD) in
Natural Resources Engineering

The Faculty of Graduate Studies
Laurentian University
Sudbury, Ontario, Canada

THESIS DEFENCE COMMITTEE/COMITÉ DE SOUTENANCE DE THÈSE
Laurentian Université/Université Laurentienne
Faculty of Graduate Studies/Faculté des études supérieures

Title of Thesis Titre de la thèse	Quantification of Seismic Responses to Mining Using Novel Seismic Response Parameters
Name of Candidate Nom du candidat	Brown, Laura
Degree Diplôme	Doctor of Philosophy Science
Department/Program Département/Programme	Natural Resources Engineering
Date of Defence Date de la soutenance	October 05, 2018

APPROVED/APPROUVÉ

Thesis Examiners/Examinateurs de thèse:

Dr. Marty Hudyma
(Supervisor/Directeur de thèse)

Dr. Eugene Ben Awah
(Committee member/Membre du comité)

Dr. Shailendra Sharan
(Committee member/Membre du comité)

Dr. Vassilios Kazadisis
(Committee member/Membre du comité)

Dr. Martin Grenon
(External Examiner/Examinateur externe)

Dr. Mostafa Naghizadeh
(Internal Examiner/Examinateur interne)

Approved for the Faculty of Graduate Studies
Approuvé pour la Faculté des études supérieures
Dr. David Lesbarrères
Monsieur David Lesbarrères
Dean, Faculty of Graduate Studies
Doyen, Faculté des études supérieures

ACCESSIBILITY CLAUSE AND PERMISSION TO USE

Abstract

Mining-induced seismic events can be loosely classified as induced events or triggered events. Induced seismic events in mines are typically proportional to mining-induced stress change. This type of rock mass failure is often successfully managed by seismically active underground mining operations, and is generally considered part of a normal seismic response to mining. Triggered seismicity represents a disproportional seismic response to mining, and often results in visible rock mass damage. The variations in space and time characteristics of induced and triggered seismicity, particularly in relation to mine blasting, are indicative of distinct seismic source mechanisms and may be useful in seismic hazard evaluation for mines.

In this work, Seismic Response Parameters (SRP's) are conceptualized using fundamental rock mechanics and mine seismicity principles, and subsequently supported with a comprehensive case study from Agnico Eagle's LaRonde mine. The primary factors considered in this thesis are space and time; how they relate a seismic response to the stimulus and how they relate individual events within a seismic response to the response itself. The four SRP's are: Distance to Blast, Time After Blast, Distance to Centroid and Time Between Events.

A normalized set of SRP's, calculated with site specific considerations, are proposed as a meaningful measure of how likely a seismic response is to be induced or triggered by discrete mine blasting. Within this thesis, Seismic Response Rating (SRR), the summation of normalized SRP's, is presented as a means of quantifying seismic responses to mining with a single numerical value. Seismic responses at LaRonde mine are used to demonstrate the application of SRP's and SRR to real mine seismic data.

A mine shutdown period, in which no mine blasting occurs, is used to provide meaningful insight into the spatial and temporal relations of mine seismicity. In the absence of mine blasting, seismic events associated with induced seismic source mechanisms cease to obscure triggered seismicity (resulting from triggered source mechanisms). Where and when both induced and triggered seismic source mechanisms interact in space and time, complex seismicity may be observed. An interpretation of complex seismic responses to mining, occurring in the transitional zone between induced and triggered seismicity, is also presented in this thesis.

Keywords: Complex Seismicity, Induced Seismicity, LaRonde Mine, Mine Blasting, Seismic Event Location, Seismic Event Time, Seismic Response Parameters, Seismic Response to Mining, Triggered Seismicity, Underground Mining,

Acknowledgments

First and foremost, I would like to thank Dr. Marty Hudyma, my supervisor and mentor. Your time and guidance has been invaluable over the past several years. I am grateful for the benefit of your knowledge and experience, which you have generously shared, and I will carry your many teachings with me. Thank you.

This work was completed primarily using the ACG software mXrap. A special acknowledgment is due to the mXrap team for their much appreciated support.

Financial support for this research was provided by Agnico Eagle's LaRonde mine, KGHM, Vale, the Natural Sciences and Engineering Research Council (NSERC), the Australian Centre for Geomechanics (ACG) and the Goodman School of Mines.

Table of Contents

List of Tables

List of Figures

List of Appendices

Glossary

DTB	Distance To Blast (m)
DTB_N	Normalized Distance to Blast
DTC	Distance To Centroid (m)
DTC_N	Normalized Distance to Centroid
MOL	Modified Omori Law
SRP	Seismic Response Parameter
SRP_N	Normalized Seismic Response Parameter
SRR	Seismic Response Rating
TAB	Time After Blast (h)
TAB_N	Normalized Time After Blast
TBE	Time Between Events (h)
TBE_N	Normalized Time Between Events

Chapter 1

1 Introduction

Mine seismicity is a naturally occurring phenomena observed in many underground hard rock mining environments. Seismic events, or dynamic stress waves, are the result of inelastic deformation in a rock mass and occur primarily in response to mine excavation geometry changes. When a volume of rock is excavated, the stress redistribution can be significant. Where mining-induced stress exceeds the strength of the rock, failure may occur. This type of rock mass failure in mines is a function of many factors, most notably: the three-dimensional stress field, rock mass and geological properties, and mining practices. All of these factors vary significantly throughout a mining environment, and over time, making it challenging to quantify and delineate the seismic response to mining.

Seismic responses commonly represent discrete rock mass failure processes, and are often naturally isolated in space and time around individual failure modes (seismic source mechanisms). This research focuses on quantifying seismic responses to discrete mine blasts in space and time, with an aim of differentiating between induced and triggered rock mass failure modes. This approach is quite novel, as little work has been done to quantify and interpret individual seismic responses to mining.

1.1 Mine Seismicity

Two main types of mine seismicity have been established in literature: Induced (Type A) and Triggered (Type B). Established seismic analysis techniques often make little effort to distinguish between induced and triggered seismicity. Induced seismicity occurs in close spatial and temporal proximity to the stimulus (i.e. mine blast), and radiates energy proportional to the experienced stress change induced by the stimulus (Gibowicz and Kijko, 1994; McGarr and Simpson, 1997; Richardson and Jordan, 2002). Because induced seismicity is spatially and temporally dependent on the stimulus (mine blasting), the locations of induced seismic responses to mining migrate over time as new mine excavations are developed.

Triggered seismic events are fundamentally different to induced events, as they occur largely independent of new mine excavations. Triggered seismicity occurs spatially distant and temporally independent of the stimulus (i.e. mine blast), and radiates energy that is disproportional to the experienced stress change (Gibowicz and Kijko, 1994; McGarr and Simpson, 1997; Richardson and Jordan, 2002). Instead of migrating over time as new mine excavations are developed, triggered seismic responses to mining typically concentrate around

larger, and relatively stationary, rock mass failure processes and seismic source mechanisms (e.g. yielding pillars and dykes).

1.1.1 Variations in Seismic Source Mechanism within a Mining Environment

Seismic responses in mines are a direct reflection of the source mechanisms driving rock mass failure. Figure 1 depicts variations in seismic source mechanism within a hypothetical underground mining environment (Hudyma *et al.*, 2003). Seismic source mechanism refers to the causative rock mass failure mode that generates a seismic event, and can be used as a means of categorizing mine seismicity. Strong spatial clustering is observed in Figure 1 part (a), which is a common phenomena in mine seismicity (Leslie and Vezina, 2001; Dodge and Sprenke, 1992; Kijko *et al.*, 1993). In part (b), the seismic sources around typical underground workings are shown. It is around these seismic source mechanisms that seismicity clusters in part (a).

Induced seismicity typically results from stress fracturing related source mechanisms, and is commonly observed within 100 metres of mine blasting (Richardson and Jordan, 2002). This type of failure is primarily controlled by the local state of stress and rock mass strength characteristics, and may occur in the presence or absence of pre-existing fractures (Woodward, 2015). In Figure 1, seismicity resulting from 'stress increase' surrounding a small excavation within a high stress pillar in part (b) is likely induced - assuming the excavation was recently blasted and the local stress increase is proportional to the blast size.

Triggered seismicity typically results from tectonic loading (McGarr and Simpson, 1997), and larger scale rock mass failure processes relative to induced seismicity. In Figure 1 part (b), a tectonic loading type source mechanism is shown as 'slip on geological features'. The majority of energy released during this type of failure (fault-slip), is not a direct result of local mining-induced stress change, but longer term tectonic processes. Mine wide failure processes, commonly resulting from the influence of many blasts over time (high extraction ratio), may also result in disproportional rock mass failure or energy release. Examples of these larger scale failure processes in Figure 1 part (b) are: 'high stress pillar' and 'crushing of pillars'. These pillars are likely yielding over extended periods, generating triggered seismicity at times independent of mine blasting.

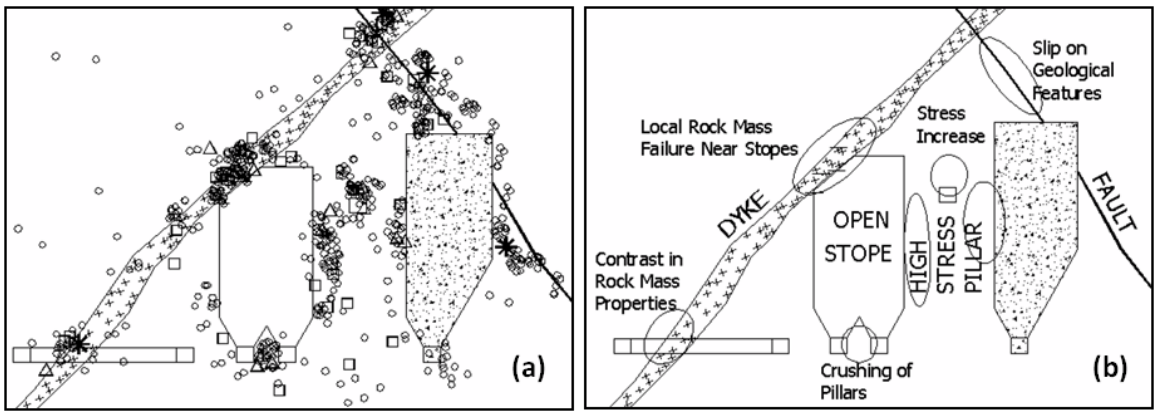

Figure 1: Variations in source mechanism within a mining environment are shown (Hudyma *et al.*, 2003). Part (a) depicts hypothetical seismicity associated with a typical underground mine. Part (b) depicts seismic sources around typical underground mine workings.

The presence of diverse rock mass failure mechanisms throughout mining environments contribute to seismic responses with distinctive spatial and temporal characteristics. Induced seismicity is synonymous with stress fracturing related seismic source mechanisms, and is highly dependent on discrete mining activities in space and time. Triggered seismicity is synonymous with larger scale and/or tectonic loading related source mechanisms, and occurs relatively independent of discrete mining activities in space and time. As a result, trends in individual seismic response event locations and times, particularly when compared to discrete mining activities, may provide insight into locations of induced and triggered seismic source mechanisms throughout a mining environment. This is significant, as it suggests a means of identifying triggered source mechanisms prior to the occurrence of large and potentially damaging seismic events.

1.1.2 Individual Seismic Events vs. Populations of Seismic Events

Source parameters may provide a measure of the local rock mass conditions at the time of failure, but they fail to describe the larger scale rock mass failure processes occurring over time throughout the mining environment. Rock mass failure processes in mines occur at various scales and over a wide range of temporal periods. Seismic source parameters describe the radiated energy, co-seismic deformation and source size for individual seismic events, however, individual seismic events represent only point measurements of rock mass failure in space and time.

Analyzing seismic source parameters with a focus on source mechanism is common practice. This type of analysis is typically performed using substantial populations of seismic events (Hudyma, 2008). Populations of seismic events can provide meaningful insight above and beyond the analysis of individual events. Performing this type of analysis commonly involves isolating populations of seismic events in space, and subsequently analyzing trends in primary and secondary seismic source parameters over time (Hudyma, 2008).

Grouping of individual seismic events into populations produces an increase in dimensionality of analysis, which often leads to more meaningful results. Seismic events are not considered individually in this thesis, but rather in population subsets referred to as individual seismic responses to mining. Unlike previous research focusing on subsets of seismic data, in this research, each seismic response is directly affiliated with a discrete mine blast (stimulus). This methodology enables each seismic response to mining to be associated as much as possible with a discrete and quantifiable mining-induced stress change.

1.1.3 Inherent Complexity in Mine Seismicity

Triggered seismicity is often considered to be distant from mining-induced stress change, but this is a simplification. Throughout the course of mining, triggered source mechanisms in a rock mass are commonly located within proximity of mining-induced stress change. Richardson and Jordan (2002) note that while induced seismicity exhibits an upper seismic event magnitude bound near magnitude zero, exceptions have been documented. They observed that anomalously large, and presumably induced, seismic events appear to defy the simple classification scheme of induced or triggered seismicity. It is from this observation, and others (e.g. Delgado and Mercer, 2006; Slade and Ascott, 2002), that the concept of a mixed or dual seismic response to mining originates.

The concept of mixed or 'complex' seismicity, as defined in this work, addresses the undefined transition zone between induced and triggered seismic responses to mining. It further works to shed light on the rock mass failure processes surrounding the occurrence of unexpectedly large seismic events in mines. Complex seismic responses to mining contain components of both induced and triggered seismicity, and consequently, may pose the most significant risk to mining operations. There is little discussion of complex seismic responses to mining in literature.

1.2 Research Scope

The primary objective of this thesis is the quantification of individual seismic responses to mining, with a focus on differentiating between induced and triggered seismicity.

In this work, Seismic Response Parameters (SRP's) are conceptualized using fundamental rock mechanics and mine seismicity concepts, and supported with a comprehensive case study from Agnico Eagle's LaRonde mine. The primary factors considered in this thesis are time and space; both how they relate a seismic response to the stimulus and how they relate individual events within a seismic response to the response itself. This thesis places relatively little emphasis on the identification of seismic responses to mining in space and time, but rather characterizing and quantifying a response once it has been identified.

Mining-induced stress conditions determined from numerical modeling are not considered in this thesis. For the purposes of delineating seismic responses to mining using SRP's, only the

maximum theoretical limits of mining-induced stress change are required. These limits can be approximated using rules of thumb based on excavation spans, and established ratios relative to excavation boundaries. Approximating mining-induced stress in this way enables the application of Seismic Response Parameters to various mining environments and seismic datasets without the need for calibrated non-linear three-dimensional numerical models.

1.3 Research Approach

In a deductive approach, a hypothesis is formed and tested by means of research processes. This research employs a deductive approach. Novel Seismic Response Parameters serve as the primary hypothesis, and are tested using a comprehensive case study of seismic responses from Agnico Eagle's LaRonde mine. Because the occurrence of seismic events is uncontrolled, data collection cannot be duplicated or repeated. This prevents the application of rigorous statistical validation or analysis.

1.4 Thesis Structure

Chapter One outlines the objectives and context of this research.

Chapter Two provides background information necessary to understand the established fundamental concepts presented in this thesis. Insights into mine seismicity, seismic monitoring, independent seismic source parameters and seismic analysis techniques are provided. Variations in seismic responses to mining are discussed, including how seismic responses are identified, and documented observations of induced, triggered and complex seismicity in mines.

Chapter Three discusses the established variations in seismic responses to mining, and defines how seismic responses are characterized within the context of this thesis. The basic space-time relations for induced, triggered and complex seismic responses to mining are outlined, and examples are provided.

Chapter Four introduces and defines the novel Seismic Response Parameters that are the focus and primary contribution of this thesis.

Chapter Five presents how Seismic Response Parameters can be used to interpret seismic responses to mining. Visualization methods and a Seismic Response Rating are introduced.

Chapter Six provides background information for the LaRonde mine case study found in Chapter Seven. The mining environment at LaRonde is introduced, along with the microseismic monitoring system and considerations surrounding the identification of individual seismic responses to mining.

Chapter Seven is composed of three independent case studies of seismic responses to mining at Agnico Eagle's LaRonde mine. A series of induced, triggered and complex seismic responses to mining are described and evaluated using Seismic Response Parameters.

Chapter Eight is a discussion of the underlying assumptions of this work, spatial versus temporal response parameters, and how Seismic Response Parameters compare to traditional seismic analysis techniques.

Chapter Nine outlines the contributions of this thesis and provides recommendations for future work. The significance of this research to the field of mine seismicity, and the mining sector, are discussed.

Chapter 2

2 Literature Review

2.1 Terminology

This section defines the basic terminology used throughout this thesis.

2.1.1 Stress

The local stress state surrounding a mine excavation is a function of the *insitu* stress and mining-induced stress (Gibowicz and Kijko, 1994; Gibowicz and Lasocki, 2001). The *insitu* stress refers to the natural stress state that exists in the rock mass prior to mining. Mining-induced stress refers to the stress state surrounding an excavation as a result of mining processes. Knowledge of local stress conditions is critical to mine planning and operation. It is one of the dominant driving factors behind seismic activity (Gibowicz and Kijko, 1994), and a key component to differentiating between types of seismic responses to mining.

Insitu stress is largely a result of tectonic forces and the compressive force from the weight of the overlying rock mass (Herget, 1974). When rock is removed as a result of mining, the remaining rock mass must account for the previously supported load. This generates additional stress for the rock mass surrounding the excavation (Herget, 1988), which is referred to as the mining-induced stress.

Mining-induced stress redistribution represents a change in stress due to mining (commonly mine blasting), and is not necessarily higher than the original stress state. Locations of relatively increased and decreased stress are dependent on the geometry and orientation of mine excavations. Figure 2 depicts the deflection of stress streamlines around a cylindrical obstruction (Hoek and Brown, 1980). Stresses are forced to redistribute around the sides parallel to the direction of the applied stress field, and are relaxed around the perpendicular sides. In instances where the mining-induced stress exceeds the strength of the rock, rock mass failure occurs (Hoek and Brown, 1980).

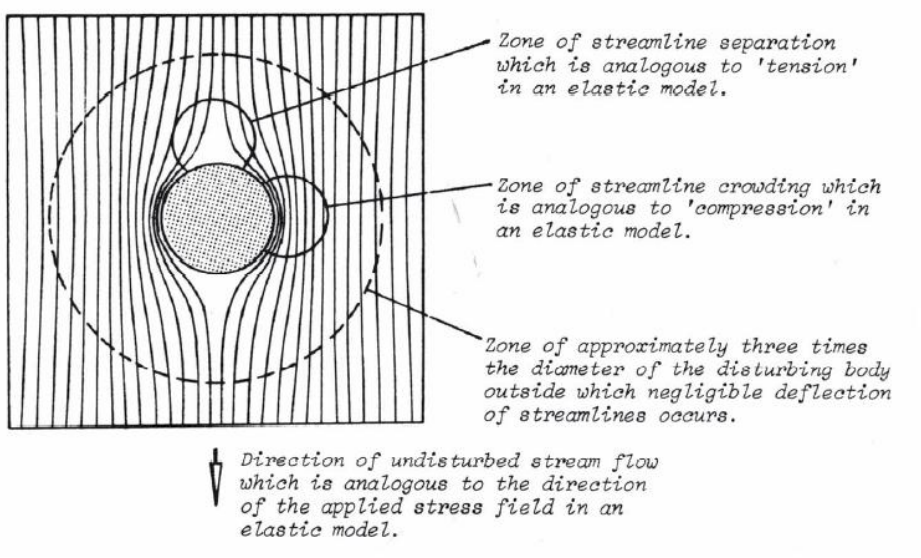

Figure 2: Deflection of stress streamlines around a cylindrical obstruction (Hoek and Brown, 1980).

2.1.2 Mine Seismicity

Mining excavations disturb and redistribute local stress fields, generating potential for mining-induced seismic events (Cook, 1976). A seismic event is the dynamic stress wave generated by a failure within a rock mass (Hedley, 1992). Mines commonly experience increased volumes of microseismic events (less than Richter magnitude zero), as a result of mining processes. This is fundamentally different from earthquake seismology, which commonly places an emphasis on macroseismic events (greater than Richter magnitude zero).

The initial elastic wave of a seismic event is referred to as the primary wave (p-wave), followed closely by the secondary wave (s-wave). Figure 3 is an example of a large seismic event with clear p and s-wave arrivals recorded by a regional seismic monitoring network. Due to the difference in travel velocities of the two waves (p and s), the degree of separation between their arrivals at a given ground motion sensor can be used to determine the approximate distance from the location of the sensor station to the source of the seismic event. In Figure 3 for example, the first sensor station experiences the p-wave ground motion first (before the second sensor), and exhibits a much smaller separation between the p and s-wave arrivals. This indicates the first station is located closer to the seismic source.

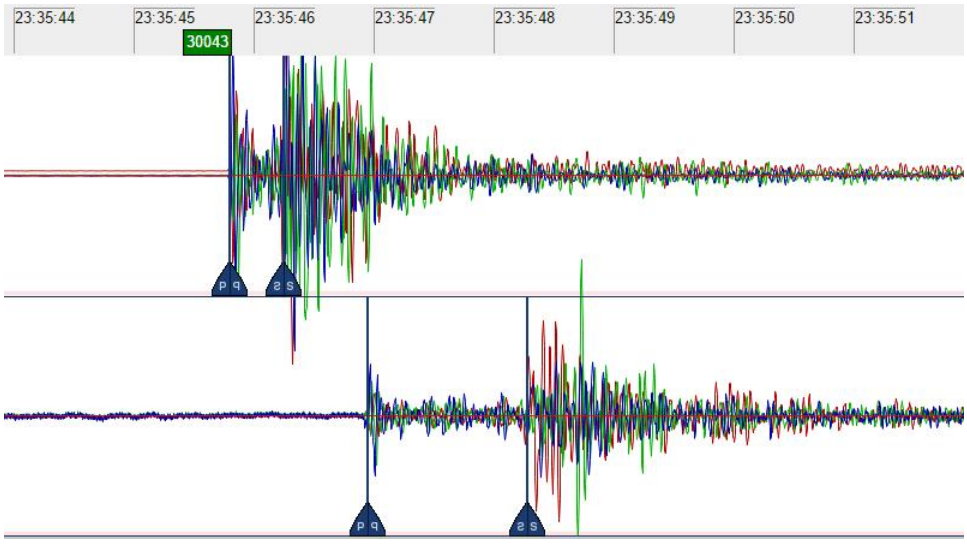

Figure 3: Example waveform for a large seismic event, with identified p-wave and s-wave arrivals, recorded by a regional seismic network.

Mining-induced seismicity was first observed and documented in hardrock Canadian mines during the mid 1930's (Hedley, 1992). It is a common phenomena and has been reported in a variety of metalliferous, potash, and coal operations worldwide (Gibowicz and Kijko, 1994). With the onset of hazardous seismic activity, mining operations typically install seismic monitoring systems to record seismic data. These seismic databases can then be back analyzed over time to identify patterns that may help to reduce seismic risk as the operations progress.

2.1.2.1 Rockburst

When a seismic event results in violent and significant damage to an excavation it is referred to as a rockburst (Ortlepp, 1997). Events that may result in significant rock mass damage pose a high risk to the safety of underground personnel, excavations and equipment. A rockburst may be further classified as bulking, ejection, or a seismically-induced fall of ground based on the damage mechanism (Kaiser *et al.*, 1996), as shown in Figure 4.

Rock bulking due to fracturing may occur as a result of an immediate or remote seismic event, and does not have to be accompanied by ejection. When this type of failure occurs rapidly, it is typically referred to as a strain burst. This is the most common type of damage observed in Canadian hardrock mines (Kaiser *et al.*, 1996).

Seismically induced falls of ground are gravity-driven failures. When a stable volume of rock is subjected to a seismic wave, the rock is accelerated with the potential to overcome the capacity of the ground support. Areas with large spans or geological conditions prone to generating blocks/wedges are more likely to experience damage resulting from this mechanism. This type of damage is the second most commonly observed in Canadian hardrock mines (Kaiser *et al.*, 1996).

Rock ejection from seismic energy transfer is a more violent damage mechanism. It occurs when the energy resulting from the seismic wave is transferred to a block/slab at the boundary of an excavation. The rock is unable to absorb the energy, and the lack of confinement enables it to be ejected into the open area of the excavation. The extent of damage is inversely proportionate to the distance of the excavation boundary from the seismic source. This type of damage is rarely observed in Canadian hardrock mines (Kaiser *et al.*, 1996).

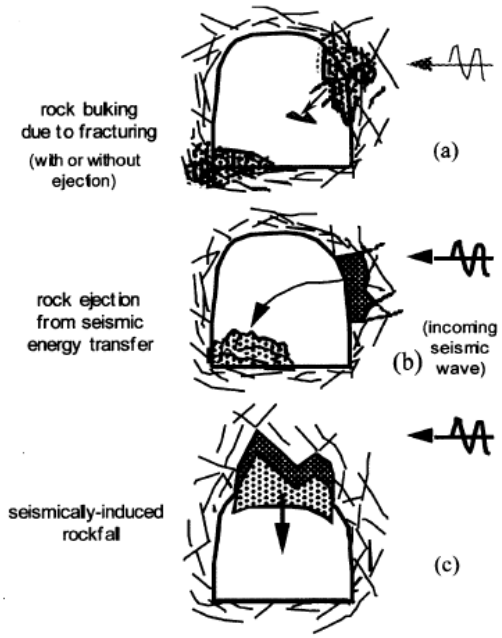

Figure 4: Rockburst classifications (Kaiser *et al.*, 1996); (a) rock bulking due to fracturing; (b) rock ejection from seismic energy transfer; (c) seismically-induced rockfall.

2.1.2.2 Mining-Induced Seismicity

Induced seismicity occurs in close spatial and temporal proximity to mining-induced stress change. This type of seismicity is highly dependent on discrete stress change stimuli (i.e. mine blasts). The energy from induced seismic events is often proportional to the experienced stress change induced by a discrete blast (Gibowicz and Kijko, 1994; McGarr and Simpson, 1997; McGarr *et al.*, 2002; Richardson and Jordan, 2002). When this is not the case, alternative factors (other than a discrete mining-induced stress change) may be driving rock mass failure.

2.1.2.3 Mining-Triggered Seismicity

Unlike induced seismicity, triggered seismic events are largely spatially and temporally independent of discrete mining-induced stress change. This type of seismicity typically results

from larger scale rock mass failure processes, making it challenging to attribute to individual mine blasts. The energy from triggered seismic events may be disproportional to the experienced stress change induced by a discrete blast (Gibowicz and Kijko, 1994; McGarr and Simpson, 1997; McGarr *et al.*, 2002; Richardson and Jordan, 2002).

2.1.2.4 Seismic Hazard

Seismic hazard is commonly defined as the likelihood of occurrence of a seismic event of a certain size (Gibowicz and Kijko, 1994). It varies in space and time within a mine and is probabilistic in nature and occurrence (Gibowicz and Kijko, 1994).The degree of hazard is often independent of the damage the event may cause, as the possibility and consequence of damage is considered in seismic risk (Owen *et al.*, 2002).

Induced seismicity, or a normal seismic response to mining, is typically associated with lower degrees of seismic hazard. The energy release expected is proportional to mine excavation geometry changes (i.e. blasting), and is usually not sufficient to generate large and potentially damaging seismic events. Triggered seismicity, or an abnormal seismic response to mining, is typically associated with elevated or high seismic hazard. Because the energy release may be significantly disproportionate to mine blasting, the likelihood of damaging seismic events increases.

2.1.3 Seismic Responses to Mining

Dynamic rock mass failure in mines is a function of many factors, most notably: the three-dimensional stress field, rock mass properties, and mining practices. All of these factors vary significantly throughout a mining environment and over time, making it challenging to quantify and delineate the seismic response to mining.

Seismic responses to mining are responses, and therefore require a causative stimulus. Mine blasting generates excavation geometry changes, resulting in mining-induced stress change. This stress change is proportional to the size of the mine blast, or excavation geometry change, and is commonly the dominate factor driving mine seismicity (i.e. induced seismicity). For the purposes of this research, response stimuli refer to discrete mine blasts.

Figure 5 depicts typical mine development associated with open stope mining. A typical production stope, raise and development drifts are shown. Production or stope blasting is a general term used to refer to the blasting of large volumes of ore from sub-vertical panels, typically in the order of thousands of cubic metres per blast. The production stope shown in Figure 5 is subdivided into two blasts. When a blast is fired, the resulting broken rock will swell in volume by 120% to 140%. The first blast (A) is relatively small, as there is limited void for the swell of the broken rock. When this broken rock is removed from the stope, it provides

additional void space for the swell of the second and larger blast (B). Production stope blasts in mines typically generate significant stress redistribution in the local rock mass.

A development drift is a general term used to refer to near horizontal mine excavations mined to facilitate ore extraction. In Figure 5, the production stope is intersected by two development drifts, on the top and bottom, to provide access for drilling and blasting, and removing the fragmented rock, respectively. Development drifts are typically 4 to 5 metres in height and width, and are typically blasted in short rounds of 3 to 4 metres per blast. Local stress change induced by development blasting is reflected in the occurrence of small magnitude seismic events, located in spatial and temporal proximity to excavation geometry changes. Mine geometry and blasts, such as those shown in Figure 5, will be referred to throughout this thesis.

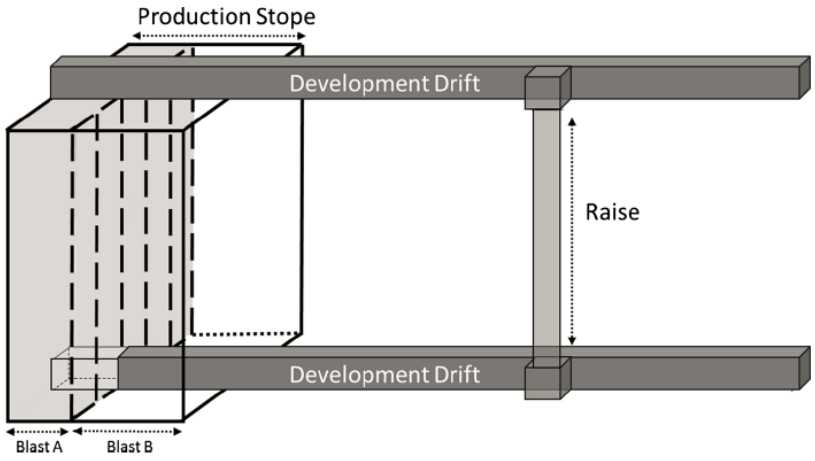

Figure 5: Diagrammatic sketch of mine geometry typical of an open stoping mining method. A single production stope, divided into two blast volumes, and two mine development drifts connected by a raise are shown (Brown and Hudyma, 2017).

Mine excavations impact local stress fields, and while seismicity is expected to accompany stress redistribution, there may be a normal and abnormal seismic response to mining (Brown, 2015). A normal seismic response to mining is relatively proportional to the scale of mining. This type of seismicity primarily consists of small magnitude seismic events (typically less than Richter magnitude zero). The normal seismic response to mining is synonymous with induced seismicity.

The occurrence of large magnitude seismic events (typically greater than Richter magnitude zero), and seismicity occurring beyond discrete blasting influences, is commonly considered an abnormal seismic response to mining. This type of activity indicates more than just small events related to local stress redistributions are occurring. Abnormal responses are often associated with unfavorable geology or very high stress conditions, and are synonymous with triggered seismicity.

2.1.4 Seismic Source Mechanism

Variations in seismic source mechanism were previously discussed in Section 1.1.1.

Seismic source mechanism refers to the rock mass failure mode resulting in a seismic event. Information regarding source mechanism can provide insights into the local rock mass stress, geological, and mining influences. Figure 6 provides depictions of six basic mechanisms driving the occurrence of seismic events in Canadian mines (Hasegawa *et al.*, 1989).

Cavity collapse, pillar burst, and tensional fault mechanism events are all subtypes of volumetric and stress fracturing source mechanisms. These events are usually associated with mining activities such as blasting, and are synonymous with induced seismicity and a normal seismic response to mining. Normal fault, thrust fault, and shallow thrust faulting all contain a shearing component and are subtypes of fault-slip seismic events. Fault-slip events tend to release disproportionate energy during rock mass failure, and are usually synonymous with triggered seismicity, and an abnormal seismic response to mining.

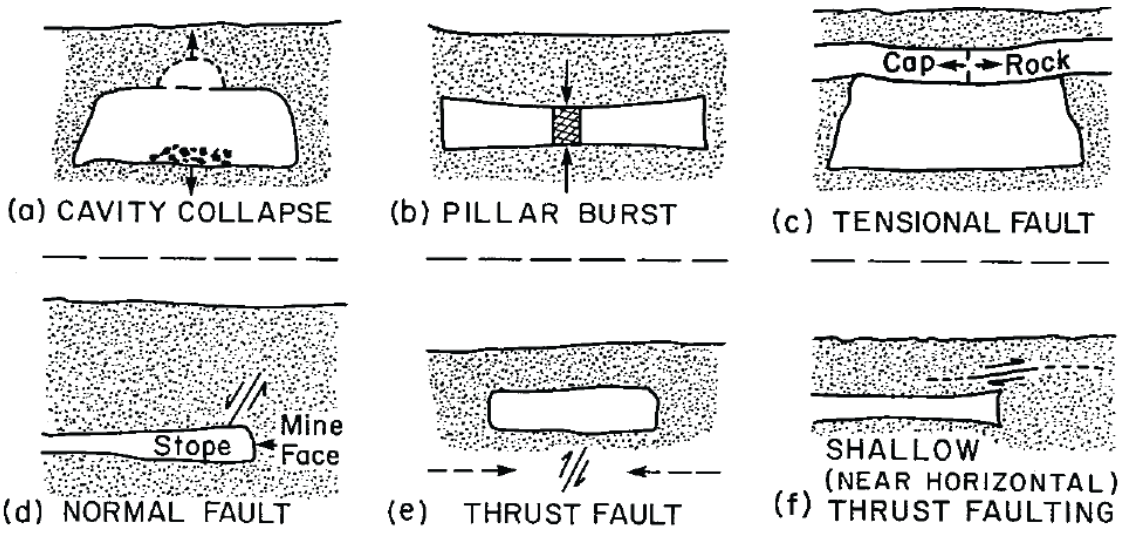

Figure 6: Six basic mechanisms driving mining related tremors in Canadian mines (Hasegawa *et al.*, 1989).

2.2 Seismic Monitoring

Seismic monitoring systems enable mining operations to detect and interpret the seismic response to mining. Though a combination of hardware and software components, ground motion can be recorded and stored as high quality seismic data. The main components of a typical seismic monitoring system include: sensors, communication networks, digitizers, data storage and software.

2.2.1 Ground Motion Sensors

In order to accurately represent a large range of seismic events, a variety of ground motion sensors must be integrated into a comprehensive seismic monitoring system. Large quantities of uniaxial sensors are typically used to surround the area of interest (the orebody), and ensure good location accuracy. Being uniaxial however, these sensors are only capable of recording movement in a single direction, limiting the ground motion information that can be inferred from them. Triaxial sensors record ground motion in three orthogonal directions simultaneously, enabling the recording of three dimensional ground motions and the calculation of seismic source parameters. A combination of uniaxial and triaxial ground motion sensors are commonly used in mine seismic arrays to provide accurate locations and source parameters for recorded microseismic events.

In Canada, piezoelectric accelerometers are the most commonly used sensor in microseismic monitoring (Brown and Hudyma, 2018a). Within this sensor, accelerometers and pressure transducers convert pressure from ground motion into an electrical signal proportional to ground acceleration. Piezoelectric accelerometers typically have an upper frequency limit of 15,000 Hz, resulting in increased sensitivity and the ability to detect very small seismic events.

Geophones are another type of sensor commonly used in Canadian mines (Brown and Hudyma, 2018a). These sensors are relatively robust, consisting of a simple mass within a spring, and cover a lower frequency range relative to accelerometers. Ground motion from a seismic event induces movement of the mass, which generates an electrical signal proportional to ground velocity.

For a given seismic monitoring system, the maximum signal level capable of being recorded in ratio to the noise level (when there is no signal), is referred to as the dynamic range (Mendecki *et al.*, 1999). Figure 7 depicts the sensitivity and dynamic range for different sensors commonly used in seismic monitoring. Dynamic range is expressed in decibels, and should be a minimum of 120 dB for a comprehensive seismic monitoring system utilizing a range of sensors (Mendecki *et al.*, 1999).

In Figure 7, noise (lower) and clip (upper) limits for an accelerometer and a variety of geophones are shown. Clip limits refer to the point at which the amplitude of ground motion exceeds the measuring capacity of a sensor. Noise limits refer to the point at which background noise on a sensor is equal to or greater than the amplitude of the ground motion. When either of these limits is exceeded, the sensor is no longer capable of accurately representing the ground motion.

Unlike geophones, accelerometers require a constant electrical input in order to function. As a result, there is a continuous electrical signal on the sensor referred to as noise. Noise affects the sensitivity of a system, dictating the smallest events that can be detected and accurately

represented. In order to develop a seismic monitoring system with a dynamic range of 120 dB, a combination of accelerometers and geophones is commonly used (Brown and Hudyma, 2018a).

Ground motion from low frequency seismic events cannot be accurately represented by close proximity accelerometers, as it falls beyond the clip limits. In order to record and utilize this data, low frequency geophones distant to mine workings must be used. Through a combination of accelerometers and geophones, a seismic system is capable of accurately representing a dynamic range of 0 to 132 dB (Figure 7) - approximately 6 orders of magnitude.

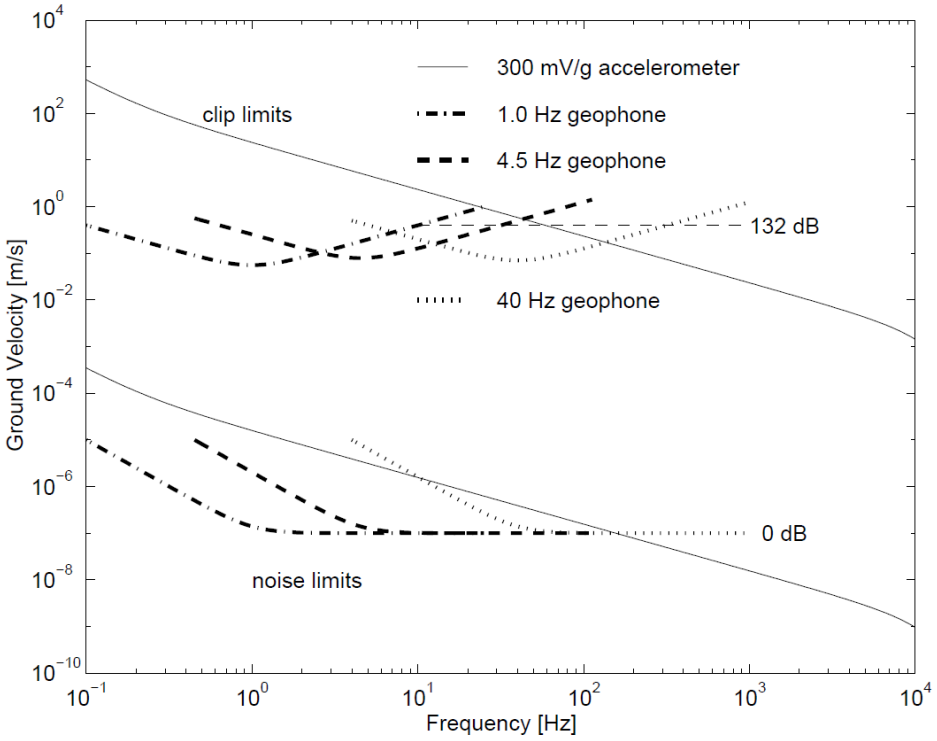

Figure 7: Sensitivity and dynamic range for sensors commonly used in mine seismic systems (Mendecki *et al.*, 1999).

2.2.2 Microseismic Monitoring Systems

Microseismic monitoring systems allow for insight into where local rock mass fracturing is occurring in relation to mining activities. In a typical ESG (Engineering Seismology Group) microseismic monitoring network, sensors record the ground motion radiated by rock mass failure and transfer the electrical signal across copper cable to Paladins (digital seismic recorders). The signal is digitized and relayed to computers on surface through a fibre-optic network. Figure 8 depicts an example of a typical ESG microseismic monitoring system (Collins *et al.*, 2014).

The networked seismic data is typically received by an acquisition computer at a central engineering office. Real time results are displayed and analyzed using various components of the ESG software suite. Data storage allows for years of seismic data to be maintained and archived,

facilitating back analysis. The strong ground motion sensors shown on surface in Figure 8, represent a macroseismic monitoring system, and are likely 4.5 Hz geophones.

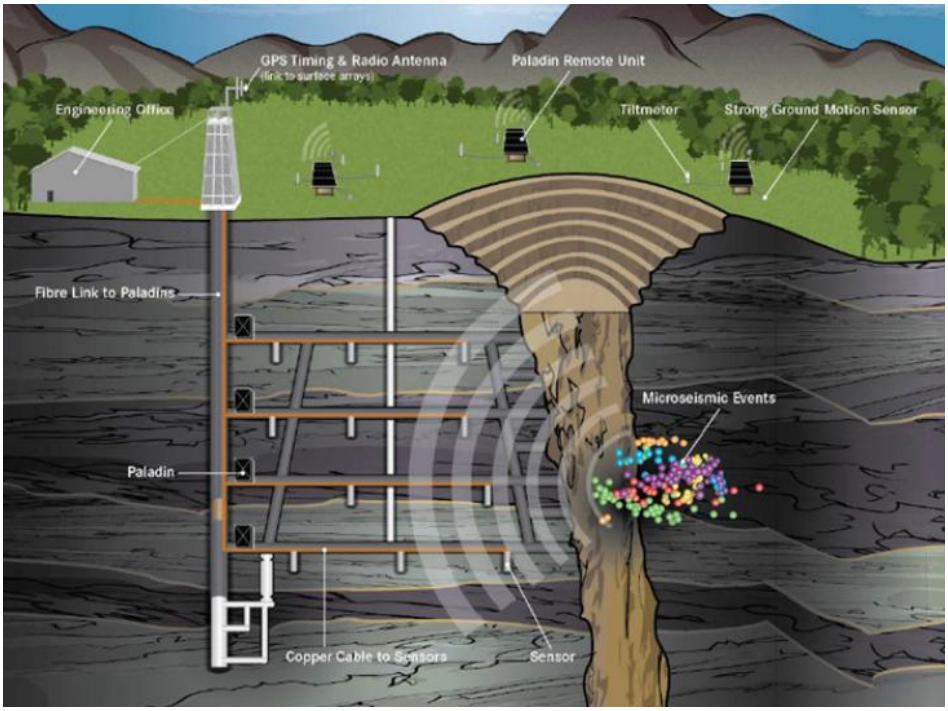

Figure 8: Example of a typical ESG microseismic monitoring system setup (Collins *et al.*, 2014).

2.3 Independent Seismic Source Parameters

Established in earthquake seismology, seismic source parameters are used to quantitatively describe the source of a seismic event. In order to provide a meaningful description of a seismic event, the event time, location and two additional independent source parameters are required (Mendecki *et al.*, 1999). Additional independent seismic source parameters are: energy, moment and source size. These parameters can be manipulated to generate secondary source parameters, such as magnitude.

2.3.1 Time

Time refers to the absolute time of occurrence of a seismic event. Proximity of event times to regular mine blasts can provide insight into the mechanisms driving rock mass failure (Cook, 1976). There is almost no error associated with event time, as it is commonly recorded as the GPS synched time of the occurrence of the event.

2.3.2 Location

Many source parameters are scaled according to distance from the seismic source to the sensor. As a result, when a seismic event occurs, the distance from the event location to each seismic sensor must be calculated. The most common methodologies used for calculating location employ a technique to minimize the difference between measured and theoretical seismic wave arrival times (Gibowicz and Kijko, 1994). Theoretical arrivals are determined from the velocity model assumed for the mine. These time residuals, between measured and theoretical arrivals, are commonly expressed as an error value (in distance), for a given seismic event location.

Location is a primary consideration of seismic analysis (Gibowicz and Kijko, 1994). Investigating the proximity of seismic event locations to active mining faces, pillars, and known geological features, can often provide valuable insight into seismic source mechanism. The error associated with a seismic event locations is often expressed in metres or feet. Figure 9 depicts cumulative distributions of location error for a variety of Canadian hard rock mining operations (Brown and Hudyma, 2018a). The median value is less than 10 metres for all operations.

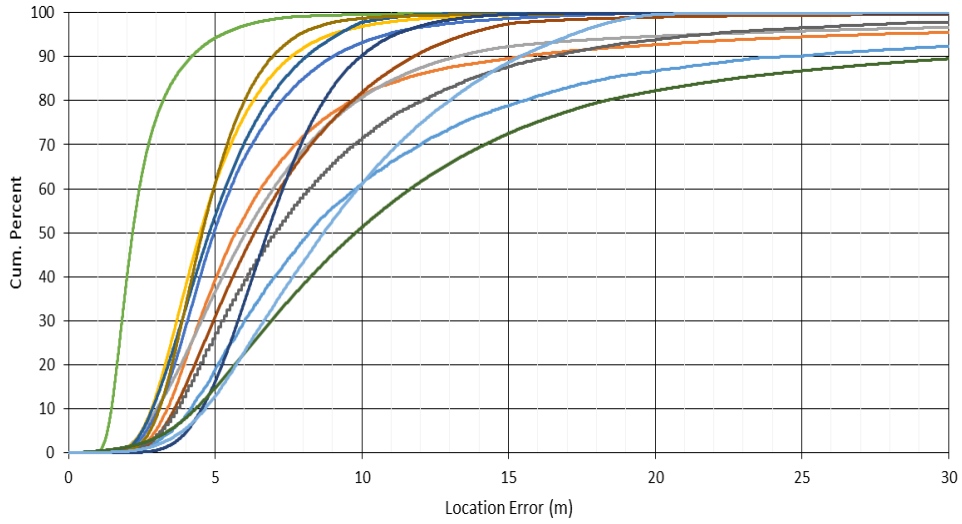

Figure 9: Cumulative distributions of location error (residuals) in metres over the most recent year of seismic monitoring for Canadian operations who participated in a Canada-Wide Seismic Monitoring Survey and provided a seismic record (Brown and Hudyma, 2018a).

2.3.3 Seismic Moment

Seismic moment (M_o) provides a widely accepted measure of size for slip-related seismic events. It is an important parameter used to describe the strength of the source, and is related to the local co-seismic rock mass deformation. Gibowicz and Kijko (1994) define seismic moment as:

$$Mo = 4\pi\rho c^3 R\frac{\Omega o}{Fc} \quad (1)$$

where,

Mo = Seismic Moment (Nm)

ρ = Rock Density (kg/m^3)

c = Velocity of the Wave in Rock (m/s)

R = Distance from the Seismic Source (m)

Ωo = Low Frequency Plateau of the Frequency Spectrum of a Seismic Waveform (see Figure 10)

Fc = Empirical Radiation Pattern Coefficient

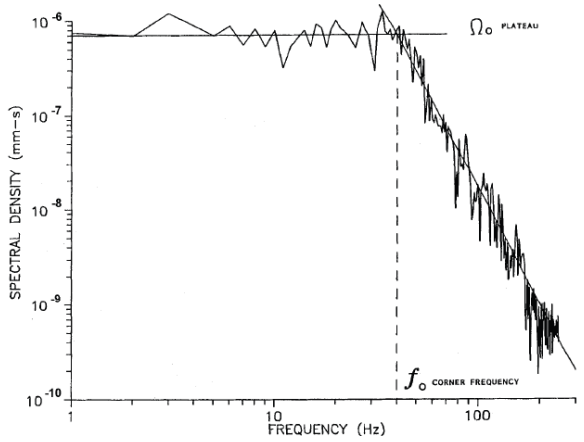

Figure 10: Corner frequency (f_0) and low frequency plateau (Ωo) for a typical seismic event (Hedley, 1992).

2.3.4 Seismic Energy

Seismic energy (E) is the total elastic energy radiated from a seismic source, and serves as a good indicator of event strength (Gibowicz and Kijko, 1994). The total radiated seismic energy is the sum of energy from the primary wave and secondary wave. Energy for each wave can be calculated as follows (Gibowicz and Kijko, 1994):

$$E = 4\pi pcR^2\frac{J_c}{Fc^2} \quad (2)$$

where,

E = Radiated Energy (Joules)

ρ = Rock Density (kg/m^3)

c = Velocity of the Wave in Rock (m/s)

R = Distance from the Seismic Source (m)

J_c = Integral of the Square of the Ground Velocity

Fc = Empirical Radiation Pattern Coefficient

2.3.4.1 Event Magnitude

Event magnitude can be expressed using numerous logarithmic scales. The well-known Richter (1935) magnitude scale is calculated using the peak ground motion from a seismic event, measured at a distance of 100 km from the seismic source, making it an amplitude based scale and consequently strongly related to seismic energy. Local magnitude is calculated similar to Richter, with considerations for local site effects.

Within this thesis, seismic events are shown according to the Local mine magnitude. As will be discussed in Chapter 6 (Section 6.1.3.1), Local magnitude values for seismic events discussed in this work are approximately one order of magnitude less than Richter. Magnitudes indicative of large and potentially damaging seismic events are Richter magnitudes greater than or equal to one (Butler, 1997); equivalent to Local magnitudes greater than or equal to zero. Table 1 details the observable rock mass response for seismic events of a particular Richter magnitude and approximate equivalent Local magnitude (adapted from Hudyma, 2004).

Table 1: Relation between varying degrees of Richter (M_R) / Local (M_L) magnitude and the observable rock mass response (adapted from Hudyma, 2004).

M_R	M_L	QUALITATIVE DESCRIPTION
-3.0	**-4.0**	-Small bangs or bumps felt nearby. Typically only heard relatively close to the source of the event. -This level of seismic noise is normal following development blasts in stressed ground. -Event may be audible but vibration likely too small to be felt. -Undetectable by a microseismic monitoring system.
-2.0	**-3.0**	-Significant ground shaking. -Felt as good thumps or rumbles. May be felt more remote from the source of the event (i.e. more than 100 m away). -May be detectable by microseismic monitoring system.
-1.0	**-2.0**	-Often felt by many workers throughout the mine. -Major ground shaking. -Similar vibration to a distant underground secondary blast. -Should be detectable by microseismic monitoring system.
0.0	**-1.0**	-Vibration felt and heard throughout the mine. -Bump commonly felt on surface (hundreds of meters away), but may not be audible on surface. -Vibration felt on surface similar to those generated by a development round.
1.0	**0.0**	-Felt and heard clearly on surface. -Vibrations felt on the surface similar to a major production blast. -Can be detected by regional seismological sensors located hundreds of kilometers away.
2.0	**1.0**	-Vibration felt on the surface is greater than large production blasts.
3.0	**2.0**	-The largest mining-induced seismic events recorded in Australia registered about Richter 3 to Richter 4.

2.3.5 Source Size

Source size is inversely proportional to the corner frequency of either the p-wave or s-wave. It is heavily model dependent and can be calculated as (Gibowicz and Kijko, 1994):

$$r_0 = \frac{K_c \beta_0}{2\pi f_0} \tag{3}$$

where,

r_0 = Source Size (m)

K_c = Source Model Constant (Hz)

β_0 = S-Wave Velocity in the Source Area (m/s)

f_0 = Corner Frequency (shown in Figure 10)

2.4 Seismic Analysis Techniques

Seismic analysis techniques allow for meaningful observations and conclusions to be drawn from seismic databases or subsets within the data. Such techniques can provide insight into source

mechanisms, seismic hazard, seismic monitoring system limitations and the seismic response to mining.

2.4.1 Gutenberg-Richter Frequency-Magnitude Relation

In 1944, Gutenberg and Richter proposed a power law relation between the frequency of seismic events and their magnitude:

$$\log(N) = a - bm \tag{4}$$

where,

N = Number of seismic events of a least magnitude 'm'

m = Magnitude

a = Constant

b = Constant

The Gutenberg-Richter Frequency-Magnitude relation is commonly considered one of the most fundamental seismic analysis techniques. For a given seismic population of sufficient size, Frequency-Magnitude charts can provide insight into data quality, source mechanism and seismic hazard. Figure 11 depicts a Frequency-Magnitude chart for a large seismic population from a deep Canadian mine. Events are plotted according to magnitude on the x-axis, with the cumulative number of events greater than or equal to that magnitude plotted on the y-axis.

The slope of the Frequency-Magnitude relation, or b-value, can provide insight into source mechanism for a given seismic population. A low b-value (less than 0.8), is indicative of a fault-slip mechanism driving seismicity. A high b-value (1.2 – 1.5), is indicative of a primarily volumetric and stress fracturing source mechanism (Hudyma, 2008). For large well-behaved populations, a b-value approximating 1.0 is expected - as seen in Figure 11.

Where the Frequency-Magnitude relation no longer approximates the real data is referred to as the M_{min} value (see Figure 11). It represents the seismic system sensitivity, or the completeness of the data record. In other words, the seismic monitoring system has reliably recorded all events greater than or equal to this magnitude for the seismic population (M_{min} = -2.0 in Figure 11). The intersection of the Frequency-Magnitude relation with this x-axis, or the 'a/b' value, is an estimation of the largest plausible event magnitude. This value is commonly used as a means of assessing long term seismic hazard. The 'a/b' value for the population shown in Figure 11 is M = 2.4, very close to the largest event contained within the population (M = 2.5).

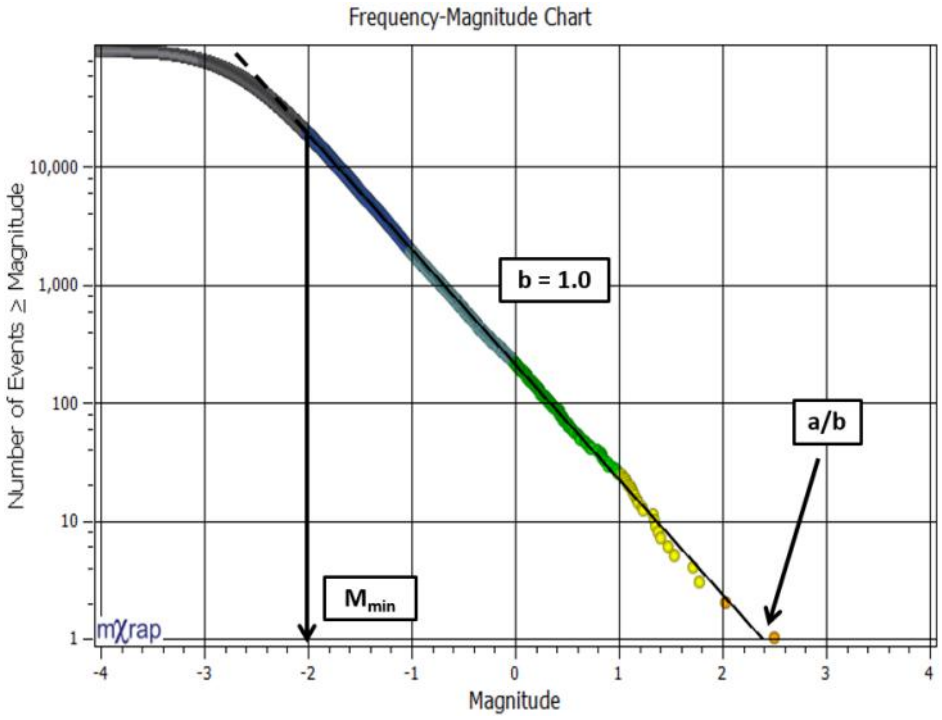

Figure 11: Frequency-Magnitude chart for a large population of seismic data from a deep Canadian mine. Colour variations correspond to magnitude.

2.4.2 Magnitude-Time History Charts

As mining is a dynamic process, time should be incorporated into seismic analysis to gain meaningful insight into the rock mass response to mining. The Magnitude-Time History analysis technique (Hudyma, 2008), allows the user to visually and quantitatively analyze a seismic response to mining over time. Events are plotted in chronological order with date/time on the x-axis, and magnitude on the primary y-axis. A line is used to represent the cumulative number of events over time, corresponding to the secondary y-axis. A flat cumulative number of events line represents no seismic activity. A constant slope reflects a constant rate of events. A slope that increases over time represents an increasing rate of events. Figure 12 is a typical Magnitude-Time History chart for a large seismic population with a relatively constant rate of events over time. Mine blasts are shown as red stars along the x-axis, and can provide further insight into the seismic response to mining. Magnitude-Time History charts are used throughout this thesis to infer temporal relations between seismic responses and discrete mine blasting.

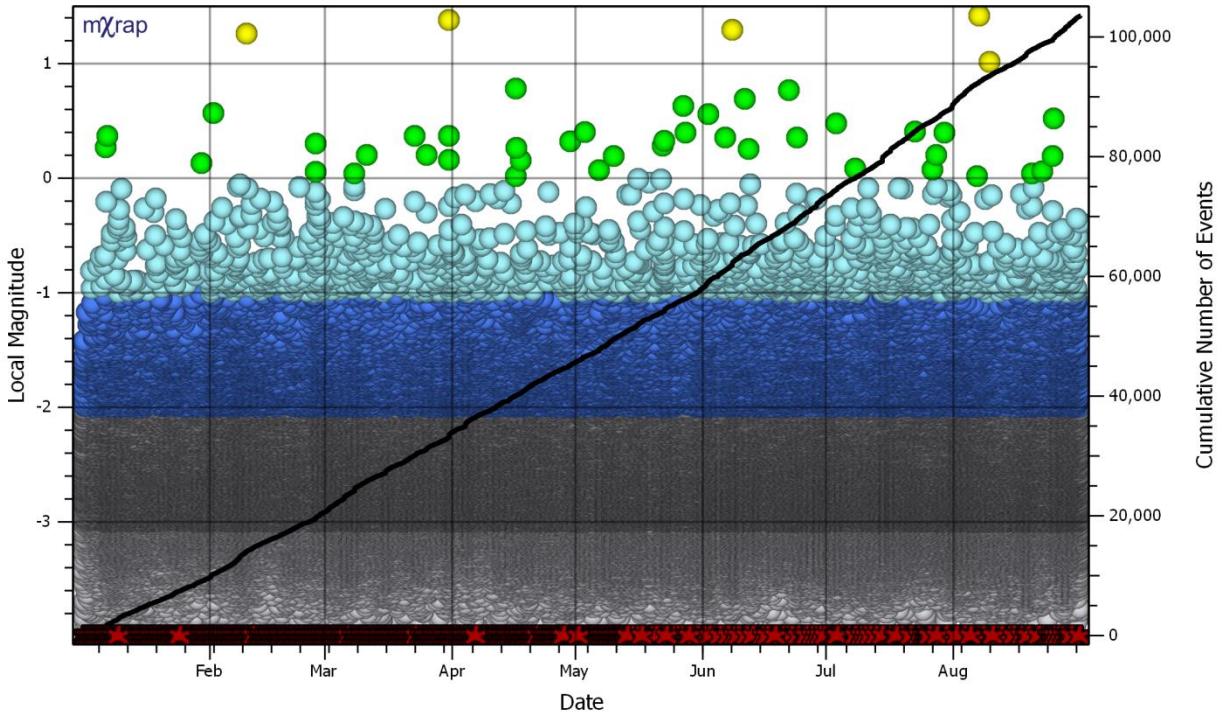

Figure 12: Magnitude-Time History chart for a large population of seismic data. Colour variations correspond to Local magnitude values. Mine blasts, which occur continuously throughout the time period, are shown along the x-axis as red stars.

2.5 Variations in the Seismic Response to Mining

Two broad types of seismicity have been described in literature. Richardson and Jordan (2002) refer to these as Type A and Type B, which are synonymous with induced and triggered, respectively. An induced seismic response to mining occurs as a direct result of the creation of new mining excavations or voids. Induced seismicity is characterized as being primarily driven by mining-induced stress change and should be proportionate to the volume change from mine blasting (Gibowicz and Kijko, 1994; McGarr and Simpson, 1997; McGarr *et al.*, 2002). Consequently, induced seismicity is largely spatially and temporally dependent on recent mine blasting activities.

Triggered seismicity is not primarily driven by discrete mining processes, but rather tectonic loading (McGarr and Simpson, 1997; McGarr *et al.*, 2002), and regional mining effects. As such, triggered seismic responses to mining commonly concentrate around geological discontinuities within a rock mass (Gibowicz and Kijko, 1994). While mine blasting may be the factor that initiates a triggered seismic response, the blast often represents only a small portion of the total energy associated with the rock mass failure. Because triggered seismicity results from the interplay of mining, geological and tectonic factors, it is spatially and temporally independent of discrete mine blasting - particularly relative to induced seismicity.

Figure 13 depicts a simple mining environment and a plausible seismic response to a production stope blast. A strong induced response is seen in close spatial proximity to the mine blast - between Level 2 and 3, as well as above Level 3. This rock mass failure is primarily driven by the discrete mining-induced stress change of the production blast, and consequently, most seismic events are spatially clustered within the *insitu* rock mass directly adjacent to the newly formed void.

A secondary cluster of seismic events is located in proximity to a known fault which intersects a mine shaft (vertical excavation), in Figure 13. Unlike the induced response however, this seismicity is significantly distant to the mine blast. The magnitude of induced stress change resulting from mine blasting is inversely proportional to the distance from the blast (Steacy *et al.*, 2005; Hudyma, 2008). While the stress change induced by blasting may be a contributing factor to the seismic response surrounding the mine fault, it is too small to be the exclusive source of energy driving rock mass failure. This seismicity is typical of a triggered seismic response to mining.

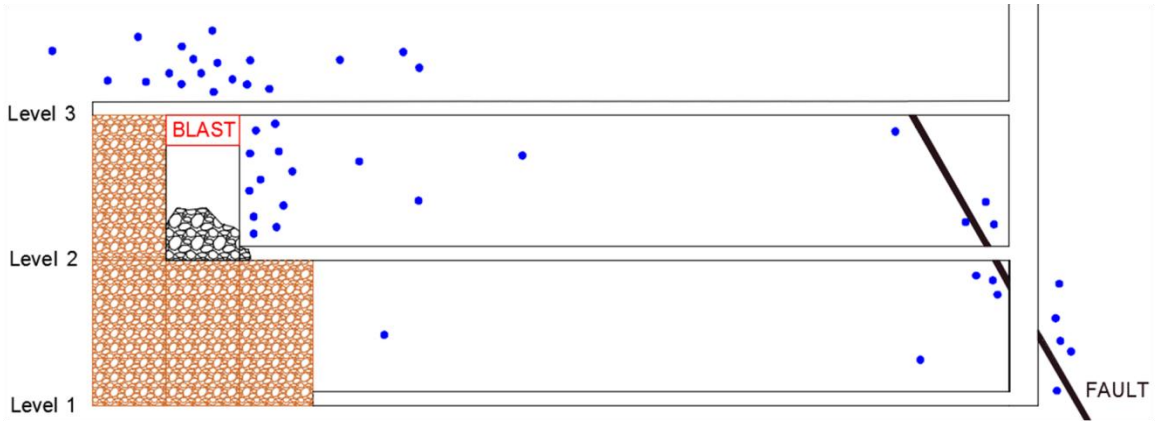

Figure 13: Diagrammatic longitudinal protection of a simple induced and triggered seismic response to mine blasting. Induced seismicity is shown in close spatial proximity to the mine blast – between Level 2 and 3, as well as above Level 3. Triggered seismicity is shown distant to the mine blast – along a known fault intersecting a mine shaft (vertical excavation). Not to scale.

2.5.1 Physical Mechanisms of Seismic Responses

While the generalized concepts used to define induced and triggered seismic responses to mining are relatively uncomplicated, there exists no unequivocally identified physical mechanism which accounts for induced and triggered seismicity (Orlecka-Sikora, 2010; Woodward, 2015). Triggered seismicity in particular, though having been observed in a variety of mining environments (Hudyma, 2008), remains relatively poorly explained. The physical processes which relate an initial stress change, such as those initiated by mine blasting, to a remote or delayed response (triggered seismicity) have limited deterministic basis (Woodward, 2015).

Earthquake interactions are commonly considered using a static stress transfer model, where stress change attenuates approximately as some inverse power of the distance (Steacy *et al.*, 2005). Steacy *et al.* (2005) define static stress changes as "changes that effectively occur instantaneously and permanently." In terms of mine seismicity, a mine blast can be considered the "mainshock", which generates a static stress transfer inducing "aftershocks" (induced seismicity) (Richardson and Jordan, 2002). Harris (1998) concludes that small, medium and large aftershocks generally occur in regions of static stress increase.

This concept does not account for triggered seismicity however, which occurs beyond the finite stress change of a static stress transfer model. Gibowicz (1990) indicates that triggered seismic events are more global, occurring in response to stress changes on a whole-mine scale and not any specific area of mining. McKinnon (2006) states that "numerical stress analysis has not been able to explain the occurrence of seismic events remote from mining." These statements suggest that triggered seismic responses are more likely to originate from a quasi-static stress transfer model; where rock mass relaxation extends significant distances beyond a static stress model due to low viscoelastic propagation speeds (Woodward, 2015).

The reader should be aware that a satisfactory model to explain the interaction of induced and triggered seismic responses to mining has yet to be defined. There are a number of site specific factors to consider, including: geometry of excavations, filling of excavations, blasting practices, mining-induced stress, non-linear rock mass strength, and location and properties of minor and major geological features. This thesis does not address this issue of ambiguity surrounding the physical mechanisms of seismic responses. The problem is sufficiently complex, and has high levels of uncertainty, suggesting a deterministic understanding is unlikely.

2.5.2 Relating Seismic Responses to Mine Blasting

Throughout literature it is suggested that relating seismicity to discrete mine blasts may provide valuable insight into seismic responses to mining, yet this task is rarely undertaken. Woodward (2015) writes: "The dependency between a seismic response and stress changes may be ambiguous due to incomplete blasting records, the influence of pre-existing stress conditions, or rock mass strength conditions." A general uncertainty regarding rock mass stress and strength conditions within mining environments appears to discourage relating individual responses to discrete stress changes from mine blasting. This suggests a need for alternative methodologies to address this issue.

Eremenko *et al.* (2009) states:

"So, the blasting to underground seismicity relationship is governed by many factors and shows itself differently in the mines. The approach to the problem may either involve an analysis of individual blast after-effects or an analysis of change in the integral probably significant

characteristics of seismicity after a series of blasts. Both analyses complement one the other and eventually produce a statistically valid physical model of blasting impact on mine seismicity."

The authors go on to apply the second analysis type to mine seismic data, however there is no further mention of the first analysis type. Richardson and Jordan (2002) also comment regarding discrete mine blast analysis, stating:

"Most of these Type A events occur shortly after blasting, and their rates are therefore casually related to the amount of blasting, which varies from mine to mine. A detailed analysis of this relationship requires the consideration of two different Types of blasting: on the stope faces (for mining gold ore) and at the development ends (for extending tunnels, haulages, and spaces for other mine infrastructure)."

Similar to Eremenko *et al.* (2009), Richardson and Jordan (2002) only define the considerations that must be made, and do not in fact attempt the analysis. The authors do note however, that the highest seismic activity rates within mining environments are associated with very high development rates and stope faces that are blasted multiple times per day.

The work of Eremenko *et al.* (2009) focuses on the distribution of seismic activity in space and time with reference to mine blasting. Figure 14 depicts the seismic event rate versus time period after blast for a series of mine blasts. Two lines are shown, with one including all seismic activity (1) and another excluding the first 10 minutes directly following blasting (2). For both lines (1 and 2), the maximum number of events occurs within one hour of the blast time. Both event rate and energy show small deviations from the mean, relative to the after-blast increase, in excess of 11 hours after the blast (Eremenko *et al.*, 2009).

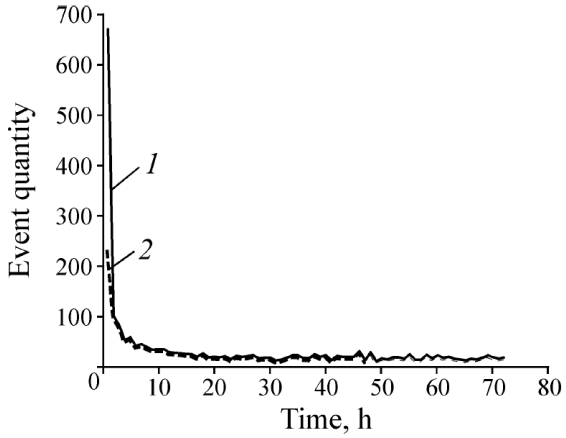

Figure 14: Event rate versus the time period after a mine blast. Two lines are shown, (1) corresponds to all the cataloged data and (2) corresponds to all the cataloged data excluding the first 10 minutes directly following the mine blast (Eremenko *et al.* 2009).

Figure 15 depicts the average distance between event locations and blast locations for three days following a mine blast (a), and one week prior to a mine blast (b). For the events occurring after the mine blast (a), there is a positive correlation between distance and time from blast -

correlation factor of 0.61. For the events occurring prior to the mine blast, and presumably with sufficient time lapse since the previous blast, there is almost no correlation between distance and time - correlation factor of -0.01. This work can be interpreted as strongly supporting a spatial relation between induced seismicity and proximity to mine blasting, while simultaneously showing a not meaningful relation between triggered seismicity and proximity to mine blasting.

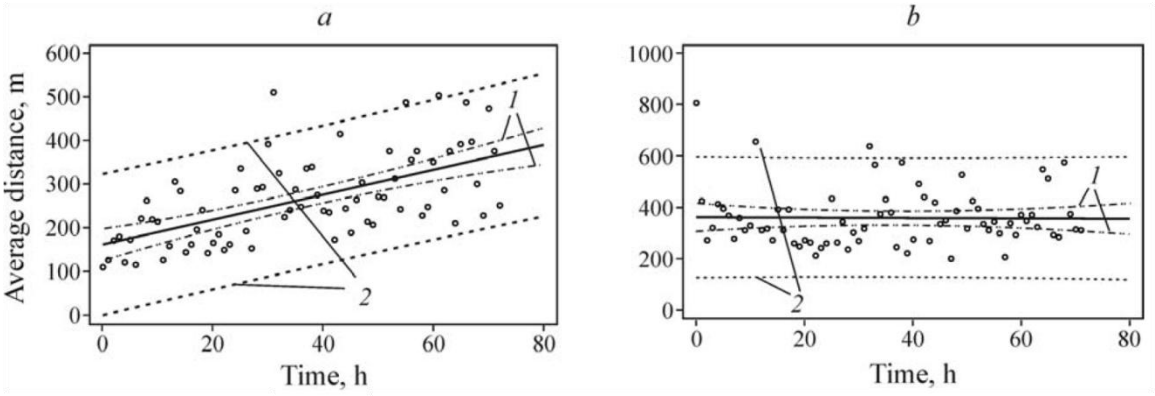

Figure 15: The mean distance between seismic event locations and mine blasts for (a) three days following a mine blast and (b) one week prior to a mine blast, with correlation factors of 0.61 and -0.01 respectively. Dashed lines (1) represent the mean position of seismic events. Dotted lines (2) represent the area of spatial distribution (Eremenko *et al.* 2009).

Woodward and Wesseloo (2015) discuss some of the inherent issues with relating seismic responses to discrete mine blasts, such as was suggested by Eremenko *et al.* (2009), within a complex mining environment, specifically:

- Mine blasting practices, such as blasting at designated times at the end of shifts, inevitably lead to seismic responses overlapping in time and separated in space.
- Mine blasting of successive headings and other near-by excavations inevitably results in seismic responses overlapping in space but not in time.
- Stress redistribution mechanisms, which can vary throughout a mining environment, may result in significant variability in the space-time relationship between seismic responses and the initial stress change.
- Within a single mine it is common practice to fire multiple blasts, of varying size and location, simultaneously. Therefore it may not be possible to associate specific seismic responses to discrete mine blasts.

Despite these challenges, the authors go on to propose four cases that characterize the space-time relation between the location and timing of seismic responses and mine blasting. These cases are summarized in Figure 16, with initial and delayed/remote seismic responses represented by red and green circles respectively. The local and immediate response (a), consists of events in close spatial and temporal proximity to the initial stress change induced by a mine blast. This type of response appears to be synonymous with induced seismicity. All other responses (b, c, d), contain seismic events both in close and distant temporal and/or spatial proximity to the initial

stress change induced by a mine blast. It is around these types of responses where there is significant ambiguity in literature.

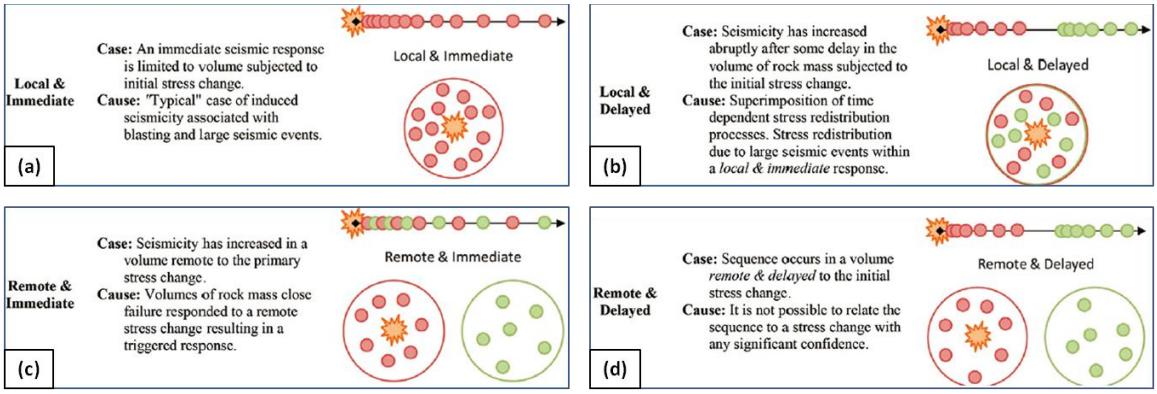

Figure 16: Descriptions of the four cases characterizing the relationship between a seismic response and a blast based on the space-time relationship. Conceptual diagram of cases is shown by an initial stress change represented by an orange splash, initial seismic response represented by red circles, and delayed/remote seismic sequences represented by green circles (redrawn from Woodward and Wesseloo, 2015).

2.5.3 Identifying Seismic Responses to Mining

As previously discussed in Section 1.1.2, this thesis focuses on groups or populations of individual seismic events referred to as seismic responses to mining. Within this thesis, relatively little emphasis is placed on the identification of seismic responses to mining in space and time, but rather quantitatively describing a response once it has been identified. For this reason, only the method employed in this research for identifying seismic responses to mining will be reviewed in detail. A discussion surrounding limitations of seismic response identification methods based on a fixed spatial distance is also presented.

2.5.3.1 Limitations of Fixed Spatial Distances for Identifying Seismic Responses to Mining

A common means of characterizing seismic responses to mining is the Modified Omori Law (MOL) (Omori, 1894; Utsu, 1961; Vallejos and McKinnon, 2010). In simple terms, MOL describes time dependent event occurrence of a seismic population or response, as shown in Equation 5:

$$n(t) = K(t + c)^{-p} \tag{5}$$

where,

$n(t)$ = Number of events per time interval, at time t

K = Constant related to productivity

c = Constant related to the time offset

p = Constant related to the event decay

Plenkers *et al.* (2010) discuss the application of MOL to five post-blast seismicity sequences in Mponeng Gold mine, as shown in Figure 17. The p-value is significant, as it describes how fast the seismic event rate decays over time. For induced seismicity, which is temporally dependent on the stress change induced by mine blasting, the event rate should decay relatively quickly. It should be noted however, that due to variability in seismic responses to mining, some observed responses are not well described by the MOL (Mendecki and Lynch, 2004).

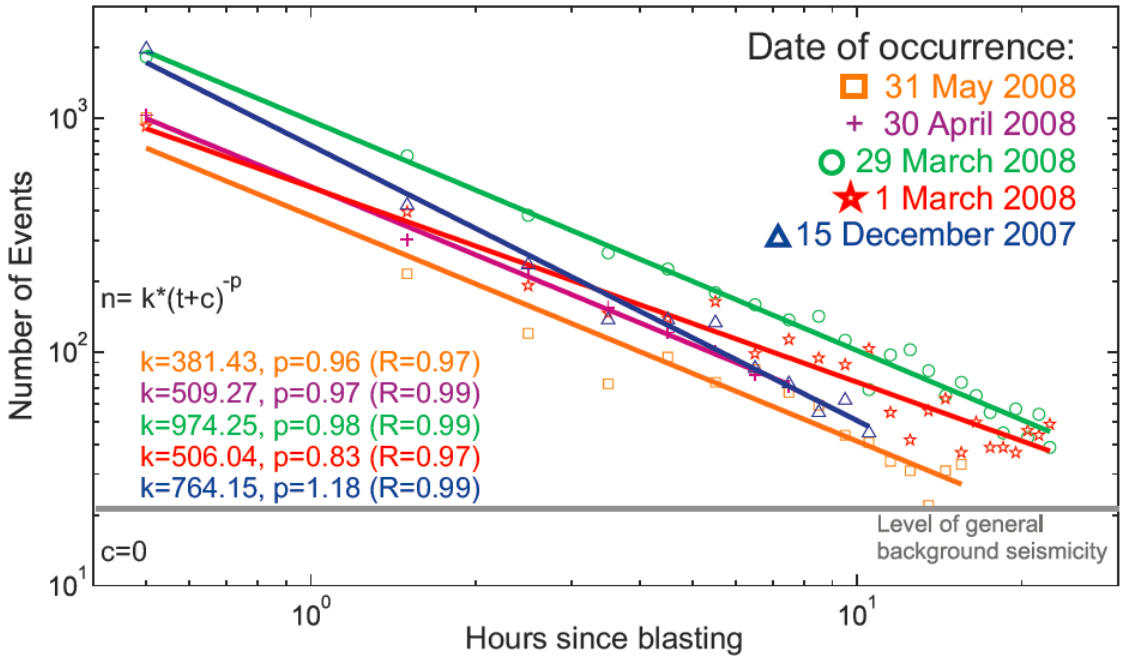

Figure 17: Analysis of Modified Omori Law. The power law was fitted using a least-squares approach minimizing the sum of squared residuals (R). The c-value was set to zero. For the post blast sequences shown, P-values between 0.83 and 1.18 are found (Plenkers *et al.*, 2010)

For the application of MOL to mining seismicity, responses are typically isolated in space using a fixed spatial distance, or search radius, from the mine blast location. This type of spatial filtering is based on an underlying assumption that response events are contained within a spherical volume around the stimulus (i.e. mine blast). This assumption is not ideal (Woodward and Wesseloo, 2015), as seismic responses may be influenced by external complexities within the mining environment, and cluster in non-spherical shapes. Furthermore, assigning a spatial limit with direct reference to the stimulus limits applicability of 'distance to blast' analysis techniques. For these reasons, this work does not employ fixed spatial distances for identifying seismic responses to mining.

2.5.3.2 Single-Link Clustering

Single-Link Clustering (SLC) is a straightforward approach to data clustering that is widely used across a variety of disciplines. Frohlich and Davis (1990) found success in applying SLC analysis to real and synthetic earthquake databases, as the hierarchical nature of the methodology ensures it is well suited for defining clusters of natural earthquakes on both a global and local scale. Kijko and Funk (1996) combined the SLC methodology used by Frohlich and Davis (1990), with a time window to assess the interaction of identified clusters. A similar methodology will be employed in the case study contained within this thesis (presented in Chapters 6 and 7).

For SLC, clusters are primarily identified through the use of a d-value. The d-value refers to the maximum linking distance between adjacent points in a group, and forms a 'd' cluster. All seismic events within a d-cluster must be located within the d-value of at least one other event within the cluster. The application of this methodology to earthquake databases requires d-values to be in the order of kilometres, as shown in Figure 18. For mine seismicity, d-values are considered in the order of metres.

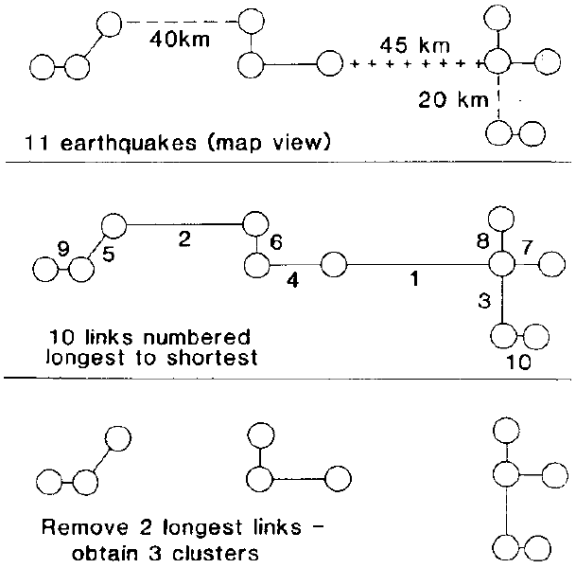

Figure 18: An example of single-link clustering applied to a series of earthquakes, shown as circles. Variations in link lines (solid, dashed, etc), correspond to varying linking distances. When the longest links are removed (40+ km in length), three distinct clusters are formed in space (Frohlich and Davis, 1990).

Single-Link Clustering is a methodology for sub-dividing seismic data into clusters using any arbitrary value of 'd'. If 'd' is too small, the resultant clusters will contain very few seismic events, and may not be of sufficient size for meaningful analysis, or be representative of a complete seismic response. If 'd' is too large, the resultant clusters will contain large quantities of seismic events, but will likely not be representative of individual seismic responses.

The distribution of link lengths may provide insight into natural ‘d’ values for a given dataset (Frohlich and Davis, 1990). Link length refers to the distance between a point and its closest neighbor, such that all data points are linked in one continuous chain. Frohlich and Davis (1990) suggest that if natural clustering exists within a dataset, the distribution of link lengths may exhibit a change in slope near the ideal d-value for natural clustering. Such a change was not present in the earthquake data presented by Frohlich and Davis (1990), shown in Figure 19.

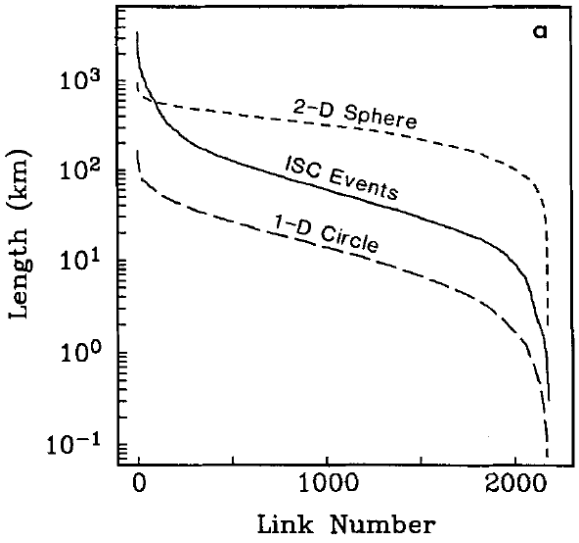

Figure 19: Cumulative distribution of link lengths for a group of earthquakes (solid line) together with the distribution of link lengths for 2178 events placed randomly on a circle (1-D) and on the surface of a sphere (2-D). The circle and the sphere both have radii equal to that of the Earth (Frohlich and Davis, 1990).

2.5.3.2.1 Limitations of Single-Link Clustering for Identifying Seismic Responses to Mining

As previously discussed, if ‘d’ is too large, the resultant single-link clusters will contain large quantities of seismic events, but will likely not be representative of individual seismic responses. Such an instance is shown in Figure 20, were two individual clusters, A and B, are merged together into a single cluster with the introduction of stray events between the two clusters (Rebuli and Kohler, 2014). When different types of seismic responses are joined, induced and triggered, it can negatively impact meaningful analysis.

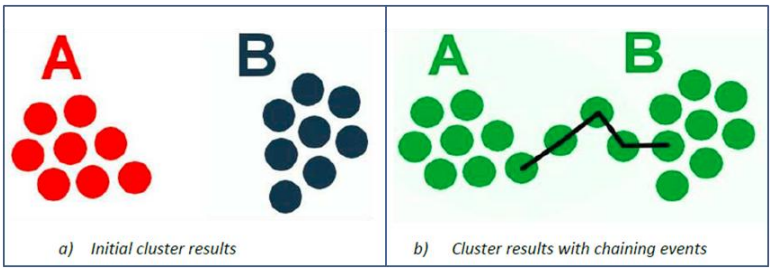

Figure 20: Example of the chaining effect produced by a single-link clustering algorithm. Part (a) depicts the original clusters A and B. Part (b) depicts the merging of cluster A and cluster B due to the occurrence of stray events between the two clusters (Rebuli and Kohler, 2014).

2.5.4 Seismic Response Observations

This section provides observations of variations in seismic responses to mining throughout literature.

2.5.4.1 Induced Seismic Responses to Mining

Throughout literature, reference is made to mining-induced seismicity as being spatially and temporally clustered close to newly formed mine excavations (Cook, 1976; McGarr, 1971; Gibowicz and Kijko, 1994; Hudyma, 2008; Plenkers *et al.*, 2010; McKinnon, 2006, Gibowicz, 1990). Table 2 summarizes literature references which make explicit statements regarding the spatial and temporal relation of mining-induced seismicity and mine blasting. In some instances, the values refer to the entire response. In others, typically where the entire mine seismicity population was considered and not an isolated response, the values refer to what the authors perceived to be the vast majority of induced events. Some values are suggestions made by authors with expertise in the subject matter.

In general, it appears that reasonable spatial bounds for induced seismic responses to mining are in the order of tens of metres. These bounds are somewhat dependent on other factors, such as the size of the mine blast and any limitations of the seismic monitoring system. General temporal bounds appear to be one to three hours following the mine blast. These observations agree with the general definition of induced seismicity employed in this thesis.

Table 2: Summary of literature references which make explicit statements regarding the spatial and temporal relation of mining-induced seismicity to mine blasting.

Reference	Spatial Relation To Blasting	Temporal Relation To Blasting
Woodward & Wesseloo (2015)	Within 10 metres (development) and within 40 metres (production).	Within 1 hour.
Kgarume *et al.* (2010)	Within 400 metres (one typical stope dimension).	Within 1 hour.
Mendecki & Lynch (2004)		Within a few hours.
Richardson & Jordan (2002)	Within 100 metres.	Within 30 seconds of the preceding event in the seismic response.
Mendecki (2001)		Within 1 to 2 hours.
Urbancic *et al.* (1992)	Confined within 90 metres, most events located within 40 metres.	
Ecobichon *et al.* (1992)	Within 10 to 20 metres (production).	
Gibowicz (1990)	Within 20 metres.	

2.5.4.2 Triggered Seismic Responses to Mining

Throughout literature, reference is made to mining-triggered seismicity as being spatially and temporally distant to newly formed mine excavations (Gay and Ortlepp, 1979; Spottiswoode, 1989; Gibowicz and Kijko, 1994; Hudyma, 2008; McKinnon, 2006; Gibowicz, 1990). Table 3 summarizes literature references which make explicit statements regarding the spatial and temporal relation of mining-triggered seismicity and mine blasting.

In general, it appears that reasonable spatial bounds for triggered seismic responses to mining are in the order of hundreds of meters beyond blasting. These bounds are somewhat dependent on other factors, such as the size of the mine blast and any limitations of the seismic monitoring system. General temporal bounds appear to be somewhat arbitrary in terms of relating a specific triggered response to a discrete mine blast.

Table 3: Summary of literature references which make explicit statements regarding the spatial and temporal relation of mine-triggered seismicity to mine blasting.

Reference	Spatial Relation To Blasting	Temporal Relation To Blasting
Woodward & Wesseloo (2015)	Beyond 100 metres.	6 hours beyond blasting.
Disley (2014)	Hundreds of metres beyond blasting.	Days beyond blasting.
McKinnon (2006)	Hundreds of metres beyond blasting.	Uncorrelated.
Whyatt *et al.* (2002)		Several months to hundreds of days beyond blasting.
Potvin & Hudyma (2001)	Several hundred metres beyond blasting.	Several days and sometimes weeks beyond blasting.

2.5.4.3 Complex Seismic Responses to Mining

Triggered seismicity is commonly defined as occurring distant to discrete mining-induced stress change, however this is not always the case. Seismic source mechanisms which generate triggered seismic responses are relatively stationary, but mine blasting migrates throughout a mining environment over time. When mine blasting approaches triggered source mechanisms (e.g. geological features or highly stressed pillar), such that the mechanism is contained within proximity of the mining-induced stress change, it is possible to observe superimposition of induced and triggered seismic responses to mining. The most evident form of this complex seismicity in literature is the occurrence of rockbursts in proximity to relatively isolated mine development. When a rockburst occurs, it is commonly considered to represent a disproportional energy release - triggered seismicity.

In early 1990, a haulage drift being driven 1,400 metres below surface at Falconbridge's Fraser Mine experienced two significantly disproportionate seismic events to typical development mining (Swan and Semadeni, 1992). With drift dimensions of 8 metres wide by 5 metres high, and considerable isolation within the mining environment (in excess of 500 metres from active mining), the static stress transfer from development blasting should not have produced any significant seismic response. Prior to the occurrence of the two large seismic events, the risk category for the excavation would have been low to non-existent (Swan and Semadeni, 1992).

The first large event (magnitude 2.0), occurred temporally distant to blasting, as crews had sufficient time to install ground support and drill new blast holes. Approximately 300 tons of material was expelled into the development drift due to the seismic event (Swan and Semadeni, 1992).

The second large event (magnitude 2.3), also occurred temporally distant to blasting, approximately 12 hours after the most recent mine blast. Approximately 600 tons of material was expelled into the development drift due to the seismic event (Swan and Semadeni, 1992).

At the time of the large seismic events, the hanging wall of a regional fault was believed to be within one or two rounds of the face (Swan and Semadeni, 1992). With 8 metre drift spans and only 4 metre development rounds, it is highly likely the fault would have been located within the mining-induced stress change zone of the excavation. This appears to be an example of a complex seismic response to mining.

Other examples of complex seismic responses to mining include:

- Delgado and Mercer (2006):
    - "At the Campbell Mine it is not typical for individual development headings to produce high levels of micro-activity under only low to moderate loading conditions...At the time of interest, this ramp was a substantial distance from any stoping activities and was, as such, considered to be under the influence of the far-field stresses."
    - In December of 2004, significant seismicity, including a magnitude 1.4 rockburst, was observed following blasting of an isolated decline. The burst was located a short distance in front of the face, presumably within the mining-induced stress change zone.
    - "At the time, it was speculated that the burst occurred due to a combination of the character of the rhyolite and the stress field being distorted by the '01' Fault some 10 m (30 ft) ahead of the face."
    - "As the face advanced towards the '01' Fault, the induced seismicity steadily increased on a round-by-round basis from approximately 70 events/day prior to the burst to nearly 500 events per day just prior to entering the '01' Fault. Once through the fault (and it was anticipated), the event rate steadily decreased until the development cycle could be returned to its pre-burst schedule."

- Slade and Ascott (2002)
    - "Two days of elevated seismic activity at the Strzelecki Mine, 22km west of Kalgoorlie, resulting in 5 rockbursts and a need to cease mining activity"
    - The seismic related damage occurred in footwall development and the decline (down ramp), at a considerable distance from production mining.
    - "...visible damage had always been strongly correlated to a fault and the damage had never extended further than 10 m from the fault."

Complex seismic responses are a phenomena observed in a variety of mines, particularly hard rock mines, and yet have not been explicitly categorized in literature.

2.6 Chapter Summary

Underground hard rock mines typically install microseismic monitoring systems with the onset of mine seismicity and visible rock mass damage (rockbursting). These systems record ground motions throughout a mining environment, and calculate quantitative seismic source parameters. The five independent seismic source parameters are: time, location, seismic moment, seismic energy and source size. From these, secondary seismic source parameters, such as magnitude, are calculated.

The primary considerations of this thesis are seismic event location and event time. Due to high quantities of uniaxial accelerometers used in Canadian mines, seismic event locations are typically good, and location errors are generally less than ten metres (Figure 9). Seismic event time is unique amongst the independent seismic source parameters, as it is associated with little to no error. Despite this advantage, it is rarely a primary factor of seismic analysis.

Variations in seismic source mechanisms in mines, or rock mass failure modes, generate seismic responses with different temporal and spatial characteristics; particularly with reference to mine blasting. Two broad types of mine seismicity are discussed in literature: induced and triggered. Induced seismicity is proportionate to mine excavation geometry changes (i.e. blasting), and typically posses a manageable risk to the viability of seismically active mining operations. Induced source mechanisms are commonly related to stress fracturing, and events occur in close spatial and temporal proximity to mine blasting - typically within tens of metres of blast locations, and within one to three hours of blast times.

Triggered source mechanisms are commonly related to failure and/or movement of significant geological features. Triggered seismic events occur spatially distant, and temporally independent of discrete mine blasting - hundreds of metres beyond blast locations and independent of blast times. Triggered seismicity is disproportionate to mine excavation geometry changes, and often represents a large uncontrolled release of stored energy within the rock mass, posing a significant risk to the viability of seismically active underground mining operations.

This chapter has introduced the terminology and basic concepts employed throughout this thesis. Many of the theories and explanations for mine seismicity are derived from earthquake seismology. Consequently, there is little accounting for the complex variations and interactions within a mining environment. Examples of seismic responses that do not conform to the definitions of induced or triggered seismicity have been discussed (Section 2.5.4.3), and are referred to within this work as complex seismic responses to mining. This thesis aims to further define and quantify seismic responses to mining, including complex responses, with explicit reference to discrete mine blasts.

Chapter 3

3 Characterizing Seismic Responses to Mining

As previously discussed in the literature review (Chapter 2), mine seismicity is typically categorized as induced or triggered. This chapter introduces the concept of complex seismicity, and discuss the characteristics of induce, triggered and complex seismic responses to mining.

Figure 21 is a diagrammatic sketch of a more realistic mining environment, relative to Figure 13 (Section 2.5), and a plausible seismic response to stope blasting. In Figure 21, a production stope blast is fired between level 2 and level 3, resulting in a significant excavation geometry change. Induced seismicity surrounds the newly formed void and consists predominantly of small magnitude seismic events. These events are spatially clustered around the blast location, and occur directly following the mine blast in time.

Triggered seismicity is located distant to the blast, and in most cases surrounds dominant geological features (Figure 21). It is the movement along these structures, and pre-existing tectonic loading, that generates disproportionate rock mass failure. For example, the large magnitude triggered seismic event located along the fault between Level 6 and Level 7 is unlikely to be exclusively driven from the blast induced stress change of the production stope, as the event occurs at a significant distance from the mine blast location.

Where geological structures are located sufficiently close to the mine blast to experience a significant mining-induced stress change, a complex seismic response is observed. This can be seen diagrammatically in the dyke between Level 2 and 3, and surrounding the fault-dyke intersection above Level 3. Complex seismicity is a common occurrence in mines, but is typically unexplored in literature due to the inherent complexity and large degree of unknowns (Section 2.5.4.3).

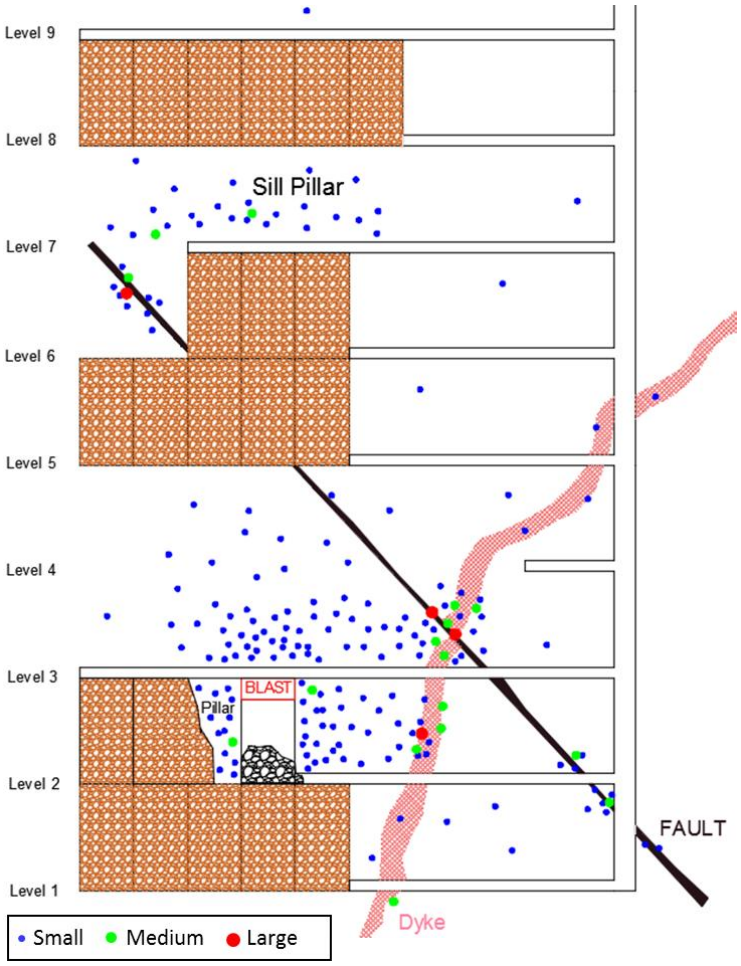

Figure 21: Diagrammatic sketch of a seismic response to production stope blasting in a mining environment. Induced seismicity is shown in close spatial proximity to the mine blast – between Level 2 and 3, as well as above Level 3. Triggered seismicity is shown distant to the mine blast – above Level 6 and 7, and surrounding Level 2 near a mine shaft (vertical excavation). Complex seismicity is shown within the near field of mine blasting and within proximity of significant geological features – between Level 2 and 3, and above Level 3. Not to scale.

3.1 Induced Seismic Responses to Mining

Induced seismic responses to mining occur in close spatial proximity to the stimulus (i.e. mine blast). This type of rock mass failure is directly driven by the mining-induced stress change resulting from the excavation of discrete mining voids. The spatial extents of this type of response therefore depend largely on the size of the void mined. In Figure 21, the void is relatively large, a production stope, and consequently the spatial distribution of the response is significant. For the mining of much smaller excavations, such as development drifts, the spatial distribution of the seismic response is reduced.

The region of stress alteration surrounding mine openings, the mining-induced stress change zone, is typically in the order of several excavation radii lengths (Brady and Brown, 1985; Hoek and Brown, 1980; Hoek *et al.*, 1995). The excavation-disturbed zone, where stress change is

relatively small and does not measurably change the rock mass properties, extends from 2 to 5 excavation radii (Kuzyk and Martino, 2008). A maximum spatial limit of an induced seismic response to mining likely approaches 5 excavation radii, as beyond this limit the rock mass experiences no appreciable mining-induced stress change.

For practical application purposes, microseismic monitoring limitations must be taken into consideration. It is common in Canadian mines to have relatively poor location accuracy surrounding new mine excavations - as there is limited accessibility for seismic sensor installation prior to mining. It was shown in Figure 9 (Section 2.3.2), that the median value of location error for a variety of Canadian underground mining operations was less than 10 metres (Brown and Hudyma, 2018a). It is suggested that an assumable spatial limit of an induced seismic response to mining is 5 excavation radii plus 10 metres to account for location error. The 'Location Error Factor', 10 metres in this work, may vary depending on mine site specific considerations, including seismic system array coverage.

Figure 22 depicts a theoretical maximum spatial limit of an induced seismic response to mining. The excavation in part (a) is shown in white as a circle with a radius of 2.5 metres. This approximates typical mine development excavations, which commonly span 5 metres. The excavation in part (b), shown as a square with a radius of 15 metres, approximates a typical mine production stope. The area in closest proximity to the excavations (shown in red), experiences the largest mining-induced stress change and is the most likely location for rock mass failure in the form of induced seismicity. Beyond this area is the excavation-disturbed zone (shown in orange to blue), where the occurrence of induced seismicity is less likely but still within theoretical limits. An additional area of 10 metres beyond the excavation-disturbed zone is used to account for microseismic monitoring limitations. In other words, seismic events that occur within the theoretical limits of failure may be located inaccurately by the monitoring system within the additional 10 metres zone. By expanding the maximum theoretical spatial limits by 10 metres, it helps to ensure these seismic events are included in the assumed mining-induced stress change zone.

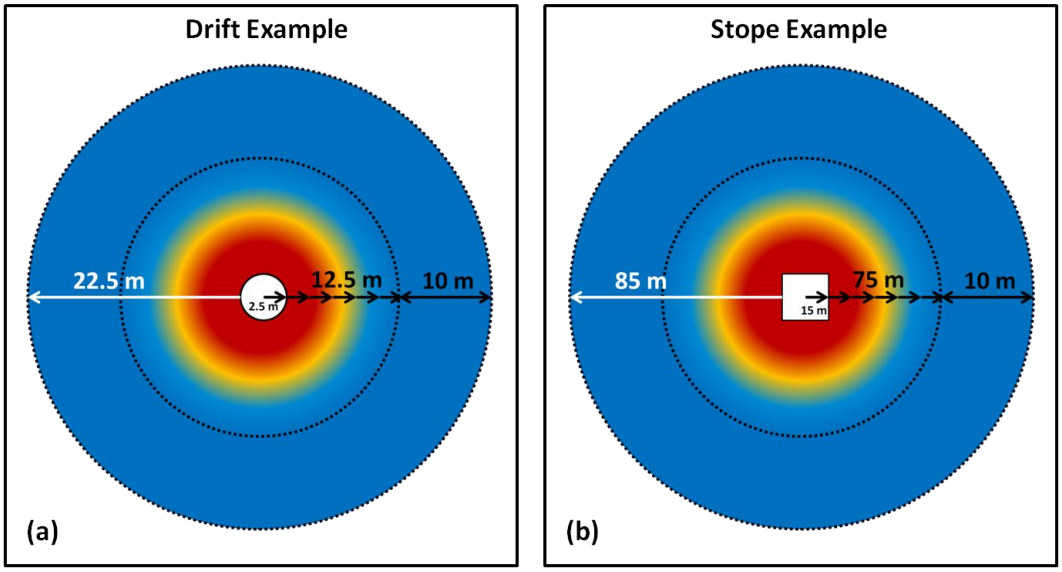

Figure 22: Maximum theoretical spatial limits of an induced seismic response to development mining (a) and production mining (b). An arbitrary excavation is shown in white with a radius of 2.5 metres for drift scale (a) and 15 metres for stope scale (b). The area surrounding the excavation is shown in hot to cold colours, corresponding to likelihood of occurrence of induced seismicity. Colour selection is arbitrary and does not correspond to quantitative stress redistribution. An area of 10 metres has been added to the outer most limits of stress redistribution to account for microseismic monitoring limitations (in terms of seismic event location accuracy).

Induced seismic responses to mining occur in close temporal proximity to the stimulus (i.e. mine blast). Eremenko *et al.* (2009) concluded that the maximum quantity of seismic events within a response occurs in the first hour following mine blasting. A detailed study of sill pillar mining at Brunswick mine reported that in all observed cases, 50% to 100% of the stress change due to blasting occurred within the first minute of the blast - as shown in Figure 23 (Hudyma *et al.*, 1994). While continued stress change occurs for hours following the mine blast, the quantity of stress change is relatively insignificant and likely a reflection of the influence of local rock mass discontinuities - to which reference is made throughout the study.

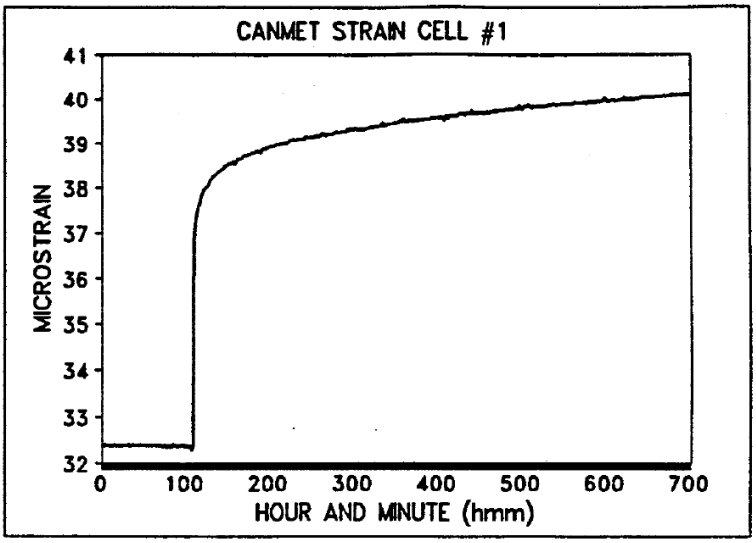

Figure 23: Response of a strain cell over time at Brunswick Mine. The mine blast (production stope) occurs just after 100 (hmm), and more than 50 metres from the strain cell location. More than 50% of the total strain change associated with the blast occurs within the first minute (Hudyma *et al.*, 1994).

Figure 24 is a Magnitude-Time History chart for a series of theoretical induced seismic responses to mining. Seismic events are plotted according to magnitude on the primary y-axis. The cumulative number of events is represented by a line corresponding to the secondary y-axis. Five days are shown, with a mine blast (denoted by a red star on the x-axis) occurring at 00:00:00h each day. Red vertical dashed lines highlight the series of seismic events induced by each mine blast. Each series of events occurs in close temporal proximity to the blast, generating distinct steps in the cumulative number of events line. The lack of seismic events occurring between steps results in distinct horizontal segments of the line between mine blasts. These trends are strong indicators of induced seismicity.

One of the defining characters of induced seismicity is proportional energy release to the inducing stimulus (McGarr and Simpson, 1997; McGarr *et al.*, 2002). Magnitude, shown on the primary y-axis of Figure 24, may be used as a proxy for radiated energy, with larger magnitude values corresponding to increased energy. Seismic events below local magnitude zero are considered relatively small, and unlikely to result in visible rock mass damage (Butler, 1997). Standard mine blasts, particularly development blasts (which constitute the vast majority of blasting in mines), are not expected to induce seismic events capable of producing visible rock mass damage. The largest seismic events shown in Figure 24 approach, but do not exceed, zero magnitude.

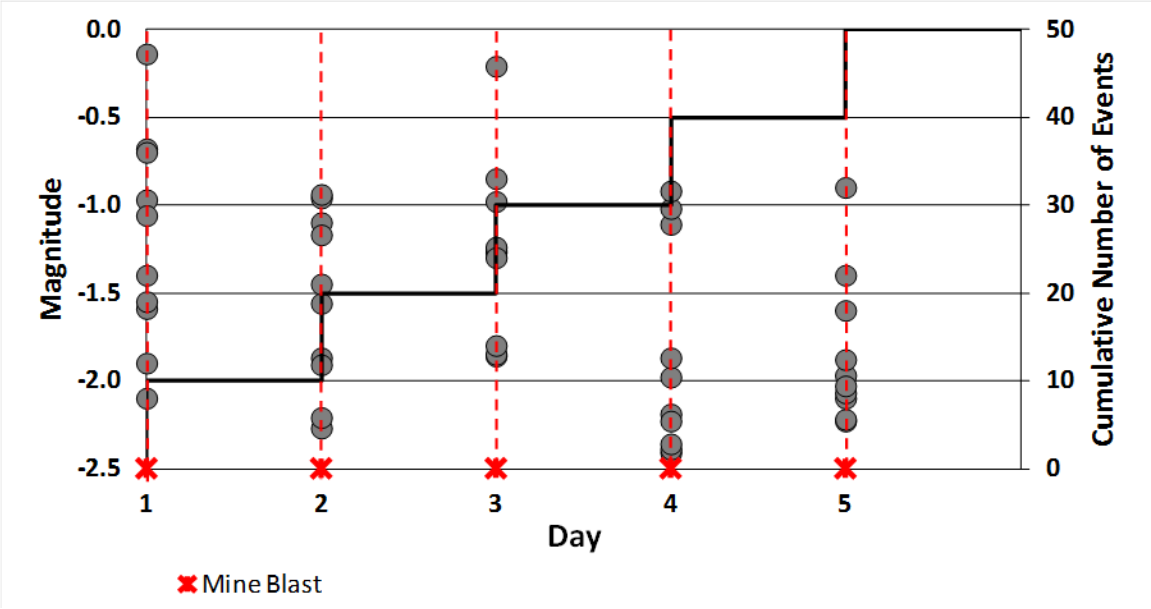

Figure 24: Theoretical Magnitude-Time History chart for a series of induced seismic responses to mining. Mine blasts are denoted by red stars along the x-axis.

Seismic responses occurring within complex real-world mining environments are not expected to behave as perfectly theoretical induced responses, but instead to exhibit the distinctive characteristics of induced seismicity. Figure 25 is a Magnitude-Time History chart of a primarily induced seismic population associated with development drift blasting at LaRonde mine (Brown, 2015). There are no disproportionately large and potentially damaging seismic events contained within the population. Mine blasts are shown along the x-axis and correspond well with steps in the cumulative number of events line. Periods of reduced seismic activity between successive development blasts, such as seen from approximately Feb 20 to Feb 25, indicate the overall event rate is strongly related to mine blasting.

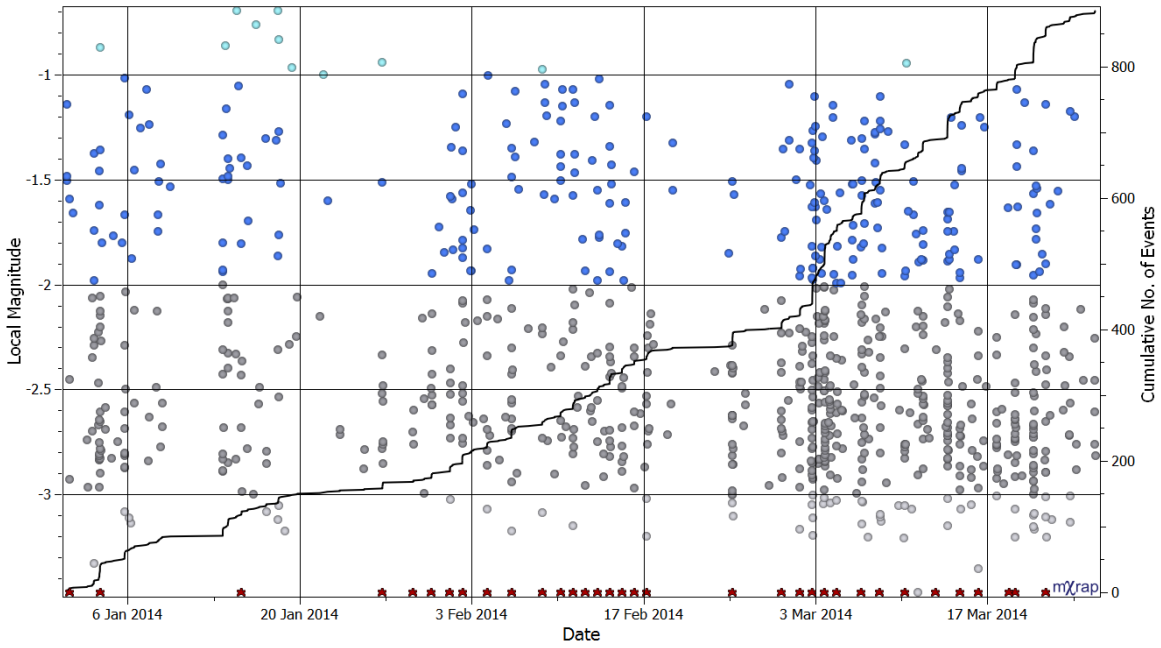

Figure 25: Magnitude-Time History chart for a population of primarily induced seismic events. Red icons along the x-axis represent development blasts, and event colours correspond to Local magnitude values (Brown, 2015).

3.2 Triggered Seismic Responses to Mining

Triggered seismic responses to mining occur spatially distant to the stimulus (i.e. mine blast). This type of rock mass failure is not directly driven by mining-induced stress change from the excavation of discrete mining voids, but rather larger scale mining failure processes occurring throughout the rock mass and tectonic loading (McGarr and Simpson, 1997; McGarr *et al.*, 2002). In Figure 21, triggered seismic responses to mining occur within a failing sill pillar between Level 7 and Level 8 (large scale failure process), and along a mine fault (tectonic loading). The triggered seismicity is significantly removed from the blast location (between Level 2 and Level 3), indicating the mining-induced stress change cannot be the exclusive driving factor of rock mass failure.

A maximum theoretical spatial limit of induced seismicity has been suggested in Section 3.1 as five times the excavation radius, plus a Location Error Factor, from the blast location. Beyond these spatial limits there is theoretically no mining-induced stress change, and consequently any seismicity occurring outside this area must be primarily driven by something other than the stress chance induced by the discrete mine blast. In Figure 21, the sill pillar is located four to five sublevels beyond the mine production blast. Assuming a sublevel spacing of 30 metres, and consequently production stope span of 30 metres, the sill pillar (and associated seismic response) occurs beyond the range of the discrete mining-induced stress change within 3 sublevels of the blast. This is indicative of triggered seismicity.

Triggered seismic responses to mining occur temporally independent of the stimulus (i.e. mine blast). Because triggered seismicity is not dependent on the mining-induced stress change from discrete mine blasts, there is little to no temporal influence from when that stress change occurs. In Figure 23, more than 50% of the total stress change occurred within the first minute of blasting, however incrementally smaller stress changes continue to occur for more than seven hours following the blast. This stress change is likely a reflection of the influence of larger scale rock mass failure processes, or local movement along geological features - triggered seismicity.

Figure 26 is a Magnitude-Time History chart for a series of theoretical triggered seismic responses to mining. Five days are shown, with a mine blast occurring at 00:00:00h each day - just as was shown for induced seismic responses in Figure 24. Red vertical dashed lines highlight when mine blasts occur, however there is no strong temporal trend of seismic events associated with blasting. Because triggered seismicity is largely temporally independent of mine blasting, the triggered seismic events occur at a constant rate over time. This is reflected in a smooth trend in the cumulative number of events line.

One of the defining characters of triggered seismicity is disproportional energy release to the stimulus (McGarr and Simpson, 1997; McGarr *et al.*, 2002). While this statement is commonly used to exclusively refer to large and potentially damaging seismic events, triggered seismicity occurs beyond the zone of discrete mining-induced stress change, and consequently any energy radiation (or size of event) is disproportional to the local stress change induced by the discrete mine blast. Steacy *et al.* (2005) indicate that triggering can occur at all scales, and hence triggered seismic events can be of any size. In Figure 26, a significant quantity of events with magnitudes greater than zero are present in the seismic response. These events are considered large, with the potential to produce visible rock mass damage (Butler, 1997), and are certainly disproportional to the stimulus.

Triggered seismic responses to mining are typically spatially disperse, relative to induced responses, and cover a larger area of the mining environment. This is particularly the case when triggered seismicity is primarily driven by larger scale rock mass failure processes, such as yielding pillars. Furthermore, triggered seismicity is temporally independent of blasting, allowing triggered responses to occur over extended time periods. Both of these conditions typically lead to an increased accumulation of individual seismic events within a single triggered seismic response (relative to an induced response).

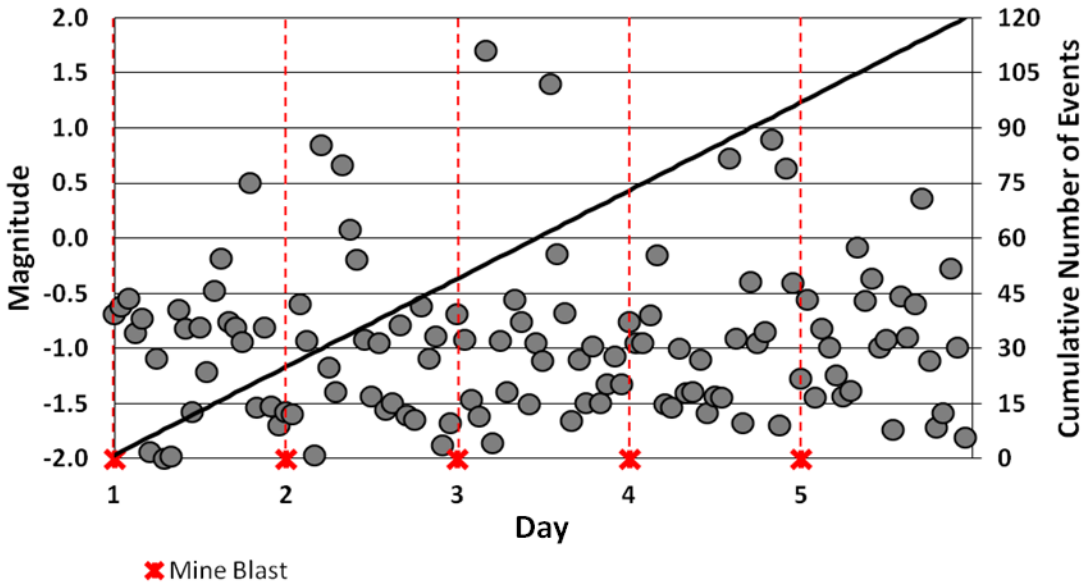

Figure 26: Theoretical Magnitude-Time History chart for a triggered seismic response to mining. Mine blasts are denoted by red stars along the x-axis.

Figure 27 is a Magnitude-Time History chart of a primarily triggered seismic population associated with a graphitic shear (Hudyma, 2008). Of particular interest is the significant quantity of disproportionately large ($M_L \geq 0$), and potentially damaging seismic events contained within the population - indicative of triggered seismicity. Over the 18 month time period shown, there are more than 100 mine blasts, all located in excess of 150 metres from the seismic event locations. Unlike the trends observed in the primarily induced response (shown in Figure 25), this population does not exhibit definitive steps in the cumulative number of events line. The relatively constant event rate over time of this seismic population suggests that the mine blasts generate only a triggered response on the shear.

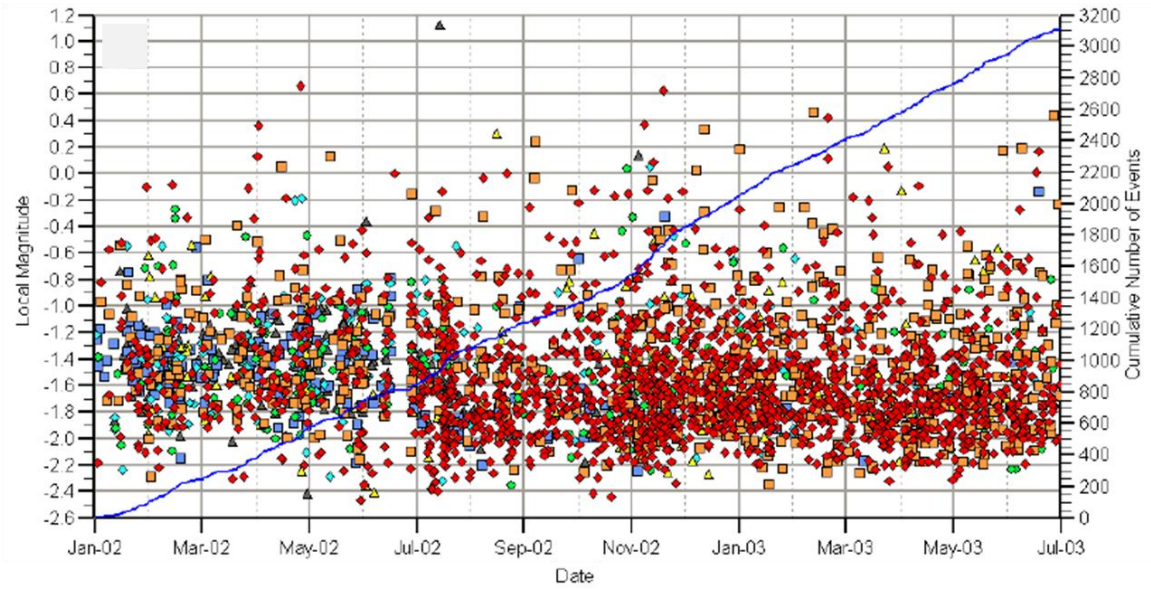

Figure 27: Magnitude-Time History chart for a seismic population associated with a graphitic shear. Events are not coloured according to magnitude (Hudyma, 2008).

3.3 Complex Seismic Responses to Mining

Complex seismic responses to mining occur when a stimulus is located sufficiently close to a geological feature, or ongoing rock mass failure process, that it experiences a significant mining-induced stress change. In Figure 21, the dyke and fault-dyke intersection are sufficiently close to the production blast that they are contained within 5 excavation radii. By this definition, the seismic response is induced. However, large seismic events, which are disproportional to the production blast-induced stress change experienced at that rock mass location, are contained within the response. By this definition the seismic response is triggered. When both of these conditions are true (induced and triggered), the seismic response is considered complex.

A further example is the strain cell measurements shown in Figure 23. Although the strain cell is located 50 metres from the mine blast, this is still within the limits of mining-induced stress change of a typical production stope (5 radii). As previously discussed, the mine blast induces a significant stress change within the first minute following the blast - induced seismicity. The subsequent stress change however, which occurs over many hours, is likely a reflection of larger scale rock mass failure processes or local movement along geological features - triggered seismicity. As this study surrounds a problematic sill pillar, with known geological features, it is likely that the majority of seismic responses in this area of Brunswick mine are complex (Hudyma *et al.*, 1994).

Because triggered seismic responses to mining are not driven by discrete mine blasts, their location remains relatively constant within the mining environment over time. In Figure 21 for example, when subsequent stopes are blasted, the location of the stimulus, and consequently

induced seismicity, will change. The location of the sill pillar, faults and dyke however will remain constant, and consequently, so will the location of triggered seismic responses to mining.

Figure 28 depicts three time periods during the development of a single mine drift. Within the mining environment shown, there is a single stationary dyke, and a mine excavation which is being developed over time. In part (a), the mine drift is approaching a dyke, but the blast location is sufficiently far that the seismic response to mining is considered as an independent induced response (outlined in blue) and an independent triggered response (outlined in red). As the mine drift is further developed, and the blast location approaches the dyke as shown in part (b), the two independent responses become sufficiently close (in space), that they are joined into a single complex response (outlined in purple). The seismicity associated with the dyke is now occurring within the mining-induced stress change zone. As the mine drift continues development however, and moves away from the dyke as shown in part (c), the induced and triggered components of the complex response become sufficiently spaced that they are again divided in to an individual induced and an individual triggered response - as was shown in part (a). This is similar to the observations of complex seismicity made by Delgado and Mercer (2006), discussed in Section 2.5.4.3.

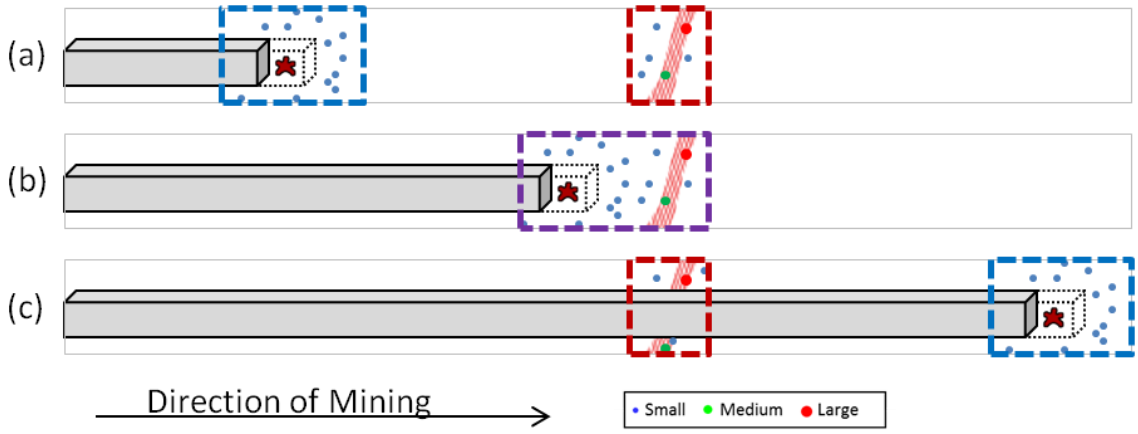

Figure 28: Diagrammatic illustration of variations in the seismic response to mining as the response stimulus (i.e. mine blast), migrates over time. Parts (a), (b) and (c) show successive migration of the mine blast, represented by a red star, over time. A geological feature, such as a dyke, is shown in pink. Induced, complex and triggered seismic responses are outlined in blue, purple and red respectively. Not to scale.

The fundamental characteristics of purely induced and purely triggered seismic responses to mining are constant, but the characteristics of an individual complex seismic response depend on the relative proportions of induced and triggered seismic events. Figure 29 is a theoretical Magnitude-Time History chart for a series of complex seismic responses to mining. Five days are shown, with a mine blast occurring at 00:00:00h each day - just as was shown for induced and triggered seismic responses in Figure 24 and Figure 26, respectively.

In Figure 29, both the characteristics of induced and triggered seismic responses to mining are present. Red vertical dashed lines highlight the series of seismic events induced by each mine

blast. Each series of events occurs in close temporal proximity to the blast, generating distinct steps in the cumulative number of events line. Unlike a purely induced response however, the cumulative number of events line is not stagnant between successive mine blasts. Instead, constant event rate line segments are observed between steps - indicative of triggered seismicity temporally independent of the mine blasts.

All seismic events directly associated with mine blasting in Figure 29 are below magnitude zero (induced seismicity). However, there is still a significant portion of large and potentially damaging seismic events contained within the seismic response (triggered seismicity). The quantity of induced events per blast is constant (equivalent to the series of induced seismic responses shown in Figure 24), however the addition of triggered seismicity between mine blasts increases the overall quantity of events in the seismic responses. For the example shown in Figure 29, the relative proportions of induced and triggered seismic events are equal, however the relative proportions are expected to vary significantly across true complex seismic responses to mining.

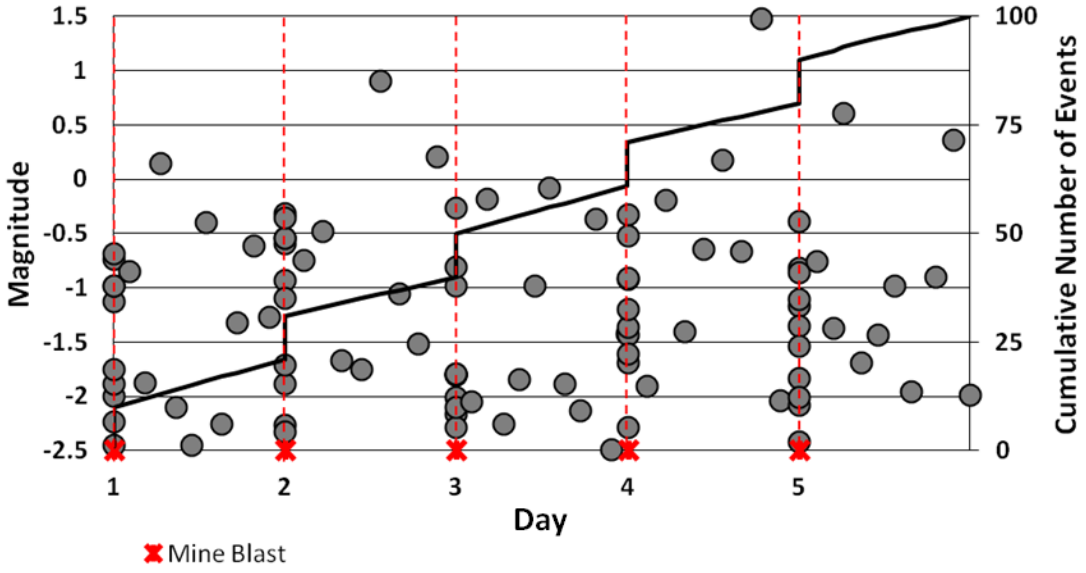

Figure 29: Theoretical Magnitude-Time History chart for a complex seismic response to mining. Mine blasts are denoted by red stars along the x-axis.

Figure 30 is a Magnitude-Time History chart for a seismic population described as representing "two different seismic source mechanisms within the same volume of ground" (Hudyma, 2008). Mine blasts are represented by red stars and black vertical dashed lines. Steps in the cumulative number of events lines indicate event rate increases associated with mine blasting, however, between blasts there are periods of significant seismic activity. This is most evident between blasts two and three, three and four, and six and seven. In Figure 30, increases in event rate directly following mine blasting are characteristic of induced seismicity, however, constant event rates temporally unrelated to mine blasting are characteristic of triggered seismicity. As this

population exhibits components of both induced and triggered seismic responses to mining, it is considered complex.

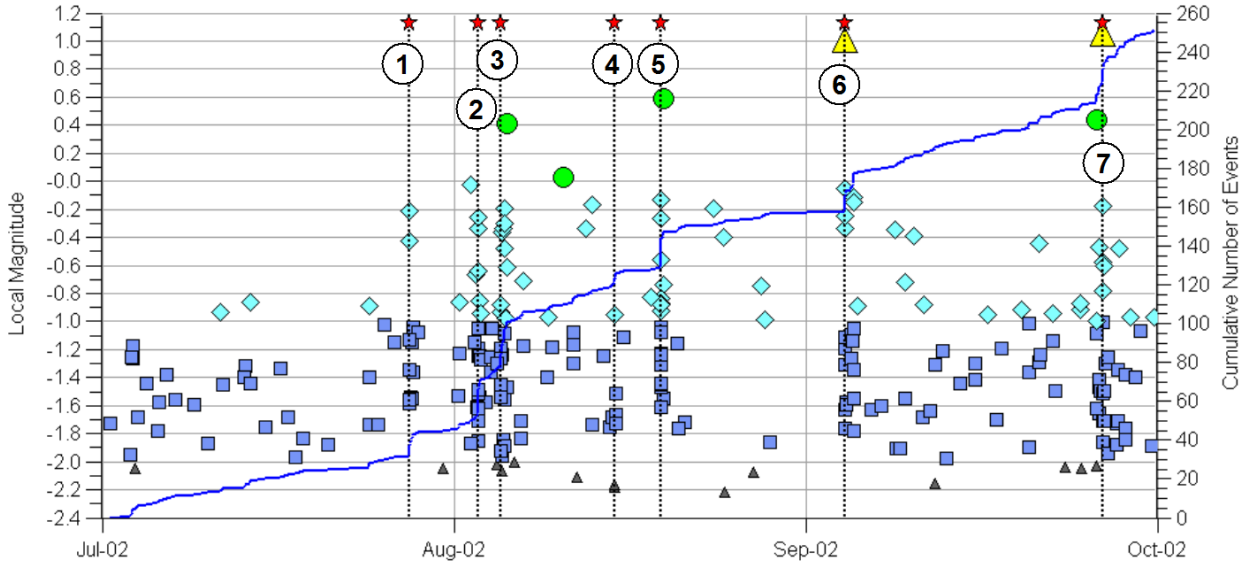

Figure 30: Magnitude-Time History chat for a single seismic population exhibiting two different seismic sources (Hudyma, 2008).

3.4 **Chapter Summary**

Within this chapter typical induced, triggered and complex seismic responses to mining have been characterized. This has been accomplished primarily through relating seismic responses to the stimulus, mine blasting, in space and time. Associated characteristics of Magnitude-Time History charts have been shown, and typical rock mass conditions leading to each type of seismic response have been described. Each of these is summarized in Table 4 for induced, complex and triggered seismic responses to mining.

Table 4: Summary table of properties and characteristics of induced, complex and triggered seismic responses to mining. Stimulus commonly refers to a mine blast.

	Induced	**Complex**	**Triggered**
Spatial Distribution	Close to Stimulus *Within 5 excavation radii (plus Location Error Factor)*	Close and Potentially Distant to Stimulus *Within 5 excavation radii (plus Location Error Factor), and potentially beyond*	Distant to Stimulus *Beyond 5 excavation radii (plus Location Error Factor)*
Temporal Distribution	Close to Stimulus *Typically within minute and up to a few hours*	Close and Independent of Stimulus *Strong response within minutes/hours and varying rates over time*	Independent of Stimulus *Varying rates over time (little to no relation to discrete mine blasts)*
Mag-Time History Chart Properties	Steps in the Cumulative Number of Events Proportional Energy - Small to Medium Magnitude Events Relatively Low Quantity of Events	Steps Separated by Periods of Relative Constant Rate in the Cumulative Number of Events Proportional and Disproportional Energy - Small to Large Magnitude Events Intermediate to High Quantity of Events	Relatively Constant Rate in the Cumulative Number of Events Disproportional Energy - Small to Large Magnitude Events Relatively High Quantity of Events
Rock Mass Properties	No Significant Geological Features	Significant Geological Features	Significant Geological Features

Chapter 4

4 Novel Seismic Response Parameters

As previously discussed in the literature review (Section 2.3), there are five independent seismic source parameters: time, location, seismic moment, radiated seismic energy and source size. Most of these parameters exclusively describe the conditions at a seismic source during point failure within a rock mass, and do little for describing the overall seismic response to mine blasting. As previously discussed in Chapter 3, radiated seismic energy can be used somewhat to differentiate between induced and triggered seismicity in terms of energy proportionality. For practical purposes however, the application of this concept using real mine seismic data can be vague and challenging.

Quantitatively determining the mining-induced stress change experienced in a specific location within a rock mass, at a specific time in a mining sequence, requires significant knowledge of local stress, rock mass conditions, and pre and post failure load deformation characteristics of the confined rock mass. This data is typically unknown or determined using significant assumptions. Furthermore, the calculation of radiated seismic energy for each individual seismic event comes with a degree of recording error. The error is dependent on a variety of factors, such as: seismic monitoring hardware (sensor) limitations, seismic energy radiation pattern, ray path obstructions, and assumptions within seismic wave processing software. Due to these intricacies, an alternative means of quantitatively distinguishing between variations in seismic responses to mining is desirable.

It has been shown in the literature review (Chapter 2) that seismic responses to mining can be characterized spatially and temporally with reference to a stimulus (i.e. mine blast). For these purposes, the seismic source parameters time and location are useful. Furthermore, significant error associated with using these parameters to quantitatively describe seismic responses to mining is unlikely. There is generally little to no error associated with seismic event time, as times are recorded using a GPS synch, and event location error is routinely quantified for individual events. Location error is also accounted for in the spatial expansion of the mining-induced stress change zone (as was shown in Figure 22).

This chapter introduces a set of novel Seismic Response Parameters (SRP's): Distance to Blast (DTB), Time After Blast (TAB), Distance to Centroid (DTC), and Time Between Events (TBE). Just as seismic source parameters describe a seismic source, Seismic Response Parameters (SRP's) describe a seismic response. The blast related SRP's, Distance To Blast and Time After Blast, use seismic event locations and times of occurrence to relate individual seismic responses to discrete stimuli (mine blasts). The response related SRP's, Distance to Centroid and Time Between Events, use seismic event locations and times of occurrence to relate individual events

within a seismic response to the response itself. Each of these concepts will be expanded on in subsequent sections of this chapter.

Individual SRP's are calculated for each seismic event contained within a seismic response. For each SRP, a normalized parameter can also be calculated. Normalized SRP's allow for easy comparison between seismic responses identified using methodology variations (e.g. varying single-link clustering d-values or space-time windows).

Normalized parameters, denoted by a subscript 'N' (X_N), are calculated from SRP's using site-specific considerations. The parameters range from zero to one (inclusive), and indicate how close a seismic event or response is to a theoretically perfect induced or triggered event or response. A theoretically perfect induced seismic response ($X_N = 0$) corresponds to the perfect definition of induced seismicity, where all events occur at the same point in space and time as the mine blast. A theoretically perfect triggered seismic response ($X_N = 1$) corresponds to the perfect definition of triggered seismicity, where all events occur beyond the discrete mining induced stress change zone and temporally independent of the blast.

4.1 Example Seismic Responses to Mining

A set of three seismic responses to mining (one induced, one triggered and one complex), are used throughout this chapter to introduce each Seismic Response Parameter (SRP). These responses are typical examples from the LaRonde mine case study presented in Chapters 6 and 7. Selection of variables used in response identification, such a temporal windows and inter-clustering distances, are discussed in detail in Section 6.3.

A typical induced seismic response to mining, identified using a single-link clustering d-value of 20 metres (see Section 2.5.3.2 for details on d-value), is shown spatially in Figure 31. The mine blast associated with the seismic response is a development blast with an excavation radius of approximately 2.5 metres. The response is relatively tightly clustered in space, with all events occurring within 11 metres of the mine blast location (shown as a red star).

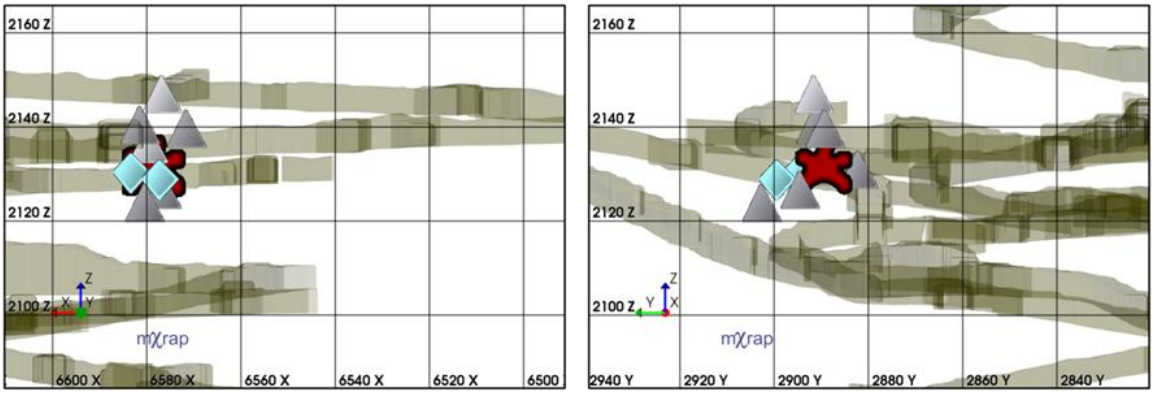

Figure 31: Longitudinal and cross-sectional projections of LaRonde mine showing an induced seismic response to mining. The inducing mine blast is shown as a red star.

The Magnitude-Time History chart shown in Figure 32, is a temporal representation of the induced seismic response to mining (shown spatially in Figure 31). The temporal window used for identifying the seismic response is 12 hours between successive mine blasts. All seismic events contained within the response are below magnitude zero, and occur within the first two hours of the blast. This seismic response exhibits a strong spatial and temporal dependency on the discrete mine blast - strongly indicative of induced seismicity.

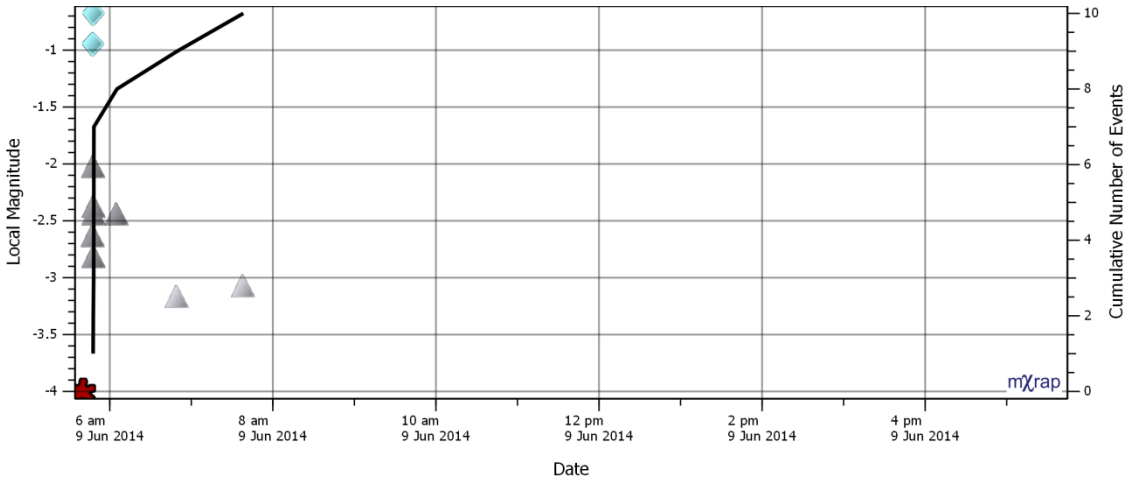

Figure 32:Magnitude-Time History chart for an induced seismic response to mining at LaRonde mine. The inducing mine blast is shown as a red star.

A typical triggered seismic response to mining, identified using a single-link clustering d-value of 100 metres, is shown spatially in Figure 33. The triggered response is visually distinct from the induced seismic response to mining previously shown in Figure 31. The mine blast associated with the seismic responses is a production blast with an excavation radius of approxamet15 metres. The events occur remote to the mine blast, with a significant distance between the blast location (red star) and response centroid (red square). The response is not tightly clustered in space, with significant distance between adjacent events.

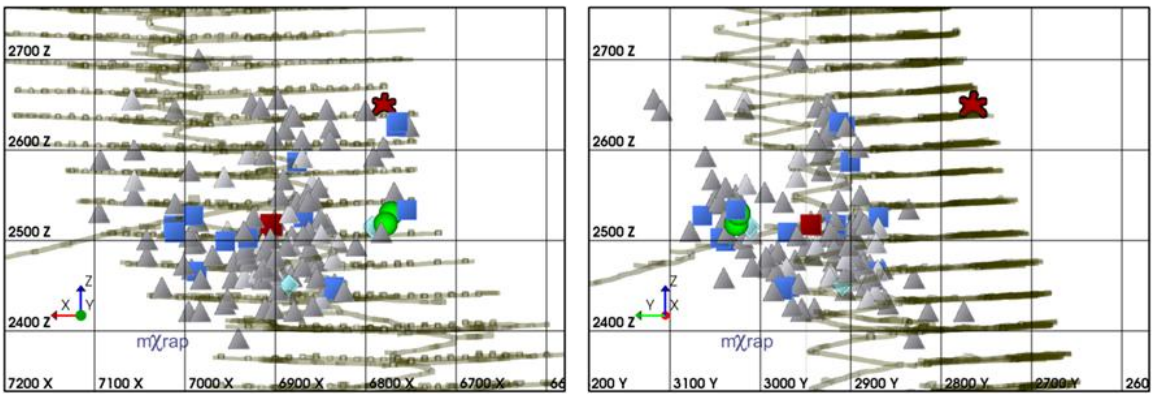

Figure 33: Longitudinal and cross-sectional projections of LaRonde mine showing a triggered seismic response to mining. The triggering mine blast and seismic response centroid are shown as a red star and red square, respectively.

The Magnitude-Time History chart shown in Figure 34, is a temporal representation of the triggered seismic response to mining (shown spatially in Figure 33). The temporal window used for identifying the seismic response is 12 hours between successive mine blasts. Seismic events occur at a relatively constant rate throughout the 12 hour time period; reflected in the relatively constant slope of the cumulative number of events line. Two events within the seismic response are large and potentially damaging (Local Magnitude ≥ 0 or Richter Magnitude ≥ 1). The energy of these events is significantly disproportionate, particularly considering the relative distance of the large seismic events to the stress change zone induced by the mine blast, indicating the likely presence of a triggered source mechanism. This seismic response exhibits no strong spatial or temporal dependency on the mine blast - strongly indicative of triggered seismicity.

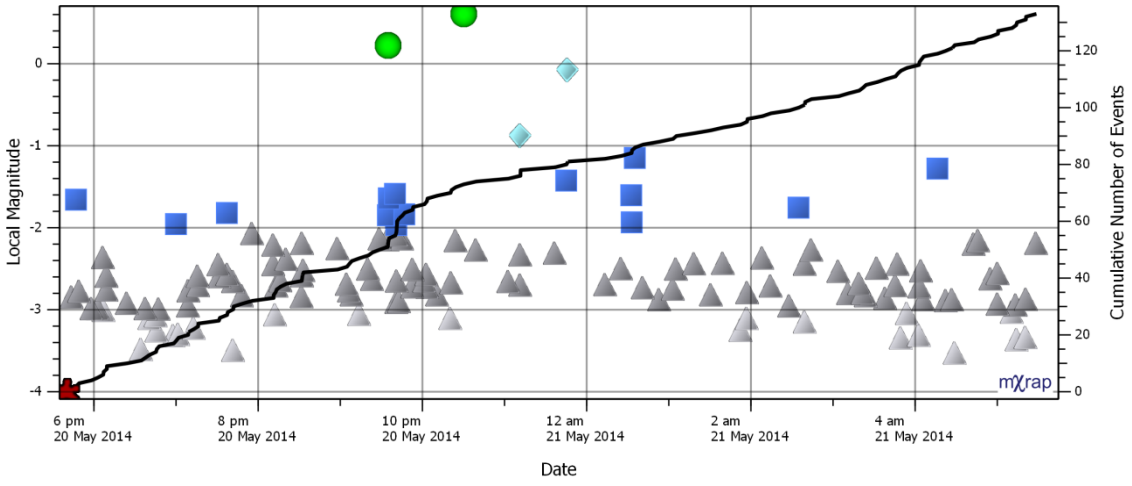

Figure 34: Magnitude-Time History chart for a triggered seismic response to mining at LaRonde mine. The triggering mine blast is shown as a red star.

A typical complex seismic response to mining, identified using a single-link clustering d-value of 20 metres, is shown spatially in Figure 35. The mine blast associated with the seismic response is a development blast with an excavation radius of approximately 2.5 metres. All events occur within 50 metres of the mine blast location (shown as a red star), with more than 80% of events

occurring within 11 metres of the mine blast (the spatial extent of the induced response shown in Figure 31). The response itself is relatively tightly clustered in space, exhibiting a slight wrap-around effect in proximity to voids/excavations, where the redistributed stress is likely concentrating.

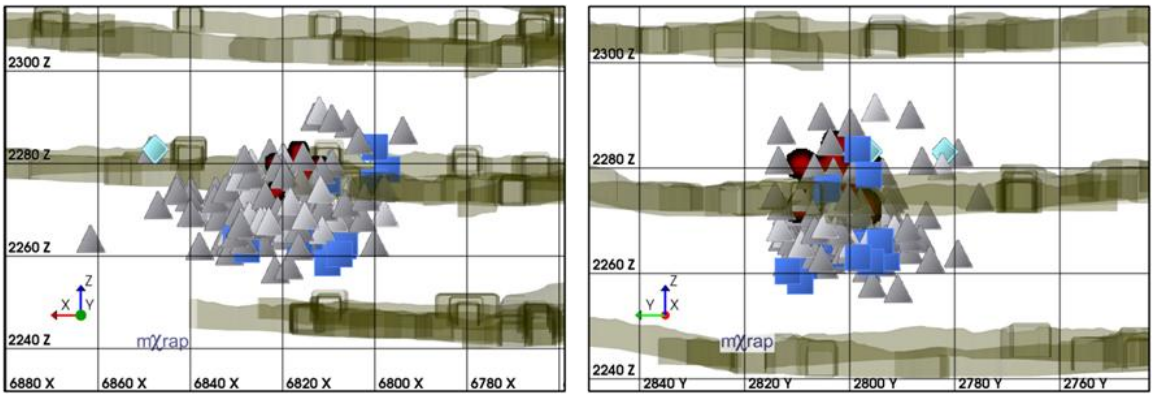

Figure 35: Longitudinal and cross-sectional projections of LaRonde mine showing a complex seismic response to mining. The initiating mine blast is shown as a red star.

The Magnitude-Time History chart shown in Figure 36, is a temporal representation of the complex seismic response to mining (shown spatially in Figure 35). The temporal window used for identifying the seismic response is 12 hours between successive mine blasts. Seismic events occur throughout the 12 hour time period, however the vast majority of events occur within the first few hours of mine blasting. All seismic events contained within the response are below magnitude zero, however events are located beyond the assumed mining-induced stress change zone of the blast (22.5 metres). These events represent disproportional energy release and likely the presence of a triggered source mechanism in the local rock mass. The largest magnitude seismic event (M_L > -0.5), occurs more than 6 hours following the mine blast; exhibiting a significant temporal delay relative to the strong and immediate induced seismicity (within two hours of the mine blast). This seismic response exhibits a strong spatial and temporal dependency on the mine blast (indicative of induced seismicity), however the response also contains seismic events that are spatially and temporally distant to the blast (indicative of triggered seismicity). This seismic response to mining is complex, and is considered predominantly induced due to the increased ratio of induced to triggered seismic events.

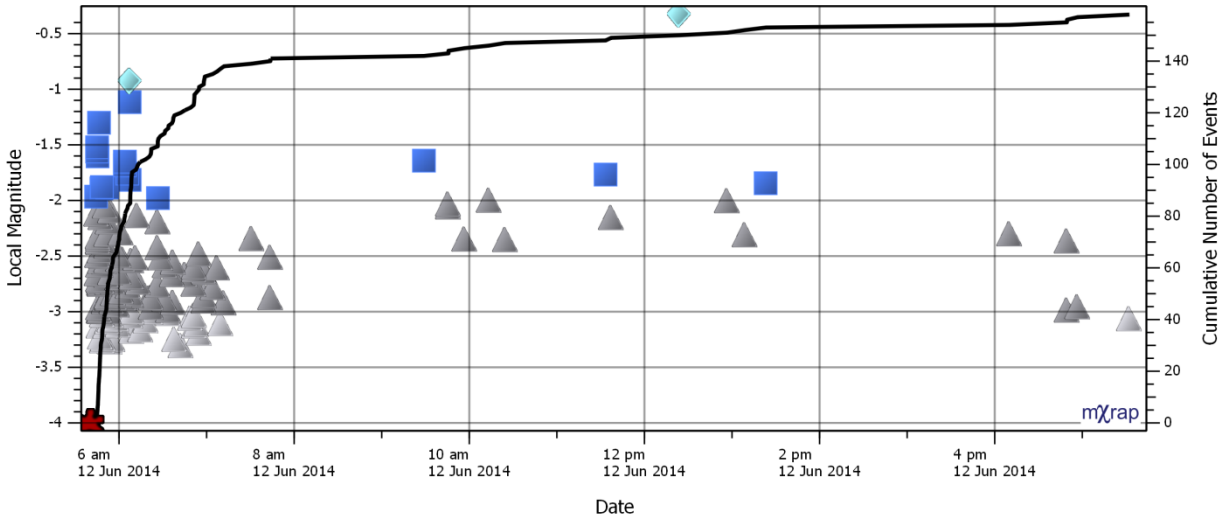

Figure 36: Magnitude-Time History chart for a complex seismic response to mining at LaRonde mine. The initiating mine blast is shown as a red star.

Each of the example seismic responses to mining described in this section will be used to demonstrate Seismic Response Parameters (SRP's). As SRP's describe the space-time relation between responses and stimuli, as well as responses and themselves, they should exhibit varying degrees of separation between induced, triggered and complex seismic responses to mining.

4.2 Distance to Blast [DTB]

Distance To Blast (DTB) is defined as the spatial distance between a seismic event and the inducing stimulus. From the examples in the previous section, it would appear that the distance between a blast and a seismic response is a possible indicator of an induced, triggered or complex response. As discussed in the literature review (Section 2.5.2), Eremenko *et al.* (2009) concluded there was a strong relation between induced seismicity and close spatial proximity to mine blasting. Distance to Blast is calculated for an individual seismic event as:

$$DTB(d,r) = \begin{cases} d - r, & d \geq r \\ 0, & d < r \end{cases} \tag{6}$$

where,

DTB = Distance to Blast (m)

r = Excavation Radius (m)

d = Distance from Seismic Event to Blast Location (m), calculated as:

$$d = \sqrt{(E_x - B_x)^2 + (E_y - B_y)^2 + (E_z - B_z)^2} \tag{7}$$

where,

$E(x, y, z)$ = Seismic Event Location (x,y,z)

$B(x, y, z)$ = Blast Location (x,y,z), Center of 3D Blasted Volume

Distance To Blast, as shown in Equation (6), uses a point location to represent a 3D blasted volume. This point location is commonly taken as the center of the blasted volume, and therefore does not account for the void space between the center and the excavation boundary, as shown in Figure 37. In order to calculate a distance from the event to the actual excavation boundary, an excavation radius must be subtracted from the standard equation for distance between two points (shown as Equation (7)). In cases where a seismic event is located within the blasted volume, DTB will be negative, and is taken as zero - as shown in Equation (6).

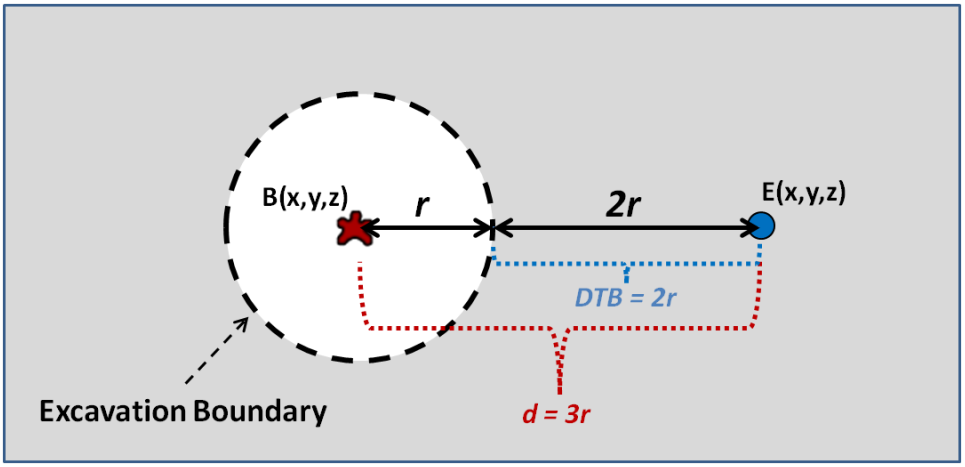

Figure 37: Diagrammatic sketch of DTB for an arbitrary blast (single point location) and an arbitrary seismic event (single point location). The excavation radius is shown as 'r'. The calculated distance between two points is shown as 'd'. In order to account for the void between the blast location and the excavation boundary, a single excavation radius is subtracted from 'd' in the calculation of DTB.

Table 5 summarizes the observation guidelines surrounding DTB for induced, complex and triggered seismic responses to mining. Induced and complex responses are discussed in relation to development mining, excavation radius of approximately 2.5 m, as the example induced and complex seismic responses referred to throughout this chapter occur in response to mine development blasting. A triggered response is discussed in relation to production mining, excavation radius of approximately 15 m, as the example triggered seismic response referred to throughout this chapter occurs in response to mine production blasting.

Table 5: Summary of observation guidelines surrounding Distance to Blast (DTB) for induced, complex and triggered seismic responses to mining. The Location Error Factor used throughout this work is 10 metres.

	Induced	Complex	Triggered
Distance To Blast [DTB]	Within 5 excavation radii (plus Location Error Factor) *Excavation Radius 2.5 m: DTB < 22.5 m*	Within 5 excavation radii (plus Location Error Factor) and potentially beyond *Excavation Radius 2.5 m: Commonly, DTB < 22.5 m*	Beyond 5 excavation radii (plus Location Error Factor) *Excavation Radius 15 m: DTB > 85 m*

To characterize an entire seismic response to mining with a single value, the median response parameter is suggested. The use of median values is common in mine seismicity (e.g. Kgarume *et al.* 2010), as it significantly reduces the impact of any anomalous outliers - a frequent occurrence in mine seismic populations. Median values will be denoted as ' $\tilde{x}$ ' throughout this thesis.

Figure 38 depicts cumulative distributions of DTB for the set of seismic responses at LaRonde mine previously discussed (Section 4.1). The entire induced response ($\widetilde{DTB}$ = 5.9 m), occurs within 11 metres of the associated mine blast. The entire complex response ($\widetilde{DTB}$ = 13.4 m), occurs within 50 metres of the associated mine blast. The entire triggered response ($\widetilde{DTB}$ = 276 m), occurs between 100 and 400 metres of the closest mine blast location. These observations match the expected observation guidelines, as proposed in Table 5.

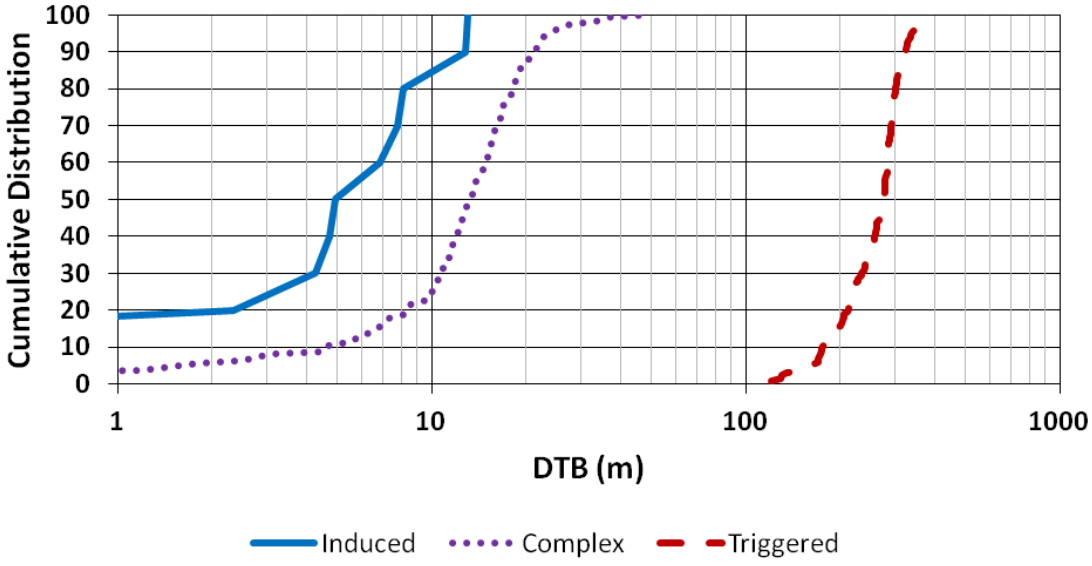

Figure 38: Cumulative distributions of Distance to Blast (DTB) in meters for an induced, complex and triggered seismic response to mining initiated by a typical mine blast (excavation radius of approximately 2.5 metres for induced and complex responses, and approximately 15 metres for the triggered response). More information regarding the individual seismic responses to mining can be found in Section 4.1.

To interpret DTB values in a more meaningful way, additional information regarding the newly blasted excavation, such as the excavation radius, is required. In the absence of this information, it is unknown if the seismic response occurs within or beyond the assumed mining-induced stress change zone of the blast. This distinction is critical to differentiating between induced, complex and triggered seismic responses to mining.

4.2.1 Normalized Distance To Blast [DTB_N]

The DTB value for a theoretically perfect induced seismic response to mining is zero, as all events occur within the blasted volume. The DTB value for a theoretically perfect triggered seismic response is greater than five excavation radii (plus a Location Error Factor), as all seismic events occur beyond the assumed mining-induced stress change zone. Knowledge of the theoretical bounds for this parameter enables DTB values to be normalized as Normalized Distance To Blast (DTB_N) values. DTB_N is calculated for an individual seismic event as:

$$DTB_N(DTB, r, E_L) = \begin{cases} \dfrac{DTB}{(5r + E_L)}, & DTB \leq (5r + E_L) \\ 1, & DTB > (5r + E_L) \end{cases} \quad (8)$$

where,

DTB_N = Normalized Distance To Blast

DTB = Distance to Blast (m)

r = Excavation Radius (m)

E_L = Location Error Factor (m)

The closer an event occurs to the blast location (approaching a DTB_N value of zero), the more likely it is to be induced. Any seismic event with a DTB_N value greater than one must have occurred beyond the assumed spatial limits of the discrete mining-induced stress change, and is taken as one - most likely triggered. Table 6 summarizes the observation guidelines surrounding DTB_N for induced, complex and triggered seismic responses to mining.

Table 6: Summary of observation guidelines surrounding Normalized Distance To Blast (DTB_N) for induced, complex and triggered seismic responses to mining. The assumed mining-induced stress change zone used throughout this work is 5 excavation radii plus an Error Location Factor of 10 metres.

	Induced	**Complex**	**Triggered**
Normalized Distance To Blast [DTB_N]	Within the assumed mining-induced stress change zone *All Events:* $DTB_N < 1$	Within the assumed mining-induced stress change zone and potentially beyond *Significant No. Events:* $DTB_N < 1$ *&* *All Events:* $0 \leq DTB_N \leq 1$	Beyond the assumed mining-induced stress change zone *All Events:* $DTB_N = 1$

Figure 39 depicts cumulative distributions of DTB_N for the same set of seismic responses to mining shown in Figure 38. With the response parameters normalized, cumulative distributions for individual seismic responses are more meaningful, and can be interpreted without a need for additional information. The entire induced response ($\widetilde{DTB_N} = 0.26$), and the vast majority of the complex response ($\widetilde{DTB_N} = 0.60$), exhibit DTB_N values less than one (indicating they are contained within the assumed mining-induced stress change zone of the blast). The entire triggered response ($\widetilde{DTB_N} = 1$), occurs beyond the mining-induced stress change zone of the blast, and consequently every event within the response has a DTB_N value of 1. These observations match the expected observation guidelines, as proposed in Table 6.

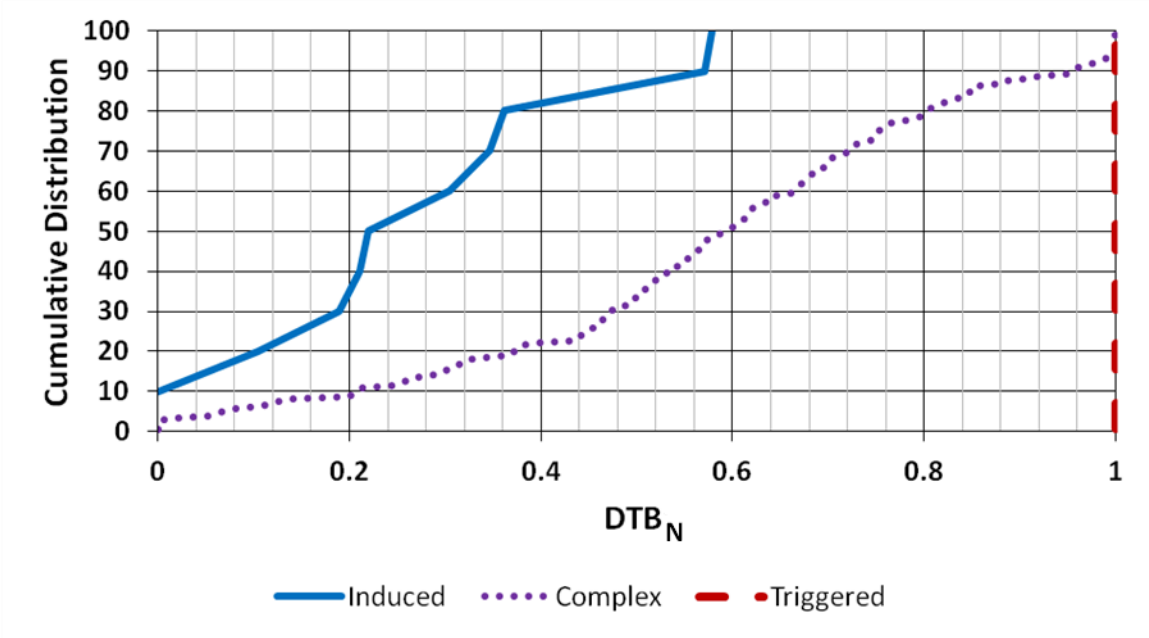

Figure 39: Cumulative distributions of Normalized Distance To Blast (DTB_N) for an induced, complex and triggered seismic response to mining. More information regarding the individual seismic responses to mining can be found in Section 4.1.

4.3 Time After Blast [TAB]

Proximity of event times to regular mine blasts can provide insight into the mechanisms driving rock mass failure (Cook, 1976). Eremenko *et al.* (2009) suggest there is value in quantifying the temporal relation between mine seismicity and blasting. As discussed in the literature review (Section 2.5.2), the largest number of induced seismic events typically occur within the first hour of mine blasting. Time After Blast (TAB) is defined as the temporal variation between a seismic event and the inducing stimulus - expressed in this work as hours (h). It is calculated for an individual seismic event as:

$$TAB = E_t - B_t \tag{9}$$

where,

TAB = Time After Blast (h)

E_t = Seismic Event Time (h)

B_t = Blast Time (h)

Table 7 summarizes the observation guidelines surrounding TAB for induced, complex and triggered seismic responses to mining.

Table 7: Summary of observation guidelines surrounding Time After Blast (TAB) for induced, complex and triggered seismic responses to mining. Maximum refers to the most distant time from the mine blast that is still contained within the temporal window used to identify the seismic response to mining.

	Induced	Complex	Triggered
Time After Blast [TAB]	Within the first few hours of mine blasting All Events: *TAB < 1-3 h*	Significant number of events within the first few hours of mine blasting and events independent of mine blasting *Significant No. Events:* *TAB < 1-3 h* *&* All Events: *0 h ≤ TAB ≤ Maximum*	Independent of mine blasting All Events: *0 h ≤ TAB ≤ Maximum*

Figure 40 depicts cumulative distributions of TAB for the set of seismic responses at LaRonde mine previously discussed (Section 4.1). The entire induced response ($\widetilde{TAB}$ = 0.14 h), occurs within 2 hours of the mine blast. The complex response ($\widetilde{TAB}$ = 0.4 h), occurs over the entire time window, with approximately 90% of the entire response occurring within the first 2 hours of the mine blast. The triggered response ($\widetilde{TAB}$ = 4.4 h), occurs at a relatively constant rate over time, with only 20% of the response occurring within the first two hours of the mine blast. These observations match the expected observation guidelines, as proposed in Table 7.

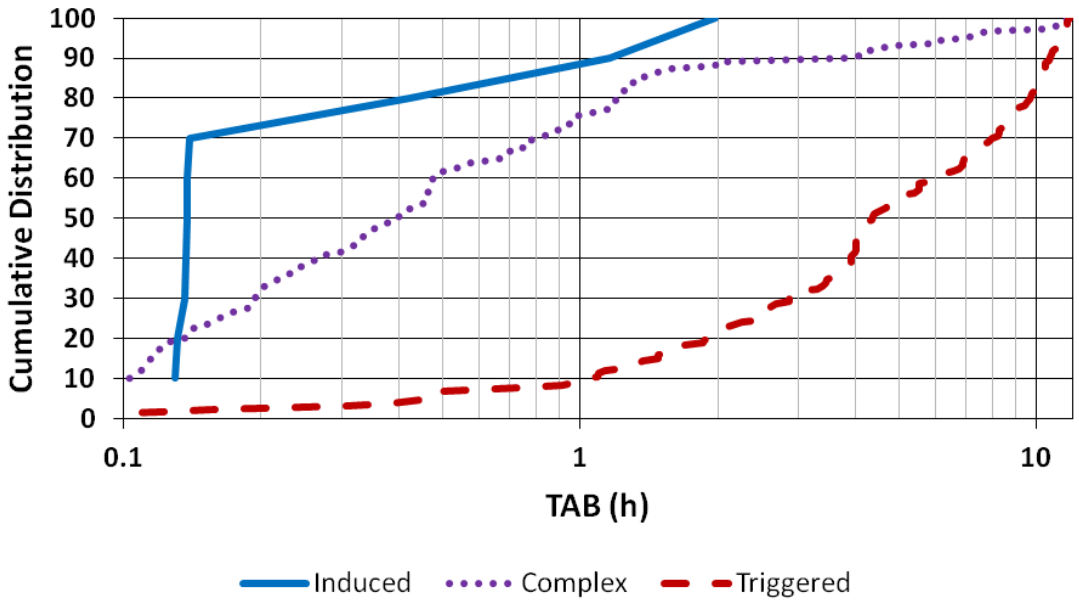

Figure 40: Cumulative distributions of Time After Blast (TAB) in hours for an induced, complex and triggered seismic response to mining. More information regarding the individual seismic responses to mining can be found in Section 4.1.

To interpret TAB values in a more meaningful way, additional information regarding how the seismic response was identified in time, such as the limits of the temporal formation window, are required. In the absence of this information, it is unknown if there is an extended time period with no seismic activity beyond the TAB values shown, or if the seismic response may be inadequately represented due to an insufficient response identification time window.

4.3.1 Normalized Time After Blast [TAB_N]

The TAB value for a theoretically perfect induced seismic response to mining is zero, as all events occur the instant after the mine blast. Seismic events within a theoretically perfect triggered response occur at a constant temporal rate, independent of mine blasting, and consequently the TAB values can be any value between zero and the end of the response identification time window. Knowledge of the theoretical bounds for this parameter enables TAB values to be normalized as Normalized Time After Blast (TAB_N) values. TAB_N is calculated for an individual seismic event as:

$$TAB_N(TAB, S_n, t_{max}) = \begin{cases} \dfrac{TAB}{(S_n)(t_{max})}, & TAB \leq (S_n)(t_{max}) \\ 1, & TAB > (S_n)(t_{max}) \end{cases} \quad (10)$$

where,

TAB_N = Normalized Time After Blast

TAB = Time After Blast (h)

t_{max} = Maximum Limit of the Response Identification Time Window (h)

S_n = Response Sequence Factor, calculated as:

$$S_n = \frac{n_x}{n} \quad (11)$$

where,

S_n = Response Sequence Factor

n_x = The Event Number (Sequential Order)

n = Number of Events in Seismic Response

Triggered seismic responses to mining occur independent of mine blasting, and consequently, there will likely be some triggered seismic events with small TAB_N values. The critical distinction between triggered and induced seismic responses for TAB_N however, is that all TAB_N values for induced seismicity should be relatively small (approaching zero and typically less than 0.2). Table 8 summarizes the observation guidelines surrounding TAB_N for induced, complex and triggered seismic responses to mining.

Table 8: Summary of observation guidelines surrounding Normalized Time After Blast (TAB_N) for induced, complex and triggered seismic responses to mining.

	Induced	**Complex**	**Triggered**
Normalized Time After Blast [TAB_N]	Within the first few hours of mine blasting *Significant No. Events:* $TAB_N \approx 0$ *Typically,* $TAB_N \leq 0.2$	Significant number of events within the first few hours of mine blasting and events independent of mine blasting *Significant No. Events:* $0 \leq TAB_N \leq 0.2$ & *All Events:* $0 \leq TAB_N \leq 1$	Independent of mine blasting *Significant No. Events:* $TAB_N \geq 0.5$ & *All Events:* $0 \leq TAB_N \leq 1$

Figure 41 depicts cumulative distributions of TAB_N for the same set of seismic responses to mining shown in Figure 40. The majority of events within the induced and complex responses occur within minutes of the blast ($\widetilde{TAB}_N$ = 0.04 and $\widetilde{TAB}_N$= 0.07, respectively). However, the complex response exhibits occasional seismicity throughout the time window; this is a key distinction between induced and complex seismic responses to mining. The triggered response is fundamentally different from the induced and complex responses, with a significant distribution offset, and a considerably larger median value ($\widetilde{TAB}_N$= 0.84). These observations match the expected observation guidelines, as proposed in Table 8.

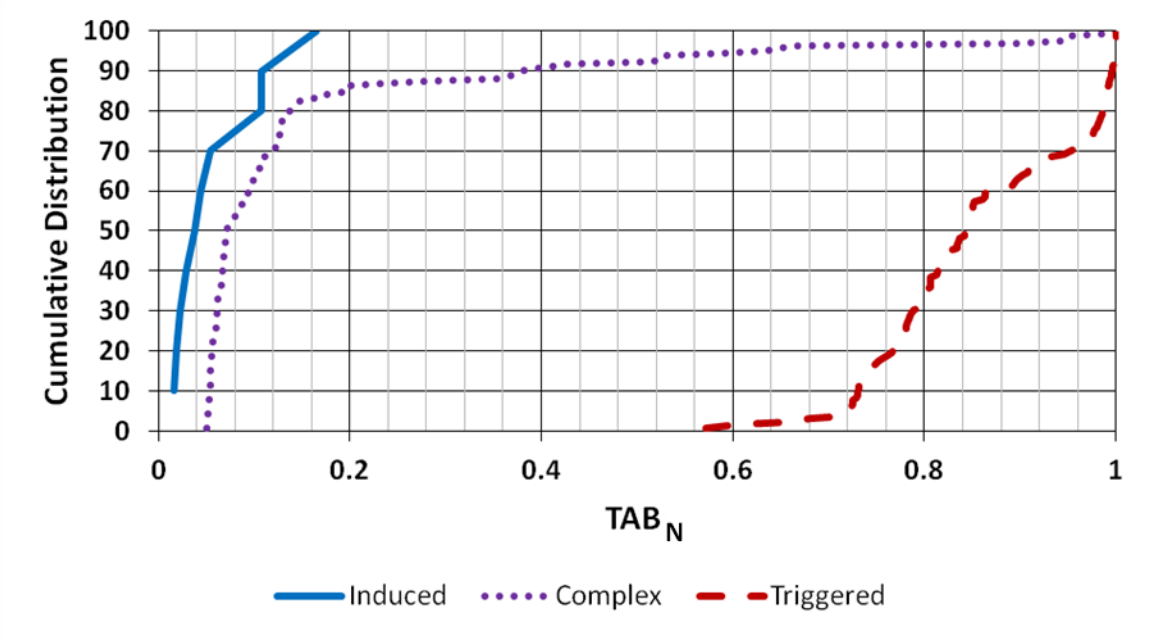

Figure 41: Cumulative distributions of Normalized Time After Blast (TAB_N) for an induced, complex and triggered seismic response to mining. More information regarding the individual seismic responses to mining can be found in Section 4.1.

4.4 Distance to Centroid [DTC]

The DTB/DTB_N and TAB/TAB_N Seismic Response Parameters relate a seismic response to a discrete mine blast (stimulus). A seismic response can be further characterized in space and time by how individual events within the response relate to the response itself. For the three dimensional cloud of events referred to as a seismic response, a centroid is used to represent the average spatial position of all points, as shown in Equation 12:

$$Centroid\ (x,y,z) = \left(\frac{x_1 + x_2 + \ ... + \ x_n}{n}, \frac{y_1 + y_2 + \ ... + \ y_n}{n}, \frac{z_1 + z_2 + \ ... + \ z_n}{n}\right) \qquad (12)$$

where,

(x_n, y_n, z_n) = Seismic Event Location 'n' (x,y,z)

n = Number of Events in Seismic Response

Woodward (2015) suggests seismic responses resulting from different source mechanisms (throughout a mining environment), may exhibit variations in spatial concentration. This is observed by Baig *et al.* (2017), who employ a diffusion index to quantitatively describe the dispersion of seismicity in a reservoir. The authors describe observing seismic clusters with different measures of spatial and temporal diffusion, and conclude it is likely due to variations in failure mechanism.

These observations suggest the relative density of a seismic response in space may be indicative of variations in seismic source mechanism. Distance to Centroid (DTC) is defined as the spatial distance between an individual seismic event, within a response, and the seismic response centroid; quantifying the relative spatial concentration of a seismic response. DTC is calculated for an individual seismic event as:

$$DTC = d \tag{13}$$

where,

DTC = Distance To Centroid (m)

d = Distance from Seismic Event to Response Centroid (m), calculated as:

$$d = \sqrt{(E_x - C_x)^2 + (E_y - C_y)^2 + (E_z - C_z)^2} \tag{14}$$

where,

E(x, y, z) = Seismic Event Location (x,y,z)

C(x, y, z) = Centroid Location (x,y,z), Equation (12)

Due to the variable complexities of underground hard rock mining environments (such as significant volumes of yielded rock mass), mining-induced stress redistribution from discrete mine blasts may be shed significantly beyond an excavation boundary. An example of stress shedding is shown by Ecobichon *et al.* (1992), in Figure 42. In part (a), a dense cluster of seismic events is circled, assumedly related to the mining-induced stress change from a production blast (shown as a shaded zone). A few weeks later, shown in part (b), the subsequent production stope is blasted, but the adjacent rock mass area is aseismic. Presumably, the rock mass volume circled had already failed at the time of the second production blast (b), and the mining-induced stress change is shed further from the excavation boundary.

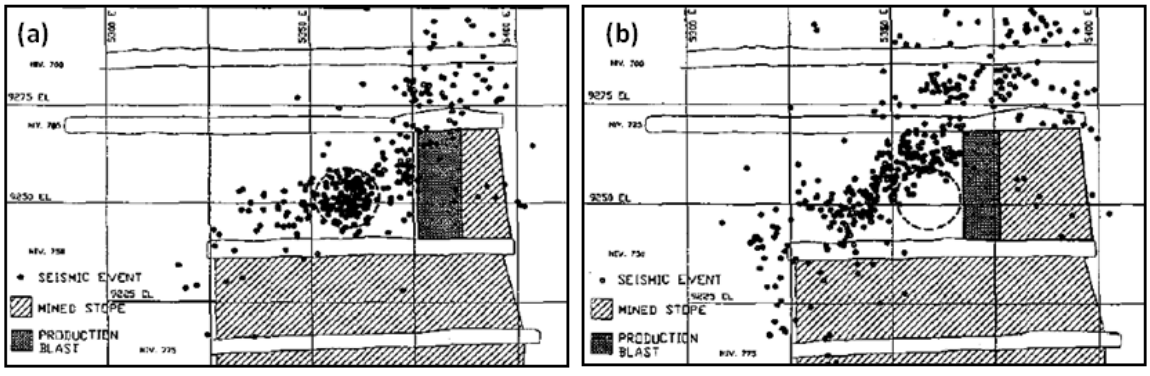

Figure 42: The location of seismic events over a period of a few weeks, spanning (a) to (b). Part (a) shows a strong concentration of events (circled). A few weeks later (and following a production blast), the circled area is aseismic (Ecobichon *et al.*, 1992).

The primary objective of DTC is to provide a measure of spatial clustering for the response, independent of the inducing stimulus (i.e. mine blast). In instances of stress shedding, induced seismic responses are still expected to be clustered within five excavation radii, but the origin measuring point is moved from the blast location to the seismic response centroid. As such, the observation guidelines from DTB (Table 5) are equivalent to those for DTC. Table 9 summarizes the observation guidelines surrounding DTC for induced, complex and triggered seismic responses to mining.

Table 9: Summary of observation guidelines surrounding Distance to Centroid (DTC) for induced, complex and triggered seismic responses to mining. The Location Error Factor used throughout this work is 10 metres.

	Induced	**Complex**	**Triggered**
Distance to Centroid [DTC]	Within 5 excavation radii (plus Location Error Factor) *Excavation Radius 2.5 m: DTC < 22.5 m*	Within 5 excavation radii (plus Location Error Factor) and potentially beyond *Excavation Radius 2.5 m: Commonly, DTC < 22.5 m*	Beyond 5 excavation radii (plus Location Error Factor) *Excavation Radius 15 m: DTC > 85 m*

Figure 43 depicts cumulative distributions of DTC for the set of seismic responses at LaRonde mine previously discussed (Section 4.1). The entire induced response ($\widetilde{DTC}$ = 8.1 m), occurs within 15 metres of the response centroid - indicating it is relatively tightly clustered in space. The majority of the complex response ($\widetilde{DTC}$ = 12 m), occurs within 20 meters of the response centroid, however some events are located beyond. DTC values for the triggered seismic response are much larger, ranging from approximately 20 to 200 meters. With a median value of approximately 100 metres ($\widetilde{DTC}$ = 99 m), the triggered response is significantly diffuse relative to the induced and complex seismic responses. These observations match the expected observation guidelines, as proposed in Table 9.

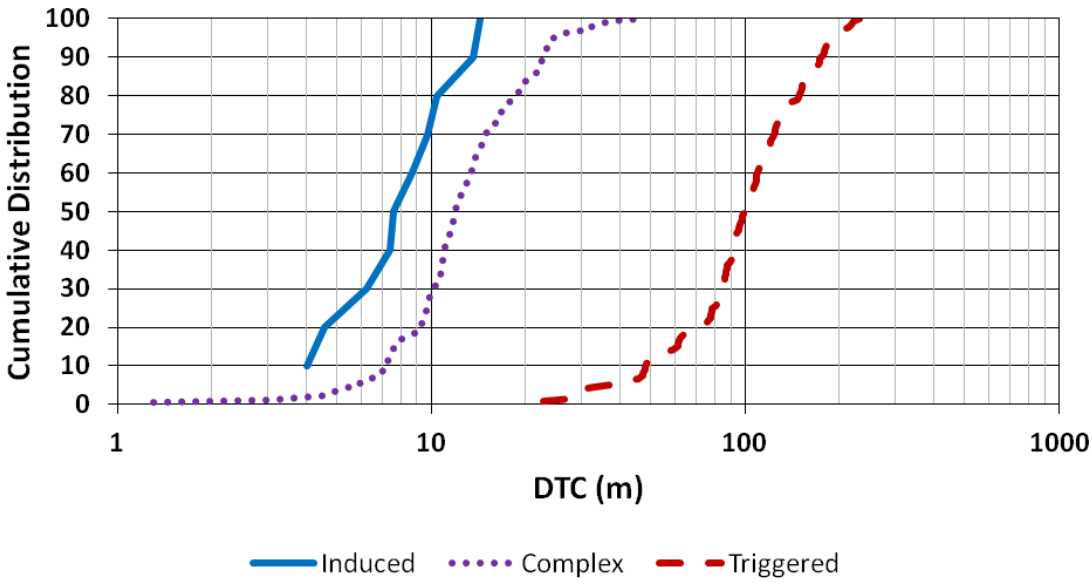

Figure 43: Cumulative distributions of Distance to Centroid (DTC) in meters for an induced, complex and triggered seismic response to mining. More information regarding the individual seismic responses to mining can be found in Section 4.1.

To interpret DTC values in a more meaningful way, additional information regarding the newly blasted excavation, such as the excavation radius, is required. In the absence of this information, it is unknown if the seismic response occurs within, or beyond, a volume equivalent to the assumed mining-induced stress change zone. This distinction is critical to differentiating between induced, complex and triggered seismic responses to mining.

4.4.1 Normalized Distance To Centroid [DTC_N]

A theoretically perfect induced seismic response to mining has a DTC value approaching zero, as all events occur within or in very close proximity to the blasted volume. Triggered seismic responses are spatially diffuse relative to induced responses however, as they are associated with significant geological discontinuities and relatively large volumes of failing rock mass (e.g. yielding pillars). The degree of spatial influence for triggered responses, represented by DTC, is expected to be significant relative to discrete mining-induced stress change from routine mine blasting. For the purposes of defining a DTC limit for a theoretically perfect triggered seismic response, the previously used value of five excavation radii (plus a Location Error Factor (E_L)), is used. This value is somewhat arbitrary, and may need to be adjusted using site-specific knowledge of local triggered source mechanisms for individual site application. Knowledge of the theoretical bounds for this parameter enables DTC values to be normalized as Normalized Distance To Centroid (DTC_N) values. DTC_N is calculated for an individual seismic event as:

$$DTC_N(DTC, r) = \begin{cases} \dfrac{DTC}{(5r + E_L)}, & DTC \leq (5r + E_L) \\ 1, & DTC > (5r + E_L) \end{cases} \quad (15)$$

where,

DTC_N = Normalized Distance To Centroid

DTC = Distance to Centroid (m)

r = Excavation Radius (m)

E_L = Location Error Factor (m)

DTC_N values approaching zero are indicative of a tightly spaced seismic response. This is characteristic of seismic responses induced by mine blasting. When DTC_N values approach or equal one, it is indicative of a relatively diffuse seismic response. This is characteristic of seismic responses resulting from larger scale rock mass failure processes (triggered seismicity). Table 10 summarizes the observation guidelines surrounding DTC_N for induced, complex and triggered seismic responses to mining.

Table 10: Summary of observation guidelines surrounding Normalized Distance To Centroid (DTC_N) for induced, complex and triggered seismic responses to mining. The assumed mining-induced stress change zone used throughout this work is 5 excavation radii plus an Error Location Factor of 10 metres.

	Induced	**Complex**	**Triggered**
Normalized Distance To Centroid [DTC_N]	Within a volume equivalent to the assumed mining-induced stress change zone *All Events:* *$DTC_N < 1$*	Within a volume equivalent to the assumed mining-induced stress change zone and potentially beyond *Significant No. Events:* *$DTC_N < 1$* *&* *All Events:* *$0 \leq DTC_N \leq 1$*	Approaching and beyond a volume equivalent to the assumed mining-induced stress change zone *Significant No. Events:* *$DTC_N = 1$* *&* *All Events:* *$0 \leq DTC_N \leq 1$*

Figure 44 depicts cumulative distributions of DTC_N for the same set of seismic responses to mining shown in Figure 43. With the response parameters normalized, cumulative distributions for individual seismic responses are more meaningful, and can be interpreted without a need for additional information. The entire induced seismic response ($\widetilde{DTC}_N$ = 0.36), is relatively well spatially clustered. The complex response ($\widetilde{DTC}_N$ = 0.53), is also well spatially clustered, but with some scatter relative to the induced response. The triggered response ($\widetilde{DTC}_N$ = 1), is significantly diffuse relative to the tight spatial clustering of the induced and complex responses. These observations match the expected observation guidelines, as proposed in Table 10.

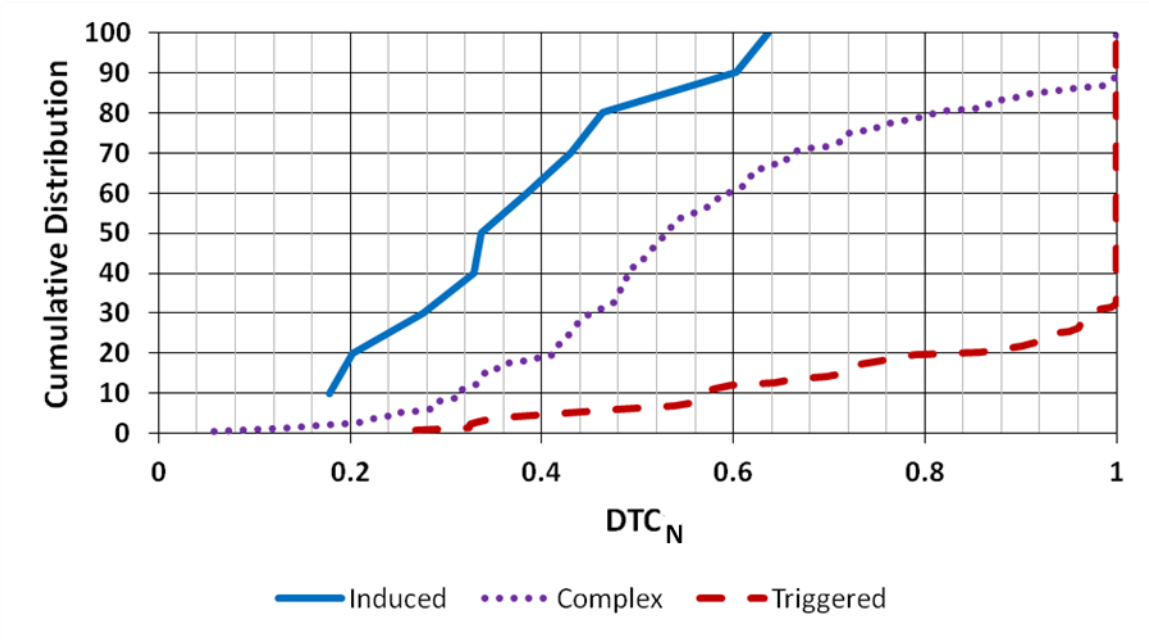

Figure 44: Cumulative distributions of Normalized Distance To Centroid (DTC_N) for an induced, complex and triggered seismic response to mining. More information regarding the individual seismic responses to mining can be found in Section 4.1.

4.5 Time Between Events

The diffusion index, discussed by Baig *et al.* (2017), considers both space and time characteristics of a seismic clusters. The authors suggest variations in temporal diffusion of seismicity may be indicative of different rock mass failure mechanisms. Time Between Events (TBE), or inter-event time, has previously been shown to provide insight into seismic source mechanism for mine seismicity (e.g. Beneteau, 2012; Beneteau and Hudyma, 2012). Because TBE is a parameter calculated using two events, there is no TBE value calculated for the first event contained within a given seismic population or response. It is calculated for an individual seismic event 'x' as:

$$TBE = t_x - t_{(x-1)} \tag{16}$$

where,

TBE = Time Between Events (h)

t_x = Seismic Event 'x' Time (h)

$t_{(x-1)}$ = Seismic Event 'x-1' Time (h)

Beneteau and Hudyma (2012) calculate Time Between Events for discrete magnitude ranges of seismic populations. Within their empirical study of 79 datasets, they show that TBE-rates (slopes of discrete percentile values for individual magnitude ranges), differ for seismic

populations driven by different source mechanisms: "Low TBE-rates...can suggest that the rock is readjusting to the new induced stress conditions caused by a blast, medium TBE-rates...can be related to shearing [triggered seismicity]."

Table 11 summarizes the observation guidelines surrounding TBE for induced, complex and triggered seismic responses to mining. The primary objective of this parameter is to provide a measure of temporal clustering independent of the inducing stimulus (i.e. blast). Induced responses are expected to cluster very closely in time, while triggered responses are expected to occur at relatively constant rates over time. Richardson and Jordan (2002) used a temporal bound of 30 seconds (approximately 0.01 hours), between successive induced seismic events when identifying induced clusters. Approximately 70% of events contained within both the induced and complex seismic responses have TBE values of 0.01 hours or less. Only 20% of events contained within the triggered seismic response have TBE values of 0.01 hours or less.

Table 11: Summary of observation guidelines surrounding Time Between Events (TBE) for induced, triggered and complex seismic responses to mining. Maximum refers to the largest theoretical TBE value. For example, a response of two events would have a maximum TBE value equivalent to the length of the time window used in response identification.

	Induced	**Complex**	**Triggered**
Time Between Events [TBE]	Temporally close together (typically within seconds to minutes) *Significant No. Events:* $0\ h \leq TBE \leq 0.01\ h$	Significant number of events temporally close together, and events over time *Significant No. Events:* $0\ h \leq TBE \leq 0.01\ h$ *&* *All Events:* $0\ h \leq TBE \leq Maximum$	Varies throughout the time period considered (relatively constant) *All Events:* $0\ h \leq TBE \leq Maximum$

Figure 45 depicts cumulative distributions of TBE for the set of seismic responses at LaRonde mine previously discussed (Section 4.1). The majority of the induced response ($\widetilde{TBE}$ = 0.002 h), and complex response ($\widetilde{TBE}$ = 0.004 h), exhibit TBE values less than 0.01. The triggered response ($\widetilde{TBE}$ = 0.07 h), exhibits many TBE values that are one to two orders of magnitude larger. Larger TBE values correspond to a relatively temporally diffuse seismic response to mining. These observations match the expected observation guidelines, as proposed in Table 11.

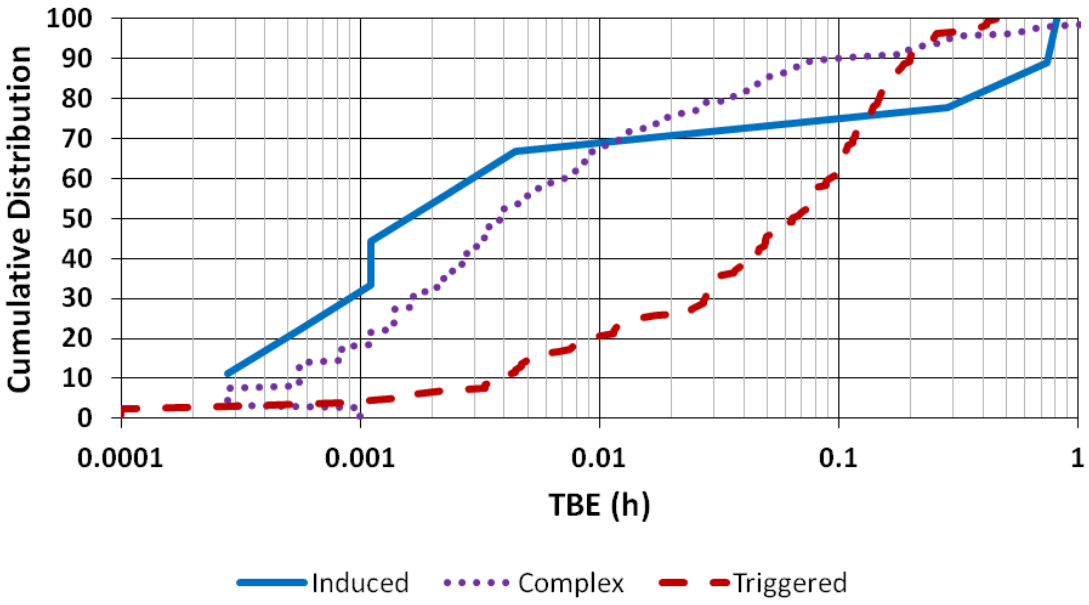

Figure 45: Cumulative distributions of Time Between Events (TBE) in meters for an induced, complex and triggered seismic response to mining. More information regarding the individual seismic responses to mining can be found in Section 4.1.

To interpret TBE values in a more meaningful way, additional information regarding how the seismic response was identified in time, such as the temporal window limit and the quantity of events, is required. In the absence of this information, the relative spacing of events throughout the temporal window, used to identify the seismic response, cannot be determined.

4.5.1 Normalized Time Between Events [TBE_N]

The TBE value for a theoretically perfect induced seismic response to mining is zero, as all events occur the instant after the mine blast. A theoretically perfect triggered response, which is temporally independent of mine blasting, has TBE values that reflect a constant event rate over the entire temporal window used to identify the seismic response. Knowledge of the theoretical bounds for this parameter enables TBE values to be normalized as Normalized Time Between Events (TBE_N) values. TBE_N is calculated for an individual seismic event as:

$$TBE_N(TBE, t_{max}, n) = \begin{cases} \dfrac{(TBE)(n)}{t_{max}}, & TBE \leq (t_{max}/n) \\ 1, & TBE > (t_{max}/n) \end{cases} \quad (17)$$

where,

TBE_N = Normalized Time Between Events

TBE = Time Between Events (h)

t_{max} = Maximum Limit of the Response Identification Time Window (h)

n = Number of Events in Seismic Response

Because triggered seismic responses typically contain a larger quantity of seismic events, relative to induced responses, there are likely to be both events with small and large TBE values contained within a triggered seismic response. In other words, as the quantity of events contained within a seismic response increases, individual TBE values must decrease, as the response identification time window is finite. A seismic event with a TBE_N value greater than one must have occurred further from the preceding event (in time), than if all events in the response were equally temporally dispersed throughout the response identification time window. The closer a seismic response is temporally clustered (TBE_N values approaching zero), the more likely it is to be induced. Table 12 summarizes the observation guidelines surrounding TBE_N for induced, complex and triggered seismic responses to mining.

Table 12: Summary of observation guidelines surrounding Normalized Time Between Events (TBE_N) for induced, complex and triggered seismic responses to mining.

	Induced	**Complex**	**Triggered**
Normalized Time Between Events [TBE_N]	Temporally close together (typically within seconds to minutes) *Significant No. Events:* $TBE_N \approx 0$ *Typically,* $TBE_N \leq 0.2$	Significant number of events temporally close together and events over time *Significant No. Events:* $0 \leq TBE_N \leq 0.2$ *&* *All Events:* $0 \leq TBE_N \leq 1$	Relatively constant rate of events over time *Significant No. Events:* $TBE_N \geq 0.5$ & *All Events:* $0 \leq TBE_N \leq 1$

Figure 46 depicts cumulative distributions of TBE_N for the same set of seismic responses to mining shown in Figure 45. With the response parameters normalized, cumulative distributions for individual seismic responses are more meaningful, and can be interpreted without a need for additional information. The majority of the induced seismic response ($\widetilde{TBE}_N$ = 0.002), is tightly clustered in time. The complex response ($\widetilde{TBE}_N$ = 0.05), is also well clustered in time, but with some scatter relative to induced. The triggered response ($\widetilde{TBE}_N$ = 0.73), is significantly temporally diffuse relative to the induced and complex responses, with 60% of events exhibiting TBE_N values greater than 0.5. These observations match the expected observation guidelines, as proposed in Table 12.

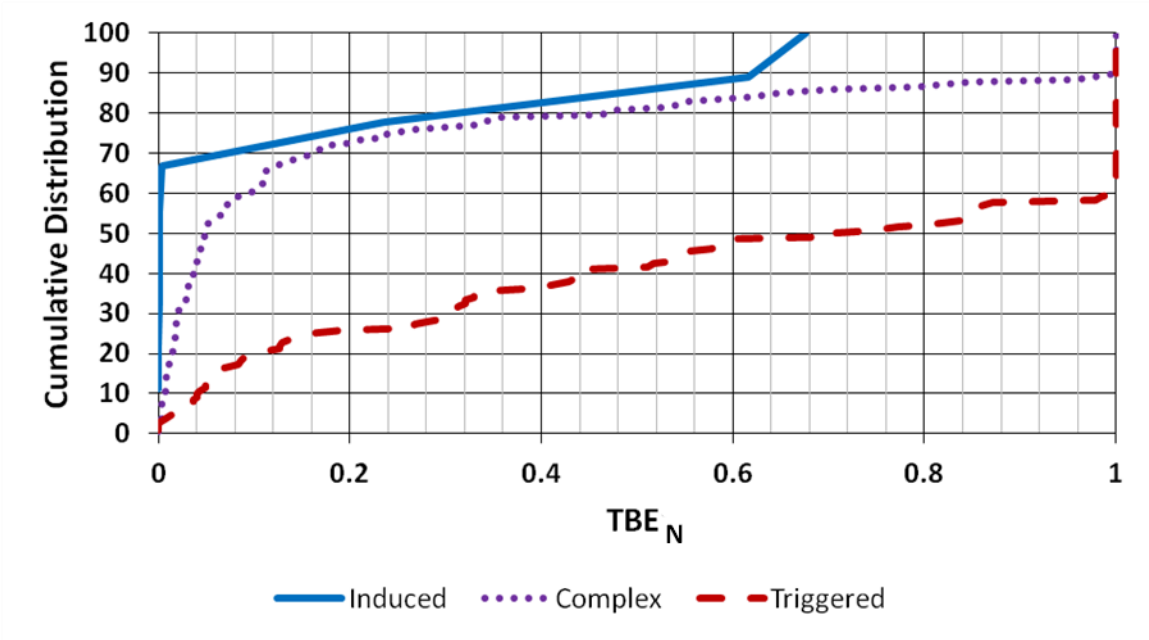

Figure 46: Cumulative distributions of Normalized Time Between Events (TBE_N) for an induced, complex and triggered seismic response to mining. More information regarding the individual seismic responses to mining can be found in Section 4.1.

4.6 Chapter Summary

Within this chapter, four novel Seismic Response Parameters and Normalized Seismic Response Parameters have been defined. Blast related $SRP_{(N)}$'s, DTB/DTB_N and TAB/TAB_N, relate seismic responses directly to discrete mine blasts. Response related $SRP_{(N)}$'s, DTC/DTC_N and TBE/TBE_N, relate individual events within a seismic response to the response itself, independent of the stimulus. Table 13 and Table 14 summarize the observation guidelines for each SRP and SRP_N, respectively, for induced, triggered and complex seismic responses to mining. Examples of typical induced, triggered and complex seismic responses at LaRonde mine have demonstrated the applicability of these guidelines to real mine seismic data. Further examples can be found in the LaRonde mine case study presented in Chapters 6 and 7.

Table 13: Summary table of observation guidelines for Seismic Response Parameters (DTB, TAB, DTC, and TBE) as they pertain to induced, complex and triggered seismic responses to mining. Stimulus commonly refers to a mine blast. Table is continued on subsequent page.

	Induced	Complex	Triggered
Distance To Blast [DTB]	Within 5 excavation radii (plus Location Error Factor) *Excavation Radius 2.5 m: DTB < 22.5 m*	Within 5 excavation radii (plus Location Error Factor) and potentially beyond *Excavation Radius 2.5 m: Commonly, DTB < 22.5 m*	Beyond 5 excavation radii (plus Location Error Factor) *Excavation Radius 15 m: DTB > 85 m*

	Induced	**Complex**	**Triggered**
Time After Blast [TAB]	Within the first few hours of mine blasting *All Events:* *TAB < 1-3 h*	Significant number of events within the first few hours of mine blasting and events independent of mine blasting *Significant No. Events:* *TAB < 1-3 h* *&* *All Events:* *0 h ≤ TAB ≤ Maximum*	Independent of mine blasting *All Events:* *0 h ≤ TAB ≤ Maximum*
Distance to Centroid [DTC]	Within 5 excavation radii (plus Location Error Factor) *Excavation Radius 2.5 m:* *DTC < 22.5 m*	Within 5 excavation radii (plus Location Error Factor) and potentially beyond *Excavation Radius 2.5 m:* *Commonly, DTC < 22.5 m*	Beyond 5 excavation radii (plus Location Error Factor) *Excavation Radius 15 m:* *DTC > 85 m*
Time Between Events [TBE]	Temporally close together (typically within seconds to minutes) *Significant No. Events:* *0 h ≤ TBE ≤ 0.01 h*	Significant number of events temporally close together, and events over time *Significant No. Events:* *0 h ≤ TBE ≤ 0.01* *&* *All Events:* *0 h ≤ TBE ≤ Maximum*	Varies throughout the time period considered (relatively constant) *All Events:* *0 h ≤ TBE ≤ Maximum*

Table 14: Summary table of observation guidelines for Normalized Seismic Response Parameters (DTB_N, TAB_N, DTC_N, and TBE_N) as they pertain to induced, complex and triggered seismic responses to mining. Stimulus commonly refers to a mine blast. Table is continued on subsequent page.

	Induced	**Complex**	**Triggered**
Normalized Distance To Blast [DTB_N]	Within the assumed mining-induced stress change zone *All Events:* $DTB_N < 1$	Within the assumed mining-induced stress change zone and potentially beyond *Significant No. Events:* $DTB_N < 1$ *&* *All Events:* $0 \leq DTB_N \leq 1$	Beyond the assumed mining-induced stress change zone *All Events:* $DTB_N = 1$
Normalized Time After Blast [TAB_N]	Within the first few hours of mine blasting *Significant No. Events:* $TAB_N \approx 0$ *Typically,* $TAB_N \leq 0.2$	Significant number of events within the first few hours of mine blasting and events independent of mine blasting *Significant No. Events:* $0 \leq TAB_N \leq 0.2$ *&* *All Events:* $0 \leq TAB_N \leq 1$	Independent of mine blasting *Significant No. Events:* $TAB_N \geq 0.5$ *&* *All Events:* $0 \leq TAB_N \leq 1$
Normalized Distance To Centroid [DTC_N]	Within a volume equivalent to the assumed mining-induced stress change zone *All Events:* $DTC_N < 1$	Within a volume equivalent to the assumed mining-induced stress change zone and potentially beyond *Significant No. Events:* $DTC_N < 1$ *&* *All Events:* $0 \leq DTC_N \leq 1$	Approaching and beyond a volume equivalent to the assumed mining-induced stress change zone *Significant No. Events:* $DTC_N = 1$ *&* *All Events:* $0 \leq DTC_N \leq 1$

	Induced	**Complex**	**Triggered**
Normalized Time Between Events [TBE_N]	Temporally close together (typically within seconds to minutes) *Significant No. Events:* $TBE_N \approx 0$ *Typically,* $TBE_N \leq 0.2$	Significant number of events temporally close together and events over time *Significant No. Events:* $0 \leq TBE_N \leq 0.2$ *&* *All Events:* $0 \leq TBE_N \leq 1$	Relatively constant rate of events over time *Significant No. Events:* $TBE_N \geq 0.5$ & *All Events:* $0 \leq TBE_N \leq 1$

Chapter 5

5 Interpreting a Seismic Response to Mining

Mining environments are complex, with significant variation due to both natural and mining processes. Individual Seismic Response Parameters are useful, but in combination they can form a comprehensive picture of the space-time relation for a seismic response to mining. This chapter presents methodologies for visually interpreting seismic responses to mining (SRP_N and SRR charts) and quantitatively describing seismic responses to mining (SRR).

5.1 Normalized Seismic Response Parameter Charts (SRP_N Charts)

Normalized Seismic Response Parameter charts (SRP_N charts) are a variation of the classic radar chart. Radar charts, also known as spider or polar plots, are a graphical means of displaying multiple quantitative variables - such as Normalized Seismic Response Parameters. Individual radar charts consist of equiangular spokes originating from a common point, as shown in Figure 47. Each spoke is used to display a single quantitative variable, with a minimum of three spokes, or Normalized Seismic Response Parameters, required to form an area.

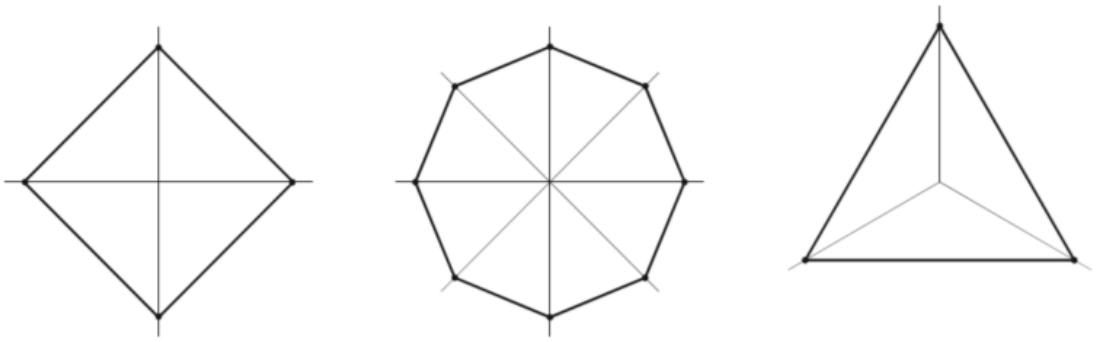

Figure 47: Radar charts with a flexible number of displayed parameters (Lechner and Weidmann, 2015)

5.1.1 Significance of Normalized Seismic Response Parameters

Normalized SRP's are capable of conveying information regarding the nature of a seismic response independent of how it was identified in space and time. For example, a DTB (Distance To Blast) value of 100 metres may appear to be large and indicative of triggered seismicity, but for a production stope blast with a radius of 30 metres, the assumed spatial limit for an induced response is 160 metres. This factor is considered in the calculation of normalized parameters however, and the DTB_N (Normalized Distance To Blast) for this example is 0.63 - less than one and therefore more indicative of induced seismicity. A significant challenge in using radar plots

is comparing data across varying scales. By using normalized parameters, which represent a variance from a theoretically perfect induced baseline, scales such as distance (m) and time (h) become uniform and unitless, from zero (induced) to one (triggered).

Figure 48 depicts a SRP_N chart for a theoretically perfect induced and theoretically perfect triggered seismic response to mining. Spatial SRP_N's (DTB_N and DTC_N), and temporal SRP_N's (TBE_N and TAB_N), are placed on individual and perpendicular axis, to facilitate a meaningful visual comparison between the two. In Figure 48 the induced response forms an area of zero, as all SRP_N values are equal to zero. The triggered response forms the largest area possible, as all SRP_N values are equal to one. Seismic responses with small SRP_N values (forming smaller areas), are tightly clustered in space and time, and are more likely to be induced.

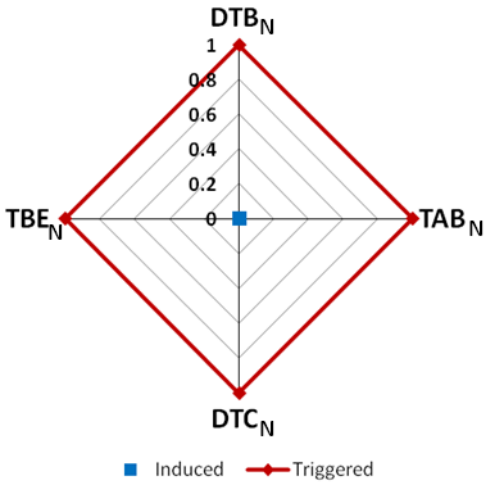

Figure 48: SRP_N chart for a theoretically perfect induced and theoretically perfect triggered seismic response to mining shown in blue and red respectively.

5.1.2 Considerations Surrounding the Use of Median Values

As previously discussed, median response parameter values can be used to characterize a seismic response to mining. Due to the inherent complexities of mining environments, particularly in deep and seismically active mines, it is unlikely to repeatedly observe completely induced seismic responses to mining. Some events, or subsets of events, within seismic responses may fall outside expected observation guidelines. Acceptable deviation will depend on many factors, most notably the seismic system limitations and seismic analysis objectives.

The induced seismic response to mining shown throughout Chapter 4, see Figure 31 and Figure 32, typically fell within the observation guidelines of induced seismicity for all $SRP_{(N)}$'s. It is most likely an induced seismic response to mining, and should plot as a relatively small area on a

SRP_N chart. Figure 49 depicts the SRP_N chart for each individual seismic event contained within the induced seismic response to mining.

A possible interpretation of the SRP_N charts is:

The seismic response to mining shown in Figure 49 *is primarily induced. Only three events deviate from the majority of the response, shown in the last full row. Seventy percent of all events within the response show little deviation from a theoretically perfect induced response in the temporal parameters ($TAB_N \approx 0$ and $TBE_N \approx 0$), and all events occur within the assumed mining-induced stress change zone of the blast ($DTB_N < 1$).*

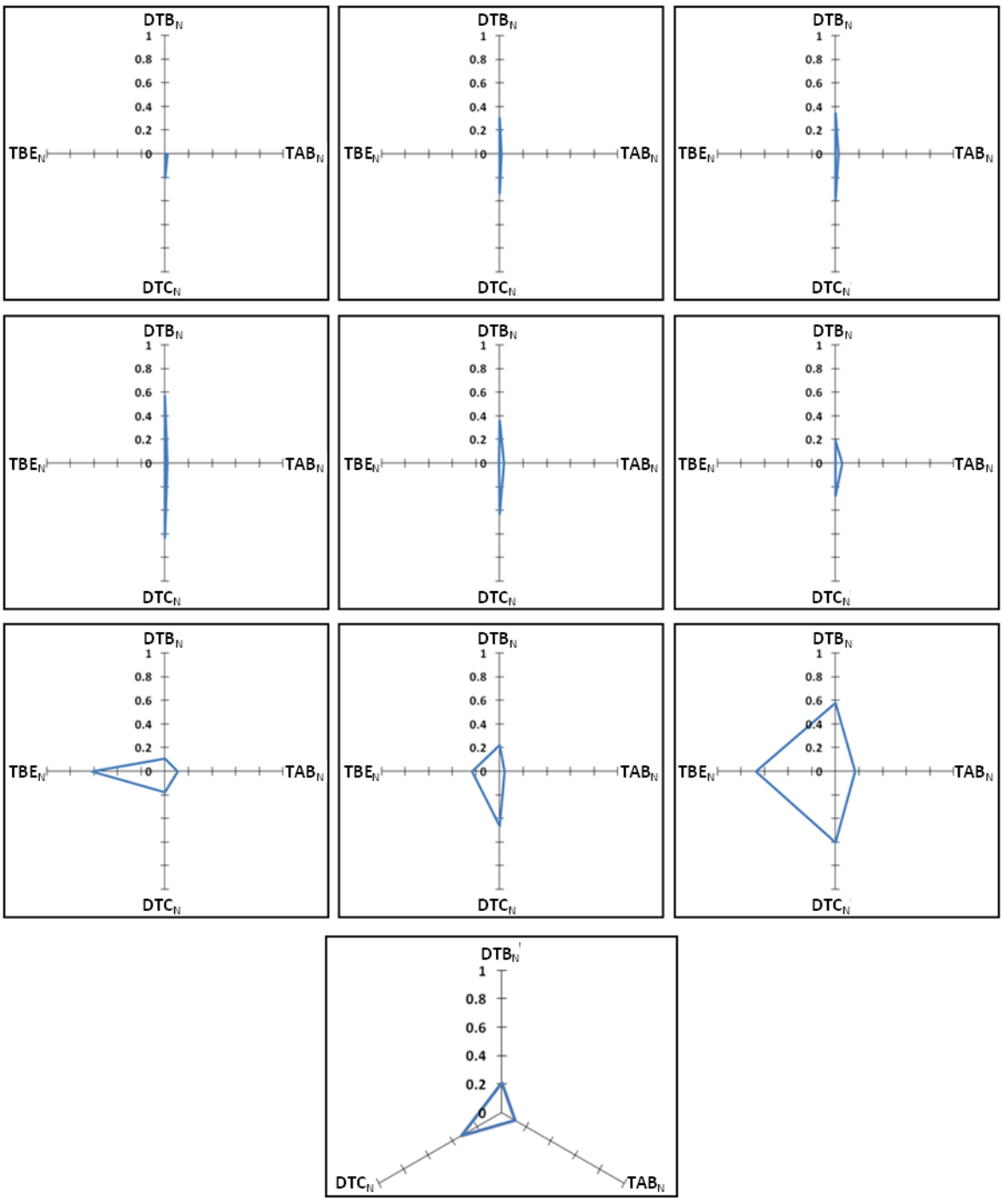

Figure 49: Individual SRP_N charts for all induced seismic events shown in Figure 31. The final plot has no TBE_N parameter, as this plot represents the first event to occur within the seismic response.

The process of examining SRP_N charts for every event contained within a seismic response can be time consuming, and is unrealistic in some cases. Triggered seismic source mechanisms, for example, can easily generate hundreds of seismic events within a single response. In such cases, it may be beneficial to plot multiple events on the same SRP_N chart, as shown in Figure 50 (a), or the median SRP_N values of the entire response, as shown in Figure 50 (b).

In Figure 50 (a), the SRP_N values for every event in the induced seismic response are plotted on the same chart. For seismic response interpretation purposes, it is recommended that the quantity of events plotted on such charts be clearly labeled, e.g. 'N = 10'. Because a well behaved seismic response to mining should consist primarily of events with similar SRP_N values, it is likely that plots for different events, contained within the same seismic response, will overlap. This overlapping of events often leads to data occlusion, where the plot of one event visually blocks the plot for another event or events. In Figure 50 (a) only four individual SRP_N plots are distinguishable, but plots for 10 events are shown. This is an example of data occlusion.

The median, or 50th percentile, is generally considered representative of a dataset. In Figure 50 (b), a single plot of the median SRP_N value for the entire induced seismic response is shown. The median SRP_N chart may be advantageous relative to the chart shown in part (a), as there is no data occlusion.

A possible interpretation of the SRP_N chart shown in (b) is:

The seismic response to mining shown in Figure 50 (b) is primarily induced. At least 50 % of all events within the response show little deviation from a theoretically perfect induced response for the temporal parameters ($\widetilde{TAB}_N \approx 0$ and $\widetilde{TBE}_N \approx 0$), and occur within the assumed mining-induced stress change zone of the blast ($\widetilde{DTB}_N < 1$).

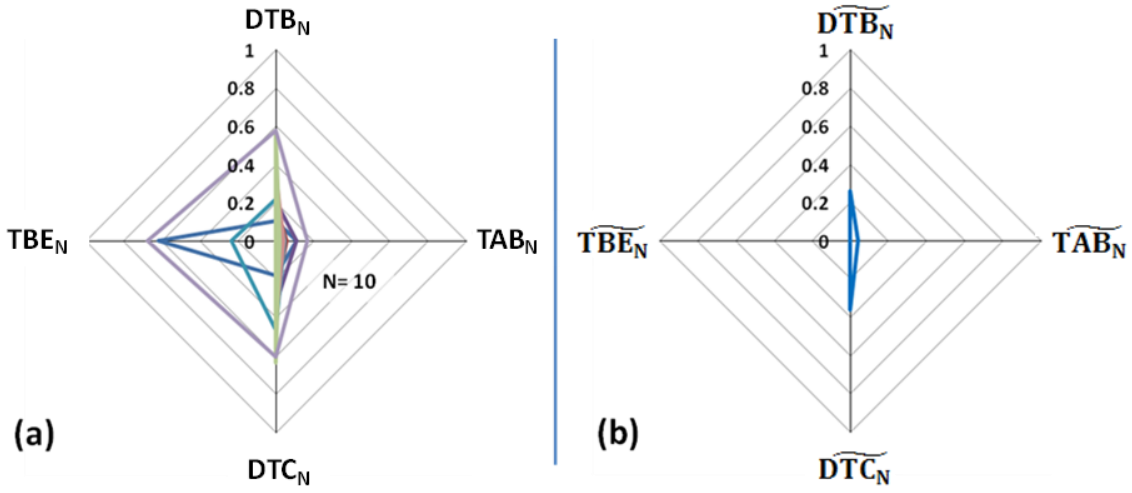

Figure 50: SRP_N charts for each individual seismic event (N =10) (a), and the median value (b), of an induced seismic response to mining at LaRonde mine. Individual plots for all events in Part (a) are shown in Figure 49.

The interpretation from the median value plot (Figure 50 (b)) and individual SRP_N charts (Figure 49) are very similar, with both interpretations concluding the seismic response to mining is likely induced. It is recommended for general analysis purposes that the median SRP_N method, as shown in Figure 50 (b), be used. Further analysis of individual events should be performed as required. When an SRP_N chart for an entire seismic response is shown as only a single SRP_N plot, it will be assumed the median SRP_N values are shown.

5.1.3 Interpreting Seismic Responses to Mining using SRP_N Charts

Figure 51 depicts two different seismic responses to mining plotted on the same SRP_N chart. Response A (shown in blue), exhibits small SRP_N values relative to Response B (shown in red).

A possible interpretation of the SRP_N chart shown is:

One of the seismic responses to mining shown in Figure 51 is likely induced (Response A), and the other is likely triggered (Response B). At least 50 % of all events within Response A show little deviation from a theoretically perfect induced response in the temporal parameters ($\widetilde{TAB}_N \approx 0$ and $\widetilde{TBE}_N \approx 0$), and the majority of events likely occur within the assumed mining-induced stress change zone of the blast ($\widetilde{DTB}_N < 1$). This indicates Response A is likely induced.

At least 50 % of all events within Response B occur beyond the assumed mining-induced stress change zone of the blast ($\widetilde{DTB}_N = 1$), but the entire response likely occurs within the maximum dimensions of the associated mining-induced stress change ($\widetilde{DTC}_N < 1$). In other words, the seismic events are spatially well clustered relative to themselves, but not in close proximity to the blast location. This is indicative of complex or triggered seismicity. There is significant deviation in the temporal parameters, relative to Response A, indicating the majority of Response B is likely triggered and not complex. A strong induced temporal component is expected to accompany a complex seismic response, this is not observed in Response B. This indicates Response B is likely triggered.

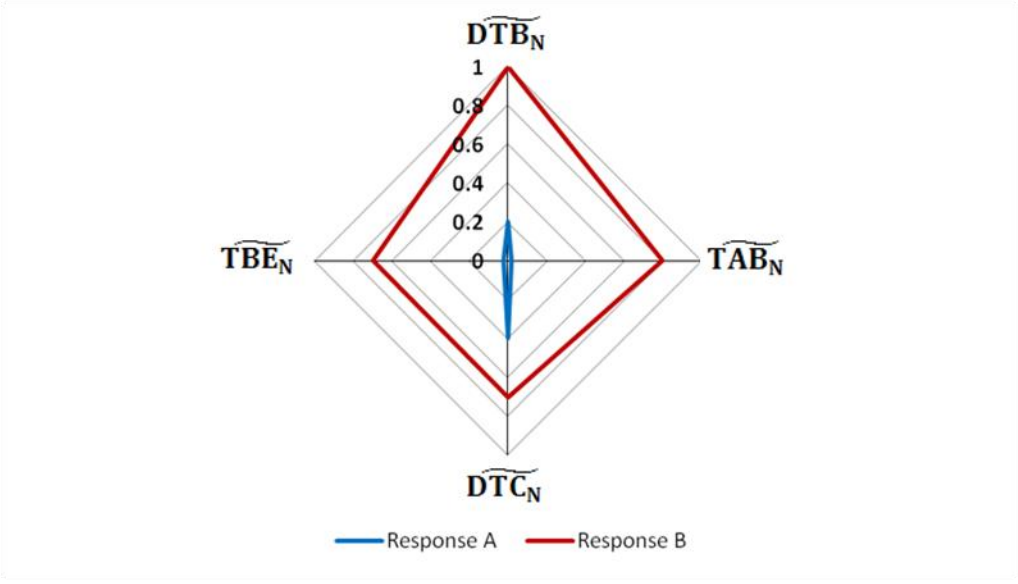

Figure 51: SRP_N chart for two seismic responses to mining A and B, shown in blue and red respectively.

Temporal parameters approaching zero are a distinct indicator of induced seismicity. A SRP_N chart for an induced seismic response at LaRonde mine has previously been shown in Figure 50

(b). Spatial parameters are more variable, and while expected to approach zero, any value less than 1 may correspond to an induced seismic response. The relatively small SRP_N values, associated with induced seismicity, typically generate small areas on SRP_N charts. Table 15 summarizes the observation guidelines surrounding SRP_N charts for induced seismic responses to mining.

Table 15: Summary of observation guidelines surrounding SRP_N charts for induced seismic responses to mining.

	Induced
SRP_N Charts	Small Area *Temporal Parameters:* *[TAB_N & TBE_N]* *Approaching 0* *Spatial Parameters:* *[DTB_N & DTC_N]* *Approaching 0*

A SRP_N chart for the triggered seismic response to mining shown throughout Chapter 4, see Figure 33 and Figure 34, is shown in Figure 52. Both of the spatial parameters ($\widetilde{DTB}_N$ and $\widetilde{DTC}_N$) equal one - a strong indicator of triggered seismicity. The temporal parameters ($\widetilde{TAB}_N$ and $\widetilde{TBE}_N$), are also characteristic of triggered seismicity. Both parameters indicate significant quantities of seismic events occur beyond the first few hours following mine blasting, with significant time between individual events and good dispersion throughout the temporal formation window.

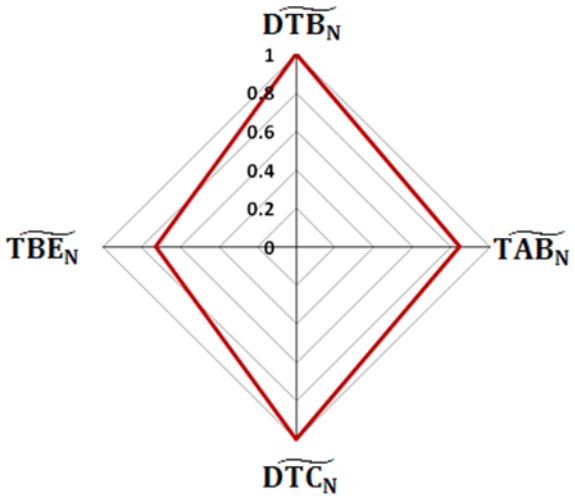

Figure 52: SRP_N chart for a triggered seismic response to mining at LaRonde mine.

The relative area of SRP_N charts can serve as an indicator of the nature of a seismic response to mining. Increasing areas correspond to larger SRP_N values, and an increased likelihood of triggered seismicity. Table 16 summarizes the observation guidelines surrounding SRP_N charts for induced and triggered seismic responses to mining.

Table 16: Summary of observation guidelines surrounding SRP_N charts for induced and triggered seismic responses to mining.

	Induced	**Triggered**
SRP_N Charts	Small Area *Temporal Parameters:* *[TAB_N & TBE_N]* *Approaching 0* *Spatial Parameters:* *[DTB_N & DTC_N]* *Approaching 0*	Large Area *Temporal Parameters:* *[TAB_N & TBE_N]* *Approaching 0.5 to 1* *Spatial Parameters:* *DTB_N = 1 &* *DTC_N Approaching 1*

A SRP_N chart for the complex seismic response to mining shown throughout Chapter 4, see Figure 35 and Figure 36, is shown in Figure 53. The complex response looks similar to the induced response (shown in Figure 50 (b)). Both responses exhibit relatively small areas, however the complex response area is nearly double that of the induced, due to the increased deviation in temporal parameters ($\widetilde{TAB}_N$ and $\widetilde{TBE}_N$). At least 50% of all events in the complex response occur within the mining-induced stress change zone of the blast ($\widetilde{DTB}_N < 1$), and the response is relatively well clustered in space ($\widetilde{DTC}_N < 1$). It is only a subset of the response, identified primarily through temporal parameters, which distinguishes the seismic response as complex.

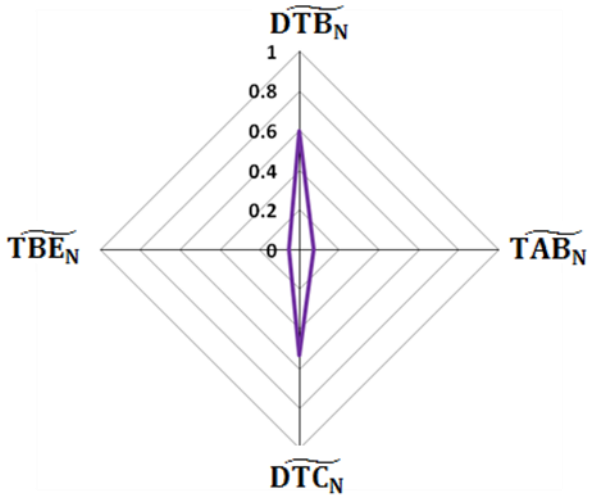

Figure 53: SRP_N chart for a complex seismic response to mining at LaRonde mine.

Complex seismic responses to mining are the most challenging to interpret from median value SRP_N charts. The median SRP_N values for a complex response can be indicative of induced or triggered seismicity, depending on the relative proportion of induced and triggered seismic events contained within the responses. Table 17 summarizes the observation guidelines surrounding SRP_N charts for induced, triggered and complex seismic responses to mining.

Table 17: Summary of observation guidelines surrounding SRP_N charts for induced, complex and triggered seismic responses to mining.

	Induced	**Complex**	**Triggered**
SRP_N Charts	Small Area *Temporal Parameters:* *$[TAB_N$ & $TBE_N]$* *Approaching 0* *Spatial Parameters:* *$[DTB_N$ & $DTC_N]$* *Approaching 0*	Medium Area *Temporal Parameters:* *$0 \leq TAB_N \leq 1$ &* *$0 \leq TBE_N \leq 1$* *Spatial Parameters:* *$[DTB_N$ & $DTC_N]$* *Typically Less than 1*	Large Area *Temporal Parameters:* *$[TAB_N$ & $TBE_N]$* *Approaching 0.5 to 1* *Spatial Parameters:* *$DTB_N = 1$ &* *DTC_N Approaching 1*

5.1.3.1 SRP_N Chart General Analysis Guidelines

The following guidelines are generalizations meant to aid in interpreting a seismic responses to mining using SRP_N charts:

- Identify any SRP_N values near zero or one, as these are strong indicators of induced and triggered seismic responses to mining respectively.

- If all SRP_N values are relatively small, particularly temporal parameters, it is indicative of an induced seismic response to mining.
- If all SRP_N values are relatively large, particularly if $DTB_N = 1$, it is indicative of a triggered seismic response to mining.
- When zero and one SRP_N values occur within the same population, it is indicative of a complex seismic response to mining.

When a clear interpretation cannot be made, complimentary seismic analysis tools and geological information may be helpful, including:

- Cumulative Distributions of Seismic Response Parameters
- Cumulative Distributions of Normalized Seismic Response Parameters
- Seismic Source Parameter Based Seismic Analysis
- Spatial Plots (such as a plan view with mine development)
- Magnitude-Time History Charts
- Knowledge of Local Geomechanical Conditions

Further examples of this are provided in the LaRonde mine case study presented in Chapters 6 and 7.

5.2 Seismic Response Rating (SRR)

The ability to express the nature of a seismic response with a single quantitative measure is desirable for many purposes. SRP_N charts provide insight into seismic responses to mining, however they require interpretation across multiple parameters. The geomechanics rating systems, RMR (Bieniawski, 1976) and Q (Barton *et al.*, 1974), are examples of rating systems which combine multiple parameters in an effort to generate a single value.

Rock Mass Rating (RMR), is a classification system commonly used in support design for underground excavations (Hoek *et al.*, 1995). It is calculated by summing the values of six individual parameters related to rock mass conditions (e.g. RQD, Condition of Discontinuities, Groundwater). The larger a RMR sum, to a maximum of 100, the higher the quality of the rock mass. Intervals of RMR are used to identify different rock quality categories, ranging from 'very poor' to 'very good', as shown in Table 18 (Bieniawski, 1989).

Table 18: Guidelines for excavation and support of 10 metre span rock tunnels in accordance with the RMR system (redrawn from Bieniawski, 1989)

Rock Mass Class	Excavation	Rock bolts (20 mm diameter, fully grouted)	Shotcrete	Steel Sets
I - Very good rock RMR: 81-100	Full face, 3 m advance.	Generally no support required except spot bolting.		
II - Good rock RMR: 61-80	Full face, 1-1.5 m advance. Complete support 20 m from face.	Locally, bolts in crown 3 m long, spaced 2.5 m with occasional wire mesh.	50 mm in crown where required.	None.
III - Fair rock RMR: 41-60	Top heading and bench 1.5-3 m advance in top heading. Commence support after each blast. Complete support 10 m from face.	Systematic bolts 4 m long, spaced 1.5-2 m in crown and walls with wire mesh in crown.	50-100 mm in crown and 30 mm in sides.	None.
IV - Poor rock RMR: 21-40	Top heading and bench 1.0-1.5 m advance in top heading. Install support concurrently with excavation, 10 m from face.	Systematic bolts 4-5 m long, spaced 1-1.5 m in crown and walls with wire mesh.	100-150 mm in crown and 100 mm in sides.	Light to medium ribs spaced 1.5 m where required.
V - Very poor rock RMR: < 20	Multiple drifts 0.5-1.5 m advance in top heading. Install support concurrently with excavation. Shotcrete as soon as possible after blasting.	Systematic bolts 5-6 m long, spaced 1-1.5 m in crown and walls with wire mesh. Bolt invert.	150-200 mm in crown, 150 mm in sides, and 50 mm on face.	Medium to heavy ribs spaced 0.75 m with steel lagging and forepoling if required. Close invert.

Employing the same methodology as RMR, individual SRP_N values can be summed to generate a Seismic Response Rating (SRR). The use of Normalized Seismic Response Parameters (SRP_N) is preferred, as all values have been normalized (discussed in Section 5.1.1). SRR is calculated for an individual seismic event as:

$$SRR = \sum SRP_N \tag{18}$$

where,

SRR = Seismic Response Rating

$\sum SRP_N$ = Sum of Normalized Seismic Response Parameters, calculated as:

$$\sum SRP_N = DTB_N + TAB_N + DTC_N + TBE_N \tag{19}$$

where,

DTB_N= Normalized Distance To Blast

TAB_N = Normalized Time After Blast

DTC_N = Normalized Distance To Centroid

TBE_N = Normalized Time Between Events

It is not necessary to possess all four SRP_N's to calculate a SRR value. When using fewer SRP_N's however, the change in the SRR theoretical maximum must be considered, as discussed in the subsequent section (5.2.1).

5.2.1 SRR Tables and Graphs

Table 19 is a SRR table for a theoretically perfect induced and a theoretically perfect triggered seismic response to mining. Because these values represent the theoretical bounds of the space-time relation for seismic responses to mining, they are also the theoretical bounds for SRR. It is expected that SRR values for true seismic responses to mining will fall between SRR = 0 (theoretically perfectly induced) and SRR = 4 (theoretically perfectly triggered).

The minimum theoretical bound for SRR is always zero, however the maximum theoretical bound is equivalent to the number of SRP_N's summed. For example, the first event in a given seismic response to mining has no TBE_N value, and would therefore have a SRR maximum bound of three.

Table 19: SRR calculation table for a theoretically perfect induced and a theoretically perfect triggered seismic response to mining.

	Induced	**Triggered**
DTB_N	0	1
TAB_N	0	1
DTC_N	0	1
TBE_N	0	1
SRR	**0**	**4**

An alternative means of visually conveying SRR is through bar graphs. By subdividing each bar into individual SRP_N values, the same information shown in Table 19 can be communicated. Figure 54 is a SRR chart for a theoretically perfect induced and a theoretically perfect triggered seismic response to mining. The triggered response spans the entire theoretical SRR range (0 to 4), with equal SRP_N values of one. No bar is shown for the induced response, as all SRP_N values equal zero.

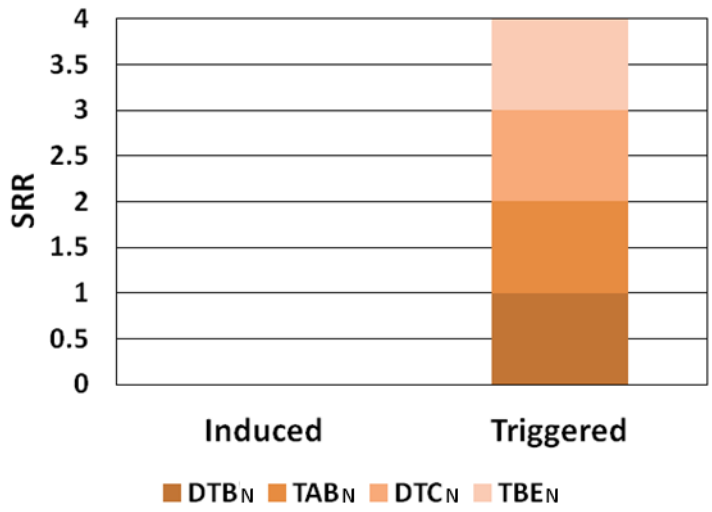

Figure 54: SRR chart for a theoretically perfect induced (SRR = 0) and a theoretically perfect triggered (SRR = 4) seismic response to mining. Colour variations correspond to individual SRP_N values used to calculate SRR.

5.2.2 Considerations Surrounding the use of Median Values

As previously discussed, median response parameter values can be used to characterize a seismic response to mining. By using the median SRP_N values of a response to calculate SRR, the space-time relation for an entire seismic response to mining can be characterized with a single quantitative value.

The induced seismic response to mining shown throughout Chapter 4, see Figure 31 and Figure 32, typically fell within the observation guidelines of induced seismicity for all Seismic Response Parameters. It is most likely an induced seismic response to mining, and should possess a relatively small SRR. Figure 55 depicts a SRR chart showing individual SRR values for all seismic events contained within the induced seismic response to mining.

A possible interpretation of the SRR chart shown is:

The seismic response to mining shown in Figure 55 is primarily induced. Only two events deviate from the majority of the response, ($SRR \geq 1$). Seventy percent of all events within the response show little deviation from a theoretically perfect induced response for the temporal parameters ($TAB_N \approx 0$ and $TBE_N \approx 0$), and all events occur within the assumed mining-induced stress change zone of the blast ($DTB_N < 1$).

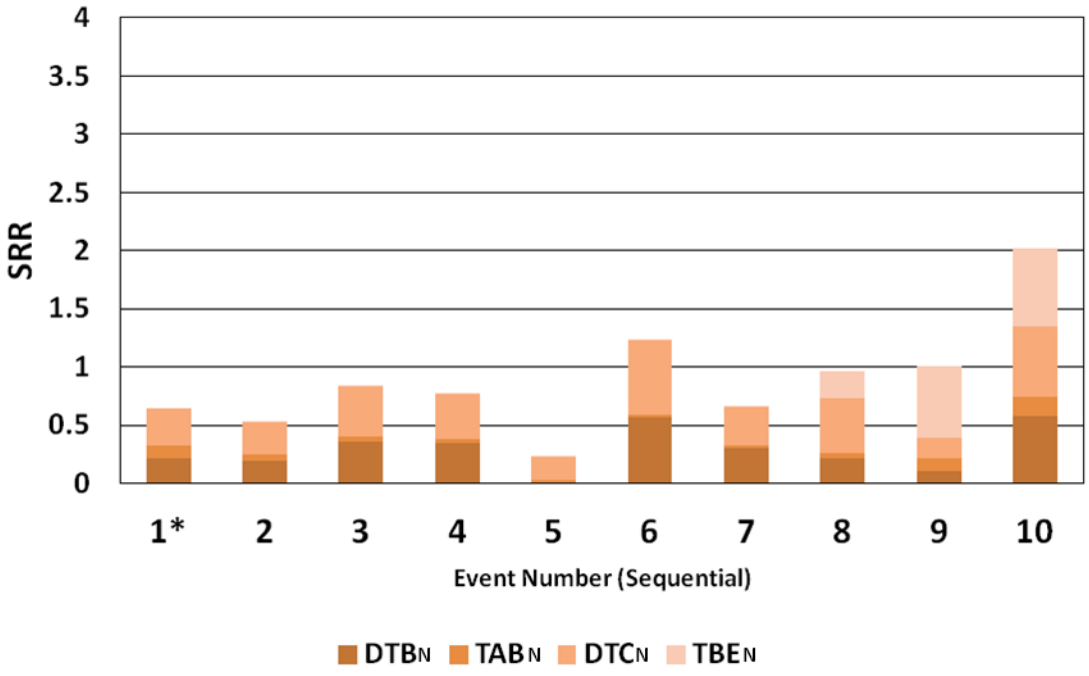

Figure 55: SRR chart for all induced seismic events shown in Figure 31. Events are shown in sequential order with reference to the time window used in response identification. The first event in the series (1*) has no TBE' value and should be considered independently as having a SRR max of 3.

The process of examining SRR for each individual event contained within a seismic response can be time consuming and is unrealistic in some cases. As was shown for SPR_N charts (Section 5.1.2), the interpretation of a seismic response across all seismic events is typically comparable to the interpretation of the response median. Figure 56 is a SRR chart of the median SRR for the entire seismic response shown in Figure 55.

A possible interpretation of the SRR chart shown is:

The seismic response to mining shown in Figure 56 is primarily induced. At least 50 % of all events within the response show little deviation from a theoretically perfect induced response for the temporal parameters ($\widetilde{TAB}_N \approx 0$ and $\widetilde{TBE}_N \approx 0$), and occur within the assumed mining-induced stress change zone of the blast ($\widetilde{DTB}_N < 1$).

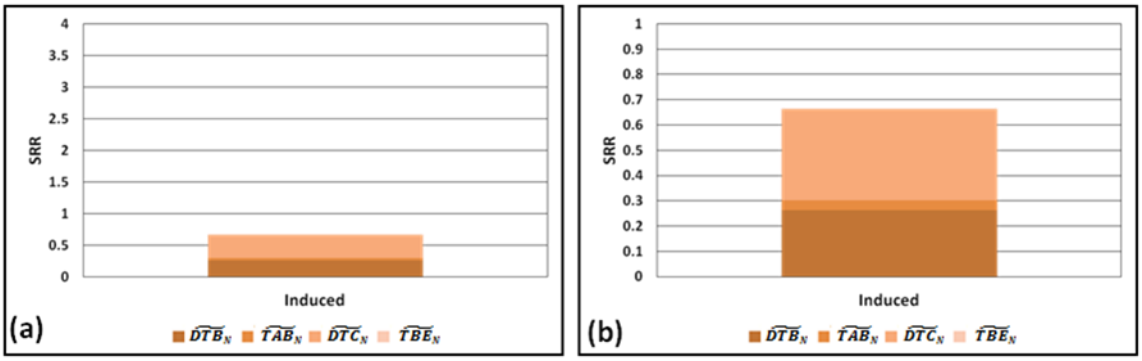

Figure 56: SRR chart for the median SRR of the induced seismic response to mining shown in Figure 31. Part (a) shows the standard SRR axis, covering all theoretical values (0 to 4). Part (b) shows only a subsection of the SRR axis, focusing on relevant values (0 to 1).

The interpretation from the median value SRR chart (Figure 56) and individual event SRR chart (Figure 55) are very similar, with both interpretations concluding the seismic response to mining is primarily induced. It is recommended for general analysis purposes that median SRR be used, as shown in Figure 56. Further analysis of individual events should be performed as required. When an SRR chart is shown with only a single bar representing an entire seismic response, it will be assumed the median SRR is shown.

5.2.3 Interpreting Seismic Responses to Mining using SRR

Figure 57 is a median SRR chart for two seismic responses to mining. Responses A and B exhibit small and large median SRR values respectively.

A possible interpretation of the SRR chart shown is:

One of the seismic responses to mining shown in Figure 57 is primarily induced (Response A), and the other is primarily triggered (Response B).The median SRR value of Response A is 0.65 - relatively small. At least 50 % of all events within Response A show little deviation from a theoretically perfect induced response in the temporal parameters ($\widetilde{TAB}_N \approx 0$ and $\widetilde{TBE}_N \approx 0$), and the majority of events likely occur within the assumed mining-induced stress change zone of the blast ($\widetilde{DTB}_N < 1$).This indicates Response A is likely induced.

The median SRR rating of Response B is 3.2 - relatively large. At least 50 % of the response occurs beyond the assumed mining-induced stress change zone ($\widetilde{DTB}_N = 1$), but the majority of events likely occur within the maximum dimensions of the associated mining-induced stress change ($\widetilde{DTC}_N <1$). In other words, the seismic events are spatially well clustered relative to themselves, but not in close proximity to the blast location. This is indicative of complex or triggered seismicity. There is significant deviation in the temporal parameters relative to the induced response, indicating the majority of Response B is likely triggered and not complex.

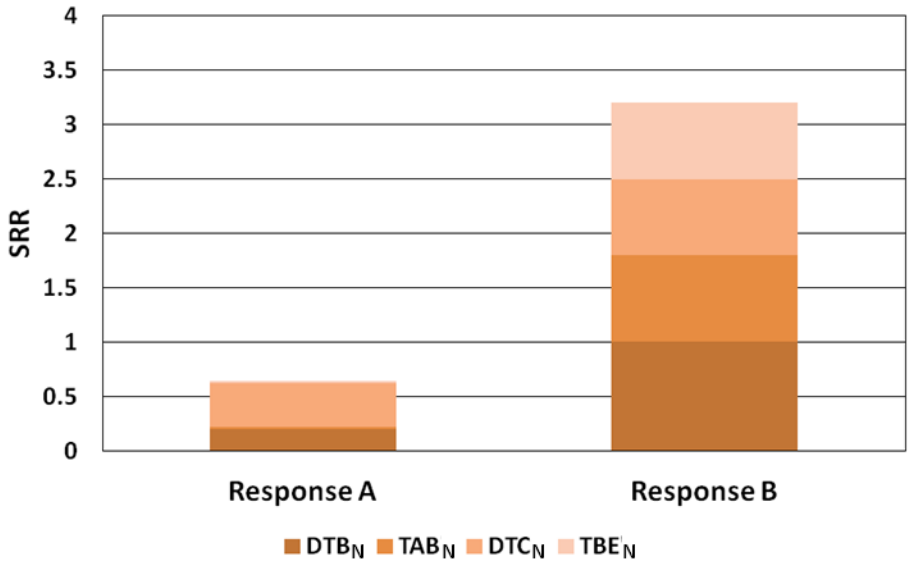

Figure 57: SRR chart for two seismic responses to mining, Response A and Response B.

An induced seismic response to mining has previously been shown in Figure 56. For induced seismicity, all SRP$_N$'s approach zero, summing to a relatively small SRR. Table 20 summarizes the observation guidelines surrounding SRR for induced seismic responses to mining.

Table 20: Summary of observation guidelines surrounding SRR for induced seismic responses to mining.

	Induced
SRR	Small SRR $0 \leq SRR \leq 1.5$

A SRR chart for the triggered seismic response to mining shown throughout Chapter 4, see Figure 33 and Figure 34, is shown in Figure 58. The previously discussed induced seismic response is also shown in Figure 58. The triggered response has a large median SRR (3.6), approximately five times the median SRR of the induced seismic response.

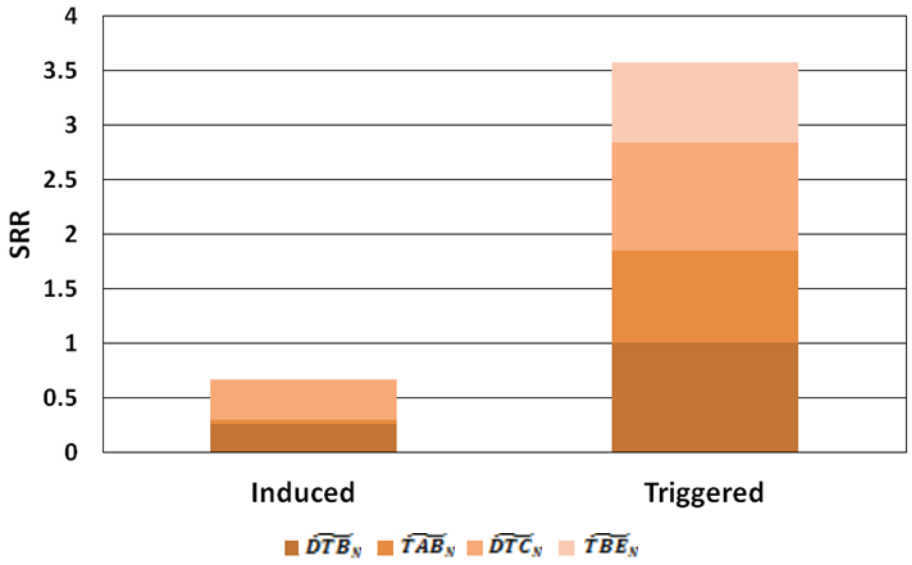

Figure 58: SRR chart for an induced and triggered seismic response to mining at LaRonde mine.

For a triggered seismic response to mining, all SRP_N values should be approaching or equal to one. As a result, triggered SRR values should be large. Table 21 summarizes the observation guidelines surrounding SRR for induced and triggered seismic responses to mining.

Table 21: Summary of observation guidelines surrounding SRR for induced and triggered seismic responses to mining.

	Induced	**Triggered**
SRR	Small SRR $0 \leq SRR \leq 1.5$	Large SRR $2.5 \leq SRR \leq 4$

A SRR chart for the complex seismic response to mining shown throughout Chapter 4, see Figure 35 and Figure 36, is shown in Figure 59. The complex response has a medium median SRR (1.25), approximately one third of the triggered and double the induced SRR values shown.

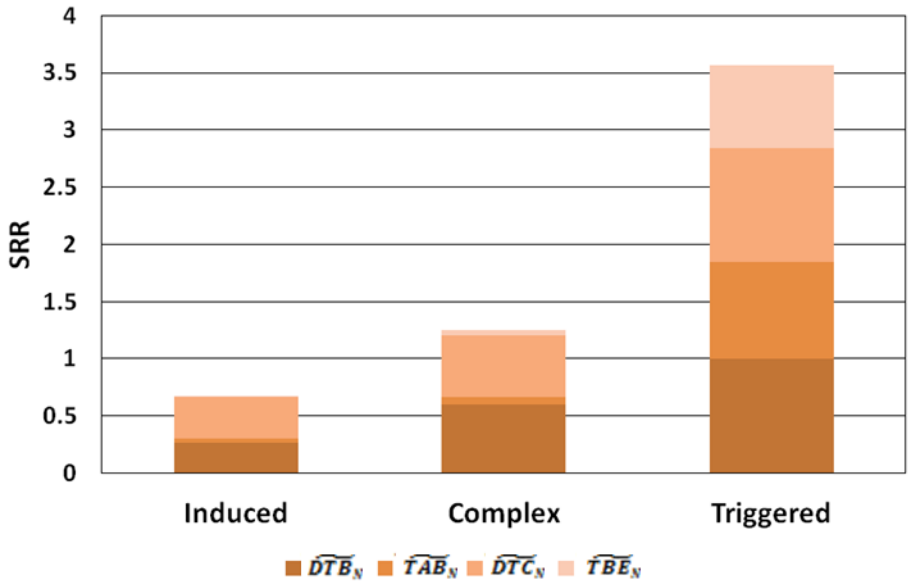

Figure 59: SRR chart for an induced, complex and triggered seismic response to mining at LaRonde mine.

Table 22 summarizes the observation guidelines surrounding SRR for induced, complex and triggered seismic responses to mining.

Table 22: Summary of observation guidelines surrounding SRR for induced, triggered and complex seismic responses to mining.

	Induced	**Complex**	**Triggered**
SRR	Small SRR $0 \leq SRR \leq 1.5$	Medium SRR $1 \leq SRR \leq 3$	Large SRR $2.5 \leq SRR \leq 4$

The median SRR depends on the relative proportion of induced and triggered seismicity contained within a seismic response, and may not be representative of the entire response. Cumulative distributions of SRR, as was shown for $SRP_{(N)}$'s in Chapter 4, can provide significant insight into seismic responses to mining - particularly for complex responses. In Figure 60, the cumulative distributions of SRR for an induced, triggered and complex seismic response at LaRonde mine are shown. The vast majority of events for each response fall into the observation guidelines range proposed in Table 22.

The more temporal and spatial outliers contained within a seismic response, the more complex it is likely to be. The 90^{th} percentile for the complex seismic response to mining at LaRonde, shown in Figure 60, corresponds to a SRR of approximately 2.5. Seismic events with a SRR $\geq$ 2.5 are most likely triggered, indicating that approximately 10% of the complex seismic response is triggered seismicity. Comparatively, the 55^{th} percentile for the complex response shown

corresponds to a SRR of approximately 1.5. Seismic events with a SRR ≤ 1.5 are most likely induced, indicating that approximately 55% of the complex seismic response is induced seismicity. The complex response contains seismic events spanning nearly the entire SRR range, however, with more than 50% of the response falling in the induced range, the response can be classified as complex and predominantly induced.

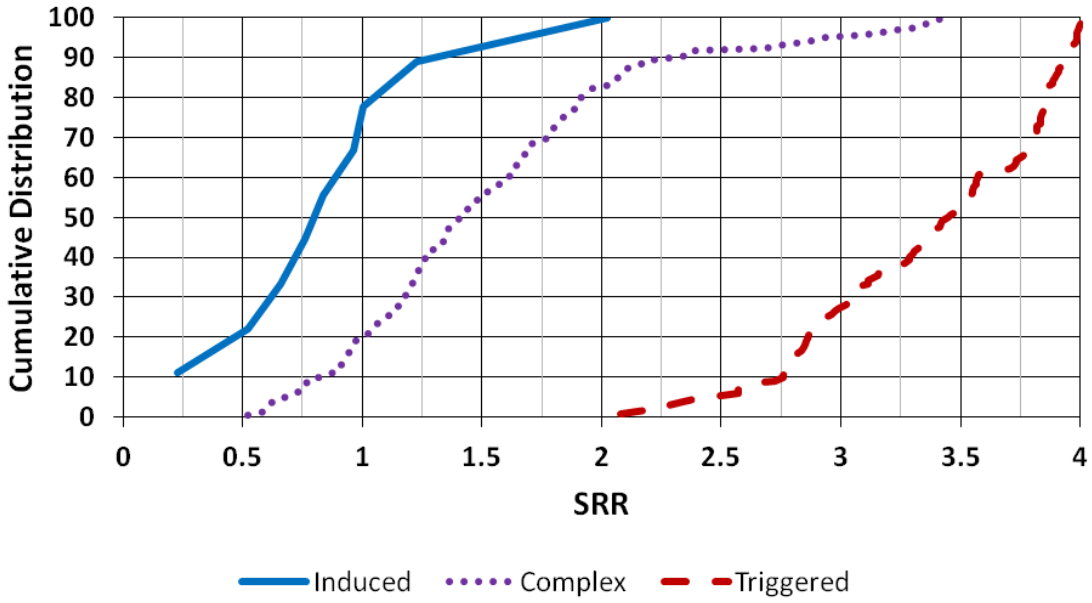

Figure 60: Cumulative distributions of SRR for all events in an induced, complex and triggered seismic response to mining at LaRonde mine. More information regarding individual seismic responses to mining can be found in Section 4.1.

5.2.3.1 SRR General Analysis Guidelines

The following guidelines are generalizations meant to aid in interpreting a seismic responses to mining using SRR:

- Identify any SRR values near zero or four, as these are strong indicators of induced and triggered seismic responses to mining respectively.
- If SRR is small, particularly temporal parameters shown on a SRR chart, it is indicative of an induced seismic response to mining.
- If SRR is large, particularly if $DTB_N = 1$ on a SRR chart, it is indicative of a triggered seismic response to mining.
- For SRR charts, identify any SRP_N values near zero or one, as these are strong indicators of induced and triggered seismic responses to mining respectively. When zero and one SRP_N values occur within the same population, it is indicative of a complex seismic response to mining.

When a clear interpretation cannot be made, complimentary seismic analysis tools and geological information may be helpful, including:

- Cumulative Distributions of Seismic Response Rating
- Cumulative Distributions of Normalized Seismic Response Parameters
- Seismic Source Parameter Based Seismic Analysis
- Cumulative Distributions of Seismic Response Parameters
- Spatial Plots (such as a plan view with mine development)
- Magnitude-Time History Charts
- Knowledge of Local Geomechanical Conditions

Further examples of this are provided in the LaRonde mine case study presented in Chapters 6 and 7.

5.3 Discussion

This chapter has introduced three tools to aid in interpreting seismic responses to mining: SRP_N charts, SRR charts and SRR. SRP_N and SRR charts are capable of conveying the same information, and the selection of one tool over the other is largely based on analysis objectives. SRP_N charts are better suited for comparing two or three discrete seismic responses to mining directly against one another, as was shown for an induced and triggered seismic response in Figure 51. The set of seismic responses at LaRonde mine, discussed throughout this chapter, are shown on a single SRP_N chart in Figure 61. When plotted directly on top of one another, the differences in individual SRP_N values, and overall area, are distinct.

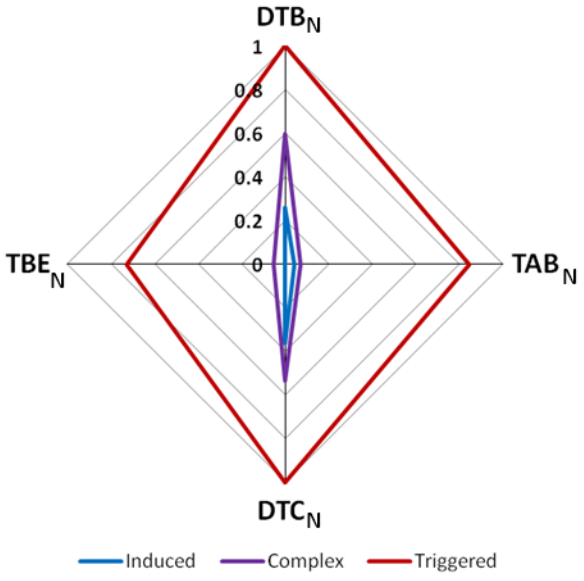

Figure 61: SPR_N chart for an induced, complex and triggered seismic response to mining at LaRonde mine.

When SRP_N values are similar across multiple responses however, or a large quantity of responses need to be plotted, SRP_N charts can become difficult to interpret due to data occlusion. In these cases, SRR charts may be better suited for seismic response interpretation. Figure 62 depicts the SRP_N chart (a) and SRR chart (b), for each individual seismic event contained within the induced seismic response to mining. While the SRP_N chart (a) is dominated by the response outliers, the inter-bar spacing of the SRR chart ensures each individual seismic event is distinguishable. Furthermore, it is possible to plot events in sequential order using a SRR chart, communicating additional information regarding trends in the nature of a seismic response over time.

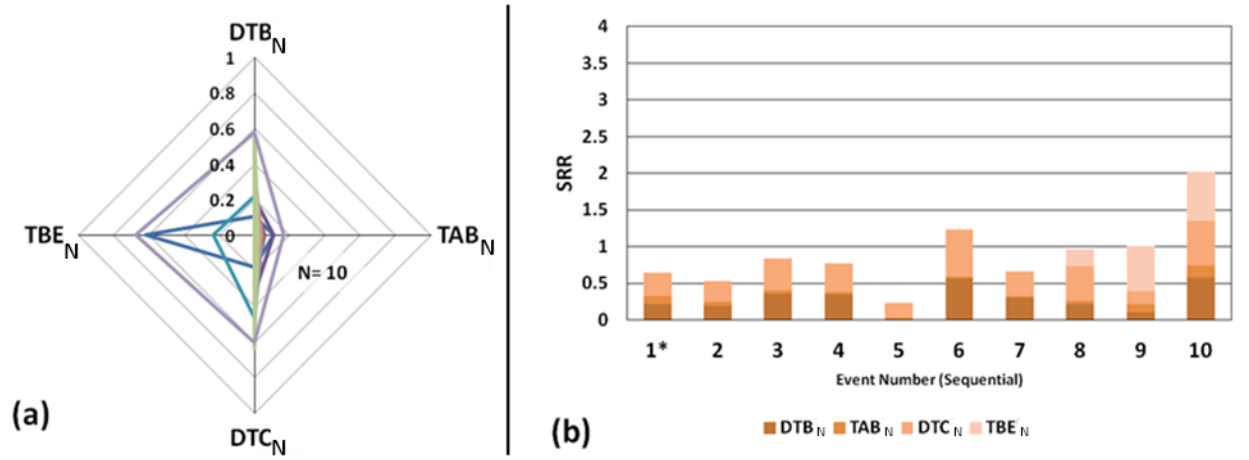

Figure 62: SRP_N chart (a) and SRR chart (b) for all individual seismic events occurring within an induced seismic response to mining at LaRonde mine.

5.4 Chapter Summary

Within this chapter, graphical and numerical tools for interpreting seismic responses to mining have been introduced. These tools have been demonstrated using examples of typical induced, triggered and complex seismic responses at LaRonde mine. Seismic Response Rating (SRR) is a single numerical value, ranging from zero to four, used to quantify the space-time relation of a seismic response to mining. SRR can provide significant insight into the nature of seismic responses, particularly when integrated with other analysis techniques, as demonstrated in the LaRonde mine case study contained within this thesis (Chapters 6 and 7). SRP_N charts and SRR use area and cumulative methods, respectively, to indicate if a seismic response to mining is more likely to be induced or triggered. Table 23 summarizes the observation guidelines of each seismic analysis tool for induced, complex and triggered seismic responses to mining.

Table 23: Summary table of SRP_N chart and SRR observation guidelines for induced, complex and triggered seismic responses to mining.

	Induced	**Complex**	**Triggered**
SRP_N Charts	Small Area *Temporal Parameters:* *$[TAB_N$ & $TBE_N]$* *Approaching 0* *Spatial Parameters:* *$[DTB_N$ & $DTC_N]$* *Approaching 0*	Medium Area *Temporal Parameters:* *$0 \leq TAB_N \leq 1$ &* *$0 \leq TBE_N \leq 1$* *Spatial Parameters:* *$[DTB_N$ & $DTC_N]$* *Typically Less than 1*	Large Area *Temporal Parameters:* *$[TAB_N$ & $TBE_N]$* *Approaching 0.5 to 1* *Spatial Parameters:* *$DTB_N = 1$ &* *DTC_N Approaching 1*
SRR	Small SRR *$0 \leq SRR \leq 1.5$*	Medium SRR *$1 \leq SRR \leq 3$*	Large SRR *$2.5 \leq SRR \leq 4$*

Chapter 6

6 Case Study Part 1: Background on Agnico Eagle's LaRonde Mine

6.1 Background on LaRonde Mine

Agnico Eagle's flagship operation, LaRonde, is a Canadian mine located near the town of Preissac in northern Quebec. It is a world-class Au-Ag-Cu-Zn massive sulphide lens complex, with over 3 million ounces of gold in proven and probable reserves (Agnico Eagle Mines Limited, 2017). Current mining extends more than 3,000 metres below surface, producing approximately 7,200 tonnes per day (Agnico Eagle Mines Limited, 2017).

LaRonde employs an open stoping bulk mining method to extract ore from three sub parallel sulphide lenses. The majority of production tonnes are extracted from a single lens, referred to as zone 20 (Turcotte, 2014), as shown in Figure 63. The other zones (7 and 21), are narrow and discontinuous sulphide lenses, ranging from 1 to 5 metres in thickness (Mercier-Langevin, 2010). All zones have a combined thickness of 1 to 40 m and a dip of 70-80° towards the South (Mercier- Langevin, 2010).

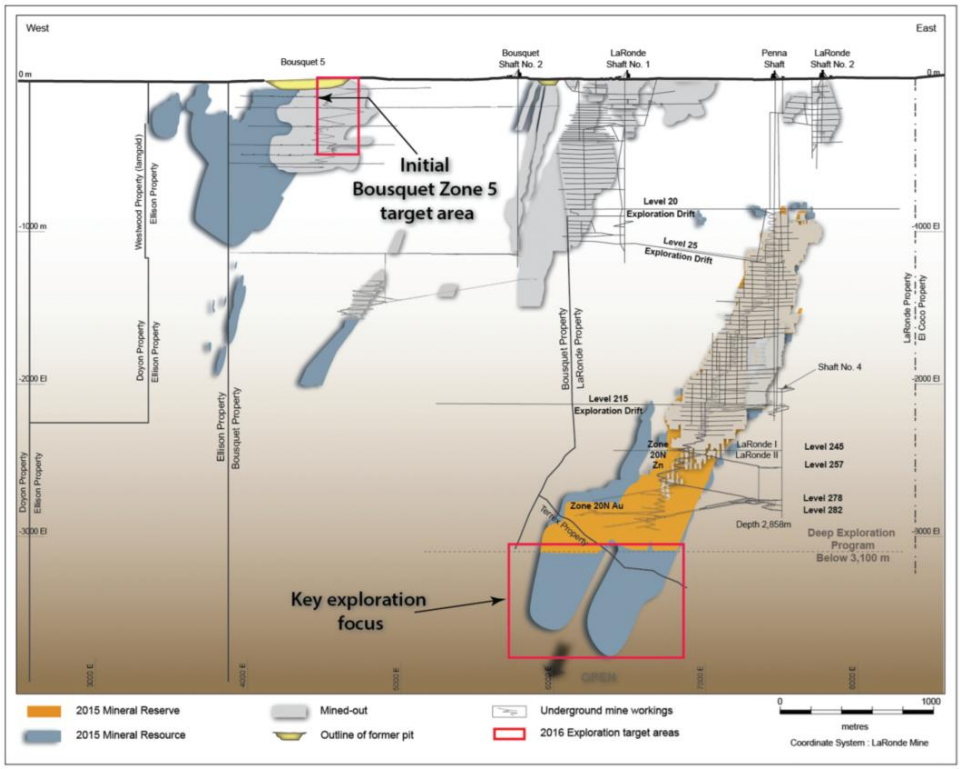

Figure 63: LaRonde mine composite longitudinal section (Agnico Eagle Mines Limited, 2017).

6.1.1 LaRonde Mining Practices

The majority of ore is extracted using transverse open stoping with a primary/secondary pyramid mining sequence. Traditional mine sequencing at LaRonde consists of stopes taken in a continuous retreating overhand pyramid. This method generates sill pillars between pyramids that have been particularly hazardous and difficult to extract in the past. In an effort to break through sill pillars as early as possible, the mine sequence was altered to include an underhand pyramid sequence as well as overhand stopes.

The average stope size at LaRonde is approximately 20,000 to 40,000 tonnes. In order to maintain the production rate of 7,200 tonnes per day, an average of 7 stopes must be turned over per month. To achieve this highly demanding schedule, both primary and secondary stopes are typically blasted in a single shot. A 30" raise bore is used to generate the initial slot void and the blast is carefully laid out using i-konTM electronic detonators. Paste fill is employed for backfilling of primary stopes, while secondary stopes are backfilled using dry rockfill (Mercier-Langevin, 2010).

6.1.1.1 Mine Excavation Size

Mine development drifts, which represent the majority of LaRonde mine excavations, measure approximately 4 metres in height by 5 metres wide. It is common however for mine drifts to intersect or require cut outs (typically for housing personnel, equipment and/or material), leading to intersections with increased spans. Typical stope sizes are 30 m high with widths for primary and secondary stopes of 13.5 m and 16.5 m, respectively (Mercier-Langevin, 2010). Stope thickness is generally the width of the orebody (to a maximum of 40 m).

6.1.2 Geology

LaRonde mine is located within the Blake River Group of the Abitibi Greenstone Belt. This belt spans Ontario and Quebec, and is home to many gold rich volcanogenic massive sulphide (VMS) deposits such as Kirkland Lake and Kerr Addison. Other deposits currently being mined in the direct vicinity of LaRonde include Agnico Eagle's Lapa mine and IAMGOLD's Westwood mine.

Complex geology plays a dominate role in the historic and current seismic response to mining at LaRonde. The orebody is located approximately 900 metres to 3,000 metres below surface, and has a strike length ranging from 240 to 530 metres. The *insitu* stress for various depths can be estimated from the equations presented in Table 24.

Table 24: *Insitu* stress gradients at LaRonde mine (Turcotte, 2014). DBS refers to depth below surface (in metres).

Component	Equation (MPa)	Plunge/Direction
σ_1	8.62 + (0.04 x DBS)	0°/000°
σ_2	5.39 + (0.0262 x DBS)	0°/090°
σ_3	0.0281 x DBS	-90°/000°

Table 25 indicates the intact rock strength for the common lithological units at LaRonde found at depth (approximately 2,900 m below surface). The basalt host rock is home to much of the permanent infrastructure, with haulage drifts and drawpoints located predominantly in the rhyolite and rhyodacite (Turcotte, 2014). The mechanical properties presented in Table 25 are further influenced by the degree of alteration present in the rock mass. The rhyolite and rhyodacite are characterized by localized sericite alteration zones, and tightly spaced (centimetre to decimetre) foliation striking parallel to the orebody and dipping south at 75-80° (Turcotte, 2014).

Table 25: Mechanical properties of intact rock at LaRonde 290 Level (Turcotte, 2014)

Rock Type	UCS (MPa)	E (GPa)
Basalt	100	50
Rhyolite	260	66
Rhyodacite	200	63
Semi-Massive Sulphide	200	70

6.1.3 Microseismic Monitoring at LaRonde

Bulk mining at such depth has resulted in a long history of seismic activity at LaRonde mine. The ESG microseismic monitoring system has undergone many upgrades since its implementation in 2003. The most influential change being a conversion from a Hyperion to a Paladin based system in late 2008. This change, from an analog to a digital system, enables greater frequency response and dynamic range. The microseismic monitoring system currently covers all active areas of the mine with more than 100 sensors, including approximately 15 triaxial sensors.

6.1.3.1 Magnitude Considerations at LaRonde

Magnitude scales have a logarithmic basis which allows for a large range of event sizes to be expressed in a short range of numbers. The main scale currently in use at LaRonde mine is Local magnitude. A Local magnitude value is calculated for all events recorded by the underground ESG microseismic monitoring system. This scale is well suited for analysis, as it provides a

consistent and accurate representation of the small and most of the large magnitude seismic events recorded. ESG does not provide a relative calibration of the Local magnitude scale.

The Richter magnitude scale is commonly recognized for reporting the magnitude of relatively large seismic events. Magnitude values are calculated using the distance of the sensors from the seismic source, and the peak displacement amplitude of the secondary seismic wave. Richter magnitudes are reported for large mining related seismic events recorded by the regional macroseismic network near LaRonde.

An empirical relation between Local and Richter magnitude for large seismic events at LaRonde mine has been suggested as (Brown, 2015):

$$M_R = M_L + 1 \tag{20}$$

where,

M_R = Richter Magnitude

M_L = Local Magnitude

This relation (Equation 20), is shown in Figure 64 for a population of large seismic events at LaRonde mine. Approximately 79% and 56% of all large events are contained within ±0.5 and ±0.3 of the relation respectively. Large seismic events have previously been defined in this thesis as having the potential to generate visible rock mass damage - Richter magnitudes one or greater (Butler, 1997). All future reference to large seismic events at LaRonde will refer to Local magnitudes zero or greater, as this approximates a Richter magnitude one.

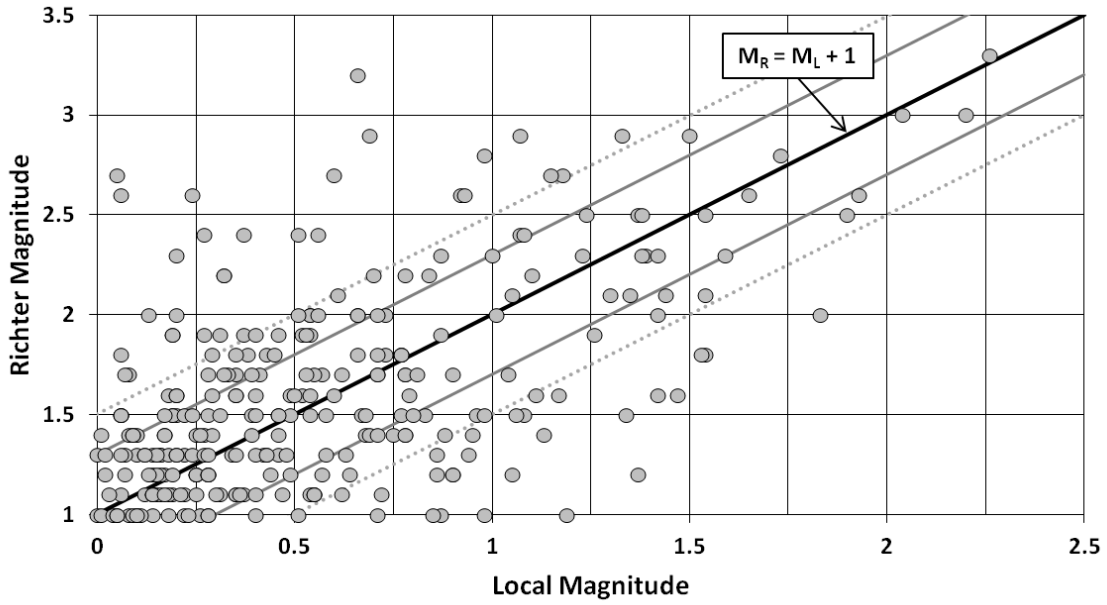

Figure 64: Relation between ESG microseismic monitoring Local magnitude and macroseismic monitoring Richter magnitude. The relation ($M_R = M_L + 1$) is shown, along with bounds of ±0.3 (solid lines) and ±0.5 (dashed lines). A total of 283 large events are considered.

6.1.4 Seismicity at LaRonde

Due to the large variations in geological conditions at LaRonde mine, the seismic response of the rock mass varies greatly - even across individual levels. Seismic responses can range from violent ejection (rockbursting) to aseismic squeezing depending on the rock mass characteristics (Turcotte, 2014). Concentrations of large seismic events correspond to concentrations of triggered seismicity, as these events represent energy release that is disproportionate to the mining-induced stress change of discrete mine blasts. The main areas at LaRonde mine with significant concentrations of triggered seismicity, as highlighted in Figure 65, are the Deep Footwall, Ramp, Hanging Wall and Sill Pillars (SP).

Figure 65 depicts a cross-sectional view of LaRonde mine showing all large and potentially damaging seismic events occurring from approximately 2009 to 2016. Concentrations of large magnitude events in the Deep Footwall are likely a reflection of failure along known geological structures - a triggered source mechanism. Concentrations of large events in the Ramp and Hanging Wall are likely a reflection of both failure along known geological structures, and large scale stress redistribution from significant orebody extraction. Locations of Sill Pillars (SP) are approximated by red boxes and also coincide with concentrations of large events. As mining pyramids converge, stress within intermediate sill pillars exceeds rock mass strength, and the pillars begin to fail and yield. This is an example of a larger scale rock mass failure process and triggered source mechanism.

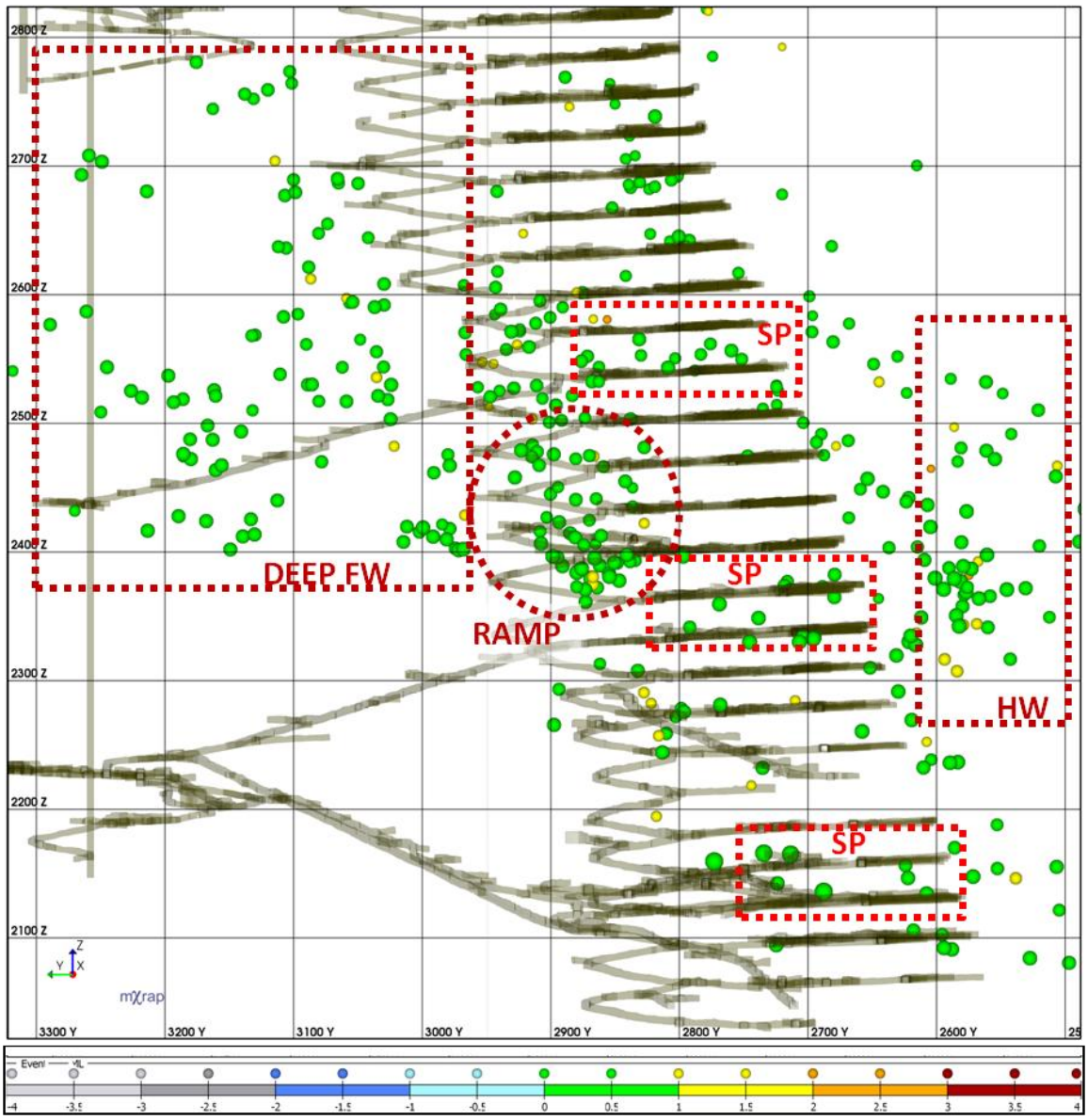

Figure 65: Cross-sectional view of LaRonde mine depicting concentrations of large and potentially damaging seismic events. Concentrations of large events in the Deep Footwall are likely a reflection of failure along known geological structures. Concentrations of large events in the Ramp and Hanging Wall are likely a reflection of both failure along known geological structures and large scale stress redistribution from significant orebody extraction. Sill Pillar (SP) locations are approximated by red boxes and coincide with concentrations of large events.

6.2 Case Study Time Period Selection

During daily blasting at LaRonde mine, both the size and location of blasts can vary significantly. For induced seismicity, this does not pose a significant challenge when identifying individual seismic responses to mining. Individual events of an induced seismic response occur in close spatial and temporal proximity to the blast location and blast time, respectively. Unlike induced seismic events however, triggered seismicity is not strongly defined in relation to

discrete stimuli or mine blasts. Triggered seismicity is related to larger scale rock mass failure processes, making it more challenging to associate specific triggered seismic events to single discrete stimuli. Mine blasting typically occurs every 12 hours at LaRonde, however in July of 2014, LaRonde mine underwent a 16 day shutdown period to facilitate routine mine maintenance. Shutdown periods, during which no excavation geometry changes occur, provide a unique opportunity to analyze seismic responses in the absence of mine blasting (Brown and Hudyma, 2018b).

Figure 66 is a Magnitude-Time History chart for LaRonde mine showing all seismicity recorded during the mine shutdown and two months preceding. The mine shutdown (approximated by a red rectangle), begins on July 1, 2014 and ends on July 17, 2014. Mine blasts, shown along the x-axis, end abruptly with the onset of the shutdown. Relative to the two months preceding, a general decline in seismicity is observed during the shutdown period. This is reflected in a slope decrease in the cumulative number of events line - particularly in the latter half of the shutdown period. The rate of occurrence for significant ($M_L \geq -1$) and large ($M_L \geq 0$) magnitude seismic events, shown in Figure 67, is particularly diminished during the shutdown.

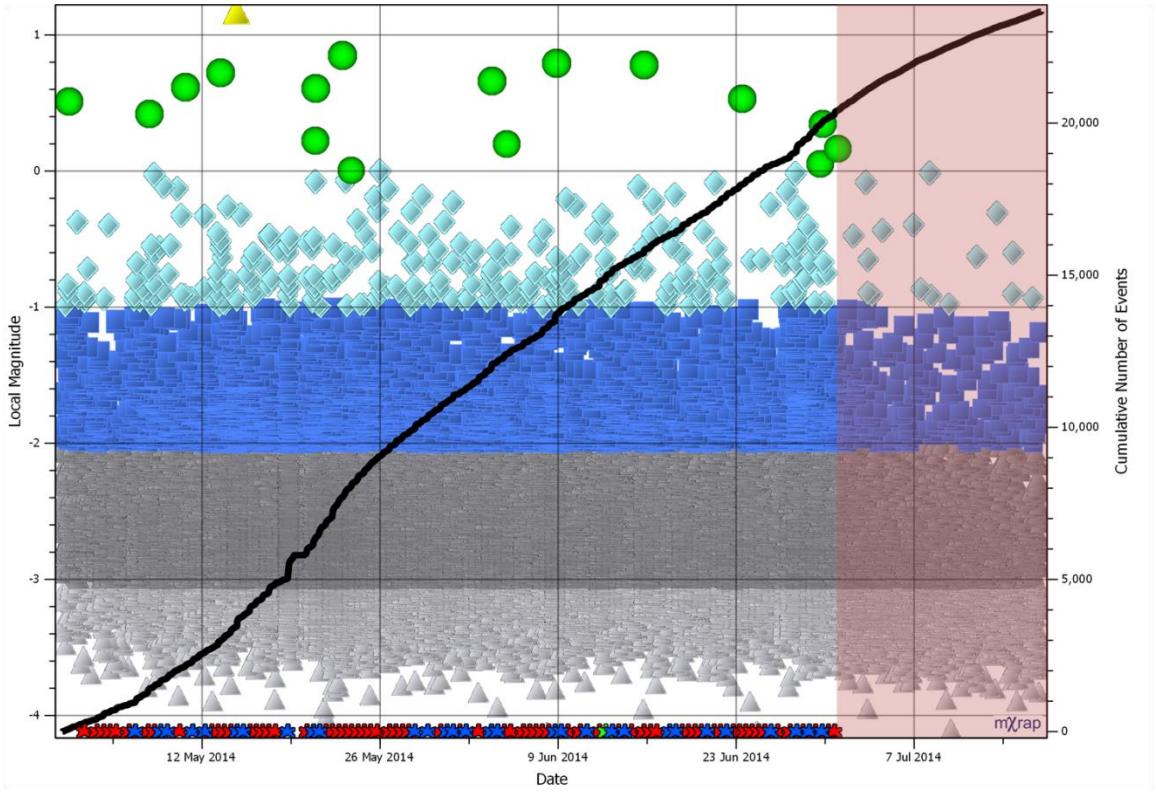

Figure 66: Magnitude-Time History chart of the LaRonde mine shutdown (July 1- 17, 2014) and two months preceding (May and June, 2014). The shutdown period is approximated by a red rectangle. Mine blasts are shown along the x-axis, coloured according to type (red for development blasts, blue for production blasts and green for raise blasts).

In the two months preceding the shutdown, a total of 267 significant ($M_L \geq -1$) and 16 large ($M_L \geq 0$) magnitude seismic events occurred at LaRonde mine. During the mine shutdown, the rate of

significant events decreased by approximately 77% - on average 1 significant event per day during the shutdown relative to 4.4 significant events per day during the two months preceding. Only one large magnitude seismic event occurred during the shutdown. This event is relatively small (M_L = 0.16), and occurred on July 1, 2014 at 00:24:08 - only 7 hours following the final mine blast preceding the shutdown. This large event is likely in part related to the recent mining-induced stress change, and is likely not a true reflection of the seismic response to mining during mine shutdown conditions. On average, LaRonde mine experienced 0.26 large events per day, or 1 large event every four days, during the two months preceding the shutdown. Subsequent to the single large event on July 1st, no large magnitude seismic events occurred during the LaRonde mine shutdown period.

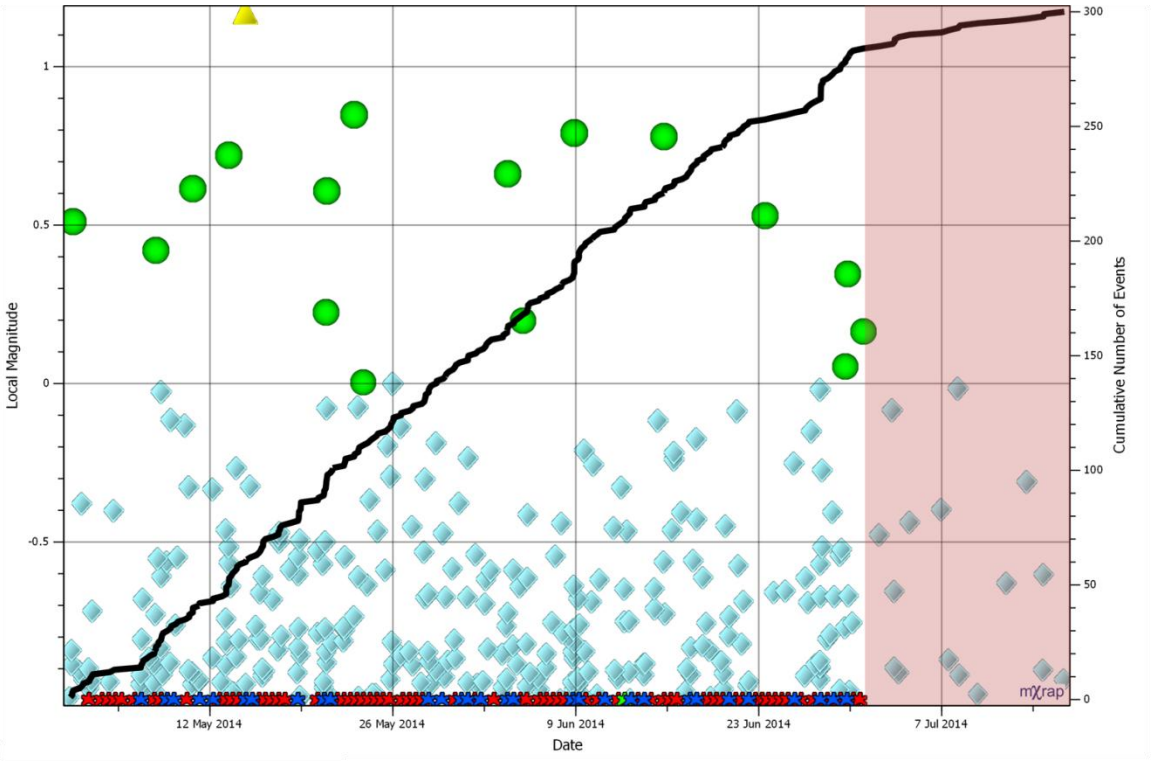

Figure 67: Magnitude-Time History chart of the LaRonde mine shutdown (July 1- 17, 2014) and two months preceding (May and June, 2014). Only significant seismic events ($M_L \geq -1$) are shown. The shutdown period is approximated by a red rectangle. Mine blasts are shown along the x-axis, coloured according to type (red for development blasts, blue for production blasts and green for raise blasts).

During the two months preceding the shutdown, May and June 2014, regular mining operations occurred and it is expected that all seismic responses will be induced, complex or triggered. During the shutdown however, no mine blasting occurred, and it is expected that all seismic responses will be triggered. In the absence of mine geometry changes, there should be no significant mining-induced stress change and consequently no induced or complex seismic responses to mining.

The use of the shutdown and pre-shutdown time periods at LaRonde mine for a case study of seismic responses is particularly advantageous for observing triggered seismicity. Relative to induced seismicity, triggered seismicity can be challenging to quantify during regular mining activities (Brown and Hudyma, 2018b). The use of a short time period, 77 days ranging from May 1, 2017 to July 17, 2017, ensures any spatial migration of larger scale rock mass failure processes (typically associated with triggered seismicity), is minimized. As such, the approximate location of triggered seismic responses at LaRonde mine should be consistent in the shutdown and pre-shutdown time periods.

6.3 Identifying Seismic Responses to Mining

The Seismic Response Parameters (SRP's), as defined in Chapter 4, are used to provide meaningful insight into seismic responses to mining at LaRonde. For the application of SRP's, seismic responses to mining should concentrate around individual and independent seismic source mechanisms. In other words, all events contained with a seismic response should exhibit similar spatial and temporal characteristics, as they are driven by the same source mechanism. The exception to this being complex seismicity, which represents the superimposition of two different source mechanisms in space and time. This assumption, that individual seismic responses to mining surround discrete source mechanisms throughout a mining environment, is discussed further in Chapter 8.

Broad spatial filtering methodologies can be ill-suited for identification of individual seismic responses to mining. Because complex seismicity represents the superimposition of two responses (or source mechanism) in space and time, characteristics of complex seismicity can be observed in both true and artificially superimposed responses. Disley (2014) describes a seismic response to mining with the spatial and temporal characteristics of both induced and triggered seismicity, as shown in Figure 68.

The response shown is associated with a small blast, indicated by a blue star. A strong seismic response, circled in red, is observed in close spatial (a) and temporal (b) proximity to the blast. This likely represents induced seismicity. A second response, located approximately 120 metres from the blast location and associated with a shear plane, is circled in black. This response is observed spatially (a) and temporally (b) distant to the blast, and likely represents triggered seismicity.

Because Disley (2014) employs a search radius of 150 metres from the blast location to spatially filter events, shown as the blue sphere in Figure 68, the induced and triggered seismic responses become joined together into a single population - artificially superimposed in space. SRP's would most likely characterize this response as complex, which is not accurate, as the induced and triggered responses are spatially distinct. All seismic responses considered in this work have

been manually checked to ensure there is no inclusion of erroneously superimposed dual or multiple responses.

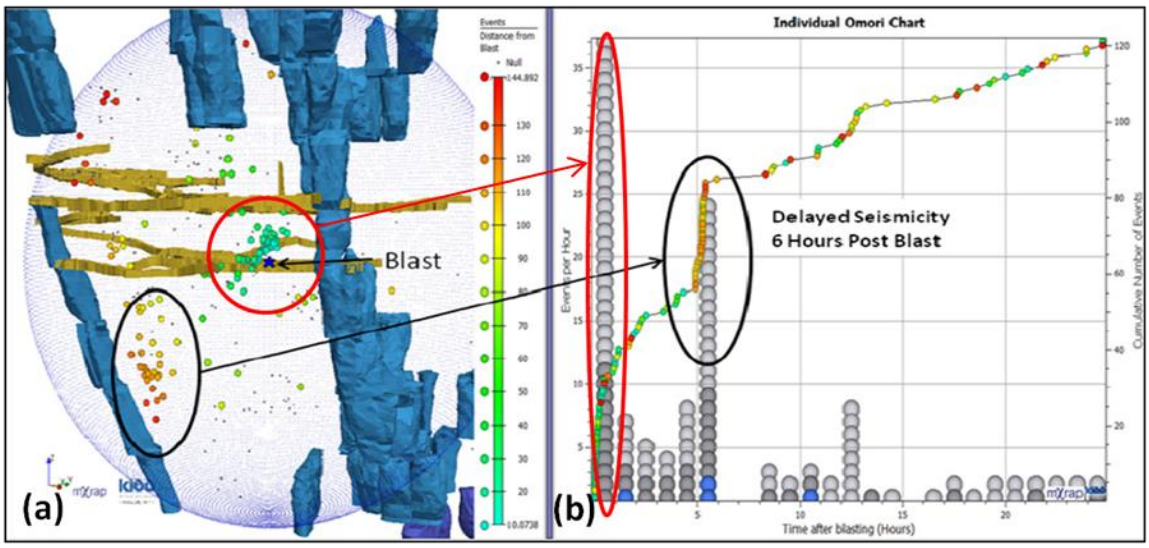

Figure 68: Spatial plot (a) of a seismic response to mining and an Omori chart (b) (adapted from Disley, 2014). The response exhibits spatial and temporal characteristics of both induced and triggered seismicity.

When selecting a methodology for identifying seismic responses to mining, the main considerations should be space and time (Woodward, 2015; Woodward *et al.*, 2017). A Single-Link Clustering algorithm paired with a moving temporal window was selected for identifying seismic responses in this case study, and is discussed throughout this section. The main considerations of this methodology are:

- Temporal Considerations
- Spatial Considerations
- Seismic Response Stimuli Considerations

6.3.1 Temporal Considerations

A primary objective of this thesis is to relate seismic responses to discrete stimuli (mine blasts). LaRonde mine blasts twice a day at approximately 05:40h and 17:40h. At each of these times, it is possible for the mine to blast multiple development headings as well as production stopes. Each blast induces a significant stress change which is reflected in the occurrence of seismicity (rock mass failure), directly following the blast. Previous research has shown the vast majority of stress change associated with mine blasting occurs within the first few minutes (Hudyma *et al.*, 1994), to few hours following the blast (Mendecki, 2001; Mendecki and Lynch, 2004; Kgarume *et al.*, 2010; Woodward and Wesseloo, 2015).

Unlike induced responses, which have a strong temporal beginning followed by an exponential event rate decay (Omori, 1894; Utsu, 1961; Vallejos and McKinnon, 2010), triggered responses

have no defined temporal limits. These types of responses appear to have neither a beginning nor end, and do not have a strong temporal association with blasting. Triggered seismicity does not result solely from the influence of a single mine blast, but rather cumulative extraction over time. Any time period used to capture triggered seismic responses to mining is therefore arbitrary.

The minimum quantity of seismic events required to identify a seismic response or population depends largely on site-specific factors and analysis objectives. As a general rule, the larger a seismic population is, the more likely it is to be well behaved, and amenable to conventional seismic analysis (Hudyma, 2008). Methodologies should aim to identify seismic responses that are as large as possible, while simultaneously ensuring individual responses are sufficiently isolated from one another in space and time.

It is common practice for mines to successively blast development headings in close spatial proximity. Because development blasts are small, approximately 200 tonnes of material broken per blast, the relative spatial change from one blast location to another can be small. This is particularly true for periods of successive blasting. To address this issue, each blasting period should be considered independently when identifying individual seismic responses to mining.

Figure 69 depicts seismicity occurring during a 12 hour time period (17:40h to 5:39h), between two successive blasting periods at LaRonde mine. Two mine development blasts, shown as red stars, are fired at the beginning of the 12 hour time window (17:40h). Throughout the mining environment, individual seismic events naturally cluster spatially around temporally isolated rock mass failure mechanisms. Induced, complex and triggered seismic responses to the development blasts are spatially approximated in Figure 69, outlined in blue, purple, and red, respectively.

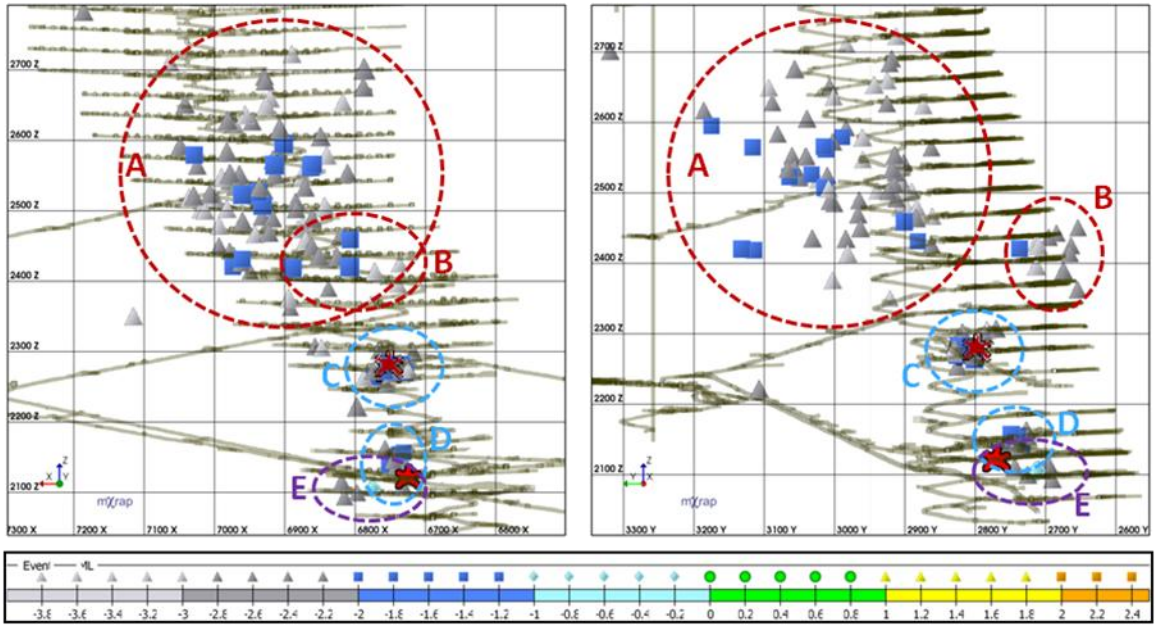

Figure 69: Longitudinal and cross-sectional projections of LaRonde mine showing two mine development blasts (red stars) and seismicity occurring within the following 12 hours. Approximate spatial clusters of seismic events are shown outlined in blue, purple and red for induced, complex and triggered responses respectively.

For LaRonde mine, the maximum temporal limits for response identification are 12 hours, as this is the time between successive mine blasts. When the time period is extended beyond 12 hours, individual seismic responses to mine blasts are no longer isolated in time, and become increasingly challenging to separate spatially. Figure 70 depicts seismicity occurring during a 24 hour time period - considering the blasting period shown in Figure 69 and the subsequent blasting period (two additional development blasts). The inclusion of the second blasting period results in a significant challenge, as seismic events shown can no longer be spatially attributed to discrete stimuli (mine blasts), and four new responses appear (F, G, H and I).

For the application of SRP's to seismic data, individual seismic responses should be identified such that they concentrate around a single source mechanism. In Figure 69, natural seismic responses are spatially isolated with few outliers (relative to Figure 70). When response stimuli locations are temporally overlapped however, as shown in Figure 70, it becomes a biased process to spatially associate individual seismic events with discrete mine blasts.

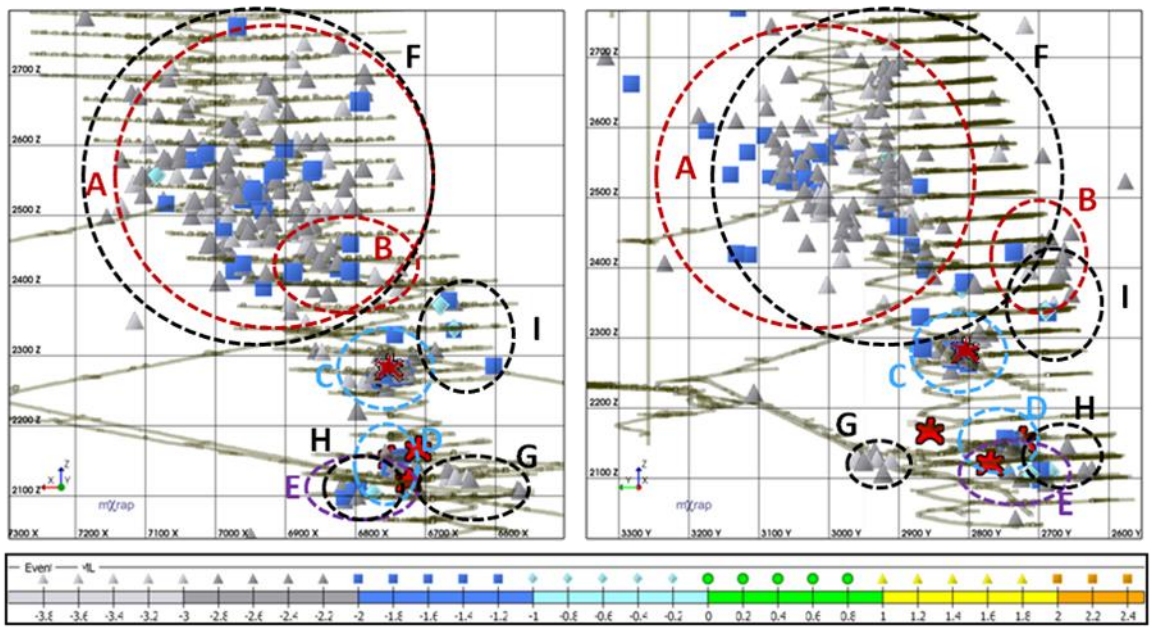

Figure 70: Longitudinal and cross-sectional projections of LaRonde mine showing four mine development blasts (red stars) and seismicity occurring over a 24 hour time period. Approximate spatial clusters of seismic events are shown outlined in blue, purple and red for previously identified clusters (Figure 69), and black for new clusters.

To achieve the objective of identifying individual seismic responses to mining, this methodology employs a 12 hour temporal window for response identification. Time windows range from approximately 05:40h to 17:39h and 17:40h to 5:39h, isolating the maximum temporal periods between successive mine blasts. The 12 hour time window will be sufficient to represent induced seismic responses, and is the maximum time period possible to represent complex and triggered seismic response to mining - based on the LaRonde specific considerations discussed above. By considering discrete blasting periods independently, individual seismic responses to mining are isolated in time, and can further be isolated in space.

6.3.2 Spatial Considerations

To investigate the applicability of single-link clustering, as discussed in Section 2.5.3.2, to the spatial identification of individual seismic responses at LaRonde mine, a sample period is used. The sample period ranges 15 days, and represents approximately one fifth of the entire time period of interest (May 1, 2014 to July 17, 2014). Figure 71 depicts the cumulative distribution of single-link lengths for seismic events at LaRonde mine within 12 hours of blasting for the sample period. Similar to the conclusions of Frohlich and Davis (1990), no change in slope is present to indicate a natural clustering length. It is evident from Figure 71 however, that a reasonable maximum single-link length (d-value) likely falls between 2 and 100 metres, as the sample slopes remains relatively constant for these link lengths.

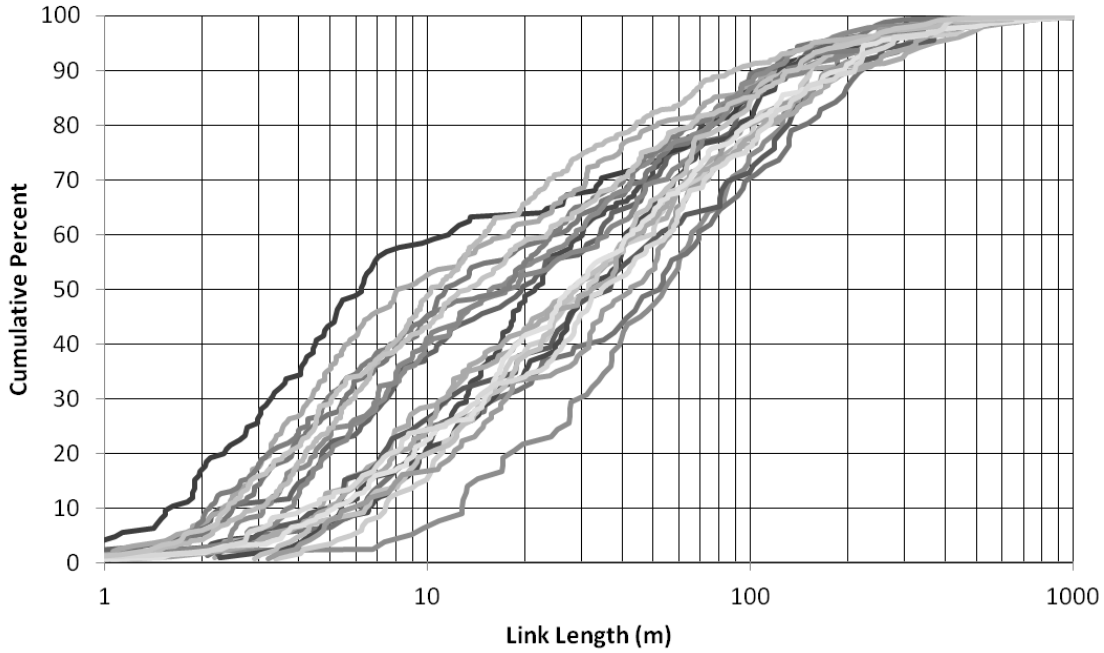

Figure 71: Cumulative distribution of single-link lengths for events occurring within 12 hours of mine blasting from May 1, 2014 to May 16, 2014 at LaRonde mine.

To facilitate meaningful seismic analysis, seismic event populations must be of a sufficient size. Sufficient size is dictated by site-specific conditions, the analysis technique being applied, and the objectives of that analysis technique. For this methodology, individual seismic response populations should aim to be as large as possible, but avoid linking spatially unrelated clusters.

Figure 72 depicts the seismic response to mining for the same time period and seismicity shown in Figure 69, however seismic events are coloured according to single-link spatial clustering using a single-link d-value of 20 metres. The primary objective of this clustering methodology is not to ensure clusters are representative of all seismicity at LaRonde mine, but instead to ensure that clusters are representative of individual seismic responses to mining (source mechanisms).

A relatively small d-value of 20 metres has been selected to best accurately represent induced seismic responses to mining. Maintaining the assumption of a 10 metre location error, a 20 metre clustering distance ensures that events located within 10 metres on either side of a single blast location will be identified as occurring within the same seismic response. In Figure 72, two clusters representative of induced seismic responses to mining are shown outlined in blue. Other event clusters are very small, in most cases with only one or two seismic events located within 20 metres.

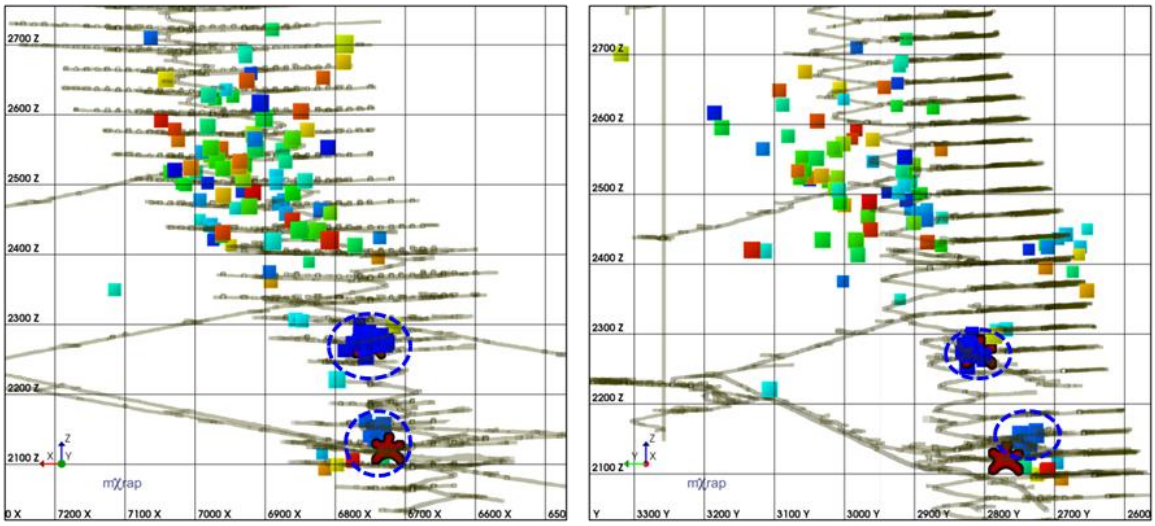

Figure 72: Longitudinal and cross-sectional projections of LaRonde mine showing two mine development blasts (red stars) and seismicity occurring within the following 12 hours. This is the same time period shown in Figure 69. Event colours correspond to spatial clusters using a d-value of 20 metres. Induced seismic responses to mining are outlined in blue.

While a d-value of 20 metres accurately captures induced seismic responses at LaRonde, it does not accurately capture triggered seismic responses. For LaRonde mine in particular, triggered responses are typically located in the deep footwall (Section 6.1.4). This area is remote from most mine excavations, and therefore exhibits relatively poor microseismic monitoring coverage. As such, location accuracy is somewhat reduced, relative to events located within the mine development, and smaller magnitude seismic events are not always reliably recorded. To accurately represent triggered seismic responses in this area of the rock mass, a larger d-value is required.

Figure 73 depicts the seismic response to mining for the same time period and seismicity shown in Figure 72. Seismic events are coloured according to single-link spatial clustering using a d-value of 100 metres. This maximum d-value was selected to better capture triggered seismic responses to mining, which are outlined in red. With the increased d-value however, induced seismic responses are no longer representative of individual source mechanisms, and become erroneous complex seismic responses - shown outlined in purple.

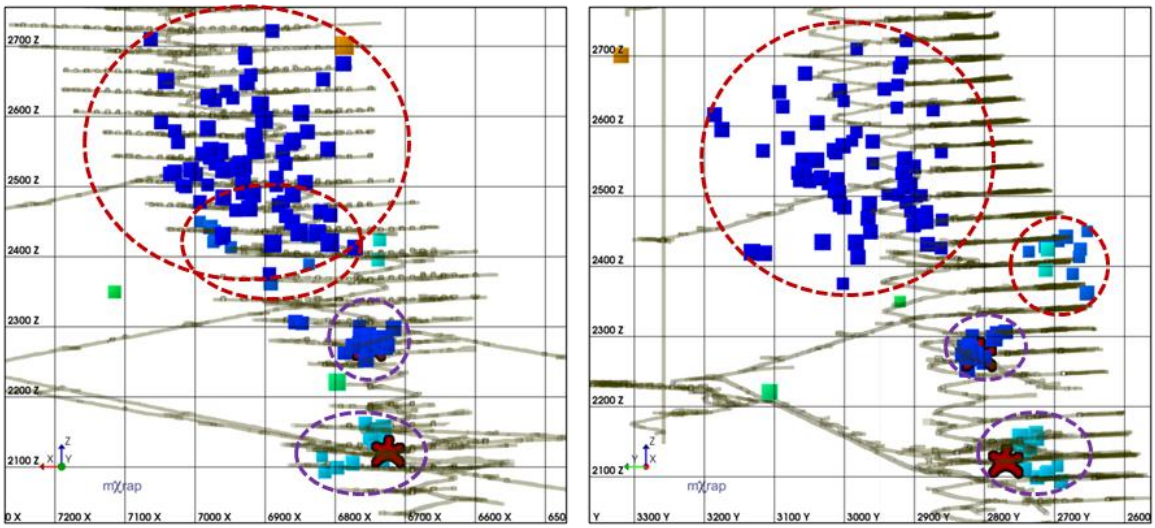

Figure 73: Longitudinal and cross-sectional projections of LaRonde mine showing two mine development blasts (red stars) and seismicity occurring within the following 12 hours. This is the same time period shown in Figure 69. Event colours correspond to spatial clusters using a d-value of 100 metres. Triggered and previously induced (Figure 72) seismic responses to mining are outlined in red and purple, respectively.

It is evident from Figure 72 and Figure 73 that while smaller d-values accurately capture induced seismic responses to mining at LaRonde, larger d-values more comprehensively capture triggered responses at LaRonde. For the purposes of this case study, a d-value of 20 metres will be used to identify induced and complex seismic responses to mining, and a d-value of 100 metres will be used to identify triggered seismic responses. A d-value of 100 metres will also be used for the mine shutdown responses, as the mine shutdown period is expected to contain triggered seismic responses to mining.

6.3.3 Seismic Response Stimulus Considerations

LaRonde mine is well suited for this type of case study as the operation maintains a blasting record. The primary purpose of the blasting record is to track production stope blasts, however development blasts are commonly recorded. This record is the primary source of information regarding blast times and locations for the time period of interest. Where blast data is not available, and cannot be inferred without ambiguity, seismic responses to mining are omitted from the case study.

The vast majority of blasts at LaRonde mine are relatively small development blasts. While the basic concepts behind induced seismic responses to mining are the same for development and production blasts, production stope blasts are much larger and consequently have a significantly increased mining-induced stress change zone. For this reason development and production seismic responses to mining are considered separately, as suggested by Richardson and Jordan (2002).

Due to the nature of bulk open stoping mining methods, there are relatively few production blasts contained within the time period of interest (May 1 - July 17, 2014). In order to ensure a sufficient quantity of production stope blasts are included in the study, the time period for identifying induced seismic responses to mine production blasts is extended by five months (January 1, 2014 to July 1, 2014).

Chapter 7

7 Case Study Part 2: Induced, Triggered and Complex Seismic Responses at LaRonde Mine

This chapter presents a series of three independent case studies focusing on variations in seismic responses to mining at Agnico Eagle's LaRonde mine:

- Case Study I - Induced Seismic Responses to Mining
- Case Study II - Triggered Seismic Responses to Mining
- Case Study III - Complex Seismic Responses to Mining

The seismic analysis software mXrap (Harris and Wesseloo, 2015), is the primary software utilized in the LaRonde mine case studies. The objective of each case study is to demonstrate the concepts developed in Chapter 4 and Chapter 5, primarily Seismic Response Parameters (SRP's), are applicable to real mine seismic data. Using 189 individual seismic responses to mining, the case studies demonstrate that SRP and SRP_N distributions exhibit the fundamental characteristics previously discussed in Chapters 3, 4 and 5.

7.1 Case Study I: Induced Seismic Responses to Mining

Within this case study, two series of induced seismic responses to mining are considered. One series corresponds to development blasting (a few hundred tonnes of fragmented rock), and the other corresponds to production blasting (several to tens of thousands of tonnes of fragmented rock). Table 26 summarizes the specific parameters used to identify the two different types of induced seismic responses to mining. Because production stopes have a significantly larger excavation radii, 15 metres relative to 2.5 metres, they also have a larger assumed mining-induced stress change zone, 85 metres relative to 22.5 metres.

Table 26: Summary of parameters used to identify the induced seismic responses to mining at LaRonde and the common factors used in the calculation of SRP_N's.

		Induced: Production Mining Response	Induced: Development Mining Response
Response Identification	**Single-Link Clustering d-value**	20 metres	20 metres
	Temporal Window	12 hours	12 hours
	Time Period	01/2014 - 07/2014	05/2014 - 07/2014
Calculation of SRP_N's	**Excavation Radius**	15 metres	2.5 metres
	Location Error Factor	10 metres	10 metres
	Assumed Mining-Induced Stress Change Zone	85 metres from Excavation Boundary	22.5 metres from Excavation Boundary

7.1.1 Induced Seismic Response Descriptions

A total of 19 production blast induced seismic responses to mining are considered in this case study. Figure 74 and Figure 75 depict the seismic event and response centroid locations, respectively, for the induced seismic responses to mining associated with production blasting. Mine production blasts are represented by blue stars, and concentrate in upper (above 2,300z) and lower (below 2,200z) areas of LaRonde mine.

The upper area corresponds to secondary stope blasting. Secondary stope blasts are typically larger (tens of thousands of tonnes of fragmented rock), and occur in rock mass areas with significant pre-existing damage. When secondary stopes are mined, the local rock mass has already experienced development and primary stope mining, which, for a deep and highly stressed mine like LaRonde, typically generates significant rock mass fracturing and failure. Where a failing volume of rock mass is spatially defined by an outline of seismic events is referred to as a seismogenic zone (Duplancic, 2001). This is most evident in the population of seismic events migrating out into the hanging wall in Figure 74 (beyond 2,600y in the cross-sectional projection shown). This seismicity wraps upwards, likely following paths of stress concentration around a failed or failing zone of the rock mass in the hanging wall.

When an area of a rock mass adjacent to a newly formed excavation has failed, the mining-induced stress is shed to more competent rock that is capable of sustaining the stress increase, and stress redistributes further away from the excavation boundary. Because the post-failure load deformation characteristics of the confined rock mass are typically quite variable, the degree to which mining-induced stress will be shed beyond an excavation boundary is also highly variable. Due to the assumed mining-induced stress change zone of SRP_N's, 5 excavation radii plus a Location Error Factor, seismicity that is not directly adjacent to an excavation boundary due to stress shedding will likely be included in the induced seismicity zone.

The lower area (below 2,200z) in Figure 74 corresponds to primary stope blasting. Primary stope blasts at LaRonde are typically relatively small (thousands of tonnes of fragmented rock), and occur in pre-failure areas of the rock mass; versus yielded ground for secondary stope blasts at LaRonde. Due to the relatively low extraction ratio during primary stope blasting, the rock mass is relatively well confined. As such, the seismic events in the lower area are concentrated tightly around mine blast locations, relative to the upper area (above 2,300z). This is further reflected in the response centroid locations, which align closely with blast locations for primary stopes but not secondary stopes, shown in Figure 75.

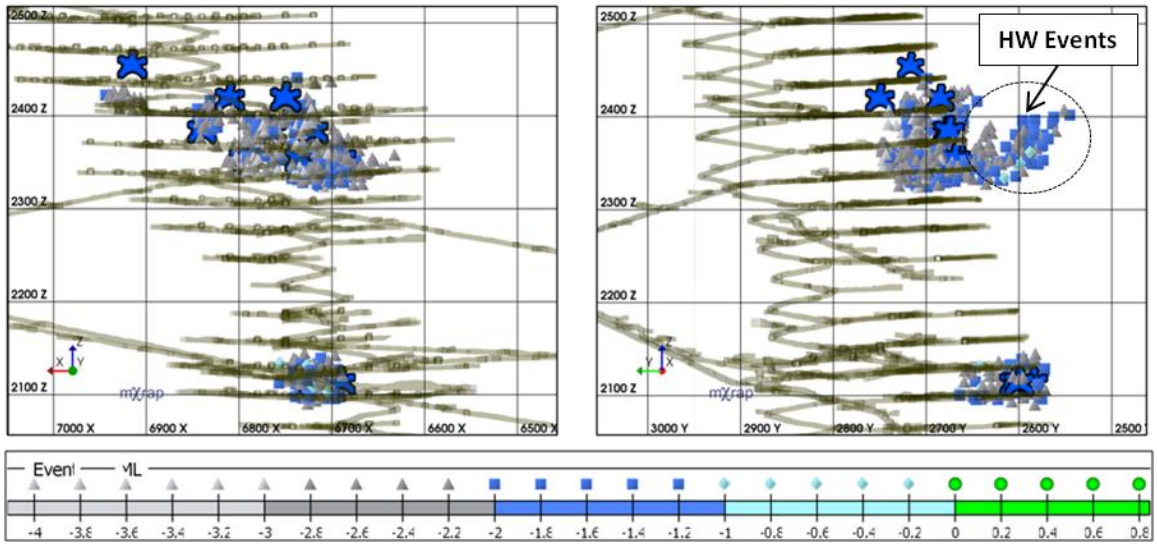

Figure 74: Longitudinal and cross-sectional projections of LaRonde mine showing induced seismic responses to mining and associated mine production blasts (blue stars).

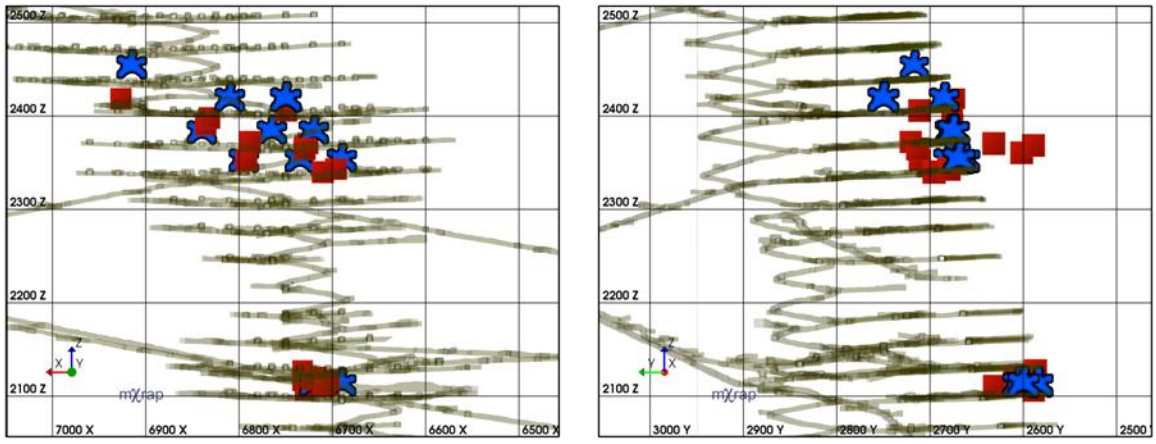

Figure 75: Longitudinal and cross-sectional projections of LaRonde mine showing the induced response centroid locations (calculated as shown in Equation 12), and associated mine production blasts (blue stars). Distances between response centroids and mine blasts are quantified in Figure 81.

Figure 76 is a Magnitude-Time History chart for the production blast induced seismic responses to mining (shown in Figure 74). Mine production blasts are shown along the x-axis as blue stars, and seismic events are coloured according to SRR. Each seismic response corresponds to a

distinct step in the cumulative number of events line - indicative of induced seismicity. SRR values are typically between 0 and 1.5, and no large magnitude seismic events ($M_L \geq 0$), are contained within the induced seismic responses to production blasting.

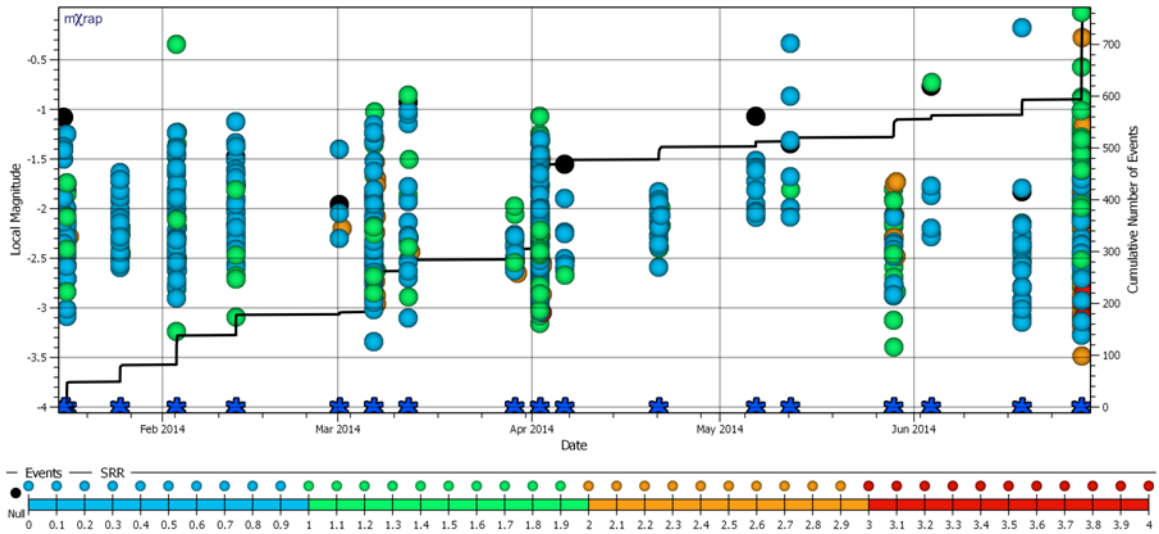

Figure 76: Magnitude-Time History chart for nineteen induced seismic responses to mining at LaRonde. Mine production blasts are shown along the x-axis as blue stars. Seismic events are coloured according to individual Seismic Response Rating (SRR). The first event in each individual seismic response is coloured black, as these events have no TBE_N parameters and consequently may exhibit uncharacteristic SRR's.

A relative frequency distribution of SRR values for the production blast induced seismic responses is shown in Figure 77. The majority of SRR values fall between 0 and 1.5, indicative of induced seismicity. There is a strong dominance of relatively small SRR values, indicating many individual SRP_N's likely approach zero. Figure 78 is a cumulative distribution of the same SRR values shown in Figure 77. The median value is slightly less than 1, with approximately 80% of all individual events exhibiting SRR values within the proposed guideline of SRR less than 1.5 (Table 23).

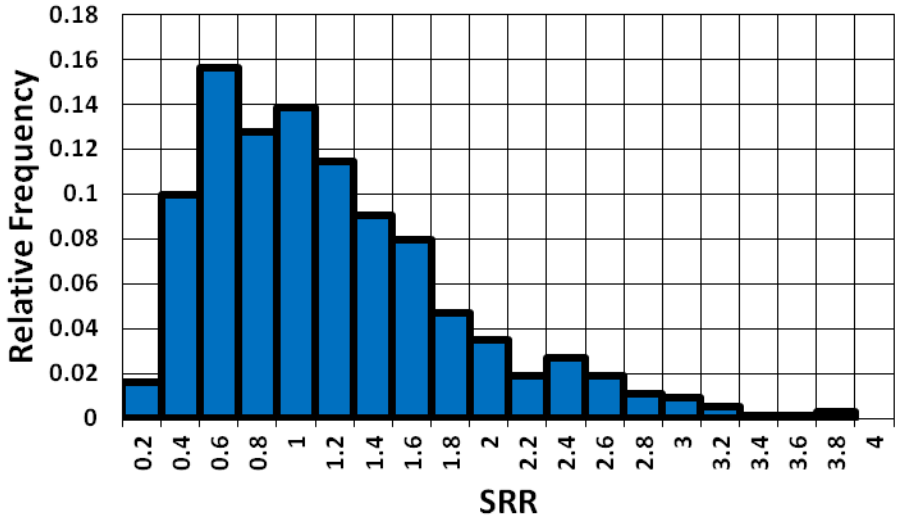

Figure 77: Relative frequency distribution of SRR values for all of the events in the nineteen production blast induced seismic responses to mining shown in Figure 76.

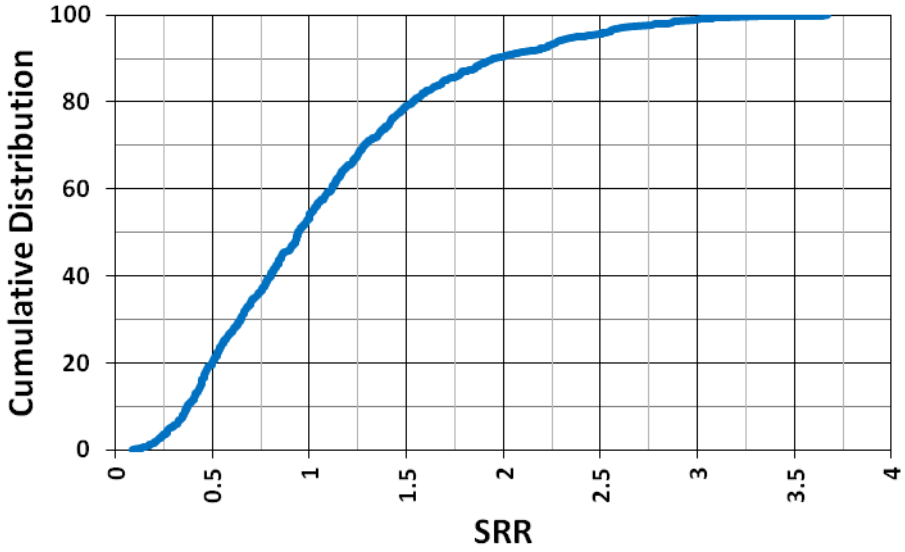

Figure 78: Cumulative distribution of SRR values for all of the events in the nineteen production blast induced seismic responses to mining shown in Figure 76.

In addition to the 19 production blast induced responses, there are 23 development blast induced seismic responses to mining considered in this case study. Figure 79 and Figure 80 depict seismic event and response centroid locations, respectively, for the induced seismic responses to mining associated with development blasting. Mine development blasts are represented by red stars, and occur throughout the mining environment at LaRonde.

Unlike the observations for production blast responses (shown in Figure 74), all development blast seismic responses to mining exhibit similar spatial characteristics. When development drifts are mined, the rock mass has experienced little to no significant localized stress redistribution or fracturing, and is likely in pre-failure. Furthermore, development blasts are relatively small, in

the order of a few hundred tonnes of fragmented rock, generating relatively small scale mining-induced stress change zones, and consequently little to no stress shedding is observed. Both development blast induced seismic responses and seismic response centroids (shown in Figure 80), concentrate closely around the development blast locations.

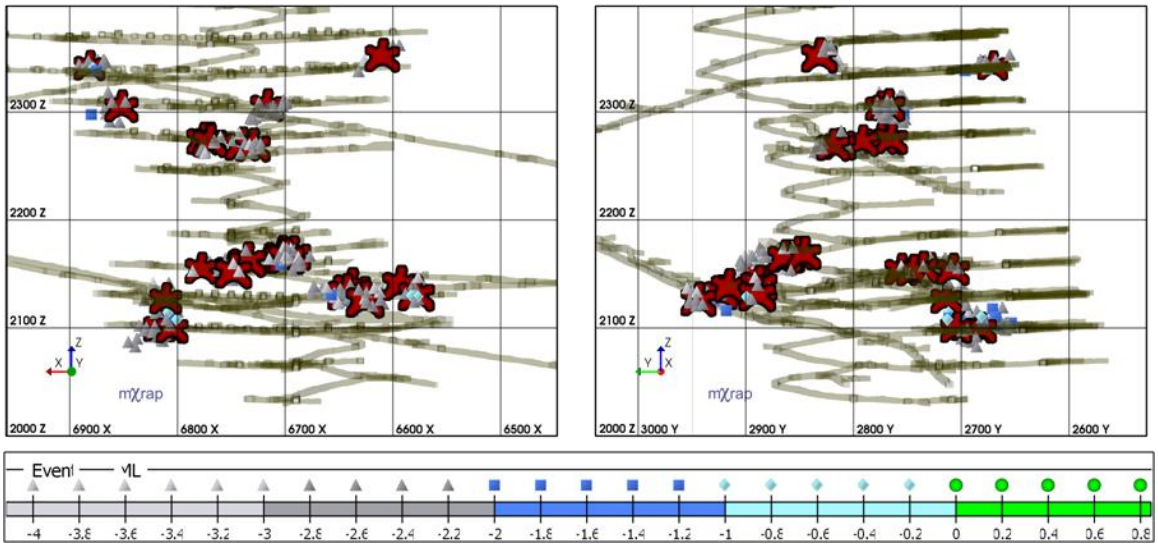

Figure 79: Longitudinal and cross-sectional projections of LaRonde mine showing induced seismic responses to mining and associated mine development blasts (red stars).

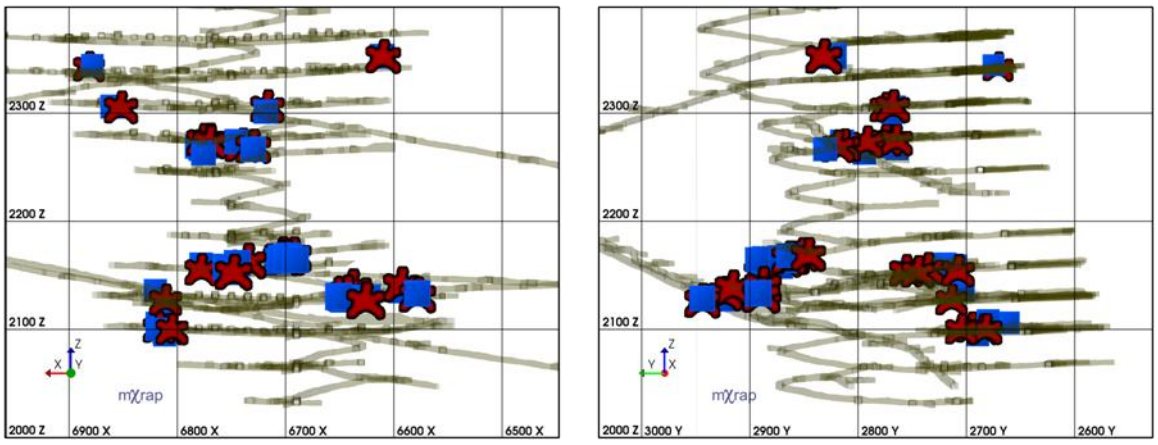

Figure 80: Longitudinal and cross-sectional projections of LaRonde mine showing the induced response centroid locations (calculated as shown in Equation 12), and associated mine development blasts (red stars). Distances between response centroids and mine blasts are quantified in Figure 81.

Figure 81 depicts cumulative distributions of distance between individual seismic response centroids and associated mine blast locations (shown in Figure 75 and Figure 80 for development and production blast induced responses respectively). The development blast induced responses exhibit low blast to response centroid distances, with 90% less than 20 metres, while the production blast induced responses exhibit relatively large distances ranging from approximately 5 to 80 metres. Production blast responses for primary stopes all exhibit blast to response centroid distances of less than 40 metres, with the majority being less than 30 metres. Very large

blast to response centroid distances in Figure 81 can be attributed to the rock mass characteristics surrounding secondary stopes (as previously discussed).

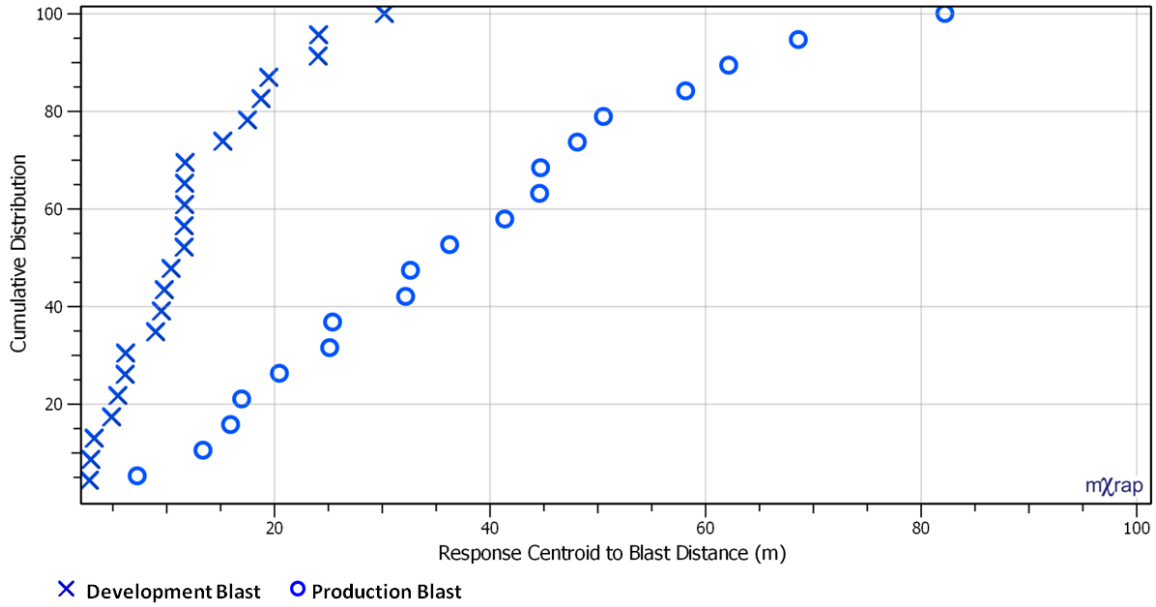

Figure 81: Cumulative distributions of the distance between response centroids and mine blast locations for Induced: Production and Induced: Development responses shown in Figure 75 and Figure 80 respectively.

Figure 82 is a Magnitude-Time History chart for the twenty-three development blast induced seismic responses to mining (shown in Figure 79). Mine development blasts are shown along the x-axis as red stars, and seismic events are coloured according to SRR. Each seismic response corresponds to a distinct step in the cumulative number of events line - strongly indicative of induced seismicity. SRR values are typically between 0 and 1.5, and no large magnitude seismic events are contained within the induced seismic responses to development mining.

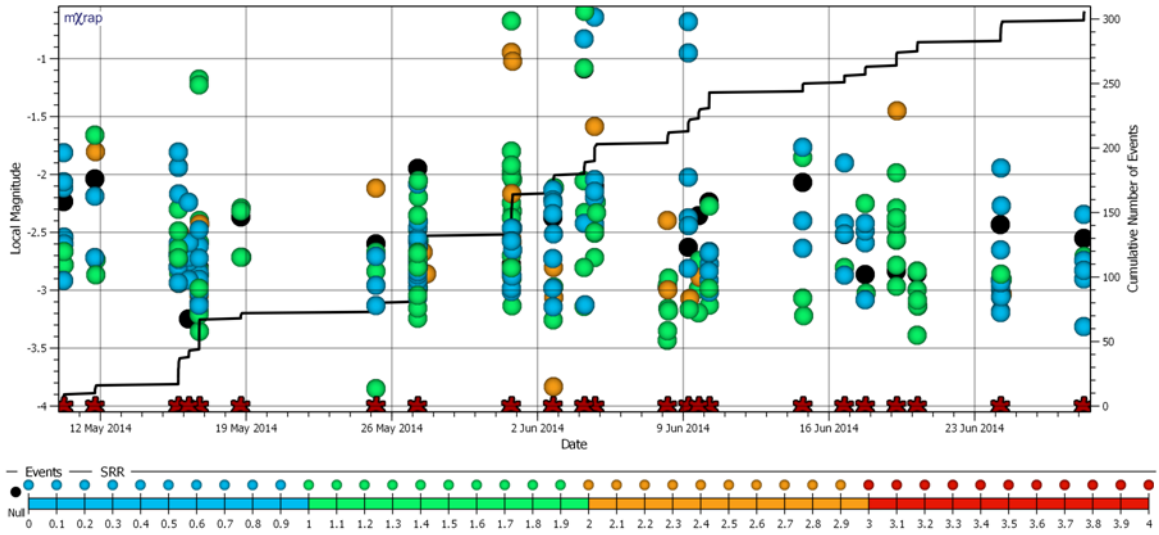

Figure 82: Magnitude-Time History chart for twenty-three induced seismic responses to mining at LaRonde. Mine development blasts are shown along the x-axis as red stars. Seismic events are coloured according to individual Seismic Response Rating (SRR). The first event in each individual seismic response is coloured black, as these events have no TBE$_N$ parameters and consequently may exhibit uncharacteristic SRR's.

A relative frequency distribution of SRR values for all of the events of the development blast induced seismic responses is shown in Figure 83. The majority of SRR values fall between 0 and 1.5, indicative of induced seismicity, with no values in excess of 3. There is a strong dominance of relatively small SRR values, indicating many individual SRP$_N$'s likely approach zero. Figure 84 is a cumulative distribution of the same SRR values shown in Figure 83. The median value is slightly more than 1, with 70% of all individual events exhibiting SRR values within the proposed observation guidelines of less than 1.5 (Table 23).

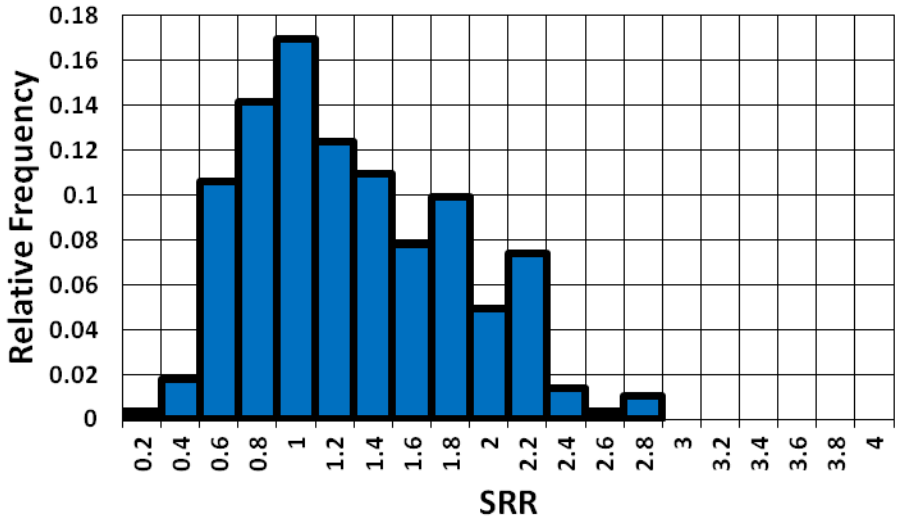

Figure 83: Relative frequency distribution of SRR values for all of the events in the twenty-three development blast induced seismic responses to mining shown in Figure 82.

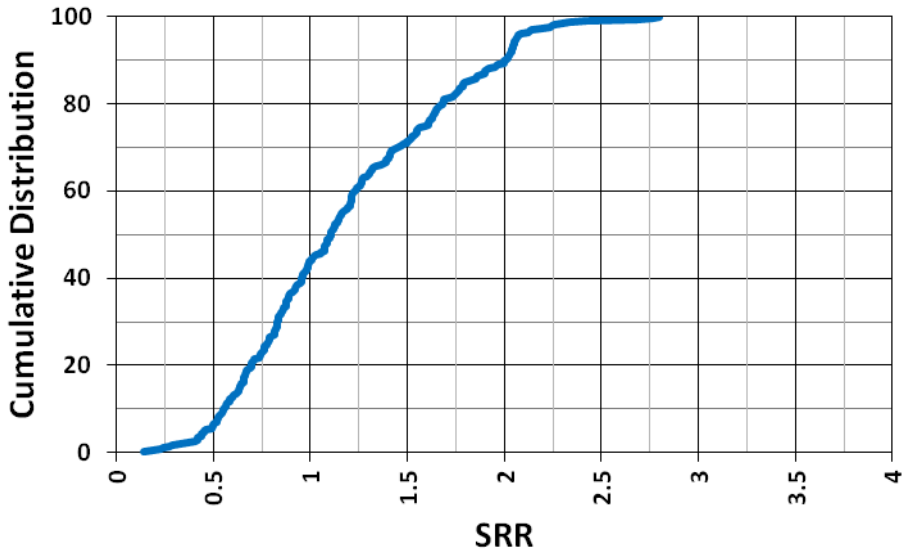

Figure 84: Cumulative distribution of SRR values for all events in the twenty-three development blast induced seismic responses to mining shown in Figure 82.

7.1.2 SRP and SRP_N Distributions for Induced Seismic Responses

The main difference between production blast and development blast induced seismic responses to mining is the size of the blast, and consequently the size of the mining-induced stress change zone. A previous section (Section 4.6), summarized the basic spatial and temporal relations between induced seismic responses to mining and mine blasts. Table 27 summarizes these relations as they pertain to Seismic Response Parameters and the induced seismic responses to mining included in this case study. A summary of observation guidelines for Normalized Seismic Response Parameters was provided in Table 14, and can be found in Appendix A for quick reference.

Table 27: Summary table of defining properties and characteristics of production blast and development blast induced seismic responses to mining (redrawn from Table 13).

	Induced: Development	Induced: Production
Distance To Blast [DTB]	*Excavation Radius 2.5 m & Location Error Factor 10 m:* *DTB < 22.5 m*	*Excavation Radius 15 m & Location Error Factor 10 m:* *DTB < 85 m*
Time After Blast [TAB]	*All Events:* *TAB < 1-3 h*	*All Events:* *TAB < 1-3 h*
Distance to Centroid [DTC]	*Excavation Radius 2.5 m & Location Error Factor 10 m:* *DTB < 22.5 m*	*Excavation Radius 15 m & Location Error Factor 10 m:* *DTB < 85 m*
Time Between Events [TBE]	*Significant No. Events:* *0 h ≤ TBE ≤ 0.01 h*	*Significant No. Events:* *0 h ≤ TBE ≤ 0.01 h*

Distributions of SRP_N's for the induced seismic responses to mining at LaRonde are discussed throughout this section. Response median values (for SRP_N's) are evaluated to aid in the interpretation of seismic responses, and are highlighted with 'X' symbols and 'O' symbols for development and production blast induced responses respectively. Figure 85 and Figure 86 depict the cumulative distributions of DTB and DTB_N, respectively, for the development and production blast induced seismic responses to mining at LaRonde. Because production blasts are significantly larger, the mining-induced stress change zone is increased, and seismic events can be located further away from the blast while still being considered induced. As expected, the production blast responses exhibit large DTB values, relative to development blast responses. The calculation of DTB_N, shown in Figure 86, accounts for this relative spatial increase, and consequently, all induced seismic responses are expected to exhibit similar DTB_N values. With the exception of two development responses (discussed further in Section 7.1.3.1), all induced seismic responses considered exhibit a $\widetilde{DTB}_N$ value less than one, and are strongly indicative of induced seismicity.

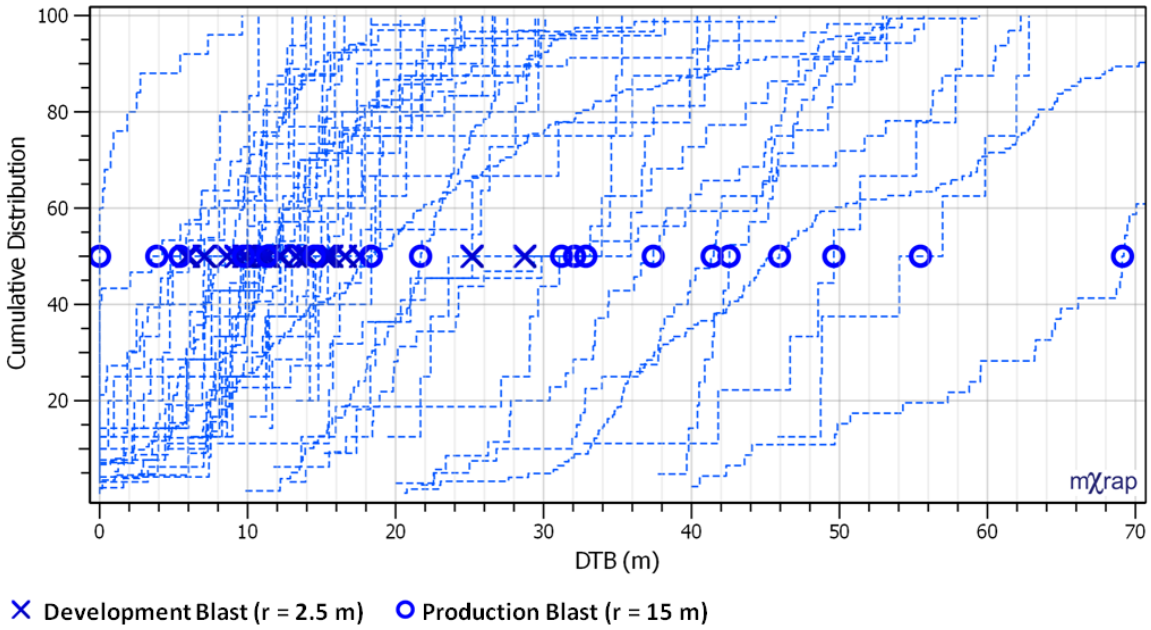

Figure 85: Cumulative distributions (post-step line shown), of the SRP Distance To Blast (DTB) for a series of induced seismic responses to mining at LaRonde. Median values for each response are shown as 'X' symbols and 'O' symbols for development and production blast responses, respectively.

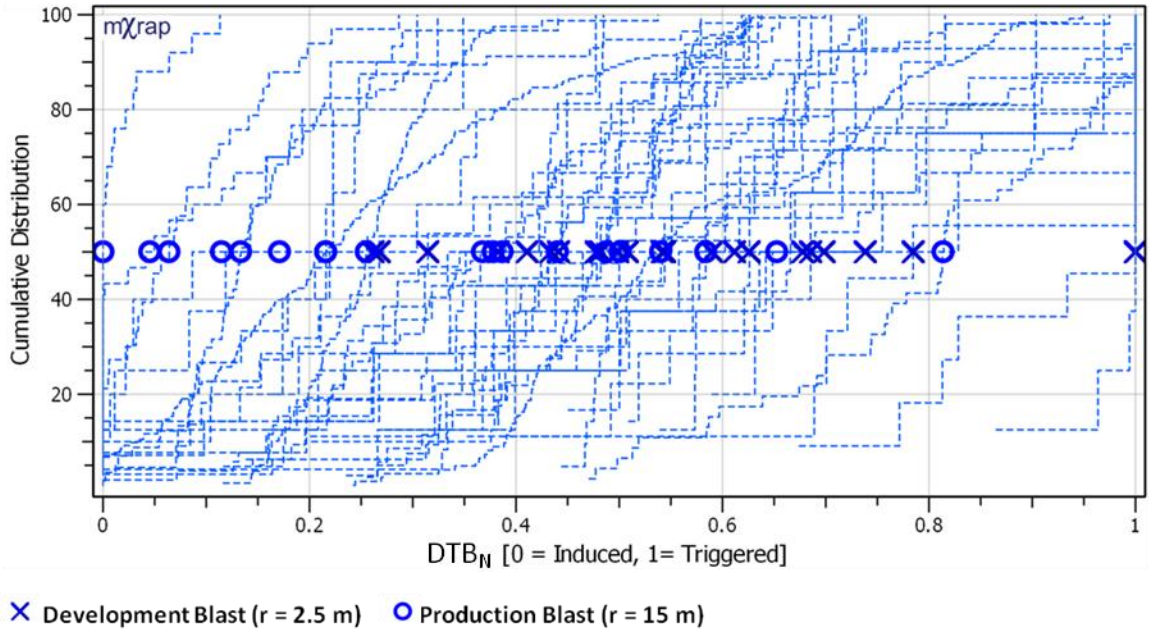

Figure 86: Cumulative distributions (post-step line shown), of Normalized Distance To Blast (DTB_N) for a series of induced seismic responses to mining at LaRonde. Median values for each response are shown as 'X' symbols and 'O' symbols for development and production blast responses, respectively.

Although the production blasting induces a larger stress change, the stress change still occurs over a very short time period. In theory, there should be no significant difference in the TAB of a induced development blast response and a induced production blast response. In practice however, larger blasts tend to exhibit longer time periods of seismic activity following mine

blasting. Relative to development blasts, production blasts in a typical mining environment are surrounded by an increased volume of yielded rock. Significant volumes of yielded rock can extend the time and distance of stress redistribution following a mine blast.

Another possible explanation for this difference is the occurrence of small numbers of triggered seismic events within the relatively large mining-induced stress change zone of production blasting. In this case study for example, the production blast mining-induced stress change zone radius is six times the radius of the development blast mining-induced stress change zone. This significantly increases the likelihood of a geological features, or other triggered source mechanism, being contained within the production blast mining-induced stress change zone, increasing the potential to generate triggered seismic events that are temporally distant to the blast.

Figure 87 and Figure 88 depict the cumulative distributions of TAB and TAB_N, respectively, for the development and production blast induced seismic responses to mining at LaRonde. The production blast ('O' symbols) and development blast ('X' symbols) induced seismic responses considered exhibit similar TAB distributions. All median TAB values are less than one, with production blast responses corresponding to larger TAB values, as expected. The TAB_N values, shown in Figure 88, indicate all induced responses occur in close temporal proximity to the mine blasts, with all median values plotting between 0 and 0.2.

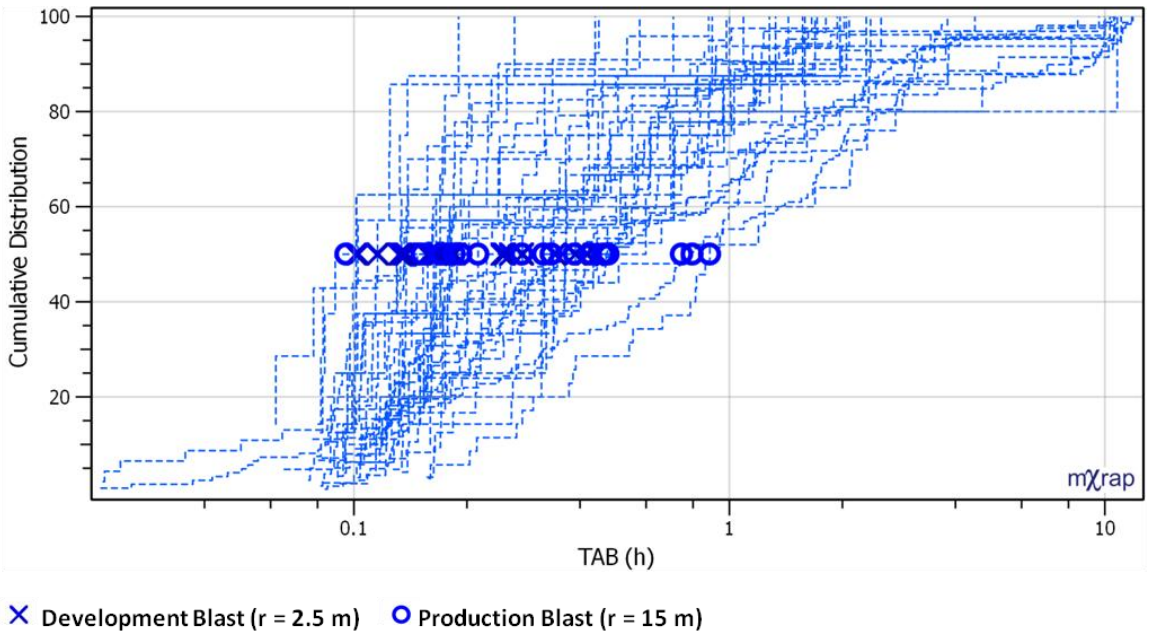

Figure 87: Cumulative distributions (post-step line shown), of the SRP Time After Blast (TAB) for a series of induced seismic responses to mining at LaRonde. Median values for each response are shown as 'X' symbols and 'O' symbols for development and production blast responses respectively.

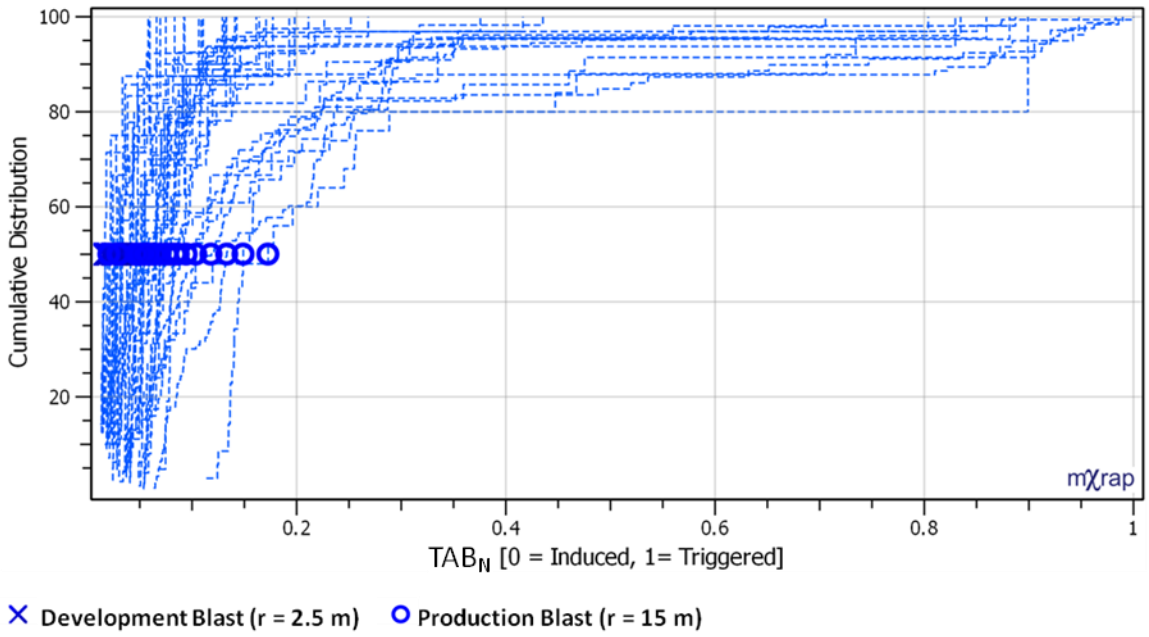

Figure 88: Cumulative distributions (post-step line shown), of Normalized Time After Blast (TAB_N) for a series of induced seismic responses to mining at LaRonde. Median values for each response are shown as 'X' symbols and 'O' symbols for development and production blast responses respectively.

Figure 89 and Figure 90 depict the cumulative distributions of DTC and DTC_N, respectively, for the development and production blast induced seismic responses to mining at LaRonde. As expected, the production blast responses ('O' symbols) exhibit larger DTC values, due to the increased size of the blast. All induced responses, generated from production and development blasting, exhibit $\widetilde{DTC}_N$ values less than one, and are strongly indicative of induced seismicity.

It is important to note that although two development blast induced seismic responses to mining exhibited uncharacteristically high values for DTB_N (DTB_N = 1 as shown in Figure 86), all development blast responses exhibit DTC_N values less than one. This may be an indication of seismic monitoring limitations or stress shedding in proximity to these two responses. These possibilities are discussed further in Section 7.1.3.1.

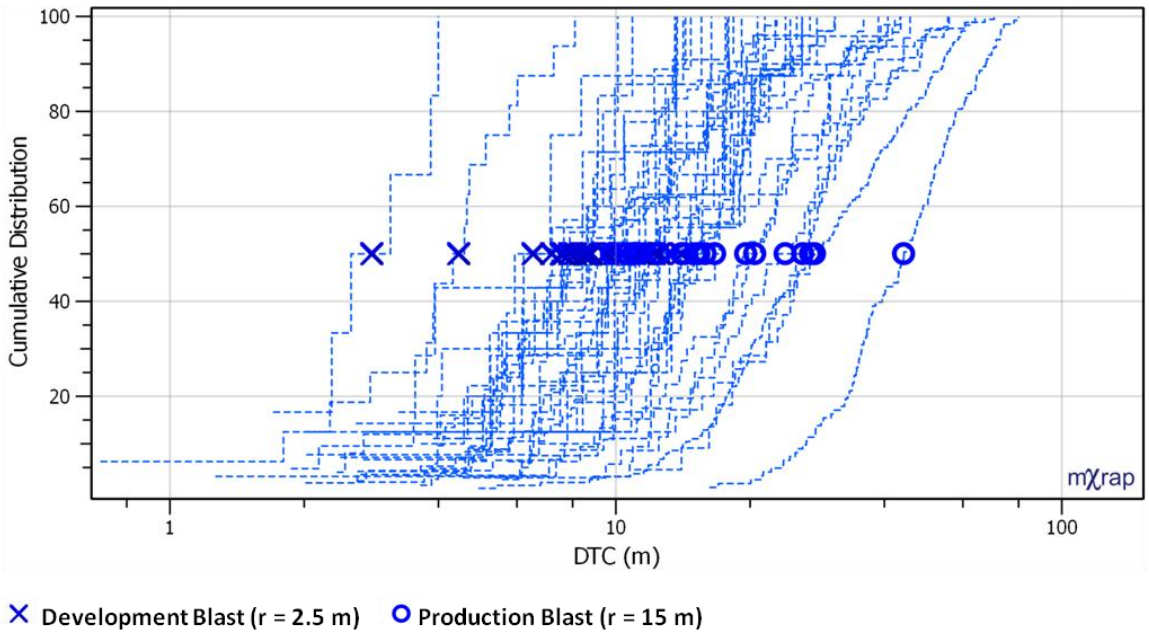

Figure 89: Cumulative distributions (post-step line shown), of the SRP Distance to Centroid (DTC) for a series of induced seismic responses to mining at LaRonde. Median values for each response are shown as 'X' symbols and 'O' symbols for development and production blast responses respectively.

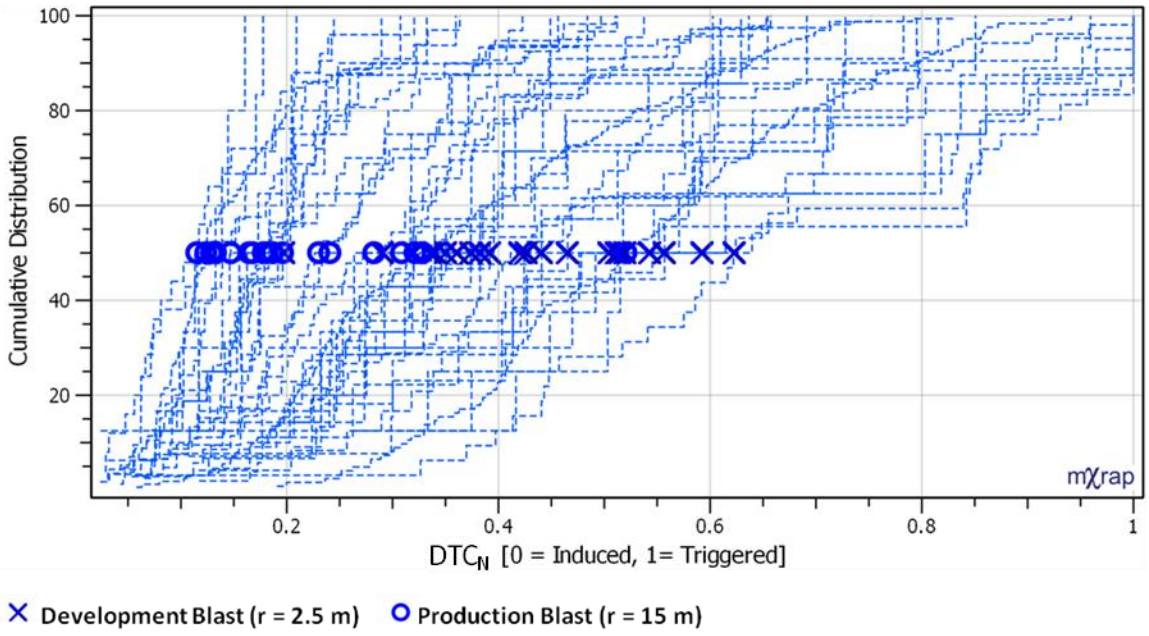

Figure 90: Cumulative distributions (post-step line shown), of Normalized Distance To Centroid (DTC_N) for a series of induced seismic responses to mining at LaRonde. Median values for each response are shown as 'X' symbols and 'O' symbols for development and production blast responses respectively.

Figure 91 and Figure 92 depict the cumulative distributions of TBE and TBE_N, respectively, for the development and production blast induced seismic responses to mining at LaRonde. The production blast ('O' symbols) and development blast ('X' symbols) induced seismic responses considered exhibit similar TBE distributions. In Figure 91, the vast majority of induced seismic

responses have median TBE values less than 0.1, or six minutes. The TBE_N values, shown in Figure 92, indicate all events within the induced responses occur in close temporal proximity to one another, with all median values plotting between 0 and 0.2.

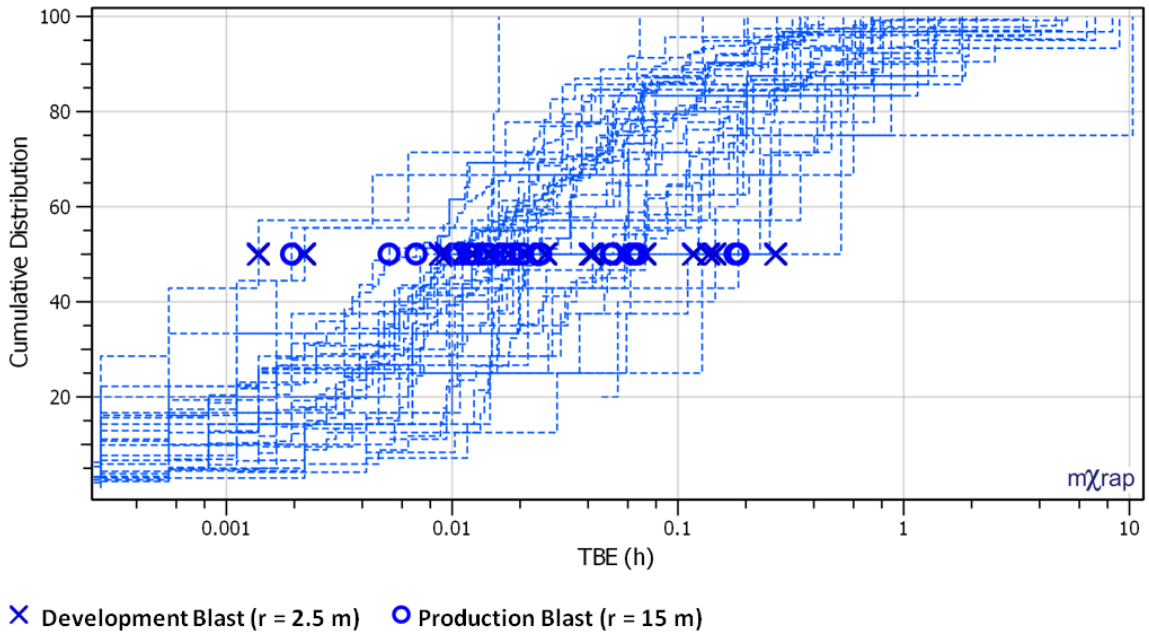

Figure 91: Cumulative distributions (post-step line shown), of the SRP Time Between Events (TBE) for a series of induced seismic responses to mining at LaRonde. Median values for each response are shown as 'X' symbols and 'O' symbols for development and production blast responses respectively.

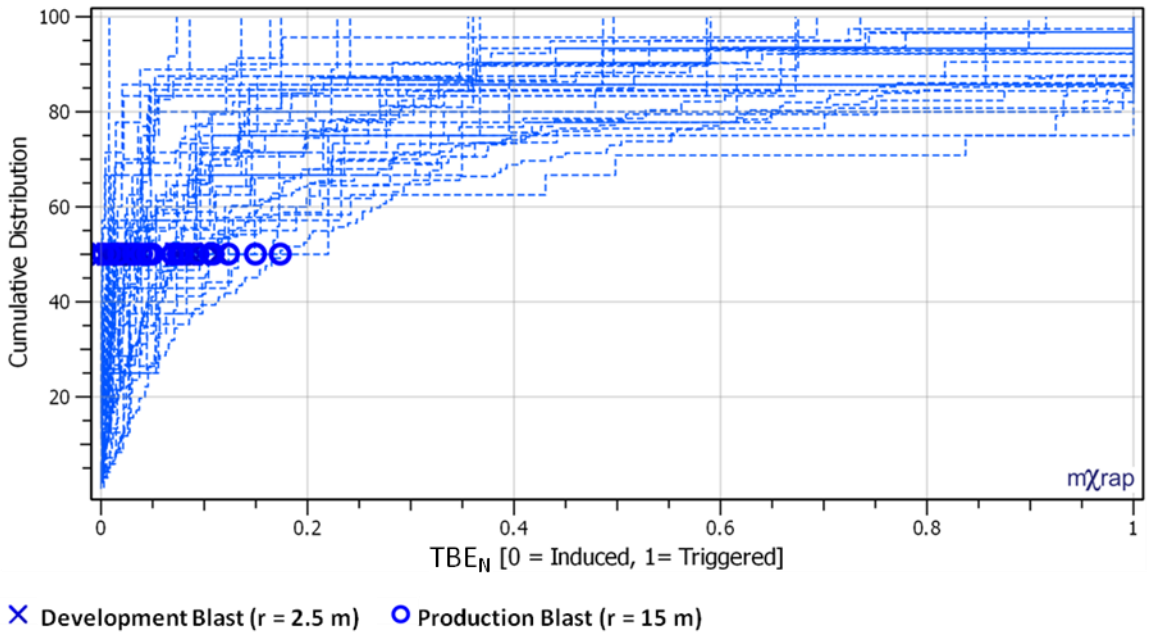

Figure 92: Cumulative distributions (post-step line shown), of Normalized Time Between Events (TBE_N) for a series of induced seismic responses to mining at LaRonde. Median values for each response are shown as 'X' symbols and 'O' symbols for development and production blast responses respectively.

7.1.3 Interpreting Induced Seismic Responses to Mining

Distributions of individual SRP_N's provide significant insight into the nature of seismic responses, but it is often more meaningful to combine multiple SRP_N's when interpreting seismic responses to mining. Table 28 summarizes the expected SPR_N chart and SRR observations for induced seismic responses to mining. These guidelines can be helpful in interpreting seismic responses using entire distributions of parameters, or representative values such as the response median values.

Table 28: Summary table of expected SRP_N chart and SRR observations for induced seismic responses to mining (Redrawn from Table 23).

	Induced
SRP_N Charts	Small Area *Temporal Parameters:* *[TAB_N & TBE_N]* *Approaching 0* *Spatial Parameters:* *[DTB_N & DTC_N]* *Approaching 0*
SRR	Small SRR *$0 \leq SRR \leq 1.5$*

Seismic Response Rating (discussed in Section 5.2), can provide significant insight into a seismic response using only a single numerical value. Figure 94 depicts the cumulative distributions of SRR for the development and production blast induced seismic responses to mining considered in this case study. The production blast ('O' symbols) and development blast ('X' symbols) induced seismic responses considered exhibit similar SRR distributions. Induced seismic responses are expected to exhibit SRR median values less than 1.5 (refer to Table 28). Only two responses, both development blast induced, exceed this guideline. These responses are discussed further in Section 7.1.3.1.

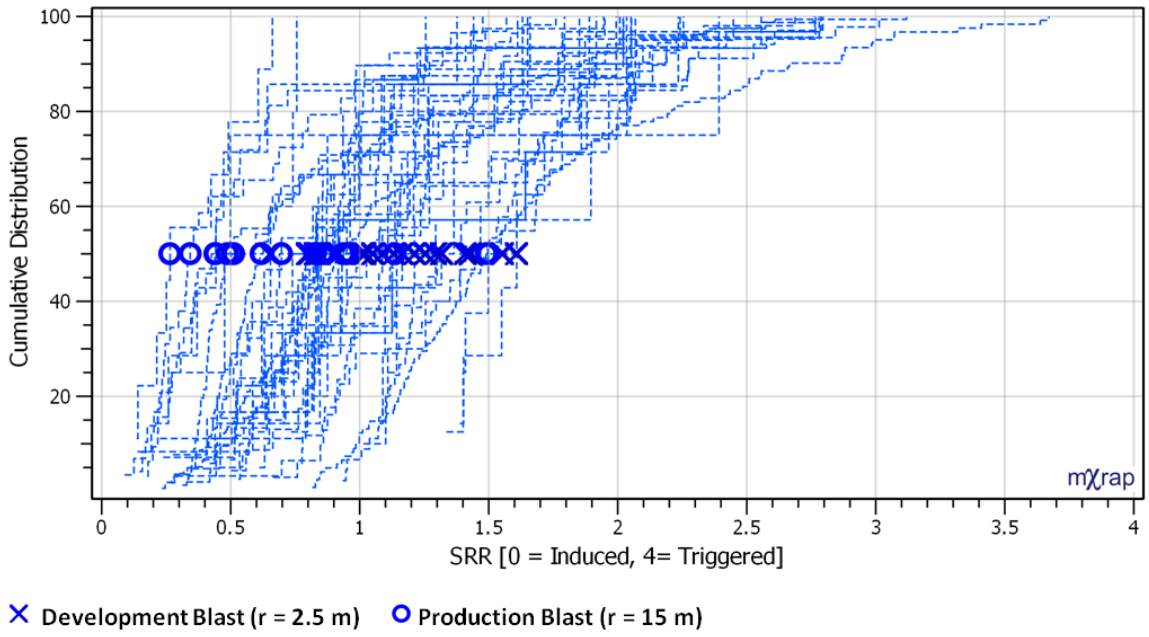

Figure 93: Cumulative distributions (post-step line shown), of Seismic Response Ratings (SRR's) for a series of induced seismic responses to mining at LaRonde. Median values for each response are shown as 'X' symbols and 'O' symbols for development and production blast responses respectively.

SRP_N charts, discussed in detail in Section 5.1, display the median SRP_N values for an individual or combination of seismic responses to mining. For interpreting seismic responses to mining, median values alone can often provide significant insight into the nature of a seismic response. Figure 94 and Figure 95 depict the SRP_N charts for the production and development blast induced seismic responses to mining, respectively.

There is some variation in the observation guidelines of SRP_N values for the induced seismic responses to mining, however the overall areas observed on the SRP_N charts for all individual responses are relatively small. Each SPR_N chart is shown along with the median SRR value and the number of events contained within the response (N). As previously discussed in Section 5.2, SRR values can be used in conjunction with other seismic analysis techniques to provide further insight into a seismic response. Responses exhibiting unexpected results, SRR values greater than 1.5, are outlined in red and are discussed further in the subsequent section (7.1.3.1). For comparison, SRR charts for production and development blast induced seismic responses can be found in Appendix B and Appendix C, respectfully.

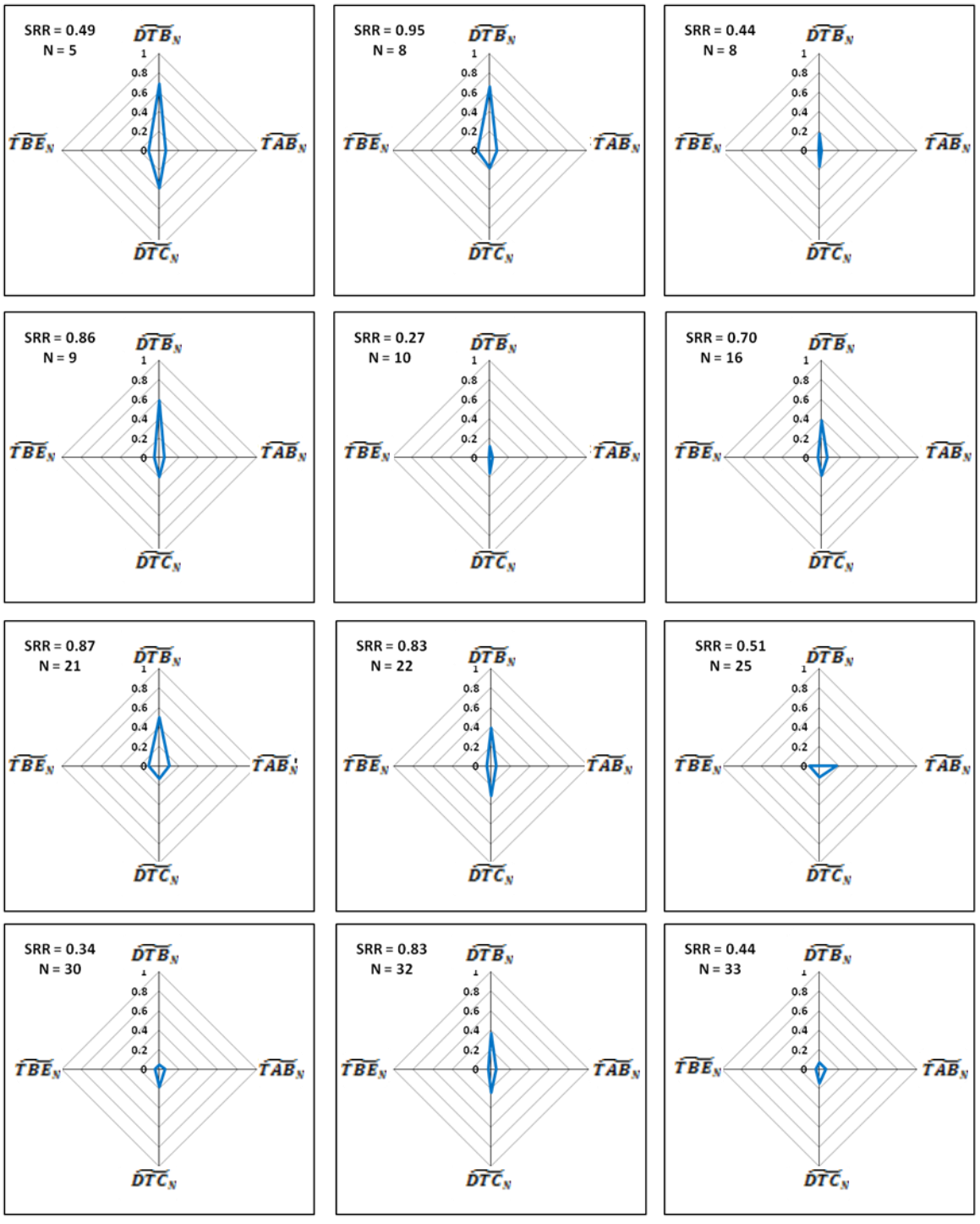
SRR = 0.49
N = 5
SRR = 0.95
N = 8
SRR = 0.44
N = 8
SRR = 0.86
N = 9
SRR = 0.27
N = 10
SRR = 0.70
N = 16
SRR = 0.87
N = 21
SRR = 0.83
N = 22
SRR = 0.51
N = 25
SRR = 0.34
N = 30
SRR = 0.83
N = 32
SRR = 0.44
N = 33
$\widehat{DTB}_N$
$\widehat{TAB}_N$
$\widehat{DTC}_N$
$\widehat{TBE}_N$
0
0.2
0.4
0.6
0.8
1

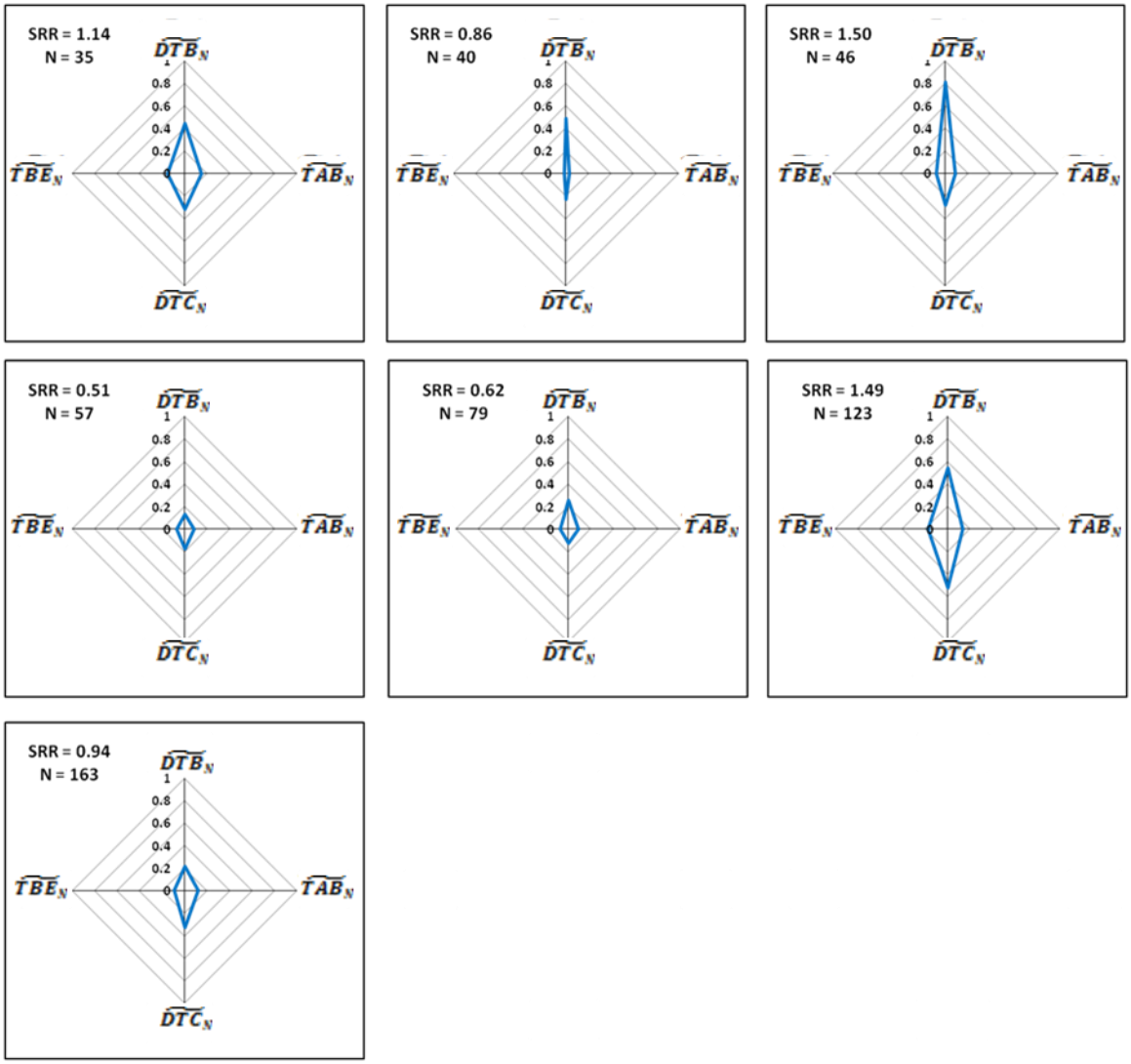

Figure 94: SRP_N charts for all production blast mining-induced seismic responses to mining at LaRonde considered in this case study. Median Seismic Response Rating (SRR) and the number of events contained within the response are also shown.

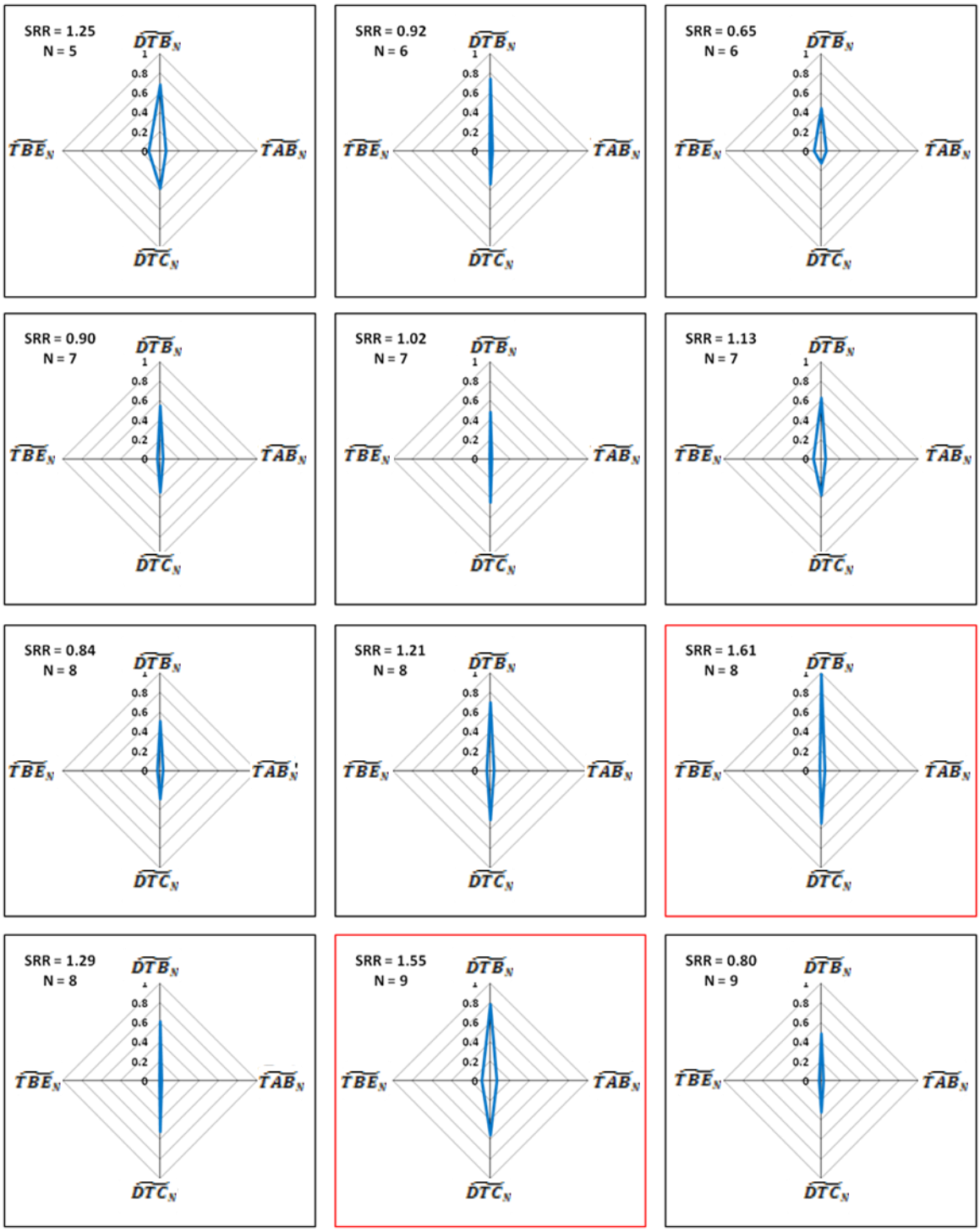
SRR = 1.25
N = 5
SRR = 0.92
N = 6
SRR = 0.65
N = 6
SRR = 0.90
N = 7
SRR = 1.02
N = 7
SRR = 1.13
N = 7
SRR = 0.84
N = 8
SRR = 1.21
N = 8
SRR = 1.61
N = 8
SRR = 1.29
N = 8
SRR = 1.55
N = 9
SRR = 0.80
N = 9
$\widetilde{DTB}_N$
$\widetilde{TAB}_N$
$\widetilde{DTC}_N$
$\widetilde{TBE}_N$
0
0.2
0.4
0.6
0.8
1

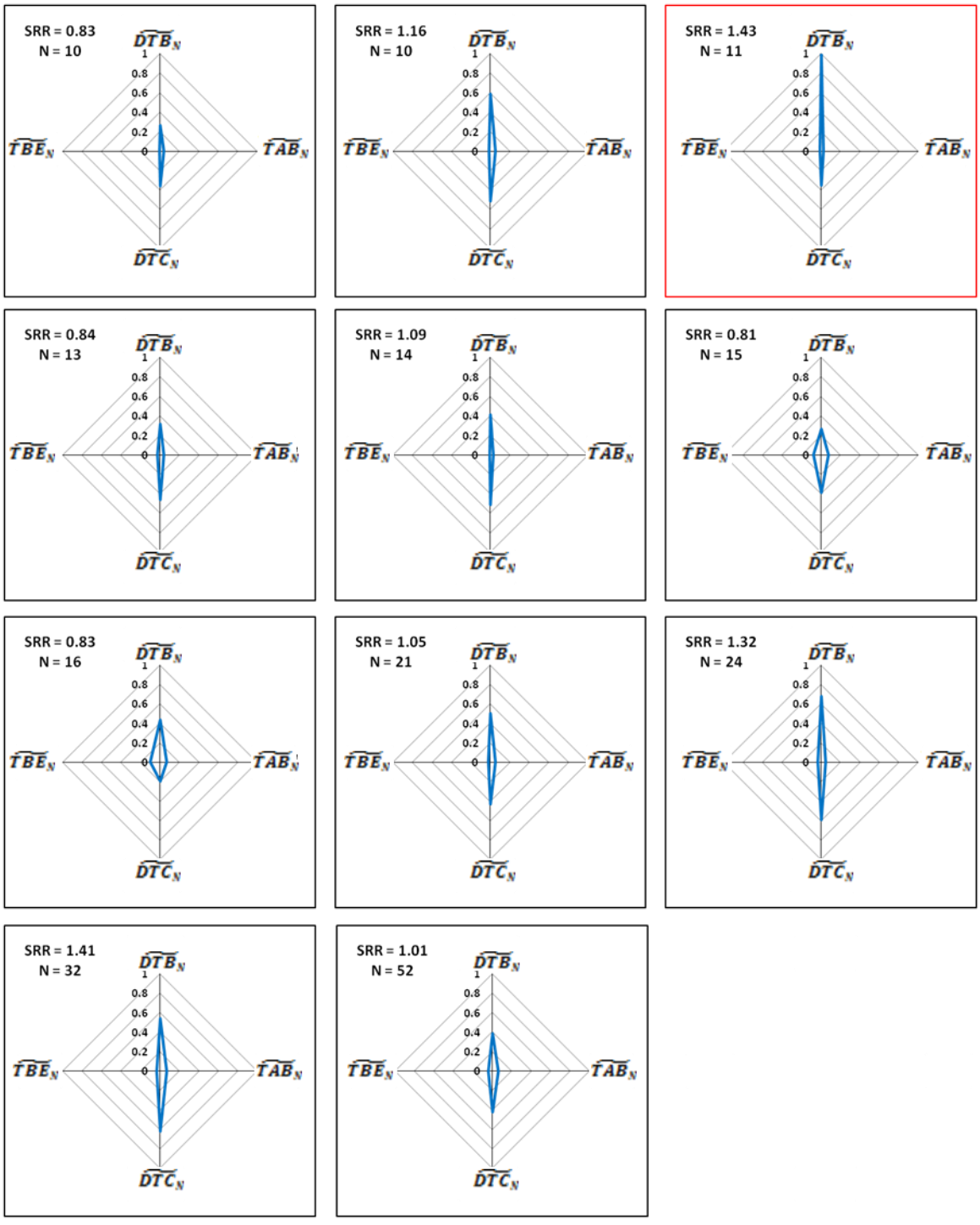

Figure 95: SRP_N charts for all development blast mining-induced seismic responses to mining at LaRonde considered in this case study. Median Seismic Response Rating (SRR) and the number of events contained within the response are also shown. Seismic responses exhibiting unexpected SRR values (SRR > 1.5) and/or DTB_N values (DTB_N = 1) are outlined in red.

7.1.3.1 Unexpected Observations for Induced Seismic Responses

More than 90% of induced seismic responses to mining considered in this case study conform to the expected observation guidelines proposed in this thesis. Three development induced responses however, shown outlined in red in Figure 95, exhibit uncharacteristically high DTB_N and/or SRR values, for the median of the response. SRR charts for these three responses are shown in Figure 96.

When median SRR values appear irregular, it typically warrants a further investigation into the seismic response. It should be noted that while two of the responses shown in Figure 96 exhibit SRR values beyond the expected range, it is exceeded by approximately 0.1. Induced seismic responses to mining are expected to exhibit DTB_N values approaching zero, and are not expected to exhibit DTB_N values equal to one. Upon further investigation, all responses shown in Figure 96 exhibit relatively large DTB_N values, contributing to uncharacteristically high SRR values.

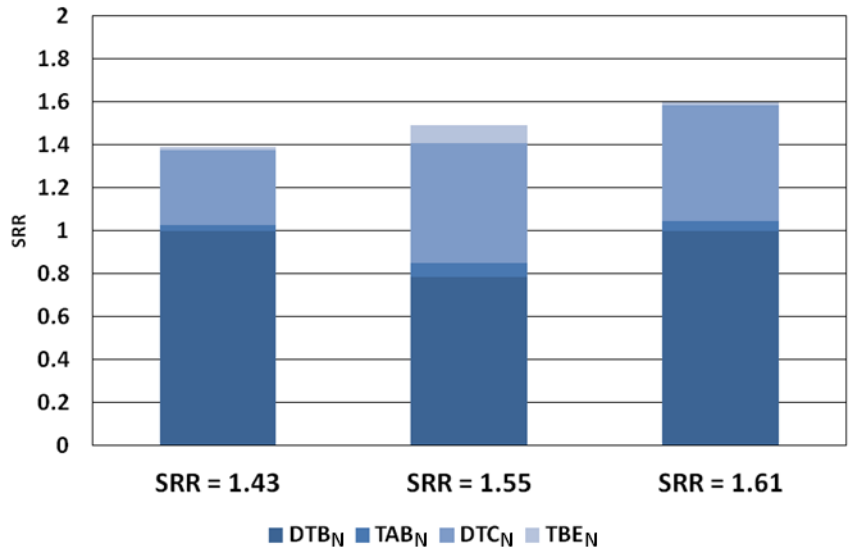

Figure 96: SRR chart for two induced seismic responses to mining that do not conform to expected SRR observations. Note that the SRR values stated on the x-axis are the median SRR values, and do not necessarily equal the sum of the individual median SRP_N.

A DTB_N value of one indicates a seismic event, or response, occurs beyond the assumed mining-induced stress change zone of the associated mine blast. Figure 97 depicts the cumulative distribution of DTB values for the three development induced seismic responses to mining shown in Figure 96. The spatial bound of the assumed mining-induced stress change zone, approximated by a red rectangle, is 22.5 metres from the mine development blast locations.

Likely reasons for induced seismicity to exhibit uncharacteristic DTB_N values are local seismic monitoring limitations and/or rock mass stress shedding. As all DTC_N values are less than one for the responses considered (see Figure 96), the individual seismic events in these responses

may have been offset from the blast location for one of these reasons. Additionally, large DTB_N values may result from the application of a uniform excavation size assumption in the calculation of normalized parameters. In this work, all mine development blasts are assumed to generate a new mine excavation with a radius approximating 2.5 metres. This assumption may not be valid in some cases (e.g. intersections with increased spans), resulting in erroneously high DTB_N values. Due to the natural complexity of the rock mass in mining environments, a degree of variability in the data should be expected.

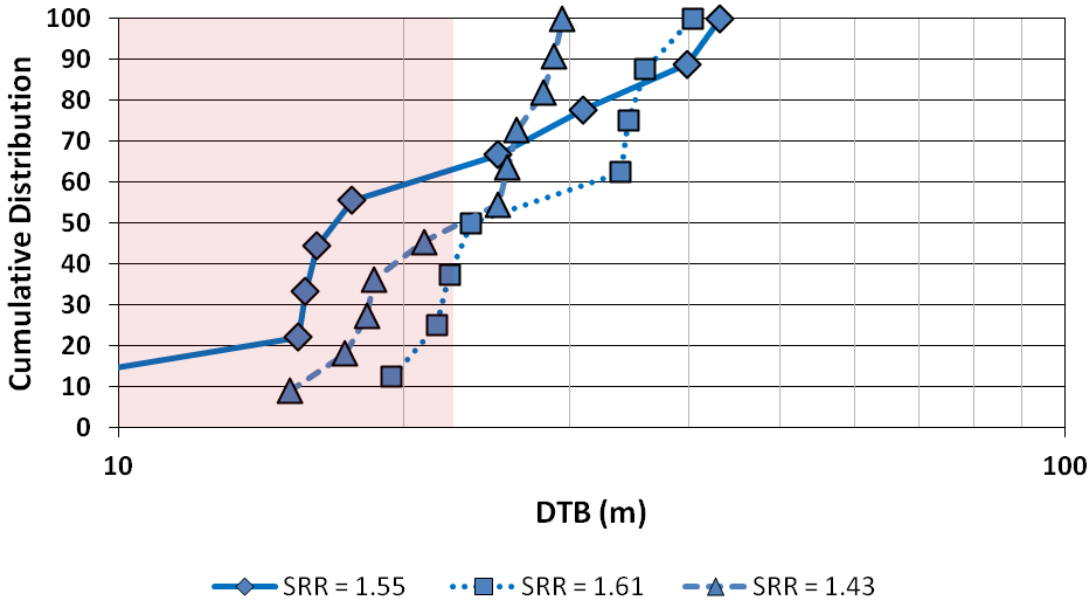

Figure 97: DTB chart for three induced seismic responses to mining that do not conform to expected SRR and/or DTB_N observations.

7.1.4 Discussion of Induced SRP_N's

This case study has demonstrated the applicability of SRP_N's (DTB_N, TAB_N, DTC_N and TBE_N) and SRR to induced seismic responses at LaRonde mine. Seismic responses induced by development and production scale mine blasting have been examined. Figure 98 depicts relative frequency distributions of the Normalized Seismic Response Parameters for the induced seismic responses considered in this case study. Distributions of temporal SRP_N's (TAB_N and TBE_N), are highly indicative of induced seismicity, with strong concentrations of values approaching zero. Relative to production blast induced seismic responses, development blast induced responses exhibit smaller temporal SRP_N values. Production blasts are typically associated with increased extraction levels, relative to development blasts, and generate a much larger stress redistribution in the rock mass. Both of these conditions suggest the rock mass may require additional time for stress redistribution following production blasting, and prior to reaching equilibrium. This may contribute to relatively large temporal SRP_N's for seismic responses to production mining.

Distributions of spatial SRP_N's (DTB_N and DTC_N) are variable relative to temporal SRP_N's in Figure 98, with a significant quantity of development blast induced DTB_N values beyond the expected range ($DTB_N = 1$). There are nominally four possibilities regarding the location of seismic events following a mine blast:

- No significant stress change occurs, and there are few or no recorded/located seismic events.
- A significant stress change occurs, and seismic events locate in close proximity to the newly blasted excavation.
- A significant stress change occurs, however stress shedding causes events to locate beyond the expected proximity to the newly blasted excavation.
- A significant stress change occurs, however seismic system design and/or software limitations incorrectly locate events beyond the expected proximity to the newly blasted excavation.

Both the influence of stress shedding, and microseismic monitoring system limitations in proximity to newly developed headings at LaRonde mine, likely contribute to the relative variability of spatial SRP_N's in Figure 98. The concept of spatial versus temporal SRP_N's is discussed in further discussed in Chapter 8 (Section 8.2).

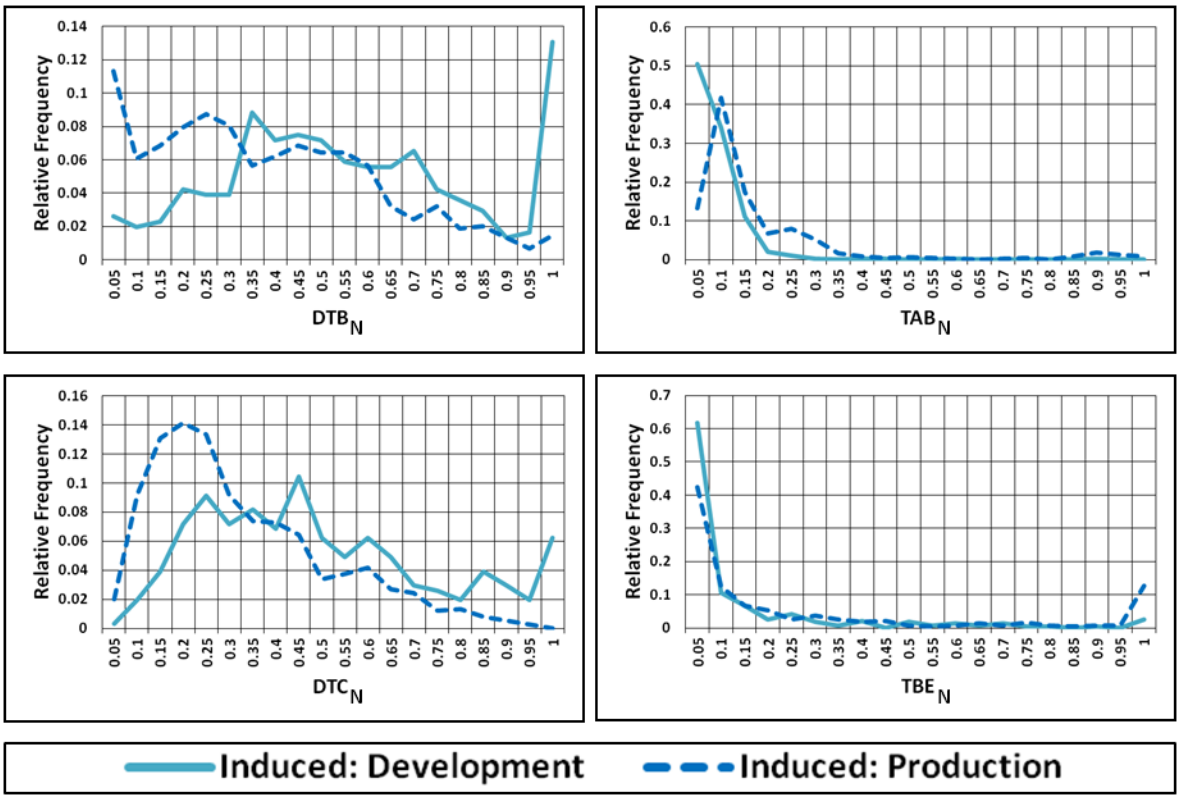

Figure 98: Relative frequency distributions for DTB_N, TAB_N, DTC_N and TBE_N for all previously shown induced seismic responses to mining at LaRonde mine.

7.1.5 Summary of Induced Seismic Response to Mining at LaRonde

Production blast and development blast induced seismic responses at LaRonde mine considered in this case study exhibit characteristics indicative of induced seismicity (as defined within the context of this thesis). No noteworthy outliers were present within the data, however, a couple relatively large median DTB_N parameters (associated with development blasts) were present. These may be an indication of complex seismicity, however it is more likely that the assumed spatial limit of the mining-induced stress change zone is not representative of the true mining-induced stress change zone for these responses. Because LaRonde is a deep and high stress mining environment with significant orebody extraction, there may be significant volumes of post-failure rock mass affecting mining-induced stress redistribution. As only two of a total of forty-two responses exhibit median DTB_N values of one, the current methodology appears to appropriately account for this challenging mining environment.

Table 29 summarizes the observation guidelines and the actual observations from the LaRonde mine case study surrounding induced seismic responses to mining. There is little to no error associated with seismic event time, while in certain cases there may be considerable error associated with seismic event locations. More variation is observed between median distributions of spatial parameters than temporal parameters, particularly when comparing production and development blast induced responses. This likely indicates that temporal parameters are more reliable for interpreting seismic responses to mining.

Table 29: Summary of SRR and SRP_N observation guidelines for induced responses and median distributions for the LaRonde case study of induced seismic responses to mining. Median distributions are shown as 'X' symbols and 'O' symbols for development and production blast responses respectively. Table continued on subsequent page.

	Observation Guidelines: Induced	Median Distributions for LaRonde Case Study: Induced
SRR	**Approaching Zero [0 ≤ SRR ≤ 1.5]**	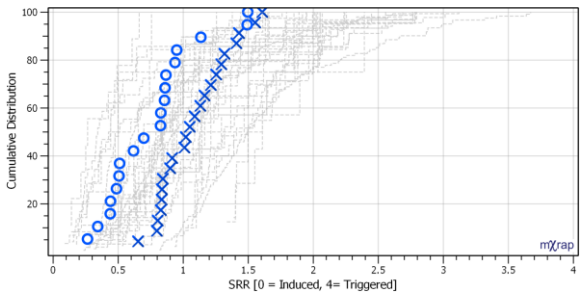

	Observation Guidelines: Induced	Median Distributions for LaRonde Case Study: Induced
DTB_N	**Approaching Zero [$DTB_N < 1$]**	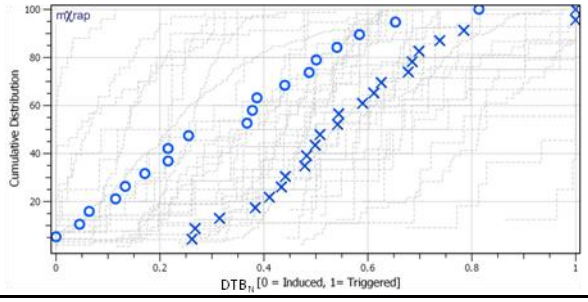
TAB_N	**Approaching Zero [$TAB_N \approx 0$]**	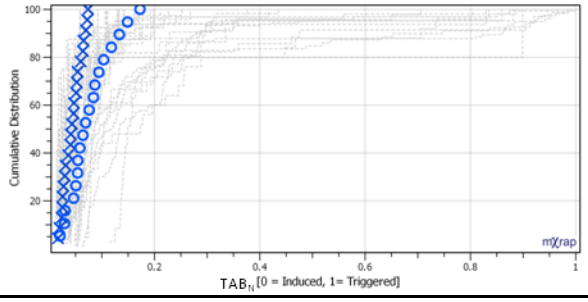
DTC_N	**Approaching Zero [$DTC_N < 1$]**	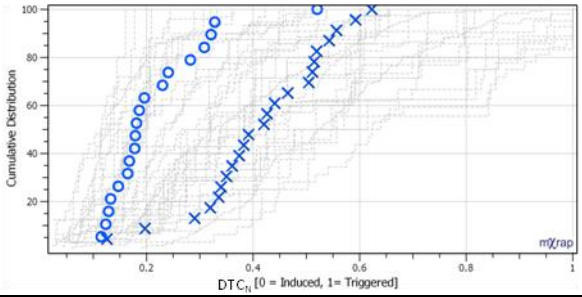
TBE_N	**Approaching Zero [$TBE_N \approx 0$]**	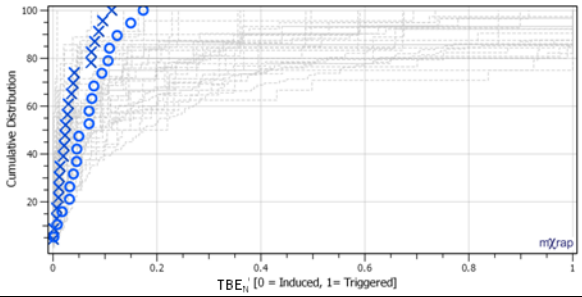

7.2 Case Study II: Triggered Seismic Response to Mining

Unlike induced responses, literature describes a poor correlation between mine blasting and triggered seismic responses. Triggered responses are characterized as being relatively spatially and temporally independent of discrete mine blasting. Triggered seismicity should therefore continue in the absence of mine blasting, as the rock mass continues to undergo larger scale failure processes. The time period for this case study was selected with the objective of using the July 2014 shutdown period at LaRonde mine to verify the space-time characteristics of triggered seismic responses to mining in the absence of mine blasting.

Seismicity occurring during mine shutdowns has previously been defined as 'background' seismicity (Mollison *et al.* 2003; Kranz and Estey, 1996). Background seismicity refers to the occurrence of seismic events independent of mining activities (i.e. blasting), and, in the context of this thesis, is synonymous with triggered seismicity. This case study focuses on triggered seismic responses to mining, including seismic responses occurring during a mine shutdown. The relation between background and triggered seismicity is discussed further in Chapter 8 (Section 8.4).

Selecting the two months prior to the shutdown to aid in identifying triggered seismic responses to mining ensures the locations of larger scale rock mass failure process do not differ significantly between the pre-shutdown and shutdown time periods. As previously discussed, any selection of temporal bounds for identifying triggered seismic responses to mining are arbitrary. To ensure a uniform comparison between pre-shutdown and shutdown period seismic responses however, all triggered responses (shutdown and pre-shutdown) are identified using the same methodology - as summarized in Table 30.

Within this case study, a series of triggered seismic responses to mining and mine shutdown responses are shown. Triggered seismicity is not often a direct result of one discrete mine blast, but the influence of many blasts over potentially months or years. As such, triggered responses correspond to mine extraction in a more general sense. In an effort to minimize the influence of discrete blasts on SRP_N's, the larger, and more conservative, mining-induced stress change zone associated with production blasting will be assumed for all triggered and shutdown period seismic responses in this case study.

Table 30 summarizes the parameters used for identifying triggered and shutdown period seismic responses to mining considered in this case study. With the exception of the response identification time period, all parameters are the same for both triggered and shutdown seismic responses to mining.

Table 30: Summary of parameters used to identify the triggered and shutdown period seismic responses at LaRonde and the common factors used in the calculation of SRP_N's.

		Triggered Response	Shutdown Response
Response Identification	**Single-Link Clustering d-value**	100 metres	100 metres
	Temporal Window	12 hours	12 hours
	Time Period	05/2014 - 07/2014	01/07/2014 - 17/07/2014
Calculation of SRP_N's	**Excavation Radius**	15 metres	15 metres
	Location Error Factor	10 metres	10 metres
	Assumed Mining-Induced Stress Change Zone	85 metres from Excavation Boundary	85 metres from Excavation Boundary

7.2.1 Triggered Seismic Response Descriptions

A total of 69 triggered seismic responses to mining are considered in this case study. Figure 99 and Figure 100 depict the seismic event and response centroid locations, respectively, for the triggered responses. Mine blast locations are shown as blue stars - indicating production blasts. Although most blasts, which concentrate below 2,400z, are relatively small development blasts, the assumed mining-induced stress change zone is considered equivalent to a production blast (85 metre radius from the blast location), as previously discussed.

Compared to the induced responses (discussed in Section 7.1), the triggered responses consist of significantly more seismic events, yet are relatively spatially diffuse. This is a reflection of the single-link clustering d-value used in response identification (100 metres relative to 20 metres), the seismic monitoring limitations in the deep footwall, and the spatially large scale rock mass failure processes that generate triggered seismicity. The response centroid locations, shown in Figure 100, are distant to mine blast locations and concentrate in the same area of the rock mass, the ramp area just below 2,600z.

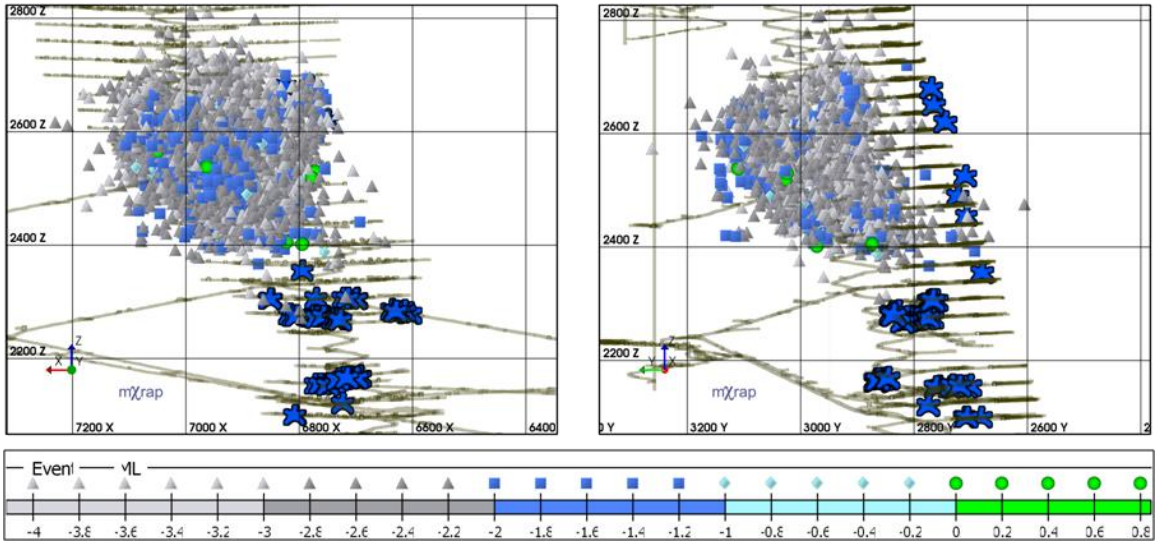

Figure 99: Longitudinal and cross-sectional projections of LaRonde mine showing triggered seismic responses to mining and associated mine blasts (blue stars).

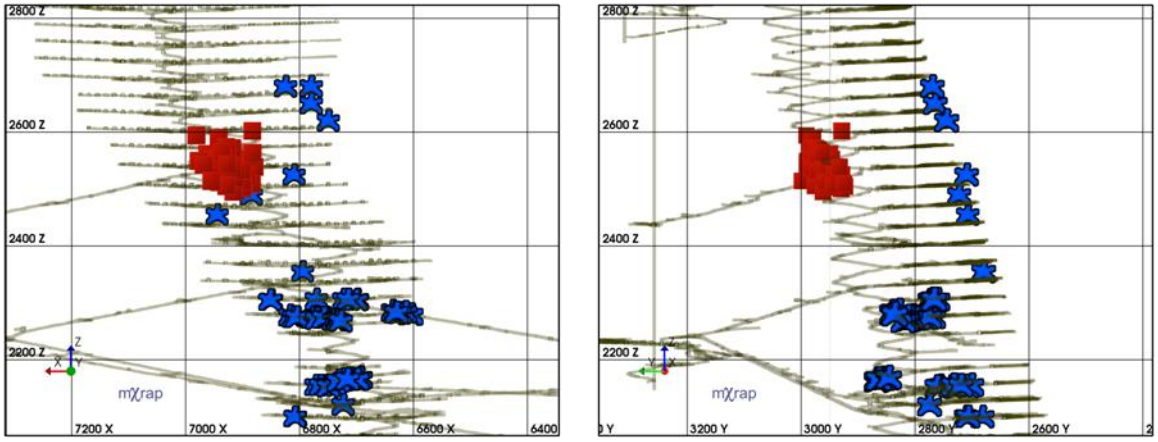

Figure 100: Longitudinal and cross-sectional projections of LaRonde mine showing triggered response centroid locations (calculated as shown in Equation 12), and associated mine blasts (blue stars).

Figure 101 depicts cumulative distributions of distance between individual seismic response centroids and associated mine blast locations for the triggered seismic responses to mining (shown in Figure 100). The distributions for the induced seismic responses at LaRonde are also shown for reference. As expected, triggered seismic responses exhibit high blast to response centroid distances, ranging from approximately 200 to 500 metres. With response centroid locations hundreds of metres from mine blast locations, the energy release associated with these seismic responses is disproportionally large compared to blast sizes, and strongly indicative of triggered seismicity.

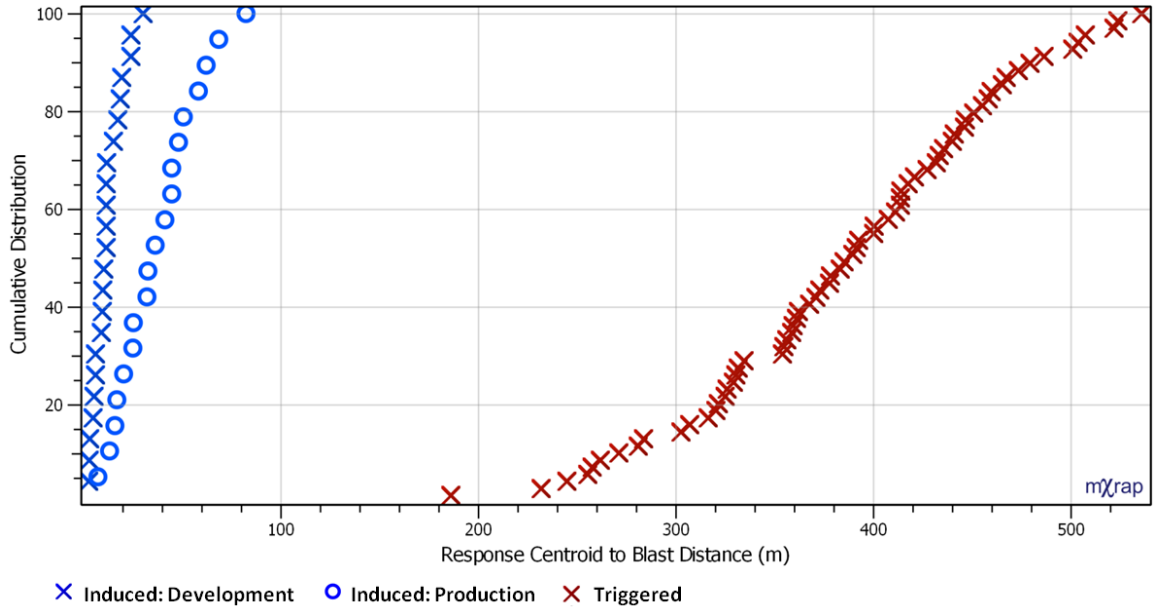

Figure 101: Cumulative distributions of the distance between response centroids and mine blast locations for Induced: Production, Induced: Development and Triggered responses shown in Figure 75, Figure 80 and Figure 100 respectively.

Figure 102 is a Magnitude-Time History chart for the triggered seismic responses to mining (shown in Figure 99). Mine blasts are shown along the x-axis as blue stars, and seismic events are coloured according to SRR. Relative to the induced responses (shown in Figure 76 and Figure 82), the slope of the cumulative number of events line is gradual and relatively constant. This supports significant differences between the temporal occurrence of triggered and induced seismic events. Slopes of zero typically correspond to time periods where there was no mine blasting or no significant triggered seismic responses to mining. Unlike induced responses, distinct steps in the cumulative number of events line are not present for the triggered responses. SRR values are typically between 2.5 and 4, and over the two month time period considered, seven large and potentially damaging seismic events ($M_L \geq 0$) occur within the triggered seismic responses to mining. In contrast, zero large events occurred within the induced seismic responses for the same time period.

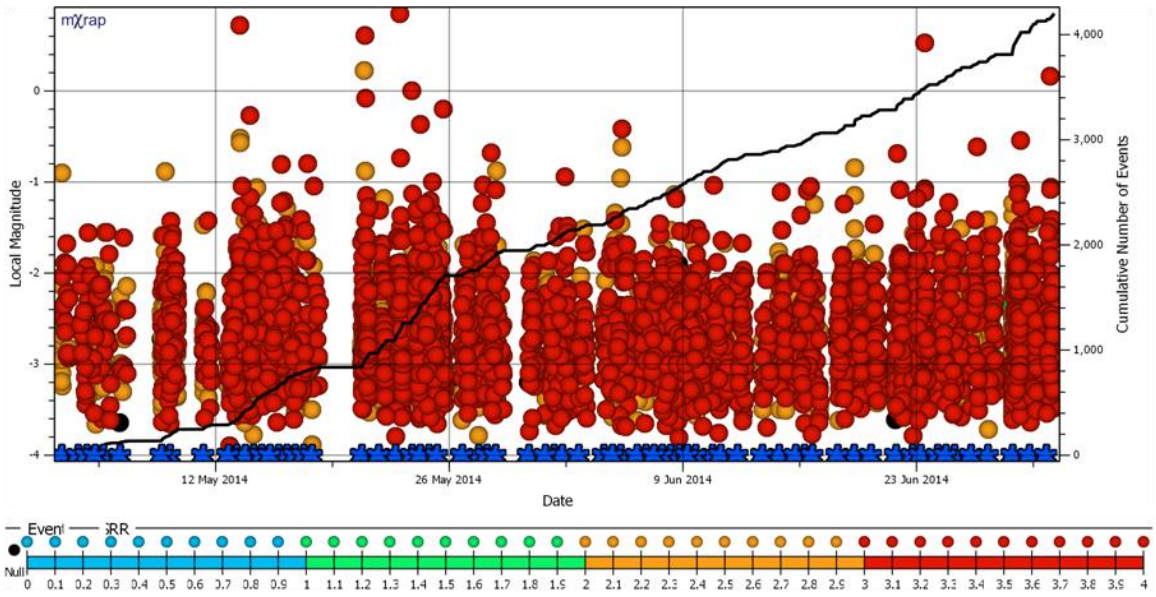

Figure 102: Magnitude-Time History chart for sixty-nine triggered seismic responses to mining at LaRonde. Mine blasts, all assumed as production blasts for simplification purposes, are shown along the x-axis as blue stars. Seismic events are coloured according to individual Seismic Response Rating (SRR). The first event in each individual seismic response is coloured black, as these events have no TBE$_N$ parameters and consequently may exhibit uncharacteristic SRR values.

A relative frequency distribution of SRR values for the triggered seismic responses is shown in Figure 103. SRR values typically fall between 2.5 and 4, indicative of triggered seismicity, with no values below 1.5. There is a strong dominance of large SRR values, indicating many individual SRP$_N$'s likely approach or equal one. Figure 104 is a cumulative distribution of the same SRR values shown in Figure 103. The median value is slightly more than 3.25, with more than 90% of all individual events exhibiting SRR values within the proposed observation guidelines of SRR greater than 2.5 (Table 23).

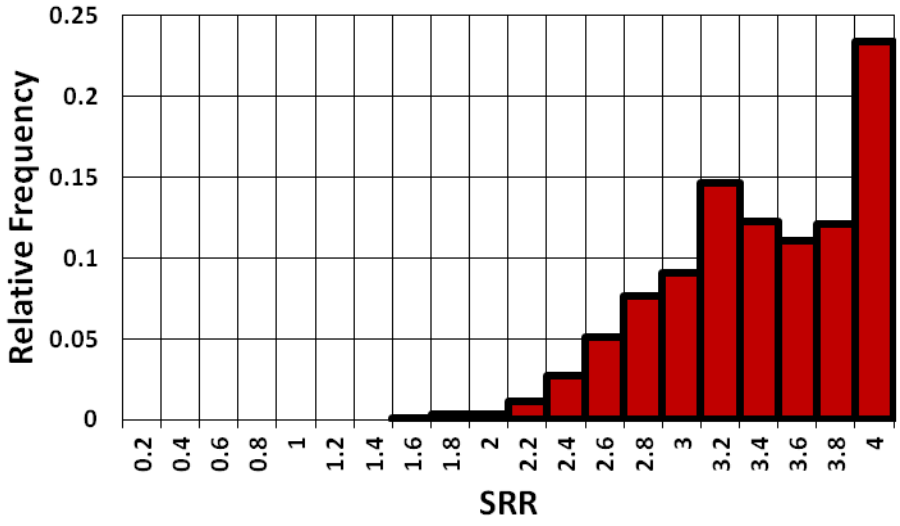

Figure 103: Relative frequency distribution of SRR values for all of the events in the sixty-nine triggered seismic responses to mining shown in Figure 102.

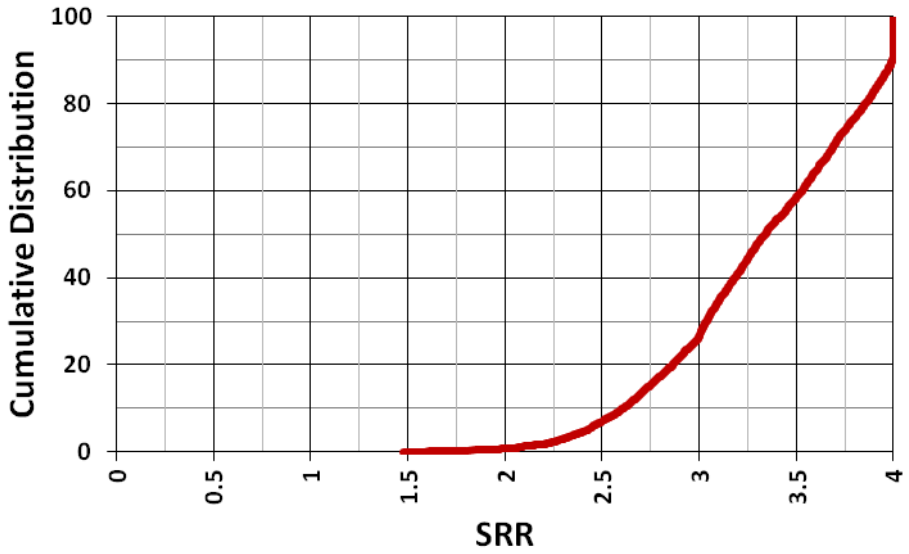

Figure 104: Cumulative distribution of SRR values for all of the events in the sixty-nine triggered seismic responses to mining shown in Figure 102.

In addition to the 69 post blast triggered responses as discussed above, there are 41 seismic responses to mining considered in this case study during the mine shutdown period. For the shutdown period responses, Figure 105 and Figure 106 depict the seismic event and response centroid locations, respectively. No mine blasts are shown, as no mine blasting occurred during the 16-day shutdown.

The vast majority of shutdown seismic responses spatially resemble the triggered responses, and occur in the same area of the rock mass (shown in Figure 99). There is however a subset of shutdown responses, occurring within the mine development below 2,400z, which are not observed in the triggered responses during regular mining. These responses likely correspond to larger scale rock mass failures that are typically masked and not identifiable during regular mine operations (blasting).

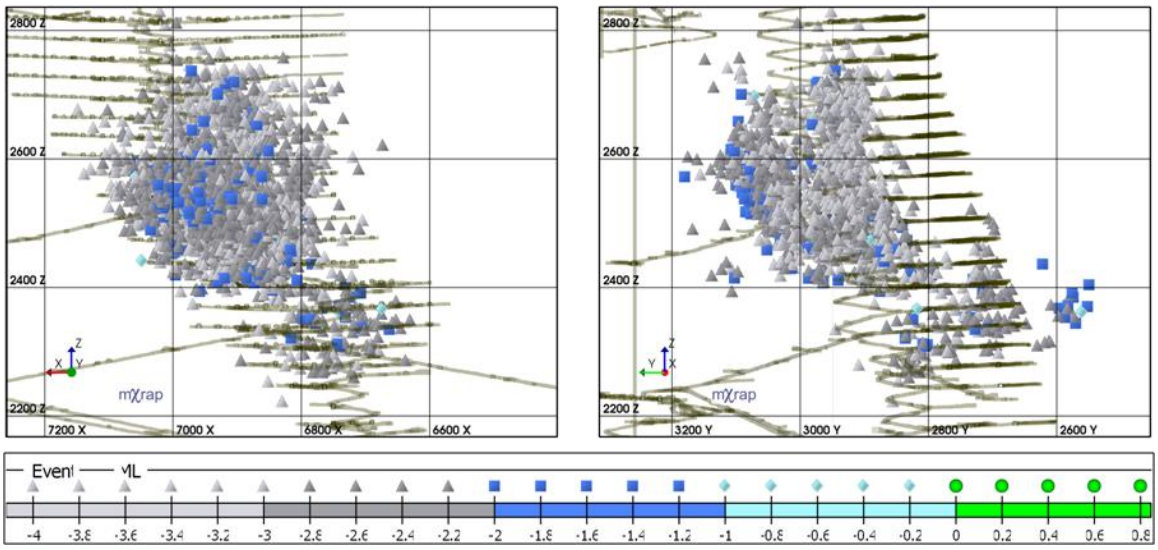

Figure 105: Longitudinal and cross-sectional projections of LaRonde mine showing shutdown seismic responses to mining. No mine blasts are shown as no mine blasting occurs during the shutdown period.

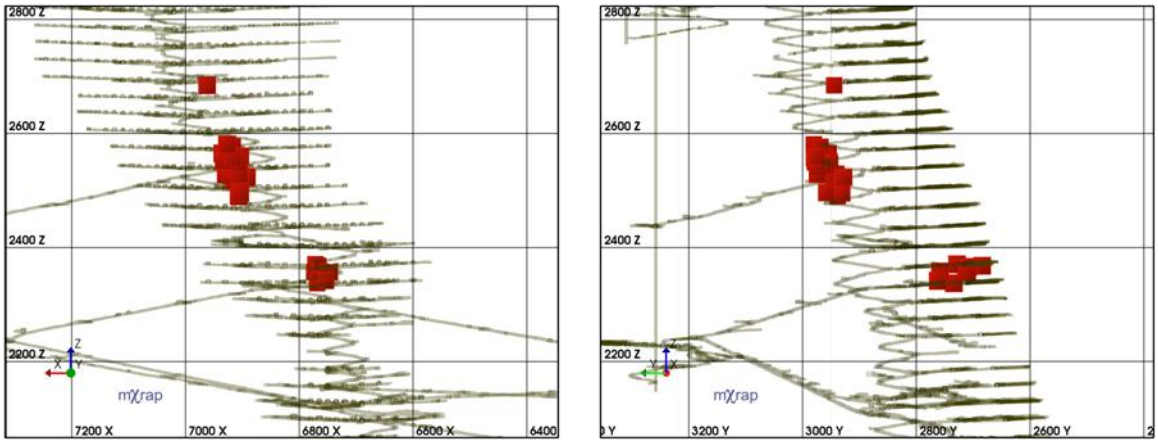

Figure 106: Longitudinal and cross-sectional projections of LaRonde mine showing the shutdown response centroid locations (calculated as shown in Equation 12). No mine blasts are shown as no mine blasting occurs during the shutdown period.

Figure 107 is a Magnitude-Time History chart for the shutdown period seismic responses to mining (shown in Figure 105). Nominal mine blast times (at 05:40 and 17:40), for when mine blasts would be if there had been no shutdown, are shown along the x-axis as blue stars. However, these are only representations used to identify the seismic responses. Individual seismic events are coloured according to SRR - assuming a DTB_N value of one. While the overall trends are the same as those observed in Figure 102 (triggered responses), the shutdown period responses are more representative of a theoretically perfect triggered response. Because the identification of responses does not depend on real mine blasting, as it does for the triggered responses shown in Figure 102, there are consistent shutdown period responses every 12 hours in Figure 107. This is reflected in the cumulative number of events line as a constant rate of events over the entire time period. SRR values are typically between 3 and 4, and while no large

magnitude seismic events are contained within the shutdown period responses, there are no mine blasts during the time period. This is indicative of triggered seismicity, as more energy is being released than injected into the mining environment.

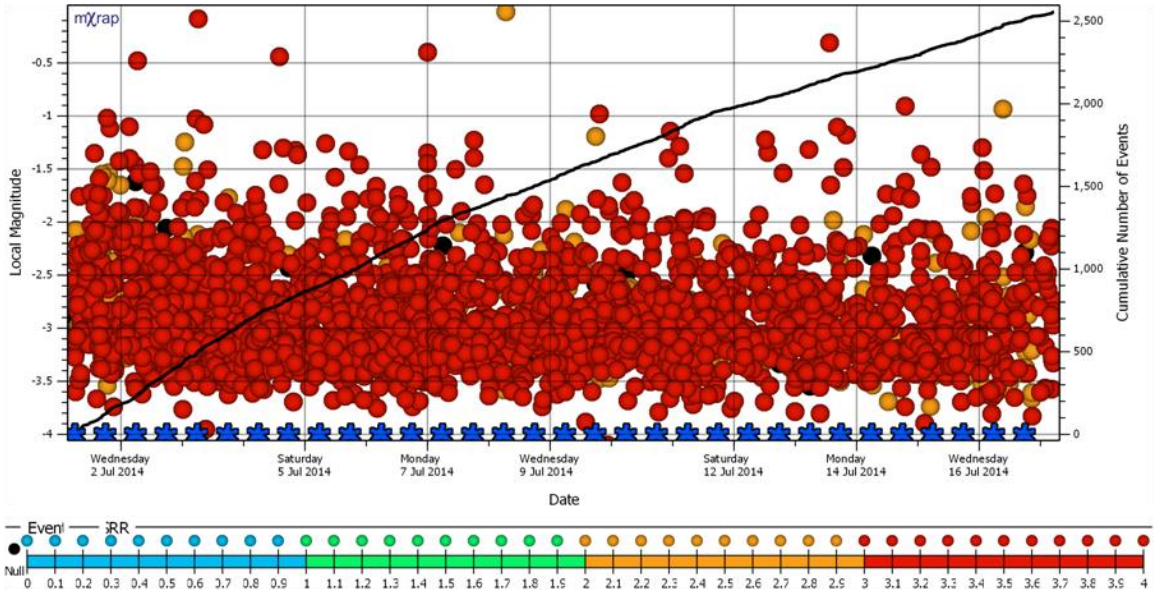

Figure 107: Magnitude-Time History chart for forty-one seismic responses occurring during a mine shutdown, where no mine blasting occurs, at LaRonde. Theoretical blast representations, used only to facilitate response identification, are shown along the x-axis as blue stars. Seismic events are coloured according to individual Seismic Response Rating (SRR), which assumes a DTB_N value of one. The first event in each individual seismic response is coloured black, as these events have no TBE_N parameters and consequently may exhibit uncharacteristic SRR's.

A relative frequency distribution of SRR values for the shutdown period seismic responses is shown in Figure 108. There is a strong dominance of large SRR values, indicating many individual SRP_N's likely approach or equal one. Relative to the triggered responses (Figure 103), the shutdown period responses exhibit larger SRR values - typically ranging 2.5 to 4. As no SRR values are below 2, this population is highly representative of triggered seismicity. Figure 109 is a cumulative distribution of the same SRR values shown in Figure 108. The median value is approximately 3.5, with more than 95% of all individual events exhibiting SRR values within the proposed guideline of SRR greater than 2.5 (Table 23).

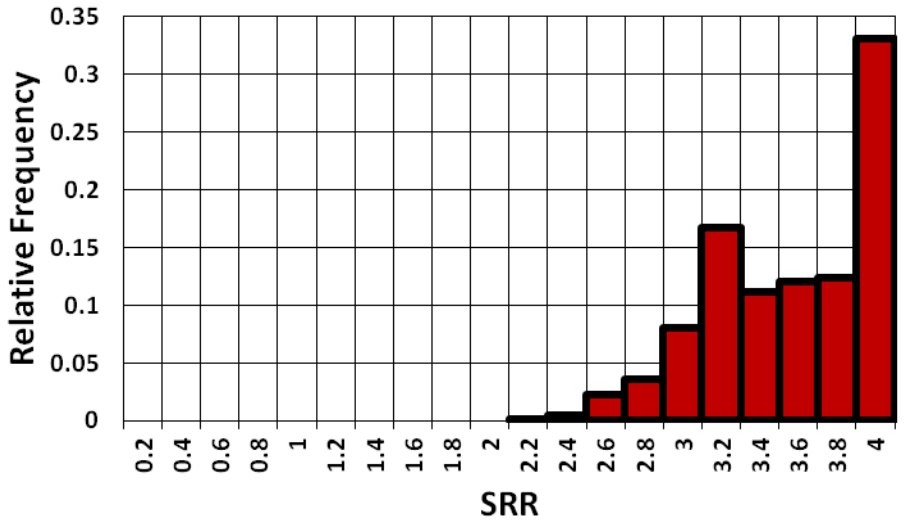

Figure 108: Relative frequency distribution of SRR values for all of the events in the forty-one shutdown period seismic responses to mining shown in Figure 107.

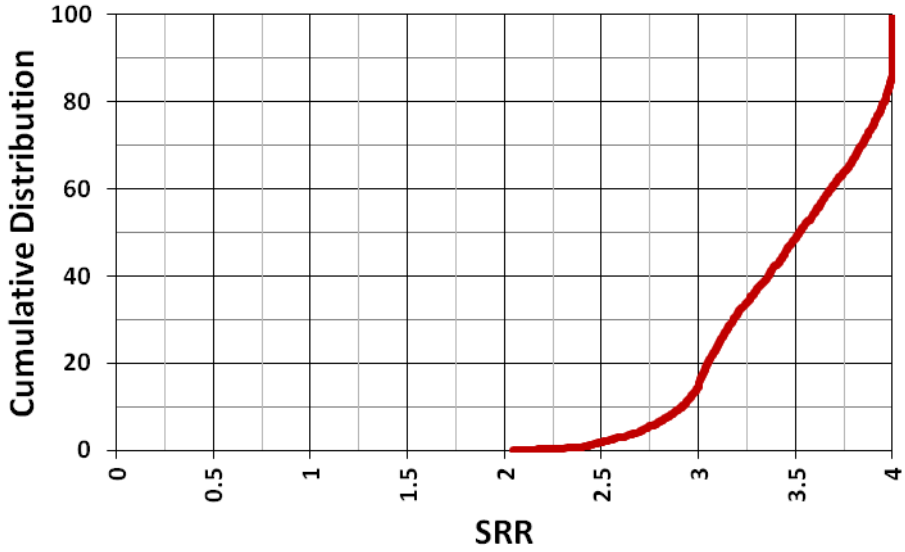

Figure 109: Cumulative distribution of SRR values for all of the events in the forty-one shutdown period seismic responses to mining shown in Figure 107.

7.2.2 SRP and SRP_N Distributions for Triggered Seismic Responses

The main difference between triggered and shutdown period seismic responses to mining is the lack of stimuli. Because there is no mine blasting during the time over which shutdown period seismic responses are identified, there is no DTB value calculated. A previous section (Section 4.6), summarized the basic spatial and temporal relations between triggered seismic responses to mining and mine blasts. Table 27 summarizes these relations as they pertain to Seismic Response Parameters and the triggered and shutdown period seismic responses included in this case study.

A summary of observation guidelines for Normalized Seismic Response Parameters was provided in Table 14, and can be found in Appendix A for quick reference.

Table 31: Summary table of defining properties and characteristics of triggered and shutdown seismic responses to mining (redrawn from Table 13).

	Triggered	**Shutdown**
Distance To Blast [DTB]	*Excavation Radius 15 m & Location Error Factor 10 m:* *DTB > 85 m*	*Not Applicable*
Time After Blast [TAB]	*All Events:* $0 \leq TAB \leq Maximum$	*All Events:* $0 \leq TAB \leq Maximum$
Distance to Centroid [DTC]	*Excavation Radius 15 m & Location Error Factor 10 m:* *DTB > 85 m*	*Excavation Radius 15 m & Location Error Factor 10 m:* *DTB > 85 m*
Time Between Events [TBE]	*All Events:* $0 \leq TAB \leq Maximum$	*All Events:* $0 \leq TAB \leq Maximum$

The SRP and SRP_N distributions for the triggered and shutdown period seismic responses at LaRonde mine are discussed throughout this section. Median values are key to interpreting seismic response and are highlighted with 'X' symbols and 'O' symbols for triggered and shutdown period responses, respectively. It is expected that triggered and shutdown responses will exhibit similar distributions across all parameters. Figure 110 and Figure 111 depict the cumulative distributions of DTB and DTB_N, respectively, for the triggered seismic responses to mining at LaRonde. There is no mine blasting during the shutdown, and consequently no shutdown DTB values are calculated. All triggered seismic events occur between approximately 100 and 400 metres from mine blasting, well beyond the conservative assumed mining-induced stress change zone. This is reflected in the DTB_N values (shown in Figure 111), as all triggered responses considered exhibits $\widetilde{DTB}_N$ values of one.

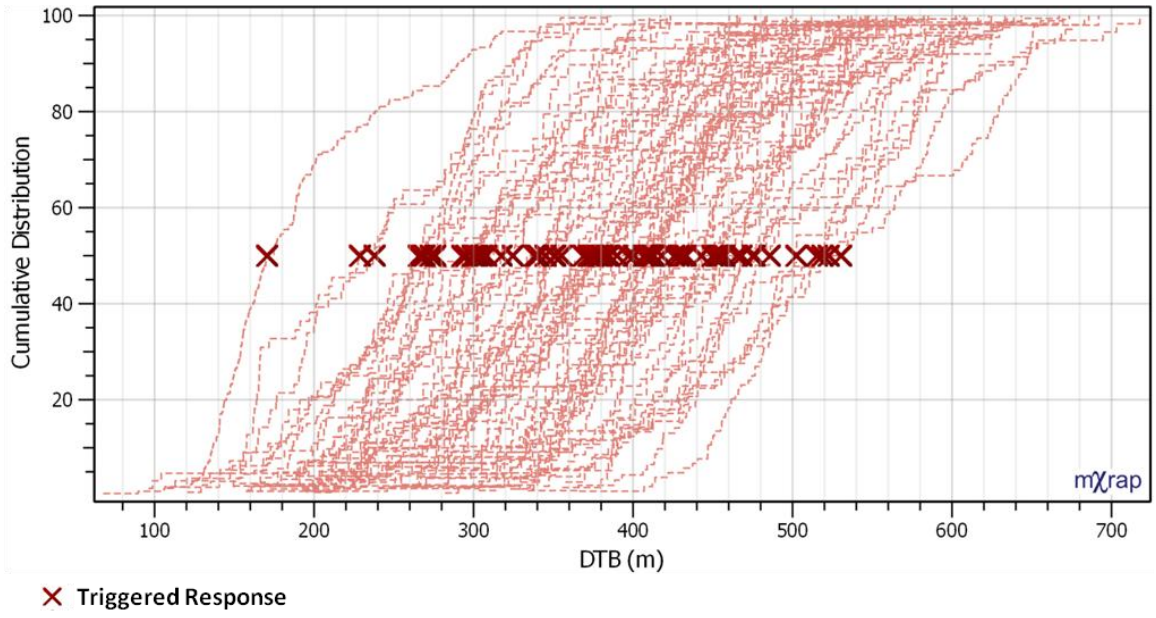

Figure 110: Cumulative distributions (post-step line shown), of SRP Distance To Blast (DTB) for a series of triggered seismic responses to mining at LaRonde. Median values for each response are shown as 'X' symbols.

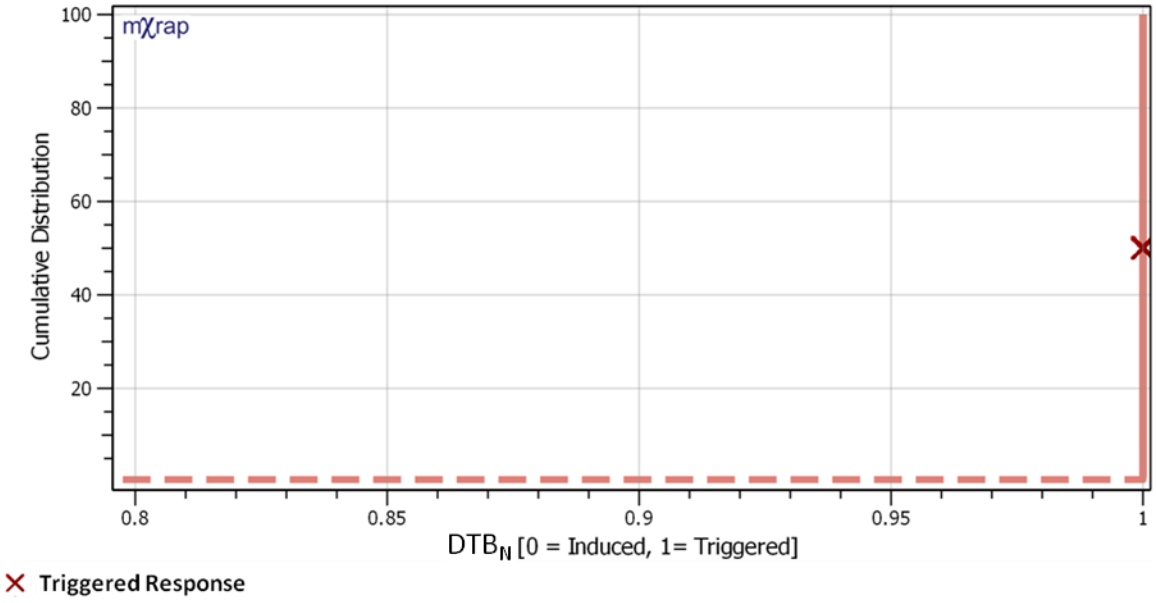

Figure 111: Cumulative distributions (post-step line shown), of Normalized Distance To Blast (DTB_N) for a series of triggered seismic responses to mining at LaRonde. Median values for each response are shown as 'X' symbols.

Triggered seismic responses to mining are expected to occur temporally independent of mine blasting. As such, the events should approach equal distribution throughout the temporal response identification window; as opposed to induced responses which concentrate at the beginning of the temporal window (i.e. blast time). Figure 112 and Figure 113 depict the cumulative distributions of TAB and TAB_N, respectively, for the triggered and shutdown period seismic responses to mining at LaRonde. The triggered ('X' symbols) and shutdown ('O'

symbols) responses considered exhibit very similar TAB distributions, as expected. All median TAB values are more than one and nearly all median TAB_N values range 0.5 to 1. All median TAB_N values for induced seismic responses to mining considered in this case study were less than 0.2 (shown in Figure 88).

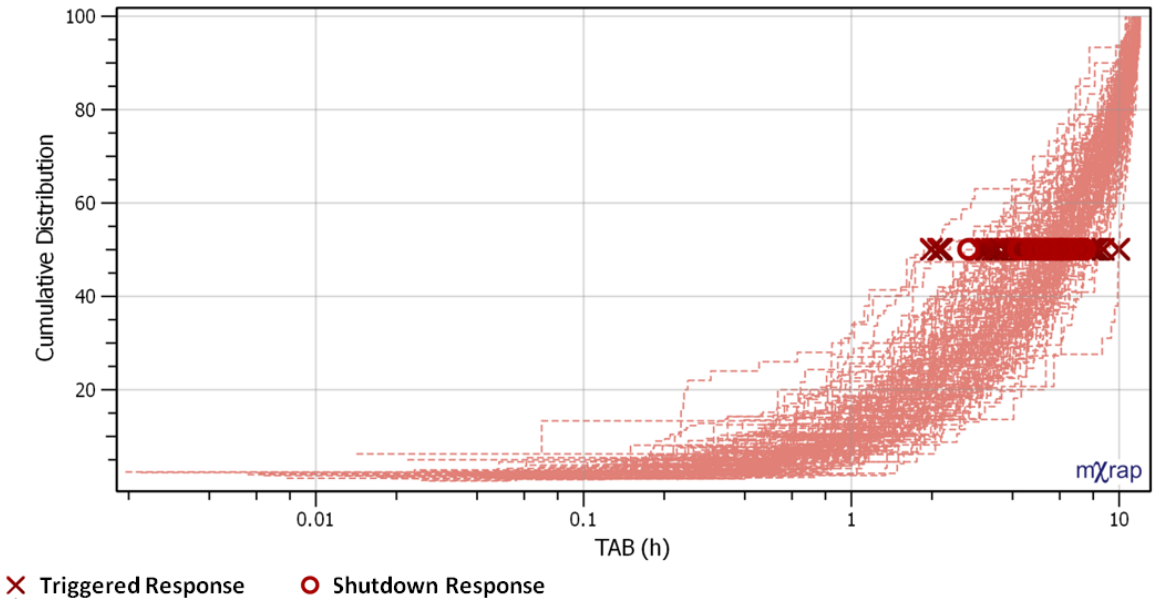

Figure 112: Cumulative distributions (post-step line shown), of SRP Time After Blast (TAB) for a series of triggered and shutdown seismic responses to mining at LaRonde. Median values for each response are shown as 'X' symbols and 'O' symbols for triggered and shutdown responses respectively.

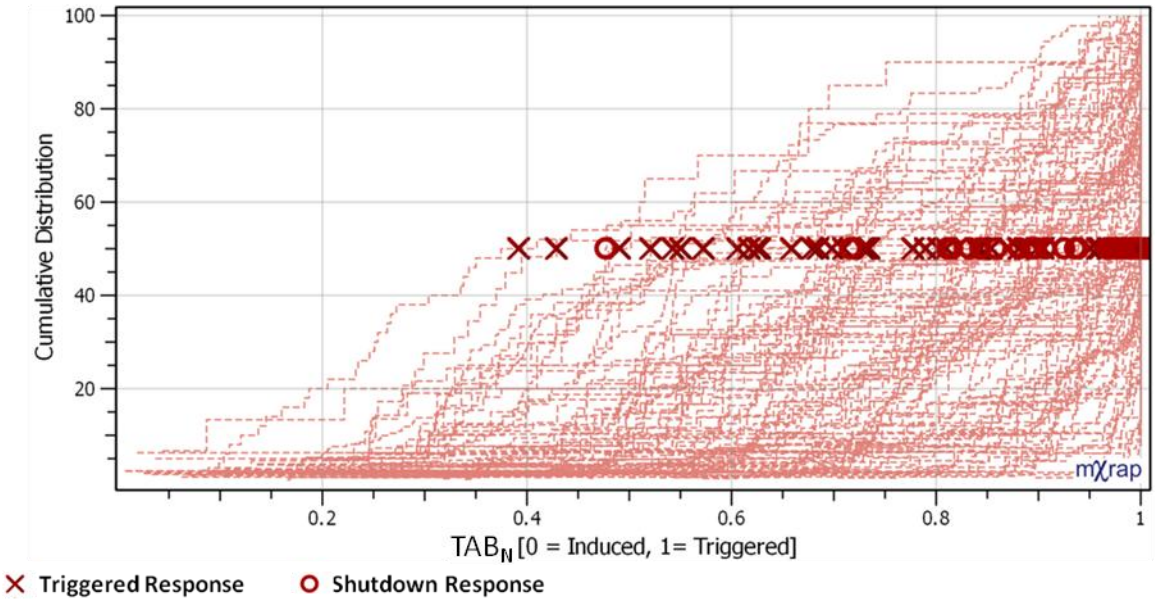

Figure 113: Cumulative distributions (post-step line shown), of Normalized Time After Blast (TAB_N) for a series of triggered and shutdown seismic responses to mining at LaRonde. Median values for each response are shown as 'X' symbols and 'O' symbols for triggered and shutdown responses respectively.

Figure 114 and Figure 115 depict the cumulative distributions of DTC and DTC_N, respectively, for the triggered and shutdown period seismic responses to mining at LaRonde. As expected, both types of responses exhibit similar distributions, and plot on top of one another (leading to data occlusion). All triggered and shutdown responses exhibit $\widetilde{DTC}_N$ values approaching one ($0.8 < \widetilde{DTC}_N < 1$), or equal to one.

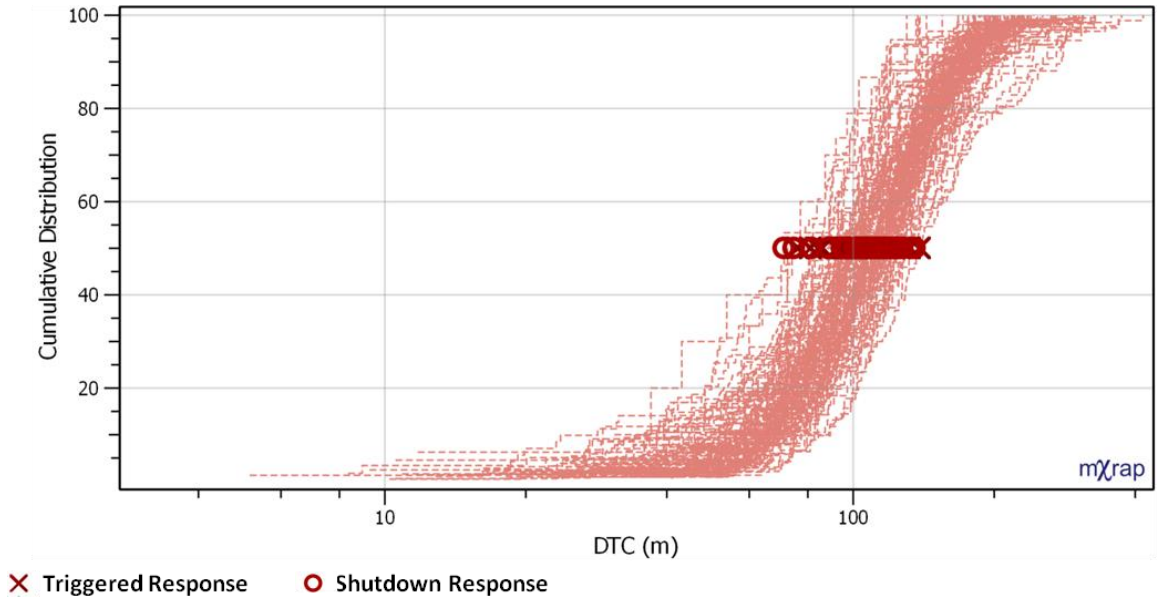

Figure 114: Cumulative distributions (post-step line shown), of SRP Normalized Distance To Centroid (DTC_N) for a series of triggered and shutdown seismic responses to mining at LaRonde. Median values for each response are shown as 'X' symbols and 'O' symbols for triggered and shutdown responses respectively.

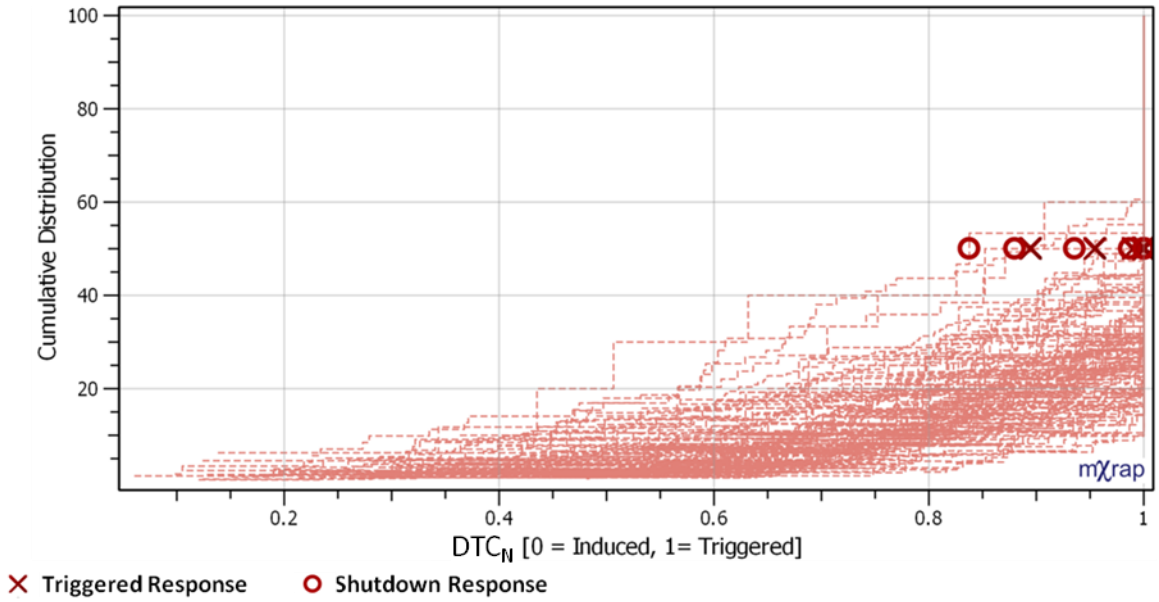

Figure 115: Cumulative distributions (post-step line shown), of Normalized Distance To Centroid (DTC_N) for a series of triggered and shutdown seismic responses to mining at LaRonde. Median values for each response are shown as 'X' symbols and 'O' symbols for triggered and shutdown responses respectively.

Figure 116 and Figure 117 depict the cumulative distributions of TBE and TBE_N, respectively, for the triggered and shutdown period seismic responses to mining at LaRonde. The triggered ('X' symbols) and shutdown ('O' symbols) responses considered exhibit similar TBE distributions. The vast majority of responses have median TBE values larger than 0.1, or 6 minutes. This is reflected in the TBE_N values, shown in Figure 117, which typically fall between 0.5 and 1 for triggered and shutdown period seismic responses to mining. All median TBE_N values for induced seismic responses to mining considered in this case study were less than 0.2 (shown in Figure 92).

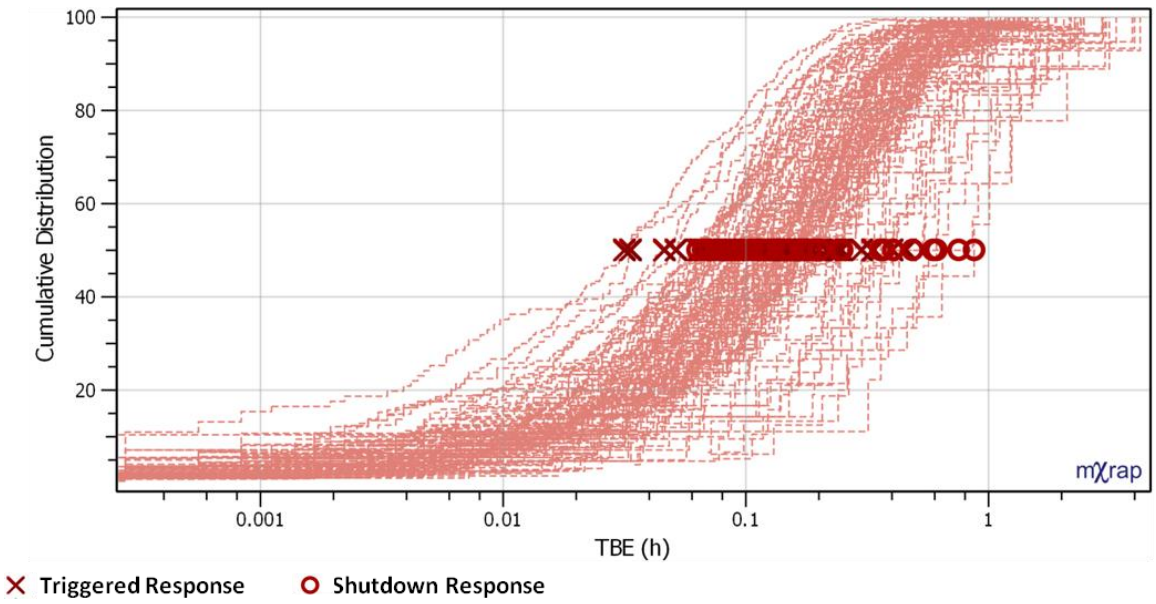

Figure 116: Cumulative distributions (post-step line shown), of SRP Time Between Events (TBE) for a series of triggered and shutdown seismic responses to mining at LaRonde. Median values for each response are shown as 'X' symbols and 'O' symbols for triggered and shutdown responses respectively.

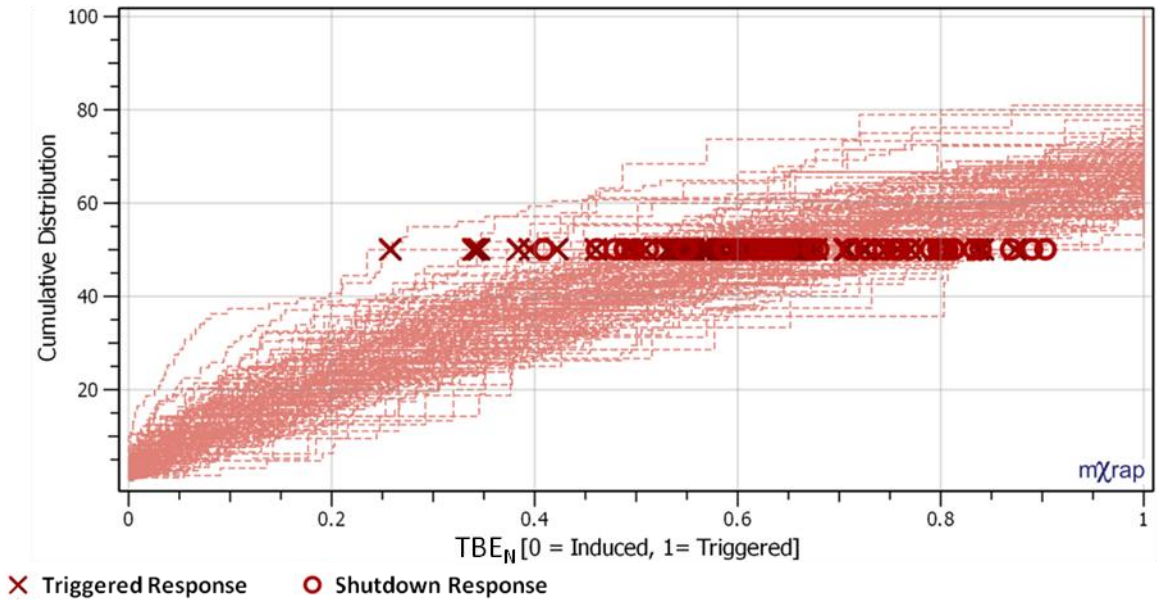

Figure 117: Cumulative distributions (post-step line shown), of Normalized Time Between Events (TBE_N) for a series of triggered and shutdown seismic responses to mining at LaRonde. Median values for each response are shown as 'X' symbols and 'O' symbols for triggered and shutdown responses respectively.

7.2.3 Interpreting Triggered Seismic Responses to Mining

Table 32 summarizes the expected SPR_N chart and SRR observations for triggered seismic responses to mining. These guidelines can be helpful in interpreting seismic responses using entire distributions of parameters, or representative value, such as the response median.

Table 32: Summary table of SRP_N chart and SRR observation guidelines for triggered seismic responses to mining (Redrawn from Table 23).

	Triggered
SRP_N Charts	Large Area *Temporal Parameters:* *[TAB_N & TBE_N]* *Approaching 0.5 to 1* *Spatial Parameters:* *DTB_N = 1 &* *DTC_N Approaching 1*
SRR	Large SRR *$2.5 \leq SRR \leq 4$*

Seismic Response Rating values can provide significant insight into a seismic response using only a single value, discussed in Section 5.2. Figure 118 depicts the cumulative distributions of SRR for the triggered and shutdown period seismic responses to mining considered in this case study. The triggered ('X' symbols) and shutdown ('O' symbols) seismic responses considered exhibit similar SRR distributions. Triggered seismic responses are expected to exhibit SRR median values between 2.5 and 4 (refer to Table 32), and all median SRR values for triggered and shutdown period seismic responses considered in this case study adhere to the proposed observation guidelines.

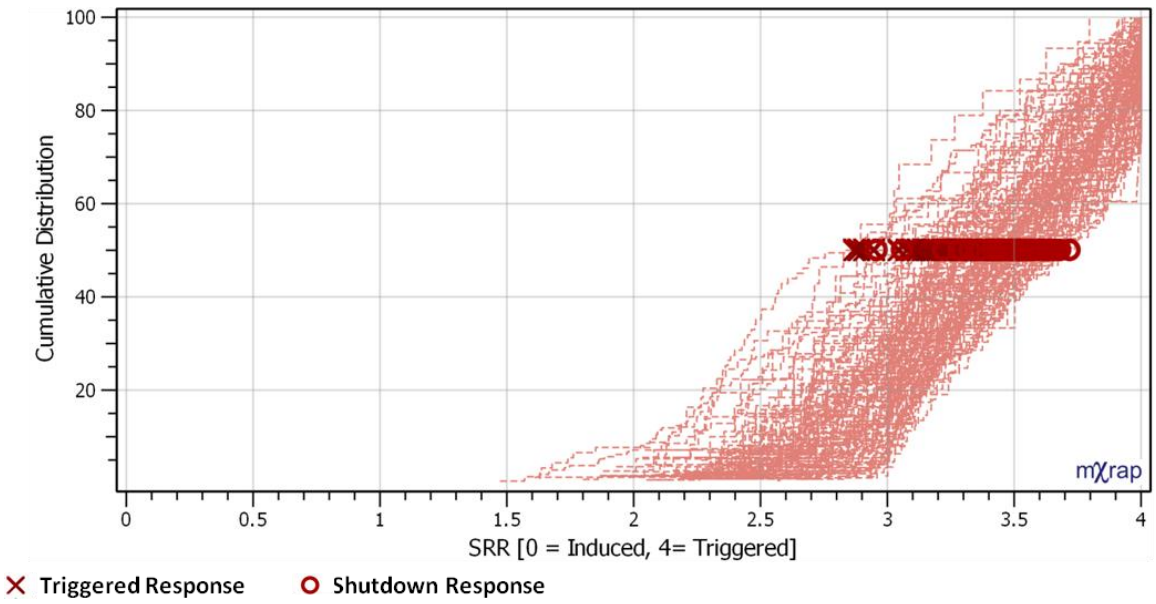

Figure 118: Cumulative distributions (post-step line shown), of Seismic Response Ratings (SRR) for a series of triggered and shutdown seismic responses to mining at LaRonde. Median values for each response are shown as 'X' symbols and 'O' symbols for triggered and shutdown responses respectively.

For interpreting seismic responses to mining, median values alone can provide significant insight into the nature of a seismic response. SRP_N charts, discussed in detail in Section 5.1, are shown in Figure 119 and Figure 120, for the triggered and shutdown period seismic responses to mining, respectively. SRR charts for each individual triggered and shutdown period response can be found in Appendix D and Appendix E, respectively. All triggered and shutdown responses exhibit SRP_N charts and SRR values indicative of triggered seismicity.

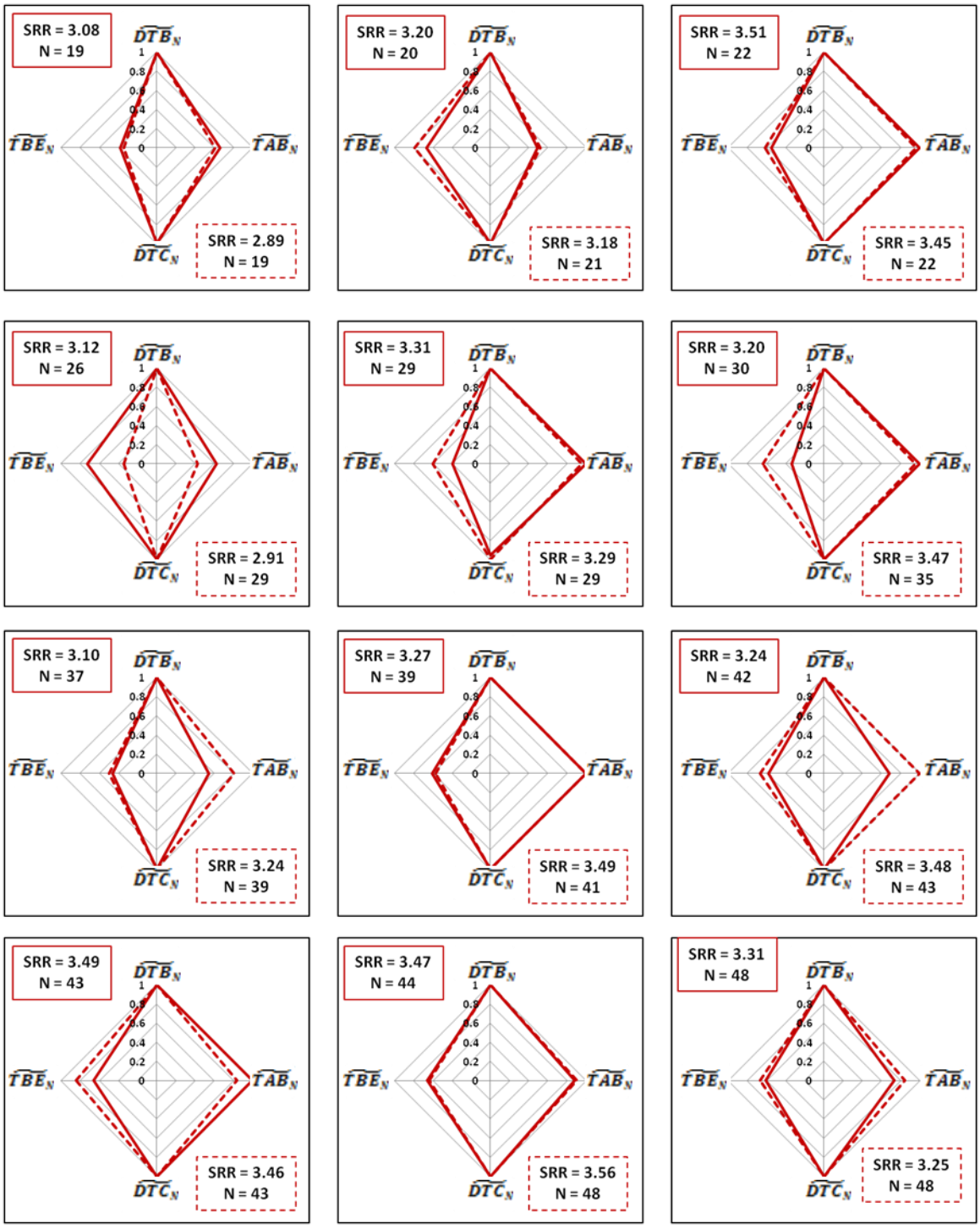
SRR = 3.08
N = 19
SRR = 2.89
N = 19
SRR = 3.20
N = 20
SRR = 3.18
N = 21
SRR = 3.51
N = 22
SRR = 3.45
N = 22
SRR = 3.12
N = 26
SRR = 2.91
N = 29
SRR = 3.31
N = 29
SRR = 3.29
N = 29
SRR = 3.20
N = 30
SRR = 3.47
N = 35
SRR = 3.10
N = 37
SRR = 3.24
N = 39
SRR = 3.27
N = 39
SRR = 3.49
N = 41
SRR = 3.24
N = 42
SRR = 3.48
N = 43
SRR = 3.49
N = 43
SRR = 3.46
N = 43
SRR = 3.47
N = 44
SRR = 3.56
N = 48
SRR = 3.31
N = 48
SRR = 3.25
N = 48

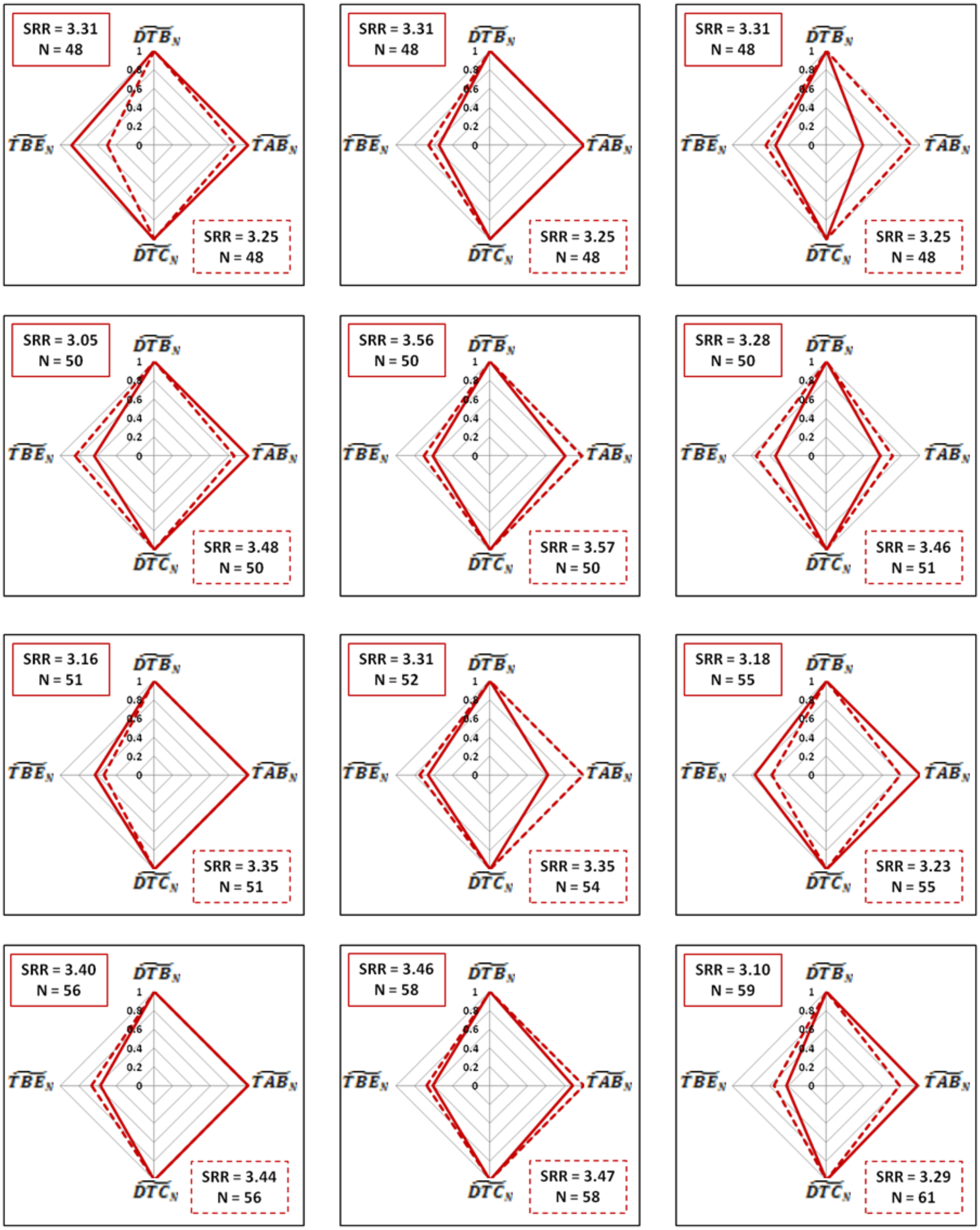
SRR = 3.31
N = 48
SRR = 3.25
N = 48
SRR = 3.31
N = 48
SRR = 3.25
N = 48
SRR = 3.31
N = 48
SRR = 3.25
N = 48
SRR = 3.05
N = 50
SRR = 3.48
N = 50
SRR = 3.56
N = 50
SRR = 3.57
N = 50
SRR = 3.28
N = 50
SRR = 3.46
N = 51
SRR = 3.16
N = 51
SRR = 3.35
N = 51
SRR = 3.31
N = 52
SRR = 3.35
N = 54
SRR = 3.18
N = 55
SRR = 3.23
N = 55
SRR = 3.40
N = 56
SRR = 3.44
N = 56
SRR = 3.46
N = 58
SRR = 3.47
N = 58
SRR = 3.10
N = 59
SRR = 3.29
N = 61
$\widetilde{DTB}_N$
$\widetilde{TAB}_N$
$\widetilde{DTC}_N$
$\widetilde{TBE}_N$
1
0.8
0.6
0.4
0.2
0

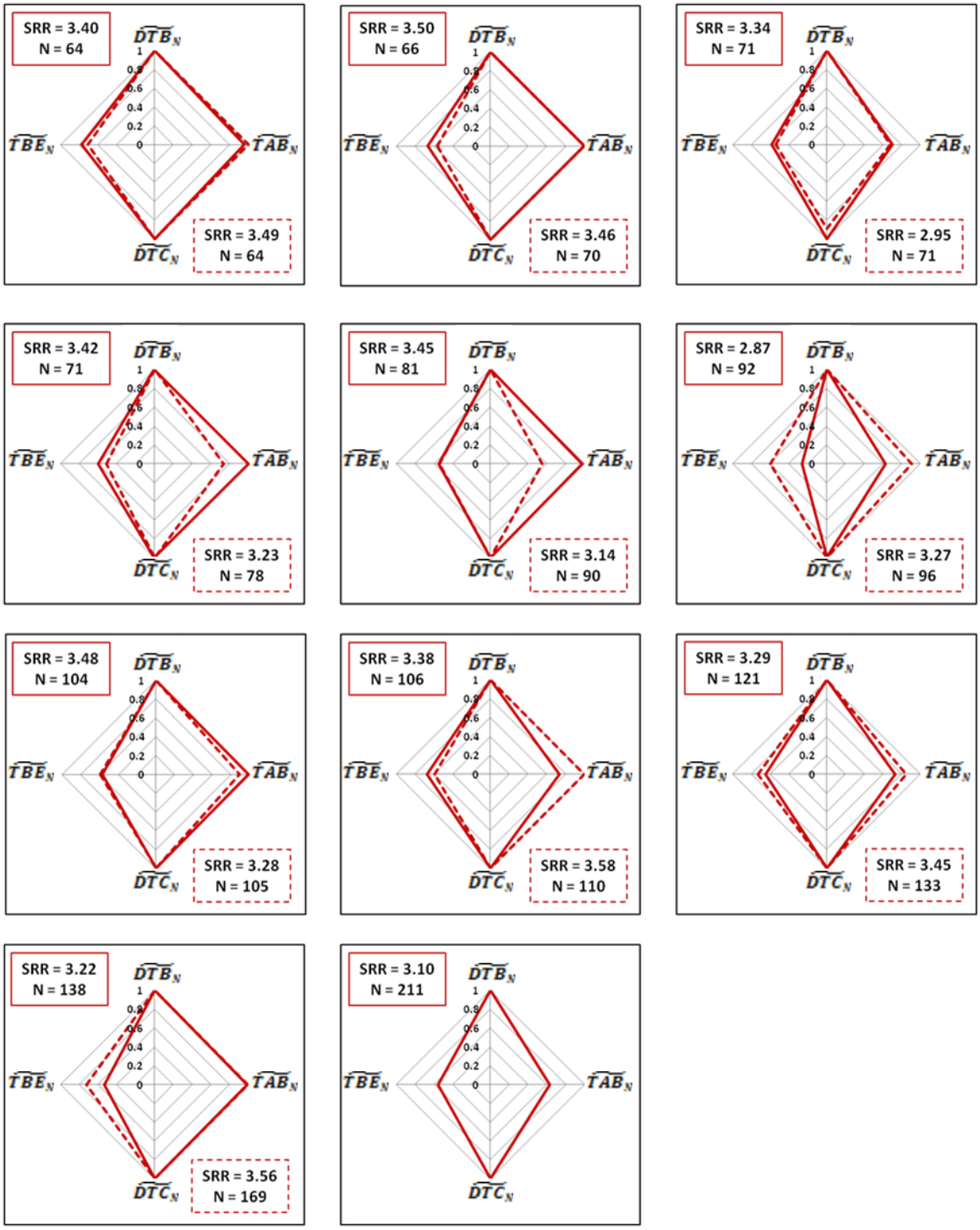

Figure 119: SRP_N charts for all triggered seismic responses to mining considered in the LaRonde Case Study. For brevity purposes, two responses are shown per SRP_N chart.

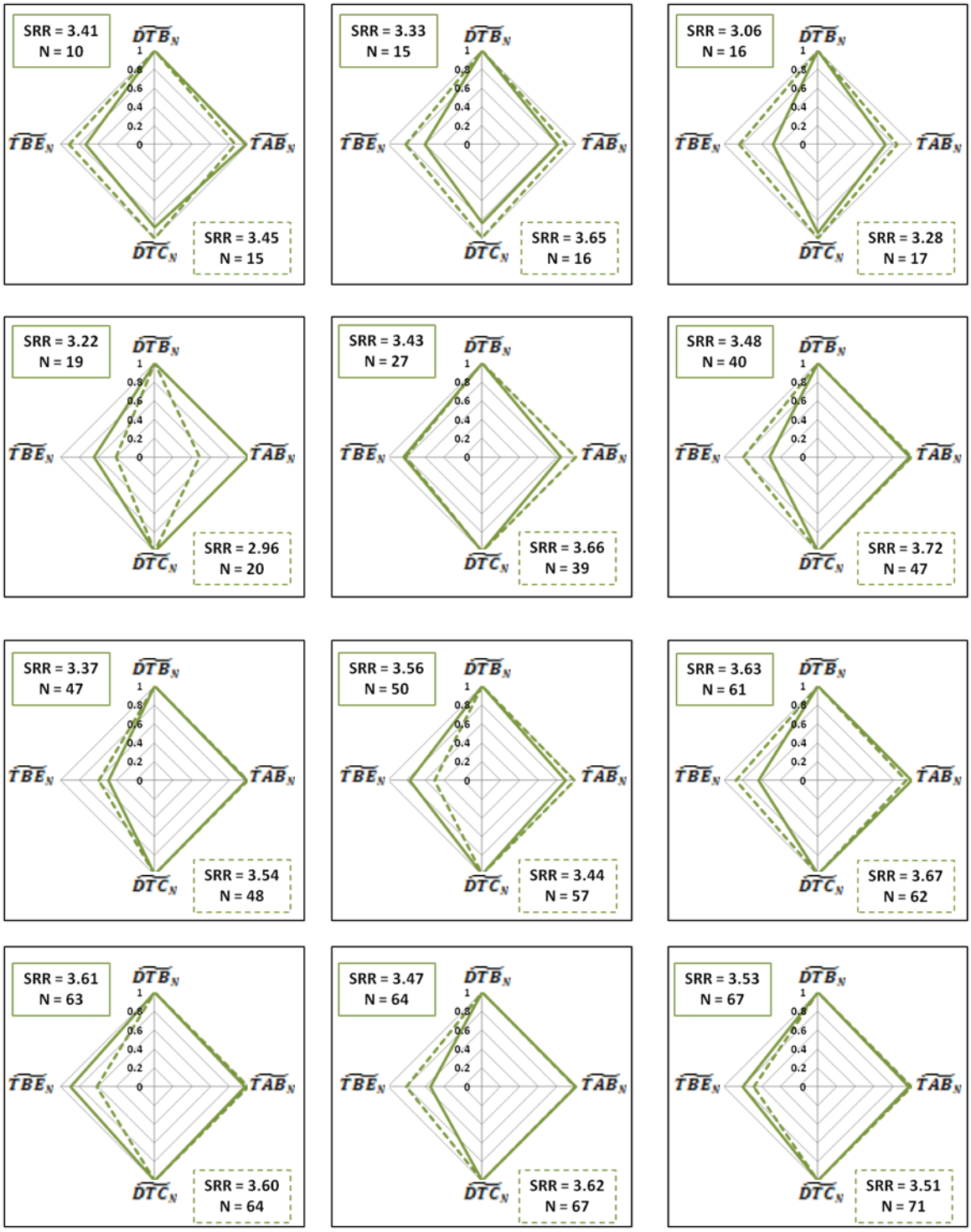
SRR = 3.41
N = 10
SRR = 3.45
N = 15
SRR = 3.33
N = 15
SRR = 3.65
N = 16
SRR = 3.06
N = 16
SRR = 3.28
N = 17
SRR = 3.22
N = 19
SRR = 2.96
N = 20
SRR = 3.43
N = 27
SRR = 3.66
N = 39
SRR = 3.48
N = 40
SRR = 3.72
N = 47
SRR = 3.37
N = 47
SRR = 3.54
N = 48
SRR = 3.56
N = 50
SRR = 3.44
N = 57
SRR = 3.63
N = 61
SRR = 3.67
N = 62
SRR = 3.61
N = 63
SRR = 3.60
N = 64
SRR = 3.47
N = 64
SRR = 3.62
N = 67
SRR = 3.53
N = 67
SRR = 3.51
N = 71

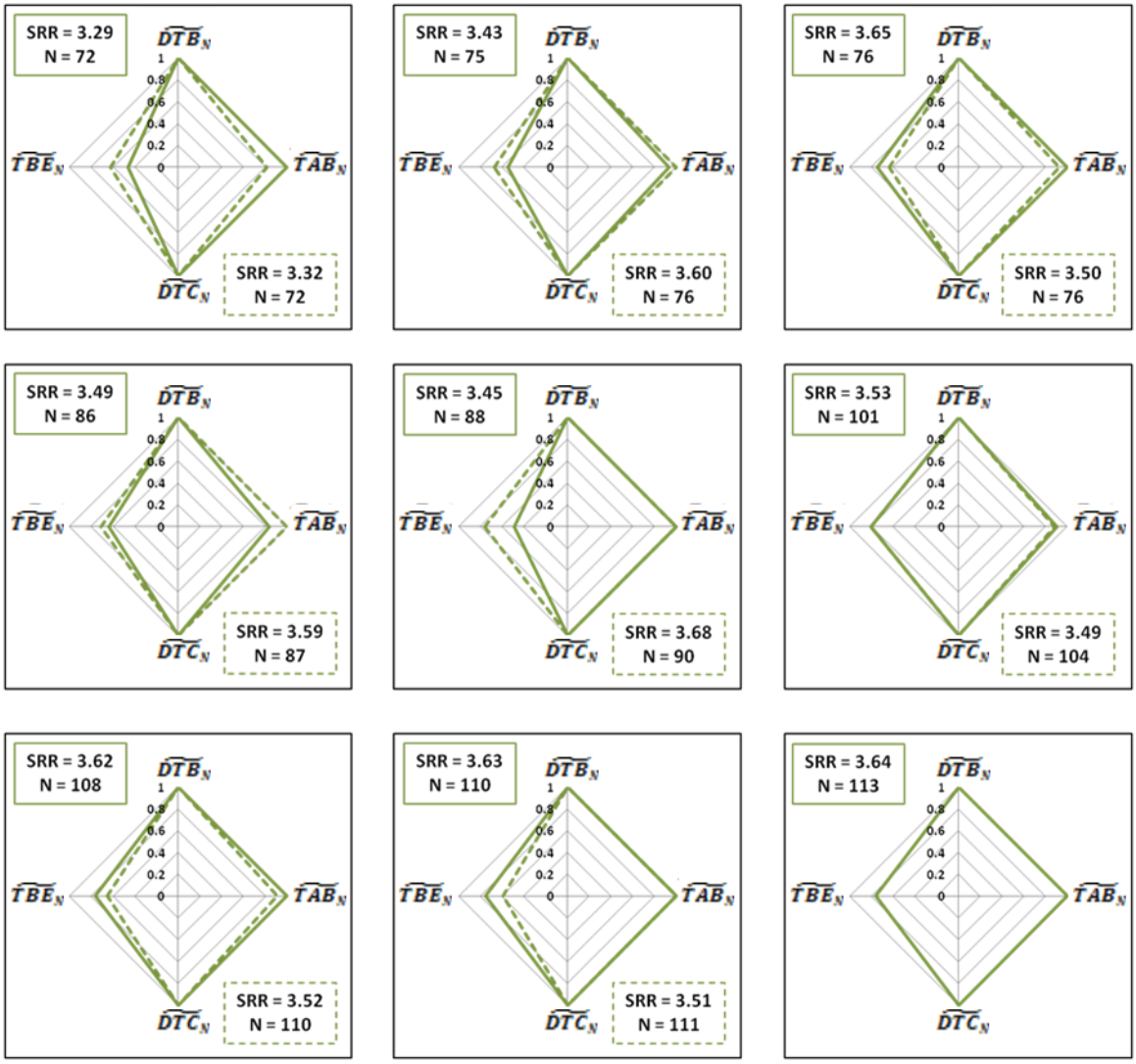

Figure 120: SRP_N charts for all shutdown period seismic responses to mining considered in the LaRonde Case Study. For brevity purposes, two responses are shown per SRP_N chart.

7.2.4 Discussion of Triggered SRP_N's

This section has demonstrated the applicability of SRP_N's (DTB_N, TAB_N, DTC_N and TBE_N) and SRR to triggered seismic responses at LaRonde mine. Seismic responses triggered during regular mining activities, and during a mine shutdown period during which no mine blasting occurred, have been examined. It should be noted that no unexpected observations were made for triggered seismic responses to mining at LaRonde. Figure 121 depicts the relative frequency distributions for the Normalized Seismic Response Parameters of triggered and shutdown period seismic responses considered in this case study. Distributions of both temporal SRP_N's (TAB_N and TBE_N), and spatial SRP_N's (DTB_N and DTC_N) are highly indicative of triggered seismicity, with strong concentrations of values approaching or equal to one.

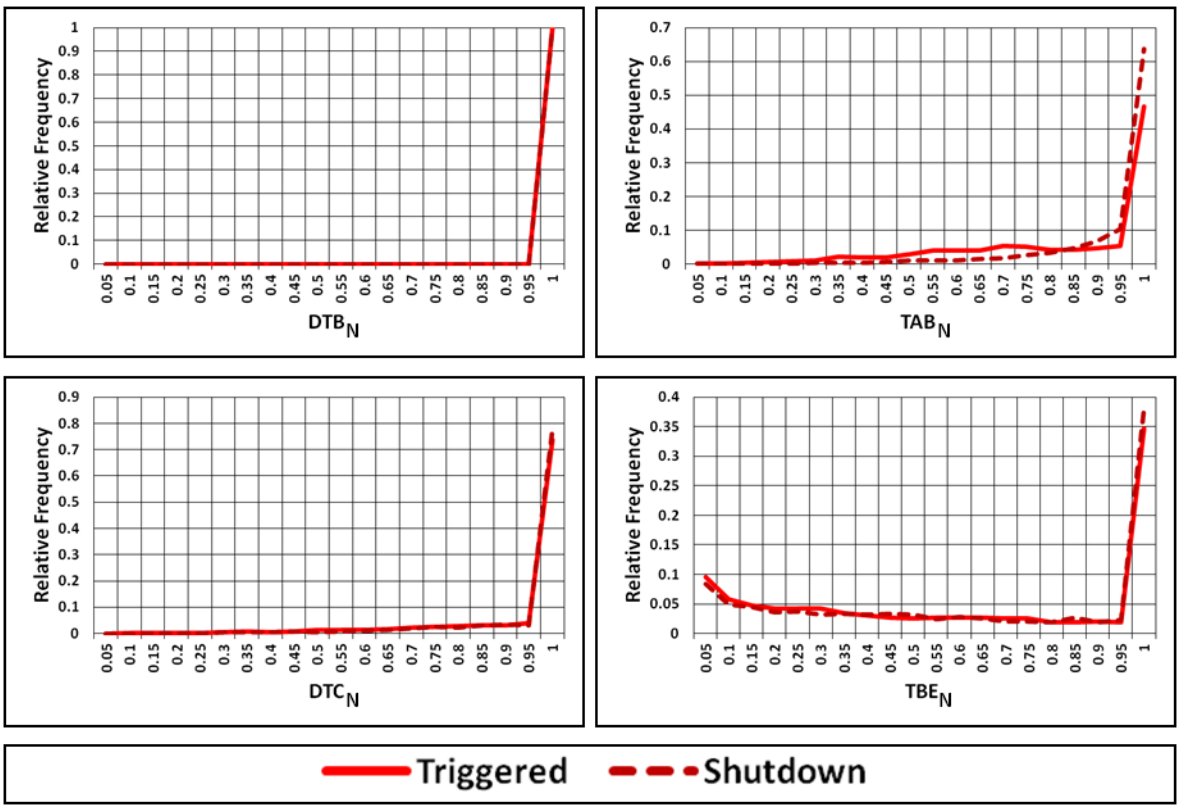

Figure 121: Relative frequency distributions for DTB_N, TAB_N, DTC_N and TBE_N for all previously shown triggered seismic responses to mining at LaRonde mine.

Both the triggered and shutdown period seismic responses considered in the LaRonde mine case study exhibit SRP_N and SRR values indicative of triggered seismicity. SRP_N distributions shown in Figure 121 are nearly identical for the two different types of seismic responses, strongly supporting that their space/time characteristics are the same. This conclusion has significant implications for the concept of background seismicity, as is discussed in Chapter 8 (Section 8.4).

Within this case study, triggered seismic responses to mining are located throughout the deep footwall of LaRonde mine, and consequently are relatively diffuse. Comparatively dense triggered responses, commonly located in proximity to mine workings (with better microseismic system coverage), are a minority in this case study. Triggered seismic responses of this nature should exhibit DTB_N values of 1, but may exhibit decreased DTC_N values, resulting in slightly lower SRR values. Examples of this type of triggered seismic response were included in the shutdown period responses, with successful application of SRP_N's and SRR. Notably, these triggered responses occurred in areas of the rock mass that commonly exhibit complex seismic responses during regular mining activities.

7.2.5 Summary of Triggered Seismic Responses to Mining at LaRonde

Triggered and shutdown period seismic responses to mining at LaRonde mine considered in this case study exhibit characteristics indicative of triggered seismicity (as defined within the context of this thesis). No outliers were present within the data. Table 33 summarizes the proposed observation guidelines and the actual observations from the LaRonde mine case study surrounding triggered seismic responses to mining.

Table 33: Summary of SRR and SRP_N expected observation guidelines for triggered responses and median distributions for the LaRonde case study of triggered and shutdown period seismic responses to mining. Median distributions are shown as 'X' symbols and 'O' symbols for triggered and shutdown period seismic responses respectively. Table continued on subsequent page.

	Observation Guidelines: Triggered	Median Distributions for LaRonde Case Study: Triggered and Shutdown
SRR	**Large SRR** $[2.5 \leq SRR \leq 4]$	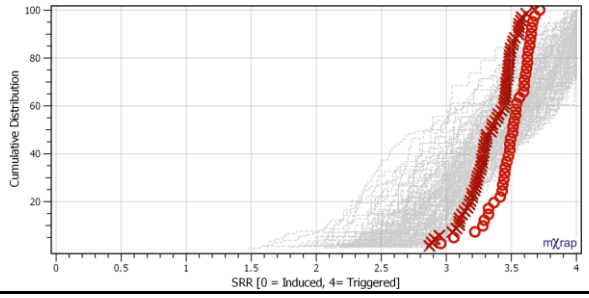
DTB_N	**Equal to One** $[DTB_N = 1]$	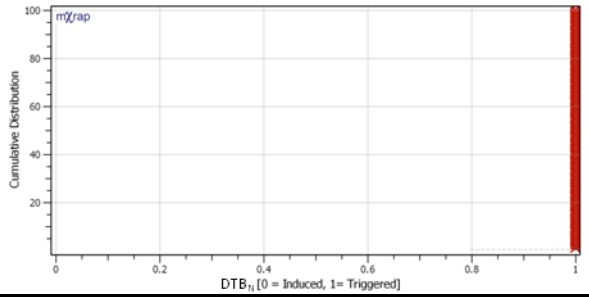
TAB_N	**Approaching One** $[0.5 \leq TAB_N \leq 1]$	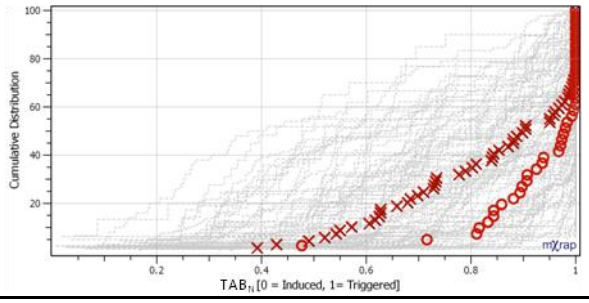

	Observation Guidelines: Triggered	Median Distributions for LaRonde Case Study: Triggered and Shutdown
DTC_N	**Approaching One [$DTC_N \approx 1$]**	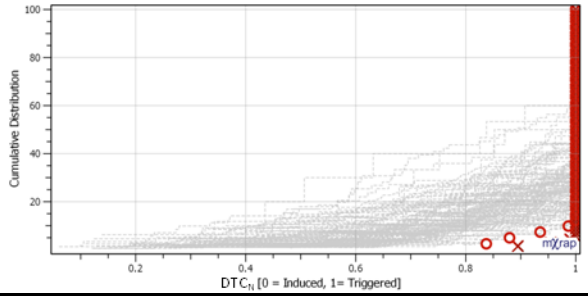
TBE_N	**Approaching One [$0.5 \leq TBE_N \leq 1$]**	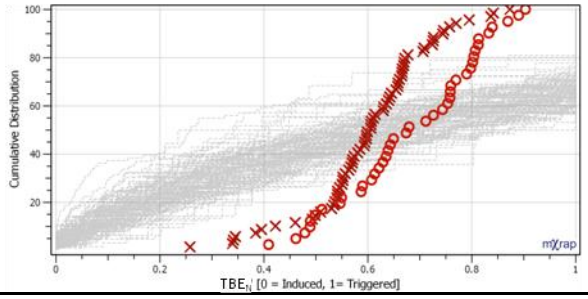

7.3 Case Study III: Complex Seismic Responses to Mining

This case study focuses on complex seismic responses to mining. The concept of complex seismicity has been defined within the context of this thesis as an induced and triggered seismic response superimposed in space and time. In other words, a complex seismic response must occur predominantly within the assumed mining-induced stress change zone of a discrete mine blast, and over a single response identification time window. Seismic clusters, or responses, can be generated using a variety of different methodologies (Woodward, 2015). When seismic responses are identified such that an induced and triggered response are arbitrarily joined, based on response identification parameters (e.g. Figure 68), they are not representative of a true complex response. In these cases, the two responses are not actually superimposed in space, as the triggered response occurs beyond the assumed mining-induced stress change zone. Seismic responses identified with the intention of using SRP_N's should always aim to minimize the probability of arbitrarily blending induced and triggered seismic responses to mining that are not directly overlaid in space and time.

The space-time relations for complex seismic responses to mining depend on the relative proportions of induced and triggered seismic events contained within each individual response. Reasonable bounds for distinguishing between induced, complex and triggered seismicity depend on data and analysis specific considerations. For example, if the objective is to use induced seismic responses to identify low seismic hazard areas of a rock mass, there may be little tolerance for induced responses to include any events more than a few hours beyond mine blasting. As such, any induced response with temporal outliers would be classified as complex, thus generating a temporal analysis bound of a few hours following mine blasting between induced and complex seismic responses to mining.

Within this case study, two sub-types of complex seismic responses to mining are considered: Complex: Induced and Complex: Triggered. Complex responses that are predominantly induced (Complex: Induced), exhibit an increased ratio of induced to triggered seismic events within a single response. Complex responses that are considered Complex: Triggered, exhibit a significant number of triggered seismic events within a single response.

All complex seismic responses require the presence of a triggered source mechanism within the mining-induced stress change zone, and are consequently more likely to be associated with larger scale mine blasts (production blasts). Complex: Induced responses considered in this case study result from mine development blasts. Complex: Triggered responses considered in this case study result from mine production blasts. Similar to the responses induced from mine production blasts, the time period for identifying Complex: Triggered responses has been extended to include a sufficient quantity of production blasts. The time period is January, 2014 to July, 2014. Table 34 summarizes the parameters used for identifying the complex seismic responses to mining considered in this case study.

Table 34: Summary of parameters used to identify the 'Complex: Induced' and 'Complex: Triggered' seismic responses to mining at LaRonde and the common factors used in the calculation of SRP_N's.

		Complex: Induced	Complex: Triggered
Response Identification	**SLC d-value**	20 metres	20 metres
	Temporal Window	12 hours	12 hours
	Time Period	05/2014 - 07/2014	01/2014 - 07/2014
Calculation of SRP_N's	**Excavation Radius**	2.5 metres	15 metres
	Location Error Factor	10 metres	10 metres
	Assumed Mining-Induced Stress Change Zone	22.5 metres from Excavation Boundary	85 metres from Excavation Boundary

7.3.1 Complex Seismic Response Descriptions

A total of 27 Complex: Induced seismic responses to mining are considered in this case study. Figure 122 and Figure 123 depict the seismic event and response centroid locations, respectively, for the Complex: Induced responses. Mine blast locations are shown as red stars - indicating development blasts. Much like the development blast induced responses (Figure 79), the Complex: Induced responses focus around areas of the mine that were under development during the time period of interest. This is expected, as complex responses require a significant induced component by definition.

Response centroids, shown in Figure 123, locate in close proximity to the mine blast locations. This indicates these complex seismic responses contain a significant induced component. In a triggered complex seismic response, a strong triggered source mechanism must be partially located within the mining-induced stress change zone, but is unlikely to be located near the exact blast location. As such, the response centroid of a triggered complex response is likely to be offset from the mine blast location (as will be demonstrated in Figure 128 and Figure 129).

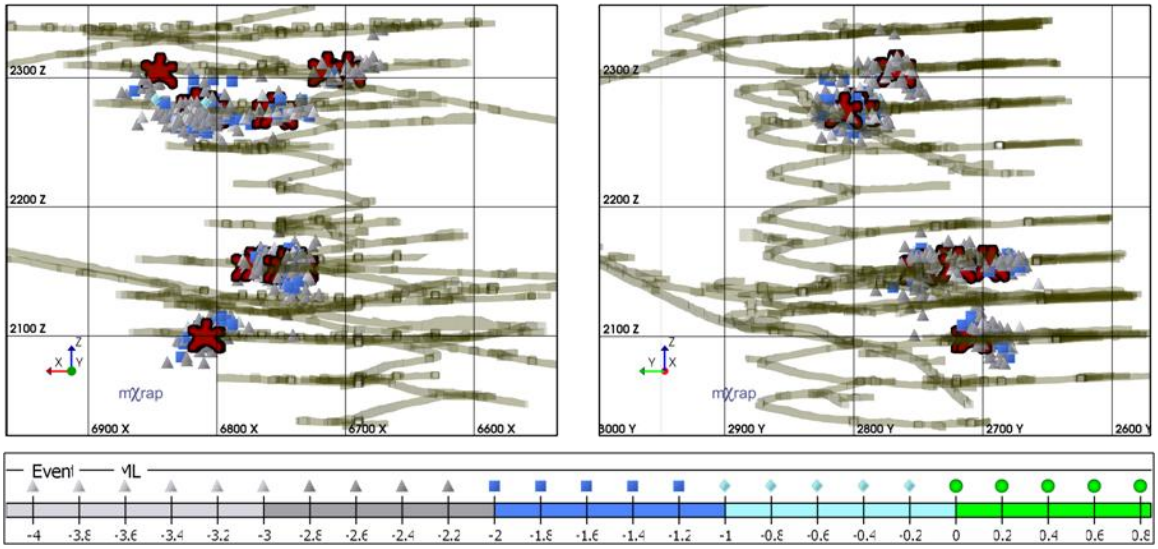

Figure 122: Longitudinal and cross-sectional projections of LaRonde mine showing Complex: Induced seismic responses to mining and associated mine development blasts (red stars).

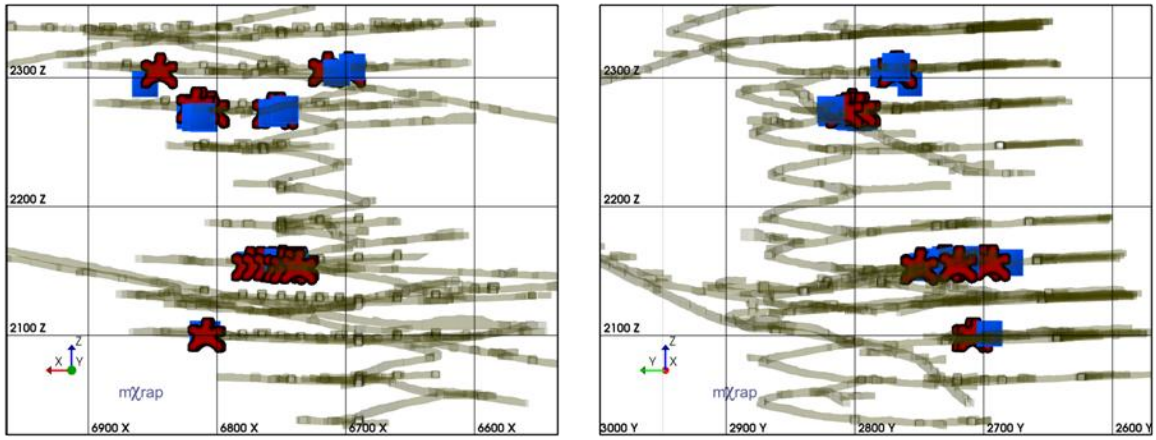

Figure 123: Longitudinal and cross-sectional projections of LaRonde mine showing Complex: Induced response centroid locations (calculated as shown in Equation 12), and associated mine development blasts (red stars).

Figure 124 is a Magnitude-Time History chart for the Complex: Induced seismic responses to mining (shown in Figure 122). Mine blasts are shown along the x-axis as red stars, and seismic events are coloured according to SRR. Distinct steps in the cumulative number of events line are present, indicating a significant induced component. There are also events occurring slightly offset from the induced lineations however, indicating a triggered component. A large magnitude seismic event ($M_L \geq 0$) , is included in the complex seismic responses - strongly indicating disproportional energy release and the presence of a triggered source mechanism.

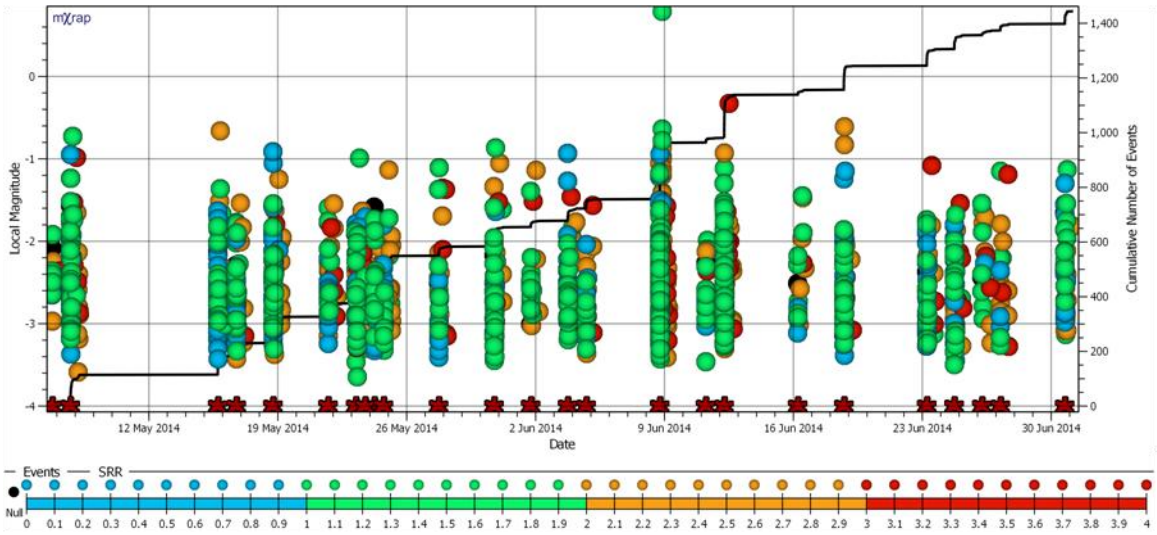

Figure 124: Magnitude-Time History chart for twenty-seven Complex: Induced seismic responses to mining at LaRonde. Mine development blasts are shown along the x-axis as red stars. Seismic events are coloured according to individual Seismic Response Rating (SRR). The first event in each individual seismic response is coloured black, as these events have no TBE_N parameters and consequently may exhibit uncharacteristic SRR's.

A relative frequency distribution of SRR values for the Complex: Induced seismic responses to mining is shown in Figure 125. SRR values typically fall between 1 and 3, indicative of complex seismicity. There is a strong dominance of relatively small SRR values however, indicative of predominantly induced complex seismicity. For a triggered complex response, a dominance of relatively large SRR values is expected. Figure 126 is a cumulative distribution of the same SRR values shown in Figure 125. The median value is slightly more than 1.25, with more than 60% of all individual events exhibiting SRR values within the proposed guideline of $1 \leq SRR \leq 3$ (Table 23).

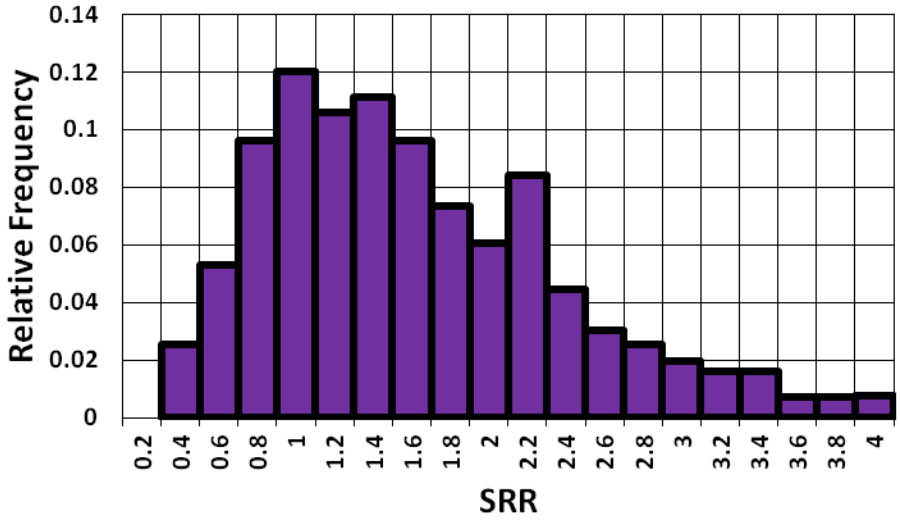

Figure 125: Relative frequency distribution of SRR values for all of the events in the twenty-seven Complex: Induced seismic responses to mining shown in Figure 124.

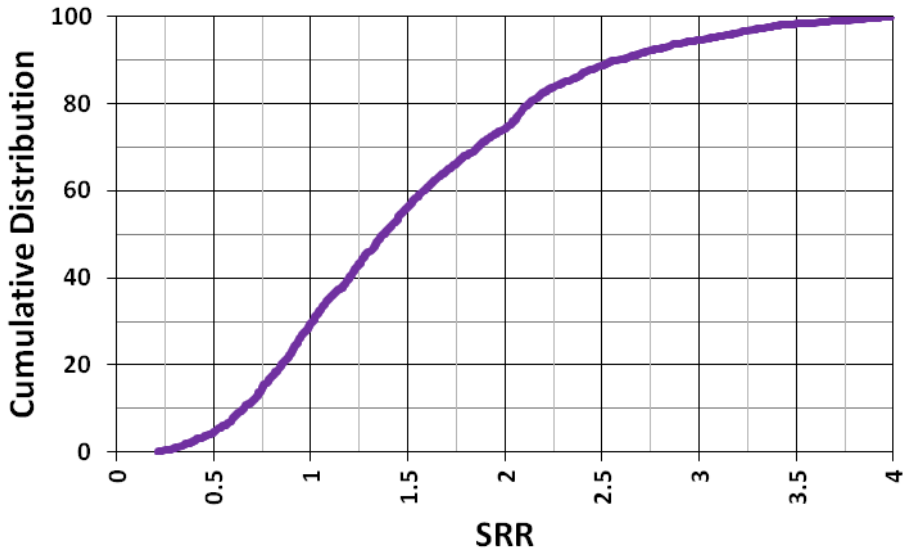

Figure 126: Cumulative distribution of SRR values for all of the events in the twenty-seven Complex: Induced seismic responses to mining shown in Figure 124.

In addition to the Complex: Induced responses discussed above, 10 Complex: Triggered seismic responses to mining are considered in this case study. Figure 127 and Figure 128 depict the seismic event and response centroid locations for the Complex: Triggered responses, respectively. Mine blast locations are shown as blue stars - indicating production blasts. Seismic responses to mine production blasts are more likely to include a significant triggered component, primarily due to their relative size and spatial influence. The increased excavation size directly increases the assumed mining-induced stress zone, increasing the potential of activating a local triggered source mechanism.

Response centroids, shown in Figure 128, are offset from mine blast locations (shown as blue stars). Rock mass failure resulting from a triggered source mechanism, located within the assumed mining-induced stress change zone, is unlikely to be located near the blast location - particularly for relatively large mine blasts. This indicates these complex seismic responses likely contain seismic events concentrated around a source mechanism different than the discrete mine blast.

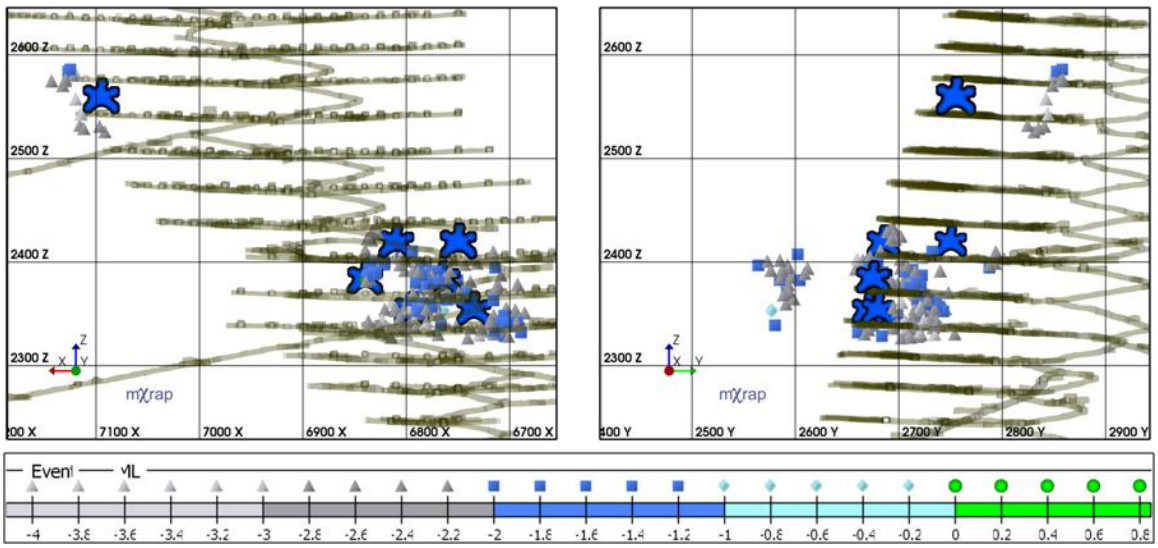

Figure 127: Longitudinal and cross-sectional projections of LaRonde mine showing Complex: Triggered seismic responses to mining and associated mine production blasts (blue stars).

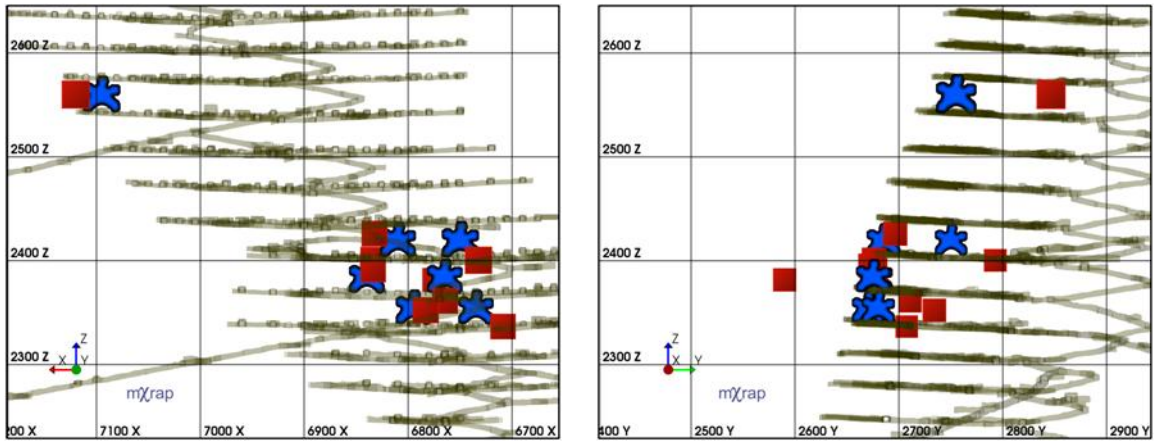

Figure 128: Longitudinal and cross-sectional projections of LaRonde mine showing the Complex: Triggered response centroid locations (calculated as shown in Equation 12), and associated mine production blasts (blue stars).

Figure 129 depicts cumulative distributions of distance between individual seismic response centroids and associated mine blast locations (shown in Figure 123 and Figure 128 for Complex: Induced and Complex: Triggered, respectively). The predominantly induced complex responses exhibit blast to response centroid distances of less than 20 metres, while the triggered complex responses exhibit distances ranging from approximately 35 to 95 metres. The increase can likely be attributed to the nature of the source mechanism, as well as the relative increase in blast size.

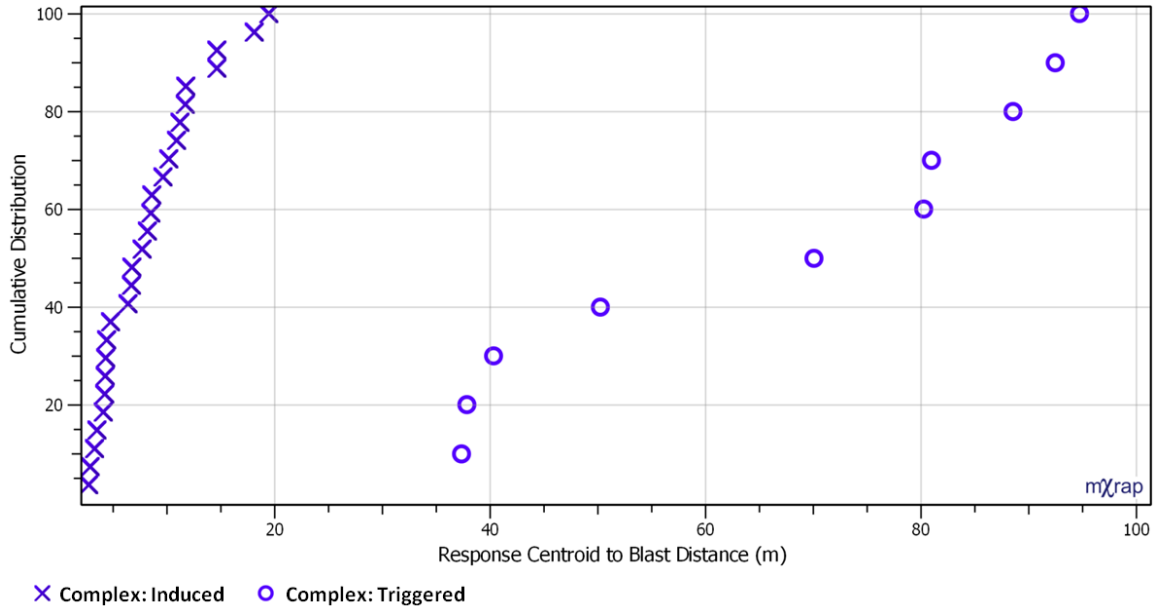

Figure 129: Cumulative distributions of the distance between response centroids and mine blast locations for Complex: Induced and Complex: Triggered responses shown in Figure 123 and Figure 128 respectively.

Figure 130 is a Magnitude-Time History chart for the Complex: Triggered seismic responses to mining (shown in Figure 122). Mine blasts are shown along the x-axis as blue stars, and seismic events are coloured according to SRR. Just as was discussed for the Complex: Induced responses, both strong lineations (steps), and offset events are contained within the Complex: Triggered seismic responses. SRR values are typically between 1 and 3, however the majority appear to be between 2 and 3 - indicating a significant triggered component. A large magnitude seismic event ($M_L \geq 0$) , is included in the complex seismic responses - indicating the presence of a triggered source mechanism and disproportionate energy release.

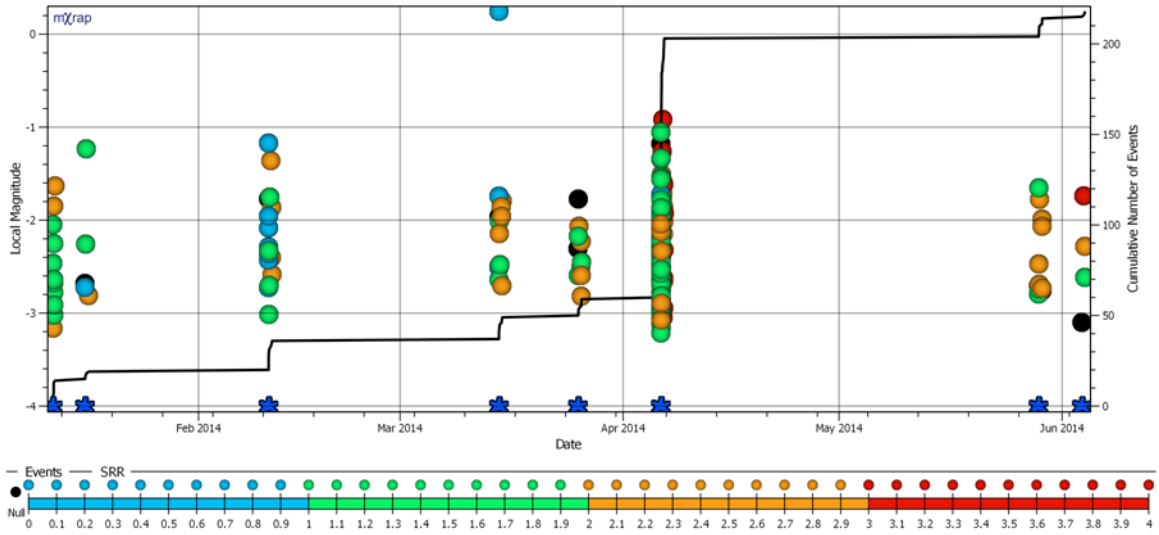

Figure 130: Magnitude-Time History chart for ten Complex: Triggered seismic responses to mining at LaRonde. Mine production blasts are shown along the x-axis as blue stars. Seismic events are coloured according to individual Seismic Response Rating (SRR). The first event in each individual seismic response is coloured black, as these events have no TBE$_N$ parameters and consequently may exhibit uncharacteristic SRR's.

A relative frequency distribution of SRR values for the Complex: Triggered seismic responses to mining is shown in Figure 131. SRR values typically fall between 1 and 3, indicative of complex seismicity. There is a strong dominance of relatively large SRR values however, indicative of a triggered complex response. Figure 132 is a cumulative distribution of the same SRR values shown in Figure 131. The median value is slightly more than 2, with approximately 70% of all individual events exhibiting SRR values within the proposed guideline of $1 \leq SRR \leq 3$ (Table 23).

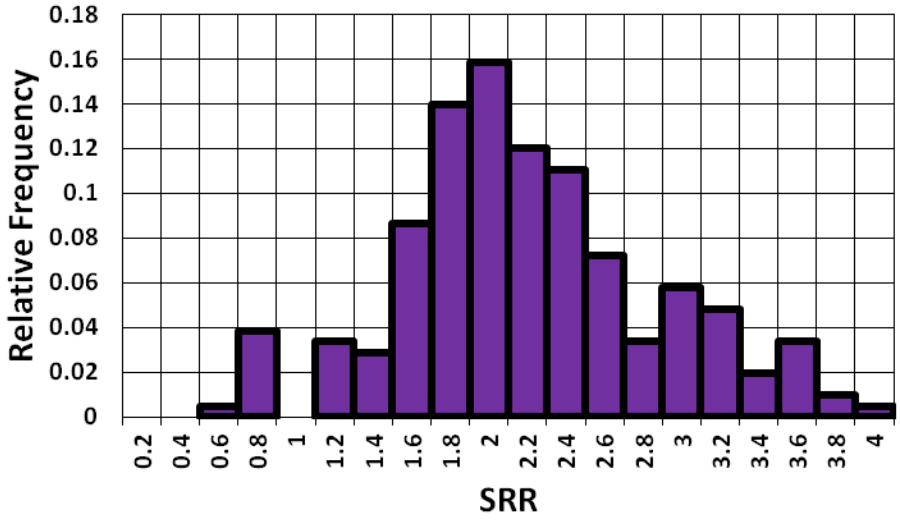

Figure 131: Relative frequency distribution of SRR values for all of the events in the ten Complex: Triggered seismic responses to mining shown in Figure 130.

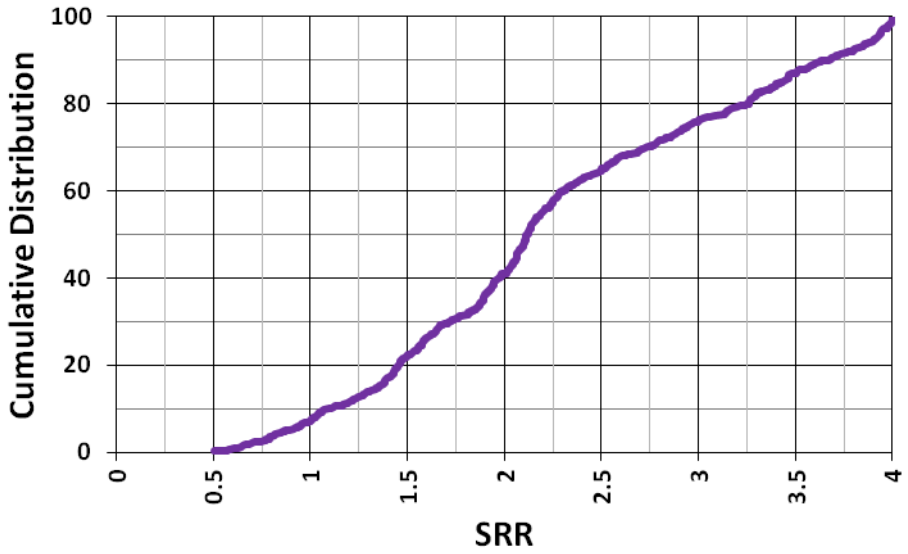

Figure 132: Cumulative Distribution of SRR values for all of the events in the ten Complex: Triggered seismic responses to mining shown in Figure 130.

7.3.2 SRP and SRP_N Distributions for Complex Seismic Responses

Both predominantly induced and triggered complex seismic responses to mining exhibit characteristics of complex seismicity. A previous section (Section 4.6), summarized the basic spatial and temporal relations between complex seismic responses to mining and mine blasts. Table 35 summarizes these relations as they pertain to Seismic Response Parameters and the Complex: Induced and Complex: Triggered seismic response included in this case study. A summary of expected observation guidelines for Normalized Seismic Response Parameters was provided in Table 14, and can be found in Appendix A for quick reference.

Table 35: Summary table of defining properties and characteristics of Complex: Induced and Complex: Triggered seismic responses to mining (redrawn from Table 13).

	Complex: Induced	Complex: Triggered
Distance To Blast [DTB]	*Excavation Radius 2.5 m & Location Error Factor 10 m:* *Commonly, DTB < 22.5 m*	*Excavation Radius 15 m & Location Error Factor 10 m:* *Commonly, DTB < 85 m*
Time After Blast [TAB]	*Significant No. Events:* *TAB < 1-3 h* *&* *All Events:* *0 h ≤ TAB ≤ Maximum*	*Significant No. Events:* *TAB < 1-3 h* *&* *All Events:* *0 h ≤ TAB ≤ Maximum*
Distance to Centroid [DTC]	*Excavation Radius 2.5 m & Location Error Factor 10 m:* *Commonly, DTC < 22.5 m*	*Excavation Radius 15 m & Location Error Factor 10 m:* *Commonly, DTC < 85 m*
Time Between Events [TBE]	*Significant No. Events:* *0 h ≤ TBE ≤ 0.01* *&* *All Events:* *0 h ≤ TAB ≤ Maximum*	*Significant No. Events:* *0 h ≤ TBE ≤ 0.01* *&* *All Events:* *0 h ≤ TAB ≤ Maximum*

The distribution of SRP_N's for the complex seismic responses at LaRonde mine are discussed throughout this section. Median values are key to interpreting seismic response and are highlighted with 'X' symbols and 'O' symbols for Complex: Induced and Complex: Triggered responses, respectively. It is expected that the Complex: Induced responses considered in this study will exhibit predominantly induced characteristic, and the Complex: Triggered responses will exhibit significant triggered characteristics.

Figure 133 and Figure 134 depict the cumulative distributions of DTB and DTB_N, respectively, for the Complex: Induced and Complex: Triggered seismic responses to mining at LaRonde. As expected, the Complex: Induced responses ('X' symbols) exhibit smaller DTB values relative to the Complex: Triggered response ('O' symbols). The median DTB_N values (shown in Figure 134), are less than one for all Complex: Induced responses, with some Complex: Triggered responses exhibiting median values of one - indicative of a strong triggered component.

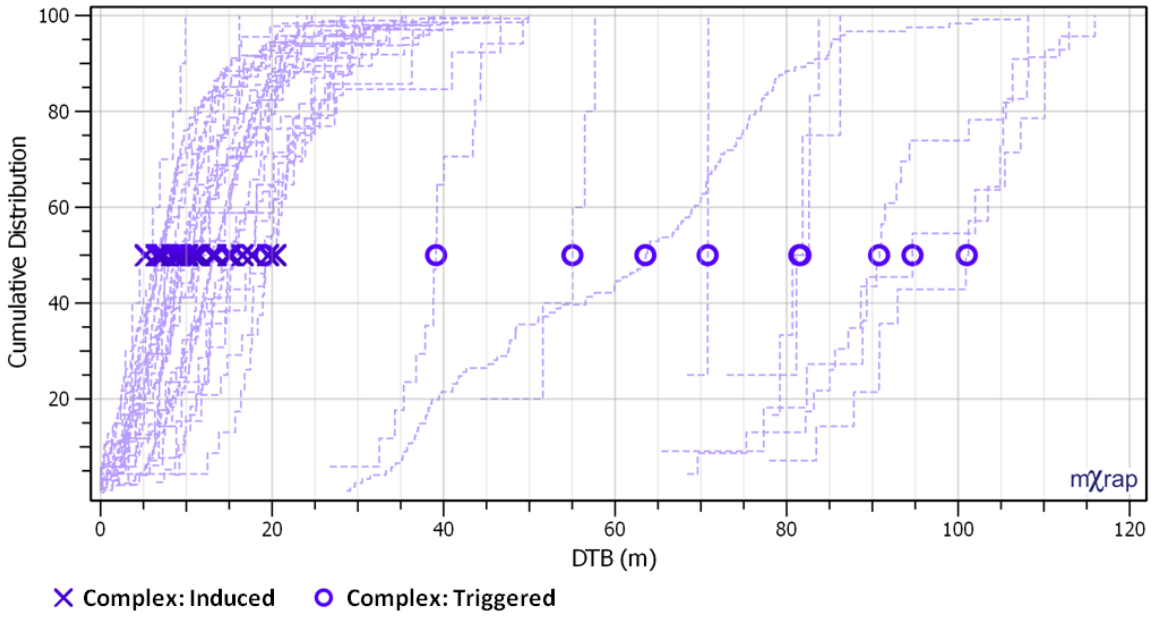

Figure 133: Cumulative distributions (post-step line shown), of SRP Distance To Blast (TAB) for a series of Complex: Induced and Complex: Triggered seismic responses to mining at LaRonde. Median values for each response are shown as 'X' symbols and 'O' symbols for Complex: Induced and Complex: Triggered responses respectively.

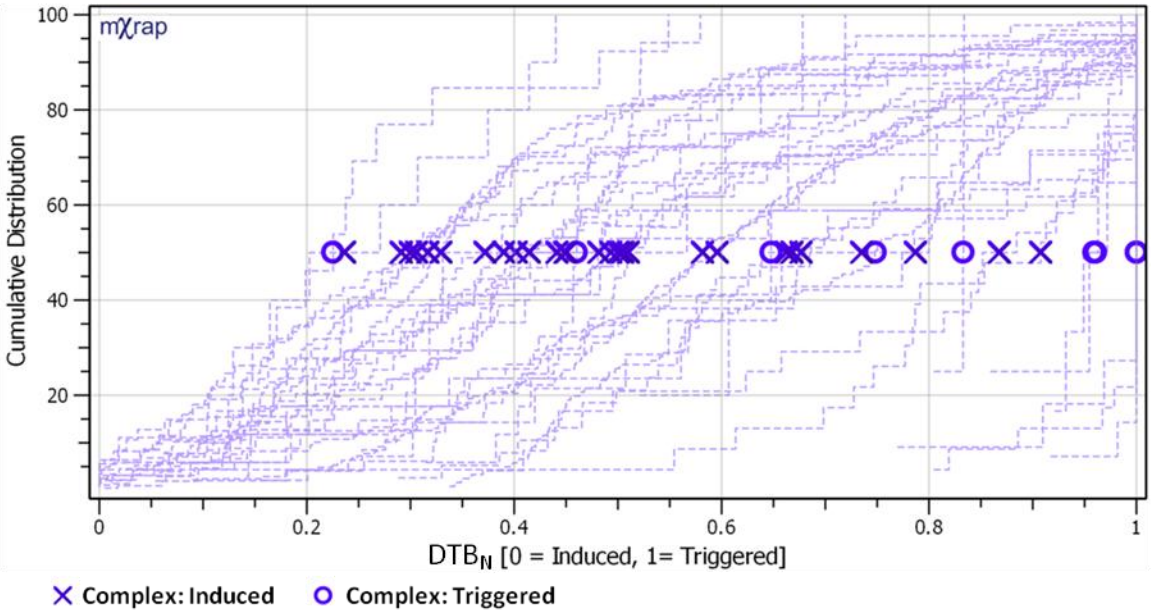

Figure 134: Cumulative distributions (post-step line shown), of Normalized Distance To Blast (TAB$_N$) for a series of Complex: Induced and Complex: Triggered seismic responses to mining at LaRonde. Median values for each response are shown as 'X' symbols and 'O' symbols for Complex: Induced and Complex: Triggered responses respectively.

Figure 135 and Figure 136 depict the cumulative distributions of TAB and TAB$_N$, respectively, for the Complex: Induced ('X' symbols) and Complex: Triggered ('O' symbols) seismic responses to mining at LaRonde. There is significant scatter between the response medians, relative to the other two case studies previously discussed (induced and triggered). This is expected, as the complex responses are not representative of a single source mechanism, but rather an induced

and a triggered source mechanism contributing to local rock mass failure concurrently. Complex: Induced responses typically exhibit smaller TAB and TAB_N values, indicative of a higher proportion of induced seismic events.

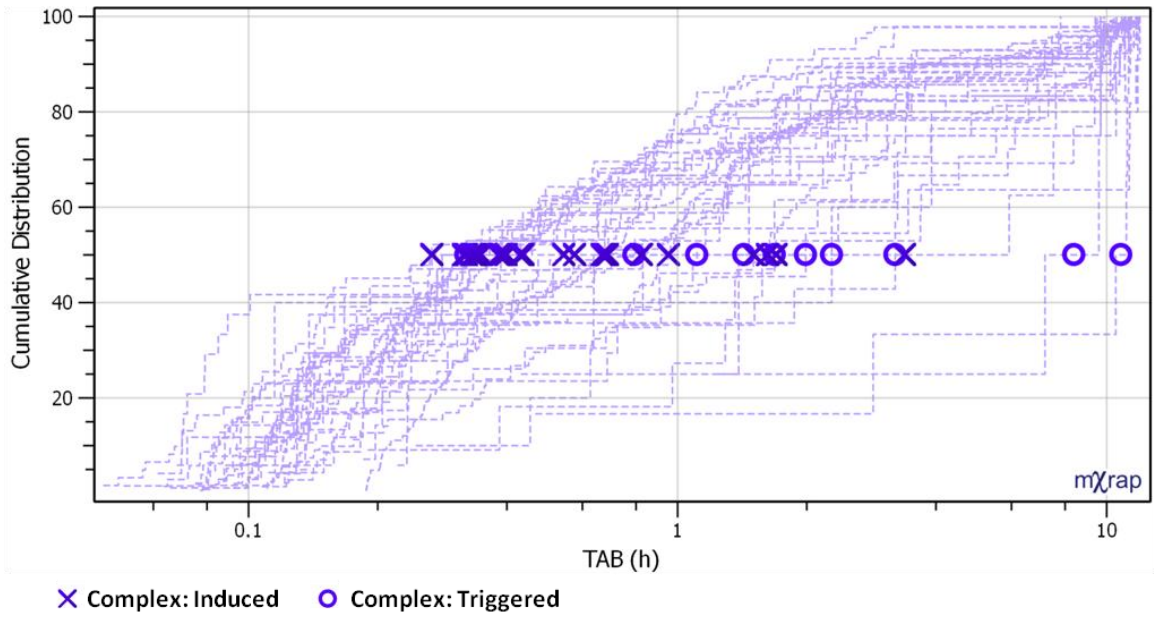

Figure 135: Cumulative distributions (post-step line shown), of SRP Time After Blast (TAB) for a series of Complex: Induced and Complex: Triggered seismic responses to mining at LaRonde. Median values for each response are shown as 'X' symbols and 'O' symbols for Complex: Induced and Complex: Triggered responses respectively.

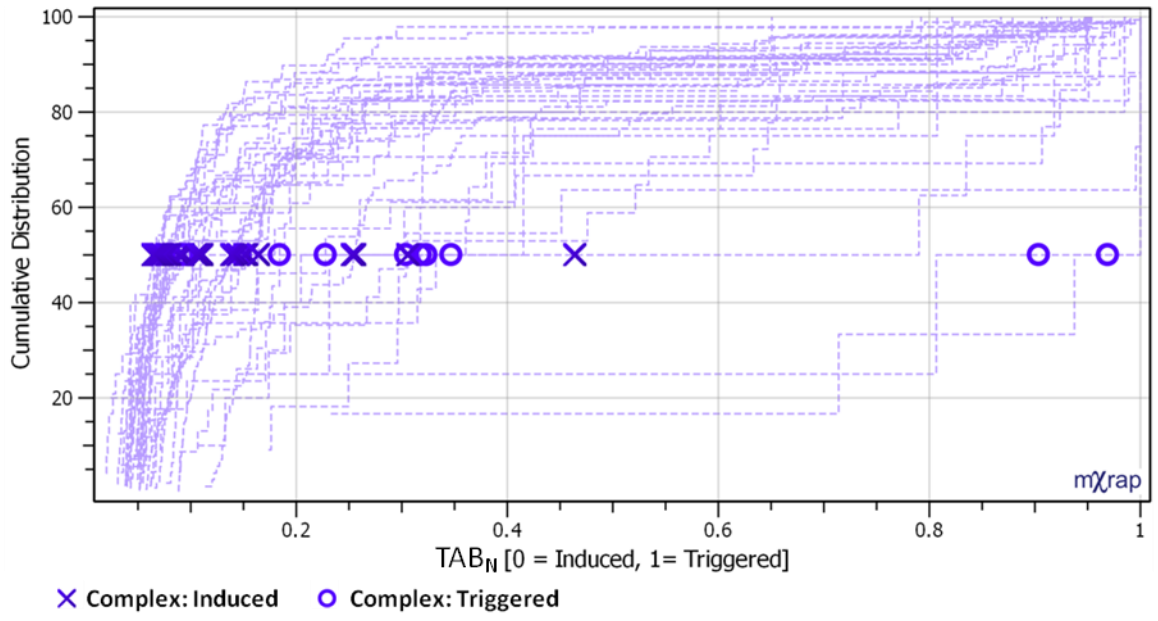

Figure 136: Cumulative distributions (post-step line shown), of Normalized Time After Blast (TAB_N) for a series of Complex: Induced and Complex: Triggered seismic responses to mining at LaRonde. Median values for each response are shown as 'X' symbols and 'O' symbols for Complex: Induced and Complex: Triggered responses respectively.

Figure 137 and Figure 138 depict the cumulative distributions of DTC and DTC_N, respectively, for the Complex: Induced and Complex: Triggered seismic responses to mining at LaRonde. As expected, both types of responses span the transitional zone between induced and triggered seismic responses. Complex: Triggered responses exhibit small DTC_N values relative to Complex: Induced responses. This is due to the relatively large assumed mining-induced stress change zone associated with mine production blasts at LaRonde.

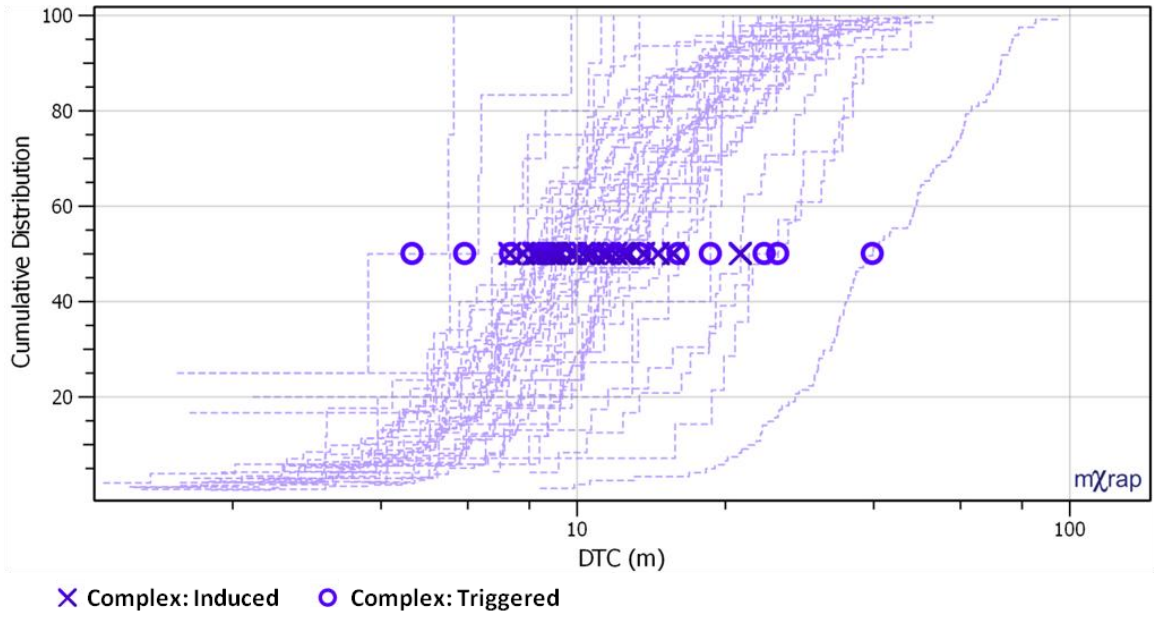

Figure 137: Cumulative distributions (post-step line shown), of SRP Distance To Centroid (DTC) for a series of Complex: Induced and Complex: Triggered seismic responses to mining at LaRonde. Median values for each response are shown as 'X' symbols and 'O' symbols for Complex: Induced and Complex: Triggered responses respectively.

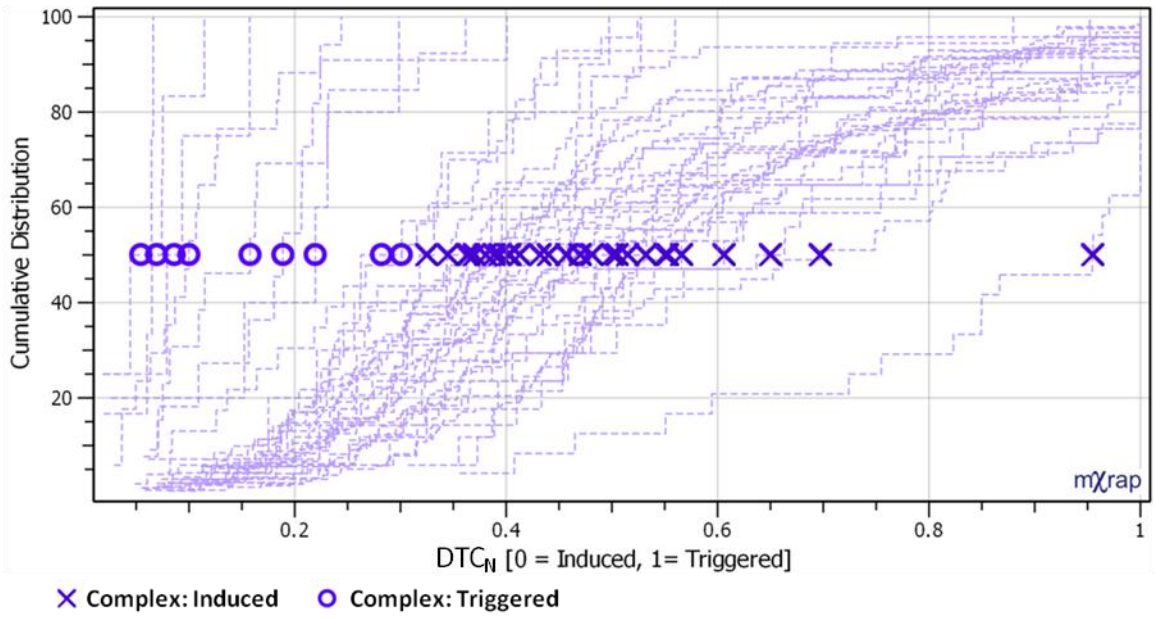

Figure 138: Cumulative distributions (post-step line shown), of Normalized Distance To Centroid (DTC_N) for a series of Complex: Induced and Complex: Triggered seismic responses to mining at LaRonde. Median values for each response are shown as 'X' symbols and 'O' symbols for Complex: Induced and Complex: Triggered responses respectively.

Figure 139 and Figure 140 depict the cumulative distributions of TBE and TBE_N, respectively, for the Complex: Induced and Complex: Triggered seismic responses to mining at LaRonde. As expected, both types of responses span the transitional zone between induced and triggered seismicity, with the predominantly induced responses exhibiting smaller TBE and TBE_N values.

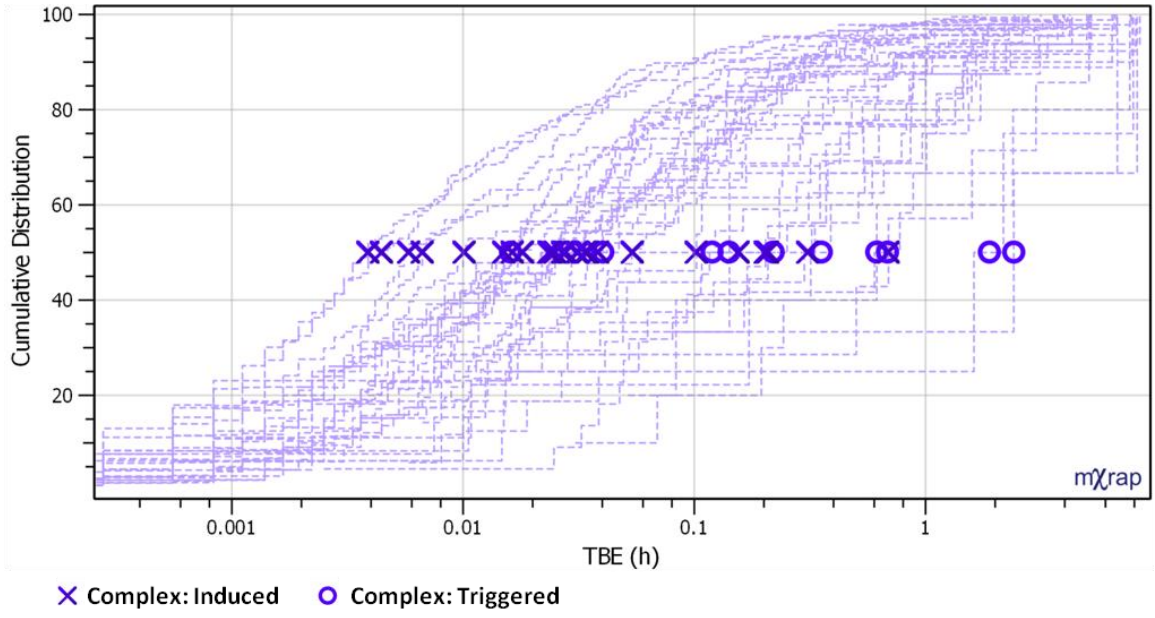

Figure 139: Cumulative distributions (post-step line shown), of SRP Time Between Events (TBE) for a series of Complex: Induced and Complex: Triggered seismic responses to mining at LaRonde. Median values for each response are shown as 'X' symbols and 'O' symbols for Complex: Induced and Complex: Triggered responses respectively.

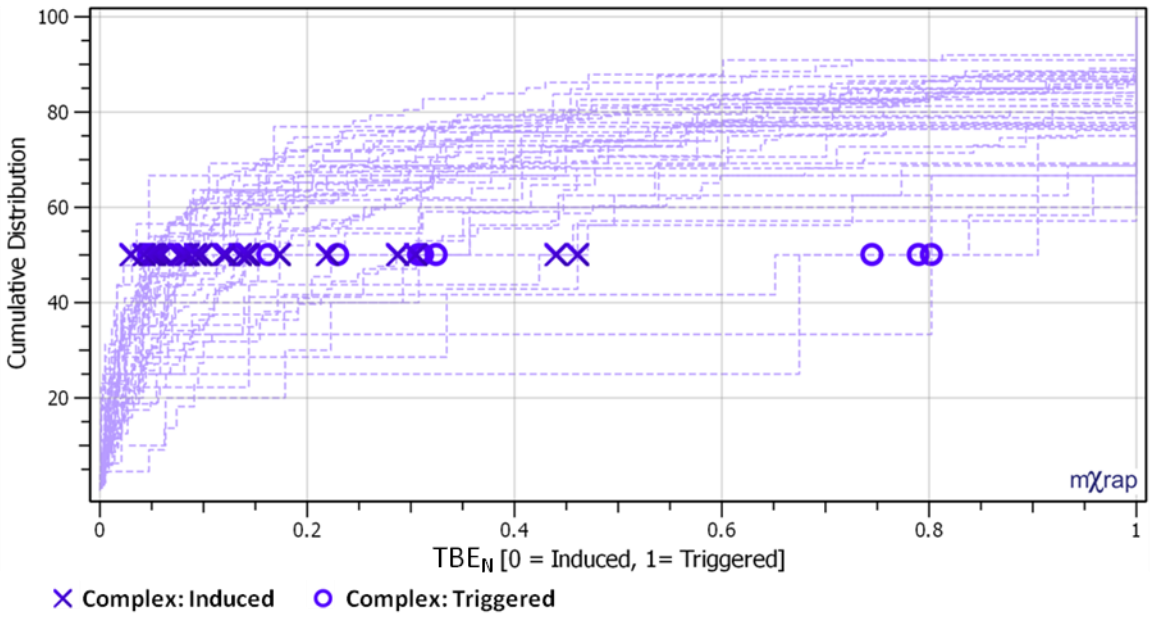

Figure 140: Cumulative distributions (post-step line shown), of Normalized Time Between Events (TBE_N) for a series of Complex: Induced and Complex: Triggered seismic responses to mining at LaRonde. Median values for each response are shown as 'X' symbols and 'O' symbols for Complex: Induced and Complex: Triggered responses respectively.

7.3.3 Interpreting Complex Seismic Responses to Mining

Table 36 summarizes the expected SRP_N chart and SRR observation guidelines for complex seismic responses to mining. These guidelines can be helpful in interpreting seismic responses using entire distributions of parameters or representative values, such as the response median values.

Table 36: Summary table of expected SRP_N chart and SRR observation guidelines for complex seismic responses to mining (Redrawn from Table 23).

	Complex
SRP_N Charts	Medium Area *Temporal Parameters:* $0 \leq TAB_N \leq 1$ & $0 \leq TBE_N \leq 1$ *Spatial Parameters:* *[DTB_N & DTC_N]* *Typically Less than 1*
SRR	Medium SRR $1 \leq SRR \leq 3$

Seismic Response Rating values can provide significant insight into a seismic response using only a single value, discussed in Section 5.2. Figure 141 depicts the cumulative distributions of SRR for the complex seismic responses to mining considered in this case study. The Complex: Induced ('X' symbols) and Complex: Triggered ('O' symbols) seismic responses considered exhibit SRR distributions concentrated in the transitional zone ($1 \leq SRR \leq 3$) between induced and triggered seismic responses.

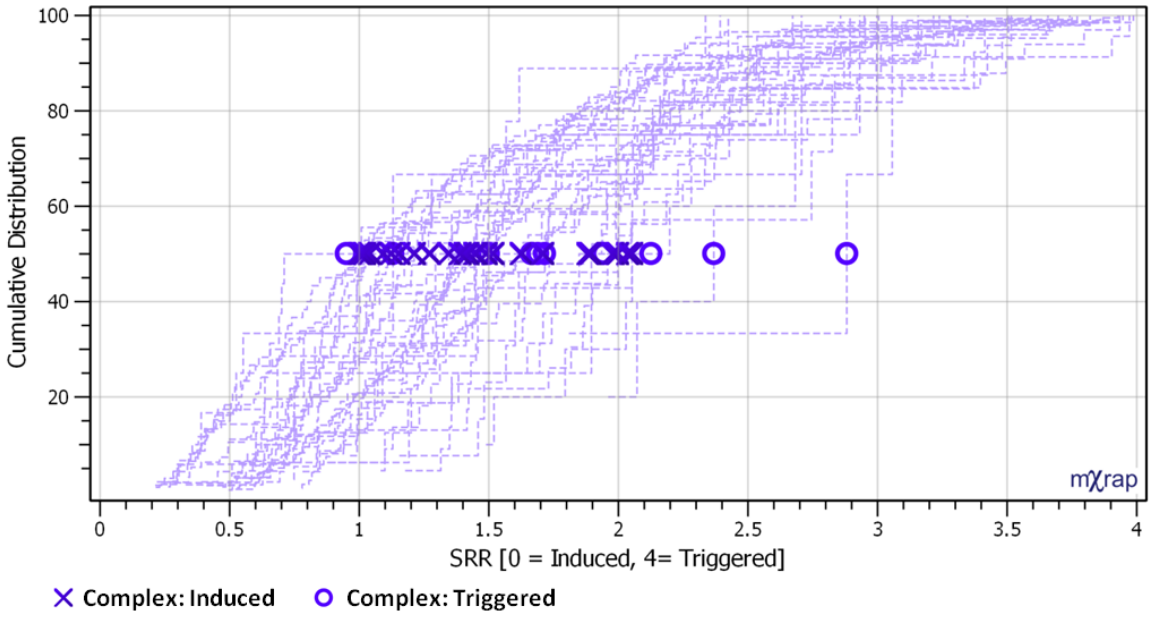

Figure 141: Cumulative distributions (post-step line shown), of Seismic Response Ratings (SRR) for a series of Complex: Induced and Complex: Triggered seismic responses to mining at LaRonde. Median values for each response are shown as 'X' symbols and 'O' symbols for Complex: Induced and Complex: Triggered responses respectively.

For interpreting seismic responses to mining, median values alone can provide significant insight into the nature of a seismic response. SRP_N charts, discussed in detail in Section 5.1, display the median SRP_N values for an individual or combination of seismic responses to mining. Figure 142 and Figure 143 depict the SRP_N charts for the Complex: Induced and Complex: Triggered seismic responses to mining, respectively. For comparison, SRR charts Complex: Induced and Complex: Triggered seismic responses can be found in Appendix F and Appendix G, respectfully.

Because complex seismic responses to mining fall in the transition zone between induced and triggered, they are represented by a relatively large range of SRR values ($1 \leq SRR \leq 3$). The expected observation ranges suggested in this thesis are only generalized guidelines, and may vary based on specific site and seismic analysis considerations. As expected, SRP_N charts for the Complex: Induced seismic responses are small to medium, and commonly exhibit SRR values less than 1.5. SRP_N charts for the Complex: Triggered responses are slightly larger medium values, with SRR values commonly greater than 1.5. An unexpected result of a SRR value less

than 1 is outlined in red for the Complex: Triggered responses, and is discussed further in the subsequent section (7.3.3.1).

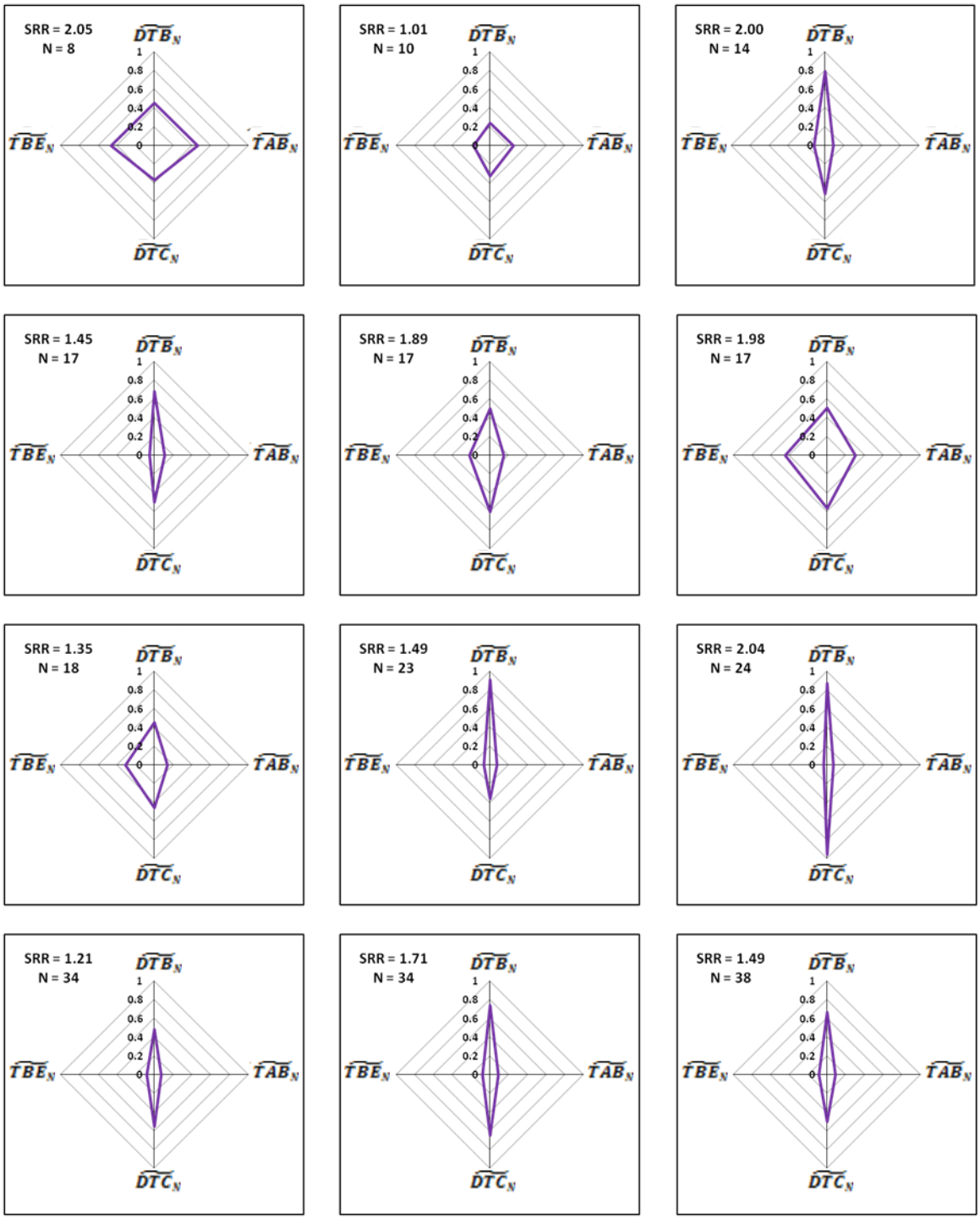
SRR = 2.05
N = 8
SRR = 1.01
N = 10
SRR = 2.00
N = 14
SRR = 1.45
N = 17
SRR = 1.89
N = 17
SRR = 1.98
N = 17
SRR = 1.35
N = 18
SRR = 1.49
N = 23
SRR = 2.04
N = 24
SRR = 1.21
N = 34
SRR = 1.71
N = 34
SRR = 1.49
N = 38
$\widetilde{DTB}_N$
$\widetilde{TAB}_N$
$\widetilde{DTC}_N$
$\widetilde{TBE}_N$
0
0.2
0.4
0.6
0.8
1

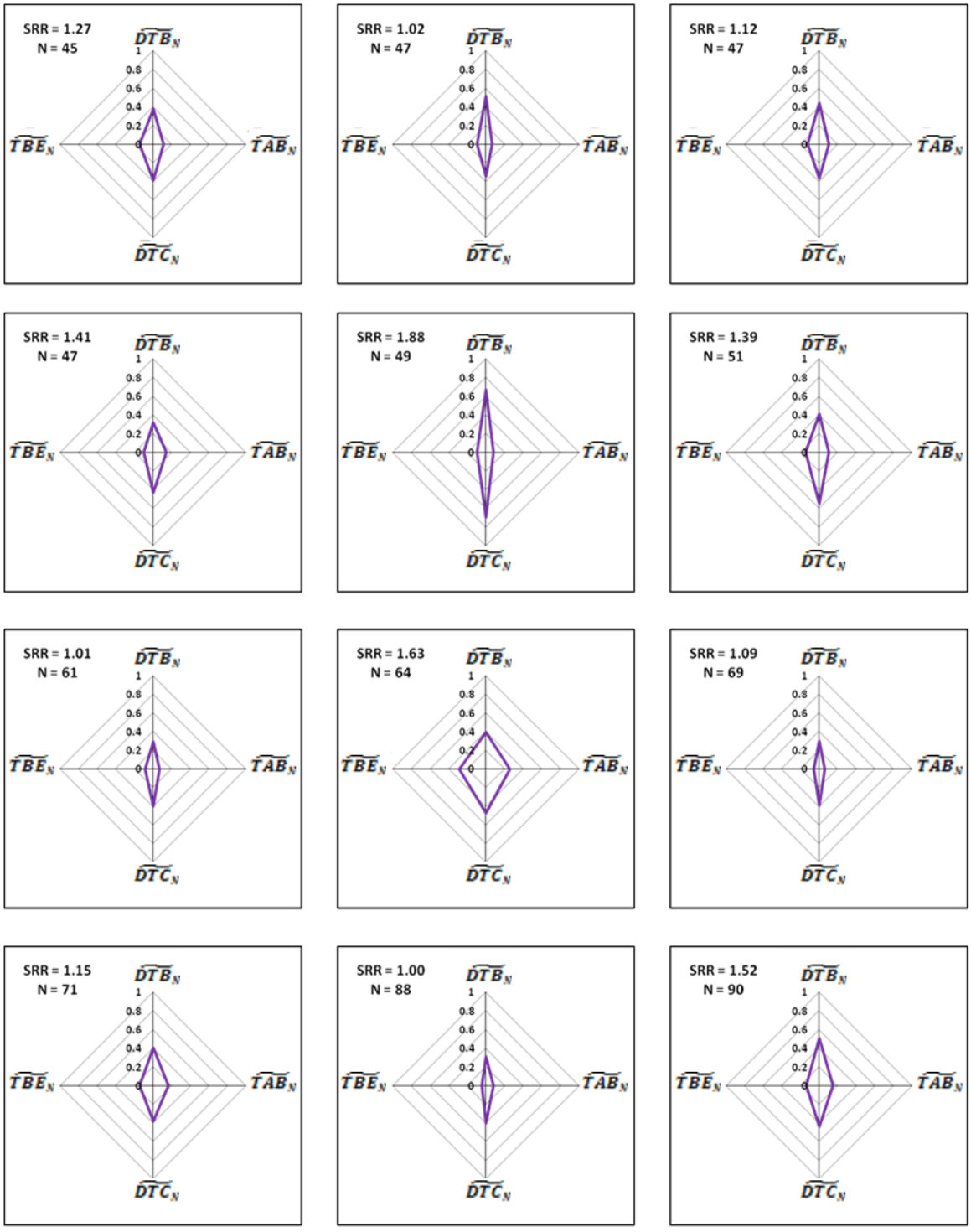
SRR = 1.27
N = 45
SRR = 1.02
N = 47
SRR = 1.12
N = 47
SRR = 1.41
N = 47
SRR = 1.88
N = 49
SRR = 1.39
N = 51
SRR = 1.01
N = 61
SRR = 1.63
N = 64
SRR = 1.09
N = 69
SRR = 1.15
N = 71
SRR = 1.00
N = 88
SRR = 1.52
N = 90
$\widetilde{DTB}_N$
$\widetilde{TAB}_N$
$\widetilde{DTC}_N$
$\widetilde{TBE}_N$
0
0.2
0.4
0.6
0.8
1

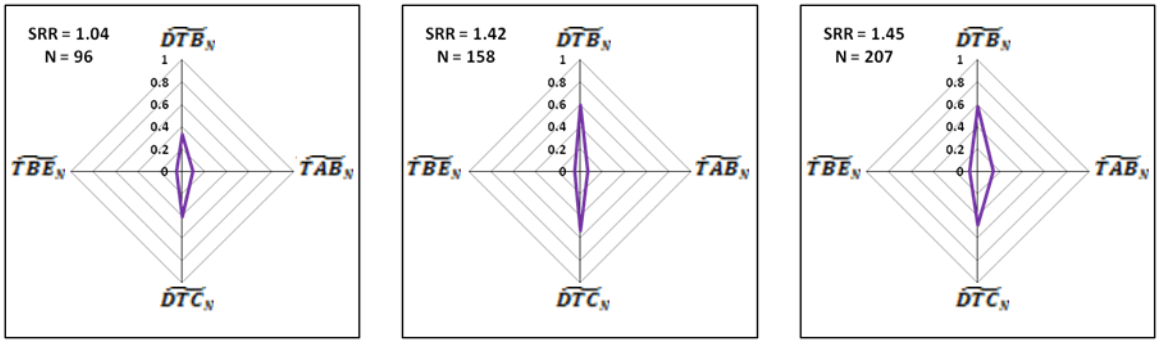

Figure 142: SRP_N charts for all Complex: Induced seismic responses to mining at LaRonde considered in this case study. Seismic Response Rating (SRR) and the number of events contained within the response are also shown.

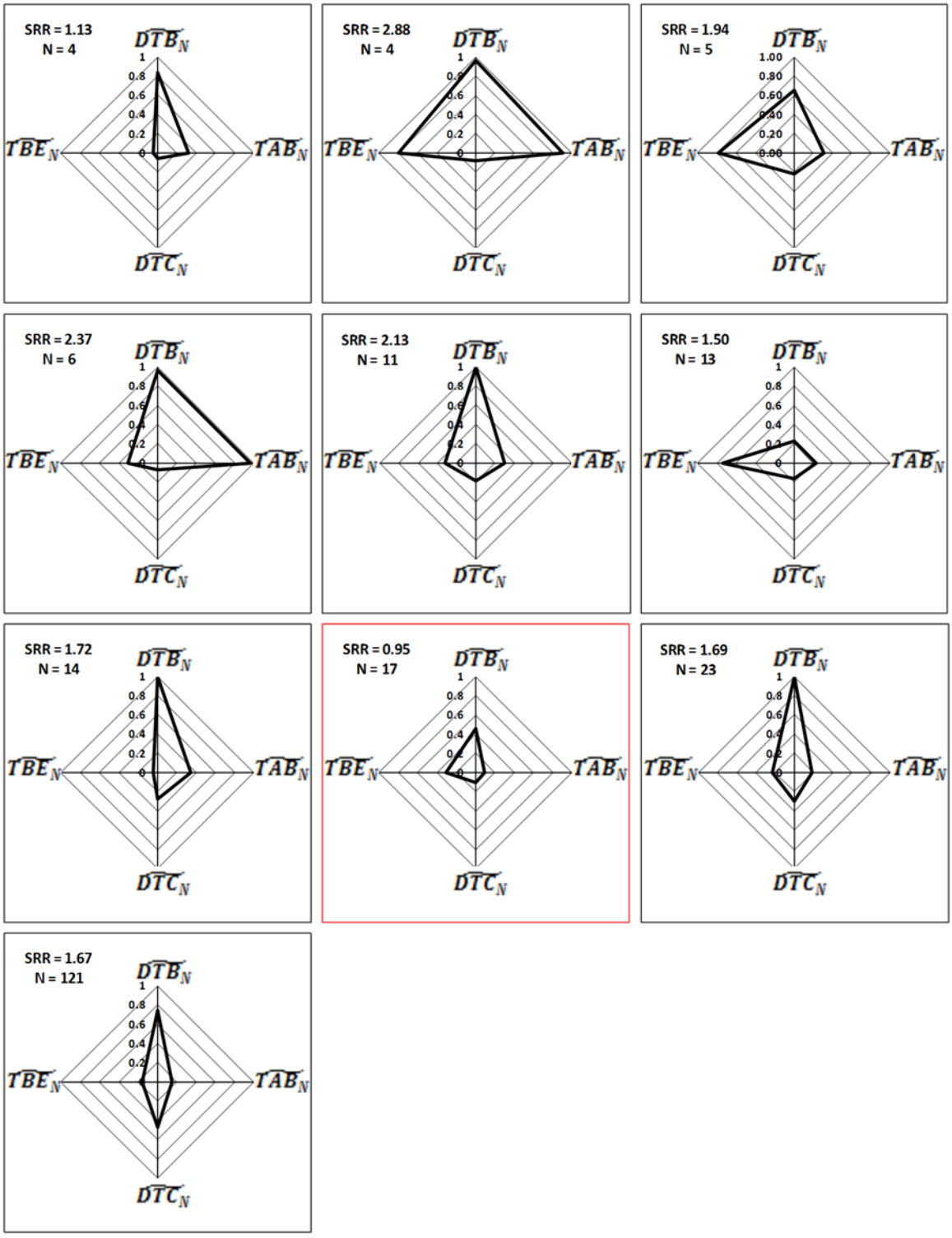

Figure 143: SRP_N charts for all Complex: Triggered mining-induced seismic responses to mining at LaRonde considered in this case study. Seismic response rating (SRR) and the number of events contained within the response are also shown. Seismic responses exhibiting unexpected SRR's (SRR < 1) are outlined in red.

7.3.3.1 Unexpected Observations for Complex Seismic Responses

All of the considered Complex: Induced, and the vast majority of considered Complex: Triggered, seismic response to mining in this case study conform to the observation guidelines proposed in this thesis. A single triggered complex responses however, shown outlined in red in Figure 143, exhibits an uncharacteristically low SRR value for the median of the response. It should be noted that while this response exhibits a SRR below the expected range, it is by 0.05.

When median SRR values do not conform to observation guidelines, it typically warrants further investigation into the seismic response. A SRR chart for the unexpected response (outlined in red in Figure 143), is shown in Figure 144. Upon further investigation, the response exhibits relatively large median DTB_N and TBE_N values, but relatively small median TAB_N and DTC_N values. This suggests that while the response is relatively tightly clustered in space, it is not clustered directly around the blast location - indicative of triggered seismicity. Furthermore, this suggests that while there may be a significant quantity of events occurring in close temporal proximity to the blast (as is required for a complex seismic responses), there are also events occurring temporally distant to the blast, generating relatively large TBE_N values.

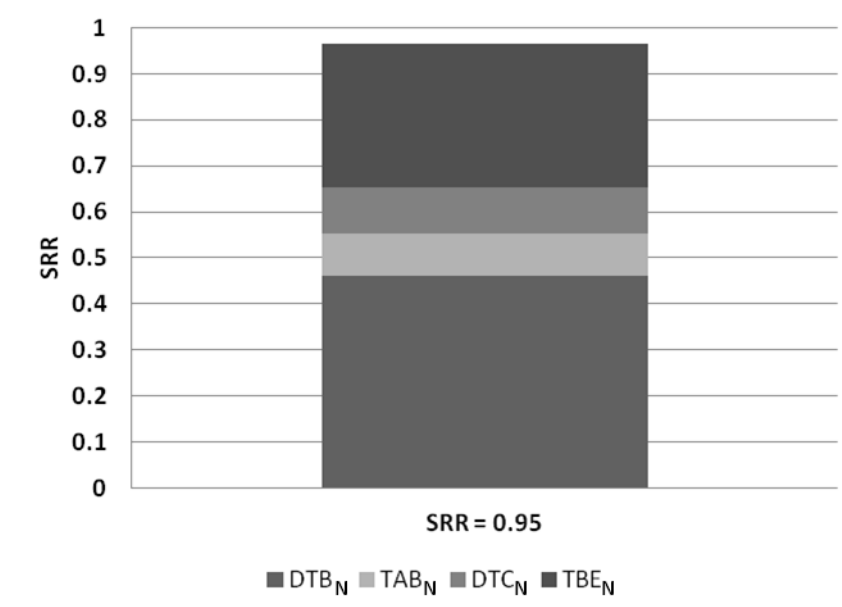

Figure 144: SRR chart for a single Complex: Triggered seismic responses to mining that does not conform to expected SRR observations. Note that the SRR value stated on the x-axis is the median SRR value, and does not necessarily equal the sum of the individual median SRP_N's.

A Magnitude-Time History chart for the complex seismic response exhibiting an unexpected SRR is shown in Figure 145. Based on the relative proportion of induced to triggered events, it may be more appropriate to designate this response as Complex: Induced. It is evident from the temporal relations between individual events and the mine blast however, that this response

contains both induced and triggered seismic events and is very likely a complex seismic response to mining.

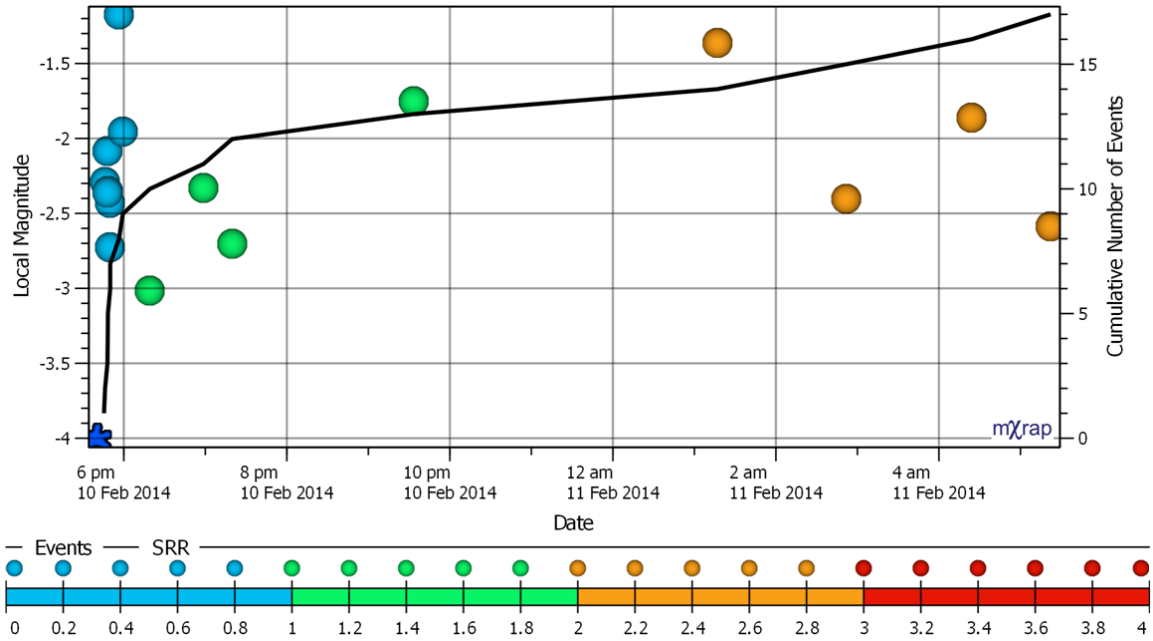

Figure 145: Magnitude-Time History charts for a Complex: Triggered seismic responses to mining at LaRonde (shown in Figure 144). A mine production blast is shown as a blue star and seismic events are coloured according to individual SRR.

7.3.4 Discussion of Complex Seismic Responses to Mining

This section has demonstrated the applicability of SRP_N's (DTB_N, TAB_N, DTC_N and TBE_N) and SRR to complex seismic responses at LaRonde mine. Complex seismic responses that are predominantly induced and triggered have been examined. Figure 146 depicts the relative frequency distributions for the SRP_N's of complex seismic responses considered in this case study. Distributions of temporal SRP_N values (TAB_N and TBE_N), are similar for both Complex: Induced and Complex: Triggered responses, with triggered responses exhibiting more variation. As expected, there is a significantly larger relative frequency of events in temporal proximity to blasting (TAB_N), for the Complex: Induced responses.

Relative to temporal parameters, distributions of spatial SRP_N values (DTB_N and DTC_N) show larger discrepancies between the two types of complex responses. Within the context of this thesis, complex seismic responses are spatially defined as primarily occurring within the assumed mining-induced stress change zone of a discrete mine blast. As a complex seismic population transitions from predominantly induced to triggered, it is expected that the relative frequency of spatial SRP_N values will increasingly shift towards one. This is observed within the LaRonde mine case study, as Complex: Triggered responses exhibit significantly larger frequencies of one, for DTB_N and DTC_N, relative to Complex: Induced responses.

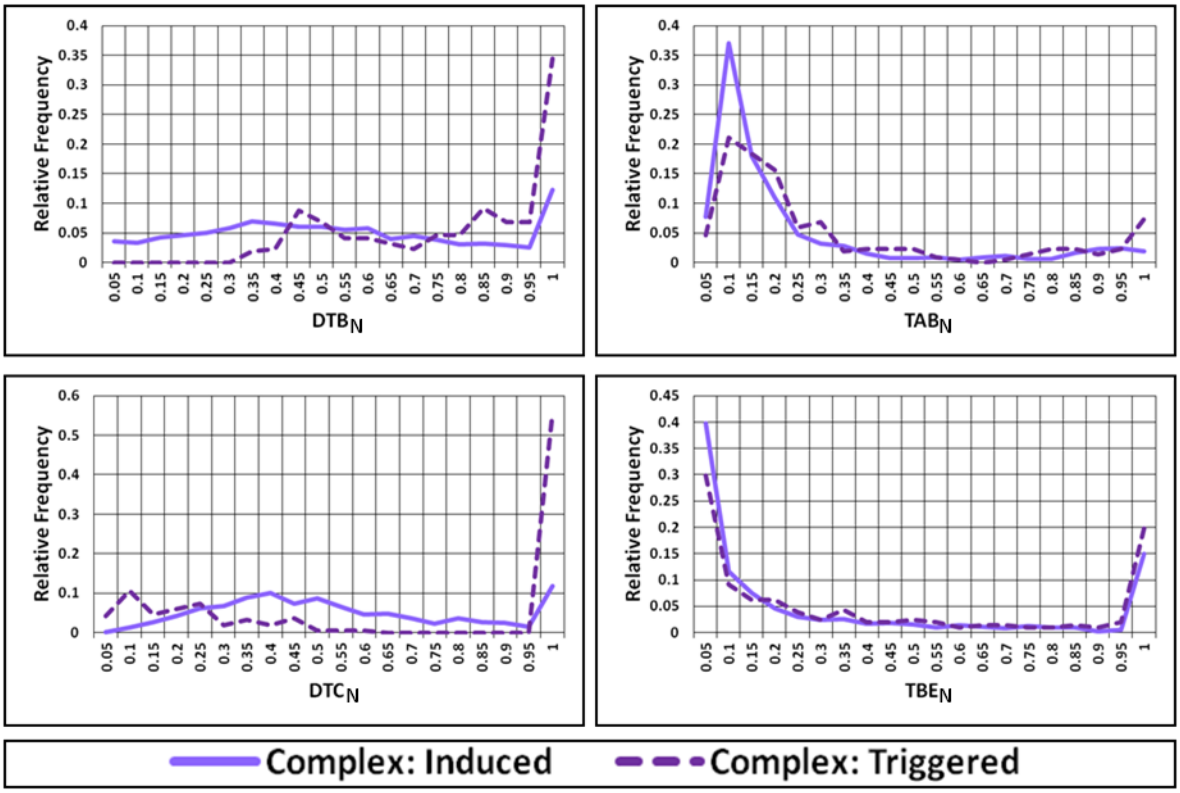

Figure 146: Relative frequency distributions for DTB_N, TAB_N, DTC_N and TBE_N for all previously shown complex seismic responses to mining at LaRonde mine.

Within this case study, mine development and production blasts were used to demonstrate predominantly induced and triggered complex seismic responses to mining, respectively. In order to generate a complex seismic response to mining, a triggered source mechanism, such as a significant geological feature, must be located within the assumed-mining induced stress change zone. Hudyma (2008) notes that temporal periods of increased seismic activity are typically longer for larger mine blasts. Due to the relative volume of rock mass that experiences a significant mining-induced stress change, mine production blasts are more likely to generate complex seismic responses to mining. Identification of complex seismic responses to mining has significant implications for seismic hazard evaluation, as is discussed in Chapter 8 (Section 8.5).

7.3.5 Summary of Complex Seismic Responses to Mining at LaRonde

Induced and triggered complex seismic responses to mining at LaRonde considered in this case study exhibited characteristics indicative of complex seismicity (as defined within the context of this thesis). No noteworthy outliers were present within the data. Table 37 summarizes the observation guidelines and the actual observations from the LaRonde case study surrounding complex seismic responses to mining.

Table 37: Summary of SRR and SRP_N expected general observations for complex responses and median distributions for the LaRonde case study of complex seismic responses to mining. Median distributions are shown as 'X' symbols and 'O' symbols for Complex: Induced and Complex: Triggered seismic responses respectively. Table continued on subsequent page.

	Observation Guidelines: Complex (Strong Induced)	Median Distributions for LaRonde Case Study: Complex
SRR	**Medium SRR** $[1 \leq SRR \leq 3]$	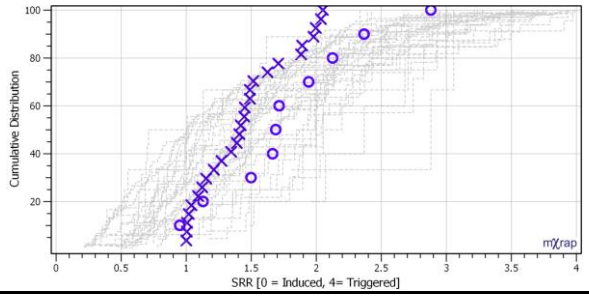
DTB_N	**Typically Less Than One** $[DTB_N < 1]$	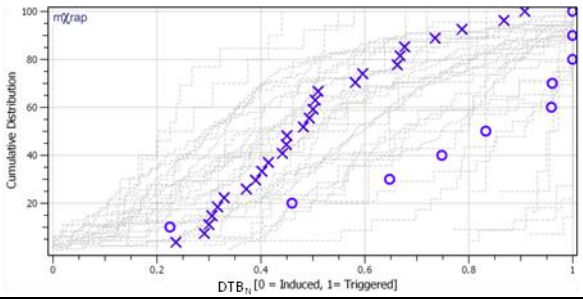
TAB_N	**Variable** $[0 \leq TAB_N \leq 1]$	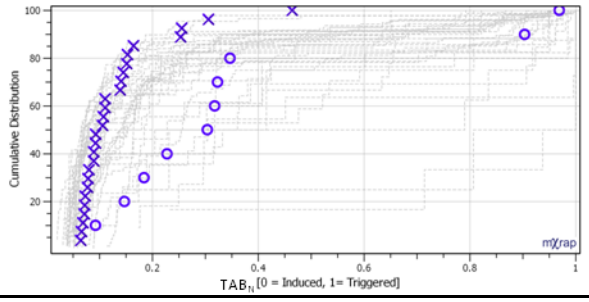
DTC_N	**Typically Less Than One** $[DTC_N < 1]$	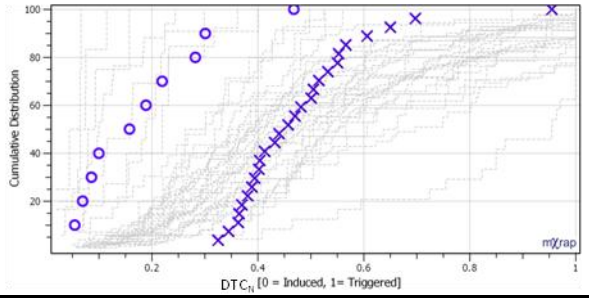

	Observation Guidelines: Complex (Strong Induced)	Median Distributions for LaRonde Case Study: Complex
TBE_N	**Variable** **$[0 \leq TBE_N \leq 1]$**	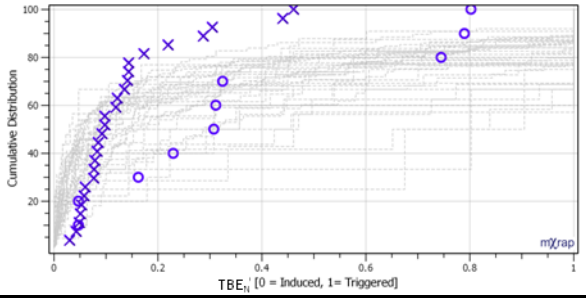

7.4 LaRonde Mine Case Study Discussion

The LaRonde mine case study is a compilation of three independent studies, each with a focus on induced, triggered or complex seismic responses to mining. Table 38 provides a breakdown of the three case studies, including: the response types observed, number of responses, average number of events contained within the responses, and the seismic event magnitude ranges exhibited by the different classifications of mine seismicity. The induced seismic responses to mining, presented in detail in Case Study I, are considered for two different scales of mine blasting: relatively large production blasts and relatively small development blasts. The Production Blast Induced responses contain approximately three times as many events, on average, as the Development Blast Induced responses. This is primarily due to the relative increase in blast size, and consequently, mining-induced stress change zone. Both types of induced seismic responses to mining contain seismic events commonly associated with a proportional seismic response and energy release ($M_L < 0$).

The triggered seismic responses to mining, presented in detail in Case Study II, are considered for two different time periods: during regular mining activities and during a mine shutdown. The average number of events contained within the two types of triggered responses are nearly equivalent, regardless of the significant change in mining practices (regular mine blasting vs. no mine blasting). This supports the notion that individual discrete mine blasts have little immediate impact on triggered seismicity. During regular mining activities, the triggered responses contain seismic events commonly associated with a disproportional seismic response and energy release ($M_L > 0$). This is not the case for the shutdown period triggered responses, however, with no mine blasting occurring, there is arguably no energy input to the mining environment and the occurrence of any magnitude seismic event represents a disproportional seismic response and energy release. As expected, relative to the induced case study (I), the triggered case study (II) contains both more responses and a higher average number of events per response.

The spatial and temporal properties of a complex seismic response to mining depend on the relative proportion of induced and triggered seismic events contained within the response. The complex seismic responses to mining, presented in detail in Case Study III, are considered for two circumstances: Complex: Induced, and Complex: Triggered. The Complex: Induced responses result from mine development blasting, and contain approximately 25% more events on average than the Development Blast Induced responses (Case Study I). This increase in the number of events can likely be attributed to the addition of triggered seismicity temporally distant to the blast. The Complex: Triggered responses are a result of secondary stope production blasting, with approximately 22 events per response on average. This value appears low compared to other responses, and is likely a reflection of the Single-Link Clustering d-value employed in response identification, as well as the relatively small quantity of responses (ten). Both types of complex seismic responses to mining contain seismic events commonly associated with a disproportional seismic response and energy release ($M_L > 0$). The presence of disproportional energy release is one of the critical factors used to differentiate between induced and complex seismic responses to mining.

Table 38: Summary table of the three independent case studies, presented in detail in Chapter 7, from Agnico Eagle's LaRonde mine.

Case Study	Response Classification		No. of Responses	Avg. No. Events in Responses	Responses Event Magnitude Range
I	Induced	Production Blast Induced	19	40.1	$(-3.48 \leq M_L \leq -0.02)$
		Development Blast Induced	23	13.3	$(-3.85 \leq M_L \leq -0.59)$
II	Triggered	Triggered During Regular Mining Activities	69	60.9	$(-3.89 \leq M_L \leq 0.85)$
		Triggered During a Mine Shutdown	41	62.4	$(-3.95 \leq M_L \leq -0.02)$
III	Complex	Complex: Induced	27	53.5	$(-3.65 \leq M_L \leq 0.80)$
		Complex: Triggered	10	21.8	$(-3.22 \leq M_L \leq 0.25)$

7.4.1 Seismic Response Rating (SRR)

As discussed in Chapter 5, Seismic Response Rating (SRR) is the sum of the Normalized Seismic Response Parameters for a given seismic response to mining. Figure 147 is a cumulative distribution of SRR for all induced, complex and triggered seismic responses to mining considered in the LaRonde mine case study. The observation guidelines for induced and triggered seismicity, as proposed in Table 22, are shaded in blue and red respectively.

The vast majority of SRR observations for the LaRonde mine case study adhere to the observation guidelines proposed in this thesis. The median SRR value for induced seismic events contained within the LaRonde mine case study is one, with nearly 80% of all induced events

exhibiting SRR values within the proposed observation guidelines. The median SRR value for triggered seismic events contained within the LaRonde mine Case Study is 3.4, with more than 90% of all triggered events exhibiting SRR values within the proposed observation guidelines.

Complex seismicity commonly falls in the transition zone between induced and triggered, approximately $1 \leq SRR \leq 3$. Complex seismic responses to mining contain significant quantities of induced seismicity, and consequently exhibit similar trends in SRP_N's and SRR as induced seismicity. This is particularly the case for the complex seismicity observed in the LaRonde mine case study, as there are nearly three times as many Complex: Induced responses as Complex: Triggered responses considered (see Table 38). In Figure 147, complex seismicity follows the induced seismicity trend, with a median SRR value of approximately 1.4, and 60% of all complex events exhibiting SRR values within the proposed observation guidelines. More detailed discussion surrounding SRR can be found in the three case studies contained within this chapter.

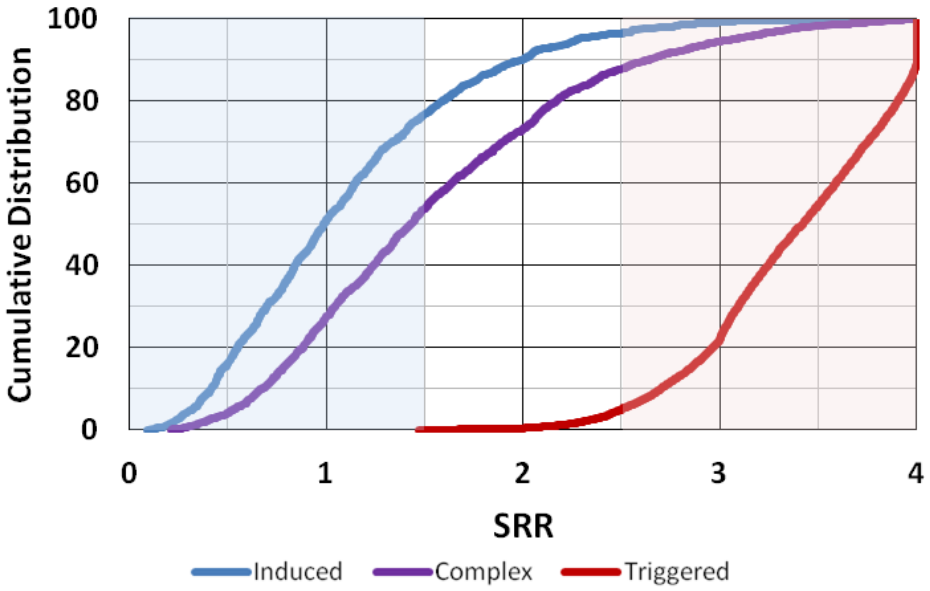

Figure 147: Cumulative distribution of SRR (Seismic Response Rating) values for the seismic events contained within the LaRonde mine case studies presented in Chapter 7. Induced, complex and triggered distributions correspond to the three independent case studies contained within Chapter 7. Background shading, in blue and red, represents proposed SRR observation guidelines for induced and triggered seismic responses respectively.

7.4.2 Normalized Seismic Response Parameters (SRP_N's)

Normalized Seismic Response Parameters (SRP_N's) are the normalized versions of the Seismic Response Parameters: Distance To Blast (DTB), Time After Blast (TAB), Distance to Centroid (DTC) and Time Between Events (TBE). Figure 148 depicts the cumulative distributions of SRP_N's for all induced, complex and triggered seismic responses to mining considered in the LaRonde mine case study. The observation guidelines for induced and triggered seismicity, as

proposed in Table 22, are shaded in blue and red respectively. Mean, median and median absolute deviation for all distributions (including SRR shown in Figure 147), are summarized in Table 39.

Induced seismicity is expected to approach zero for all SRP_N's; typically less than one for spatial SRP_N's (DTB_N and DTC_N) and less than or equal to 0.2 for temporal SRP_N's (TAB_N and TBE_N). All induced response median values adhere to the guidelines proposed in this work. More than 90% of induced event spatial SRP_N's are less than one and more than 70% of temporal SRP_N's are less than 0.2. Similar to previous observations, complex seismicity closely resembles the trends observed in induced seismicity.

Triggered seismicity is expected to approach or be equal to one for all SRP_N's; equal to one for spatial SRP_N's (DTB_N and DTC_N) and greater than or equal to 0.5 for temporal SRP_N's (TAB_N and TBE_N). All triggered response median values adhere to the guidelines proposed in this work. More than 70% of triggered event spatial SRP_N's (99% of DTB_N) are equal to one, and more than 55% of temporal SRP_N's (more than 90% of TAB_N) are greater than 0.5.

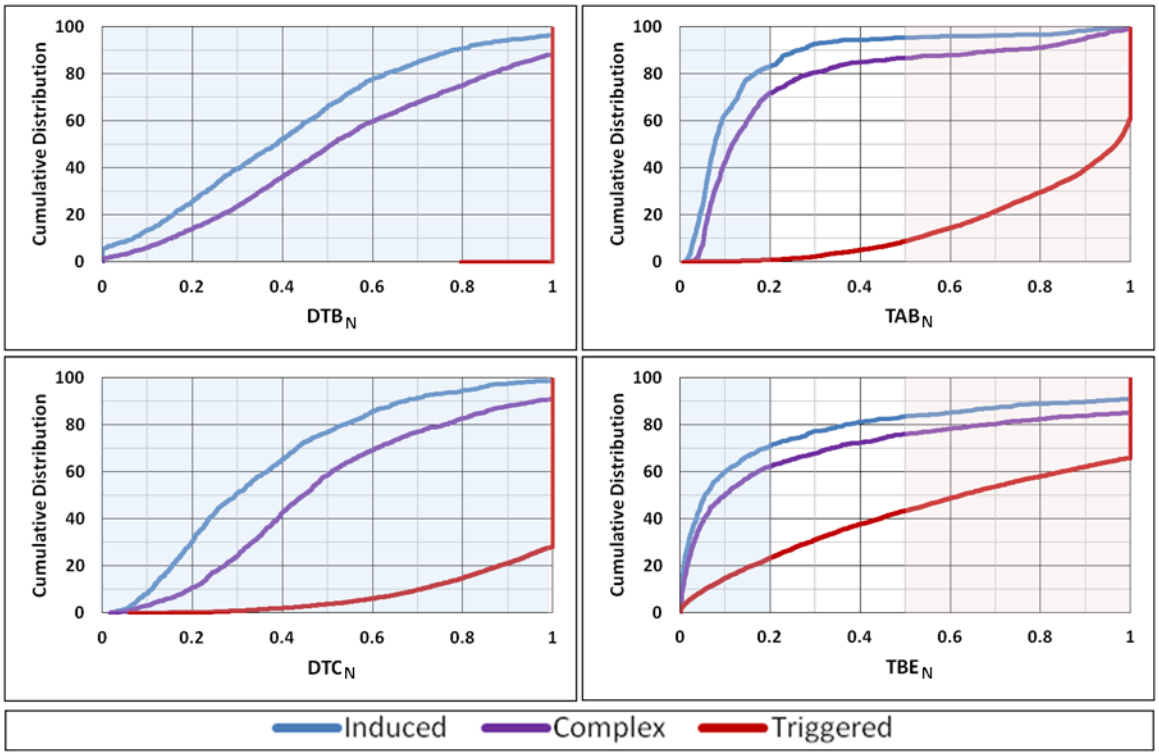

Figure 148: Cumulative distributions of SRP_N's for the three case studies, presented in detail in Chapter 7, from Agnico Eagle's LaRonde mine. Background shading, in blue and red, represents proposed SRP_N guidelines for induced and triggered seismic responses respectively.

Throughout this work, median SRP_N's are typically considered representative of seismic responses to mining. The mean, median and median absolute deviation for each of the SRR and SRP_N distributions discussed above is summarized in Table 39. Median absolute deviation (MAD) values represent the average absolute distance between a single observation and the

median. MAD is a measure of statistical dispersion, and a strong indicator of variability for quantitative data. SRP_N and SRR values are not normally distributed, as discussed in the subsequent section, and consequently deviations around the mean are not provided. A considerable difference exists between the mean and median of the temporal SRP_N's. This is significant, as unlike median values, the mean temporal SRP_N's do not fall within observation guidelines. This further suggests that median values can lead to meaningful conclusions regarding seismic response interpretation and classification.

Table 39: Summary table of the mead, median and median absolute deviation (MAD) of the induced, complex and triggered seismic response to mining SRR and SRP_N's as shown in Figure 147 and Figure 148.

	Induced			Complex			Triggered		
	mean	median	MAD	mean	median	MAD	mean	median	MAD
DTB_N	0.40	0.38	0.22	0.54	0.51	0.25	1.00	1.00	0.00
TAB_N	0.14	0.08	0.09	0.22	0.12	0.15	0.85	0.97	0.15
DTC_N	0.35	0.30	0.18	0.50	0.45	0.21	0.93	1.00	0.07
TBE_N	0.22	0.06	0.20	0.29	0.10	0.26	0.59	0.63	0.34
SRR	1.10	0.99	0.48	1.55	1.43	0.61	3.38	3.42	0.42

As discussed in Chapter 2, seismic event time and location are independent seismic source parameters. SRP_N's consider seismic event time in the calculation of temporal SRP_N's (TAB_N and TBE_N). For a seismic response resulting from a single source mechanism, both temporal SRP_N's should approach the same value (zero for induced and one for triggered). The same is true for spatial SRP_N's (DTB_N and DTC_N), which should be less than one for induced, and approach or equal to one for triggered. Figure 149 is a scatter plot of the sum of temporal SRP_N's versus the sum of spatial SRP_N's, for events contained within the LaRonde mine Induced Case Study (I). In part (b), the relative percent of all induced seismic events is shown by scatter plot quadrant. Induced seismicity is expected to approach a sum of zero, and nearly 65% of all induced events plot in the minimum quadrant (containing (0,0)). A significant divide exists between spatial and temporal SRP_N's, as more than 88% of induced events plot below a temporal SRP_N sum of one. This suggests temporal parameters may be more meaningful for induced response classification, relative to spatial parameters, as discussed in Section 8.2.

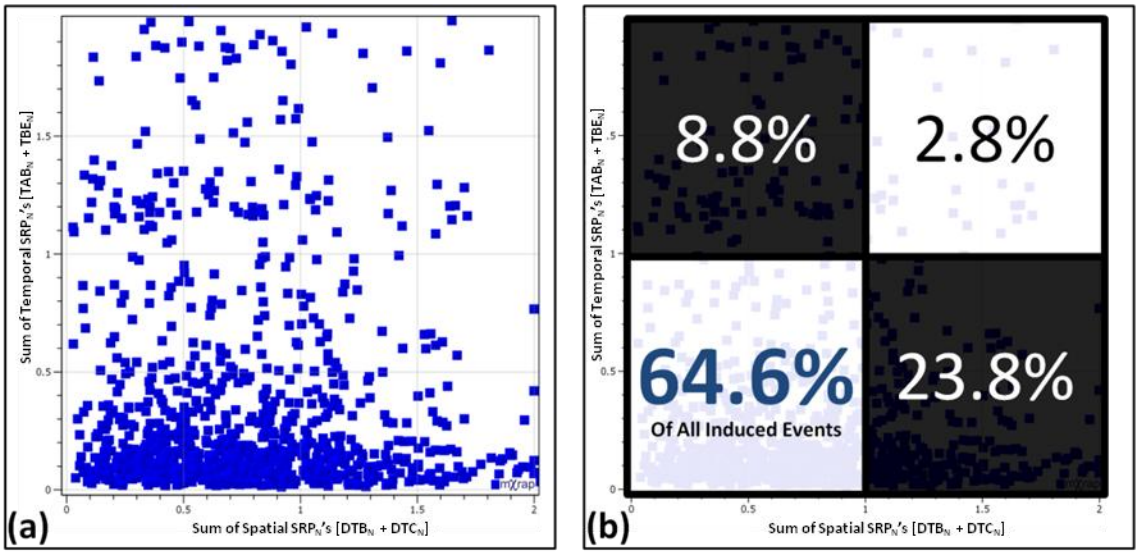

Figure 149: Scatter plot of spatial SRP$_N$'s (DTB$_N$ + DTC$_N$) versus temporal SRP$_N$'s (TAB$_N$ +TBE$_N$), for all induced seismic events contained within the LaRonde mine Case Study I - presented in Chapter 7. Part (b) depicts the relative percent of events that are contained within each quadrant of the scatter plot shown in Part (a).

Figure 150 is a scatter plot of the sum of temporal SRP$_N$'s versus the sum of spatial SRP$_N$'s, for events contained within the Triggered Case Study (II). In part (b), the relative percent of all triggered events is shown by scatter plot quadrant. Triggered seismicity is expected to approach sum values of two, and more than 83% of all triggered events plot in the maximum quadrant (containing (2,2)). Just as was observed for induced events, a significant divide exists between spatial and temporal SRP$_N$'s of triggered seismicity. Triggered seismicity occurs distant to mine blasting in space, and 99% of DTB$_N$ values for the triggered seismic responses are equal to one. This leads to spatial SRP$_N$ sums greater than one, and all triggered seismic events in the LaRonde mine case study plot above a spatial SRP$_N$ sum of one.

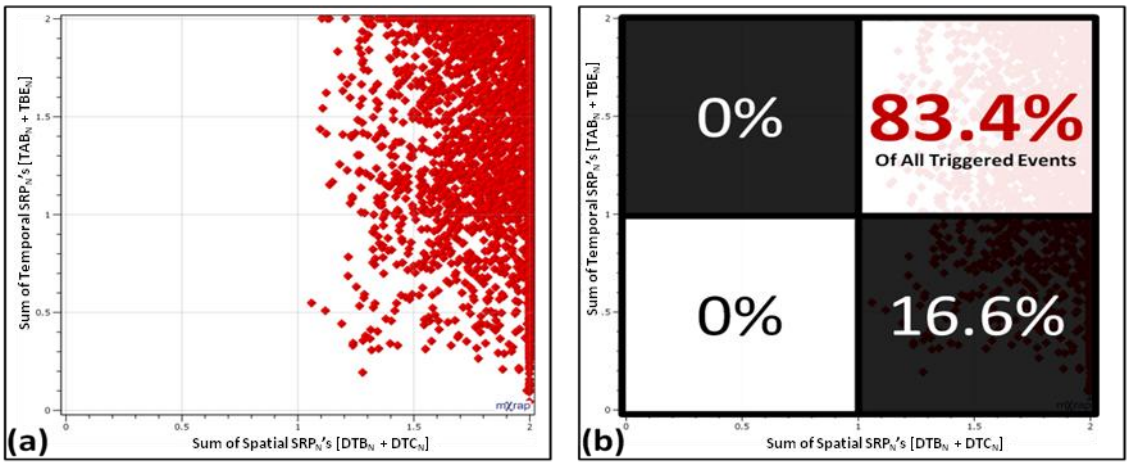

Figure 150: Scatter plot of spatial SRP$_N$'s (DTB$_N$ + DTC$_N$) versus temporal SRP$_N$'s (TAB$_N$ + TBE$_N$), for all triggered seismic events contained within the LaRonde mine Case Study II - presented in Chapter 7. Part (b) depicts the relative percent of events that are contained within each quadrant of the scatter plot shown in Part (a).

Figure 151 is a scatter plot of the sum of temporal SRP_N's versus the sum of spatial SRP_N's, for events contained within the Complex Case Study (III). Complex seismicity is expected to span the transition zone between induced and triggered seismicity (shown in Figure 149 and Figure 150, respectively). Approximately 10% or more of complex events plot in each individual quadrant shown in part (b). The majority of seismic events, approximately 43%, concentrate in the same quadrant as the induced seismicity. This is expected, as complex seismic responses contain a significant induced component. Unlike the induced seismicity shown in Figure 149 however, the complex seismicity exhibits a nearly equal split between the two bottom quadrants (sum of temporal SRP_N's less than one). This is largely a reflection of the triggered seismic events contained within the complex seismic responses to mining.

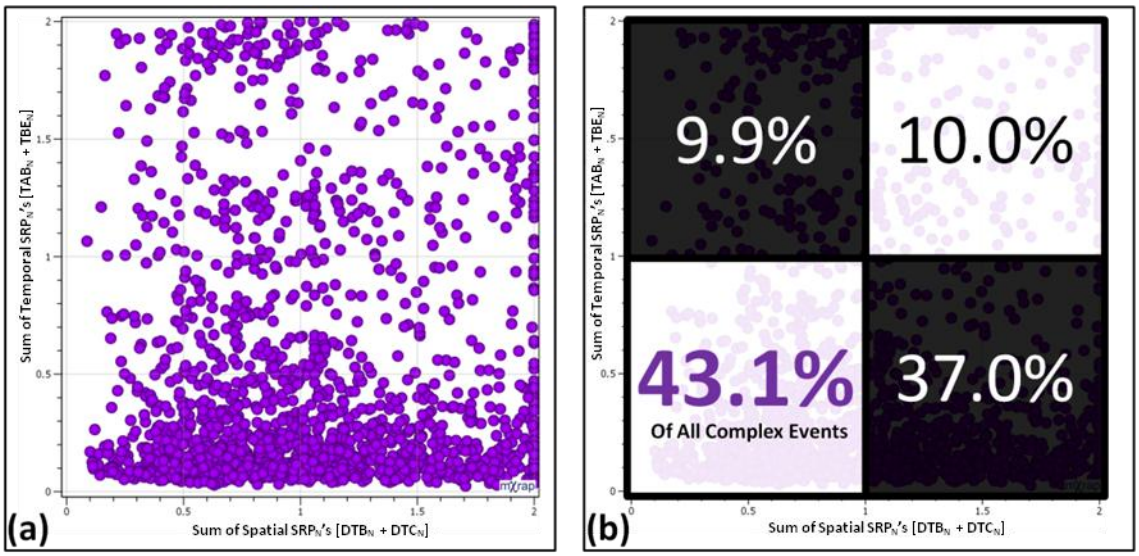

Figure 151: Scatter plot of spatial SRP_N's ($DTB_N + DTC_N$) versus temporal SRP_N's ($TAB_N + TBE_N$), for all complex seismic events contained within the LaRonde mine Case Study III - presented in Chapter 7. Part (b) depicts the relative percent of events that are contained within each quadrant of the scatter plot shown in Part (a).

When the induced, complex and triggered seismic events contained within the LaRonde mine case study are shown on the same scatter plot, Figure 152, nearly the entire range of SRP_N sums is represented. In part (b), the number of individual seismic events is shown by plot quadrants. The induced, complex and triggered seismic responses to mining examined within the LaRonde mine Case Study strongly support the proposed observation guidelines for SRP_N's and SRR. The transitional quadrants (shown in black in part (b)), contain the largest relative proportions of complex seismicity. Induced and triggered seismic events concentrate in the minimum (0,0) and maximum (2,2) quadrants, respectively.

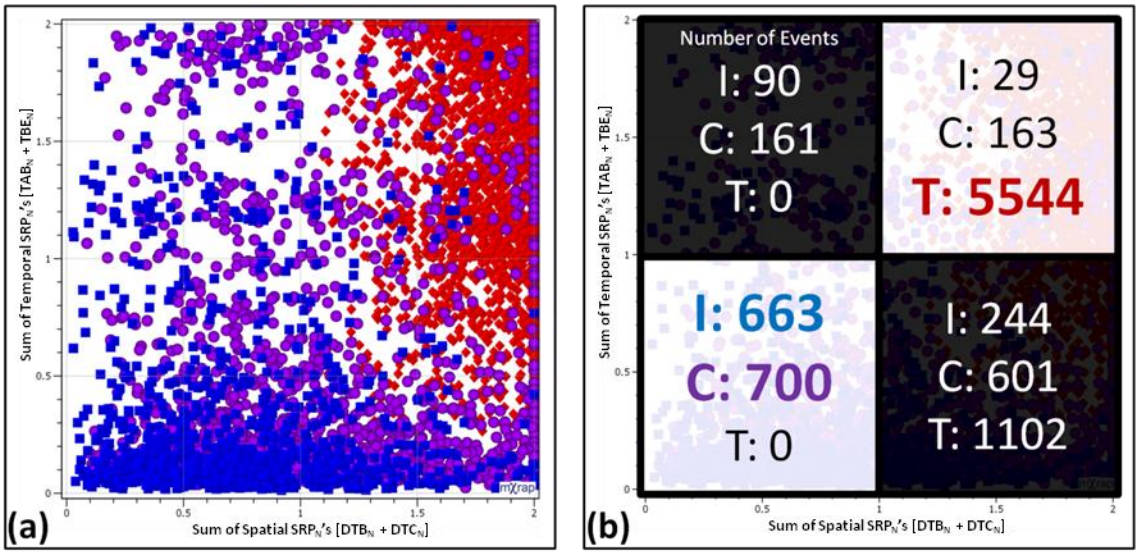

Figure 152: Scatter plot of spatial SRP$_N$'s (DTB$_N$ + DTC$_N$) versus temporal SRP$_N$'s (TAB$_N$ + TBE$_N$), for all induced, complex and triggered seismic events contained within the three case studies presented in Chapter 7. Events are coloured according to seismic response classification, with blue, purple and red corresponding to induced, complex and triggered respectively. Part (b) depicts the quantity of individual events, by classification, that are contained within each quadrant of the scatter plot shown in Part (a).

7.4.3 Statistical Considerations

Seismic events represent observations of rock mass failure, with significant dependencies on seismic monitoring hardware and software limitations. The occurrence of seismic events is uncontrolled, and consequently, data collection cannot be duplicated or repeated. In general, this complicates the application of statistical validation or analysis.

SRP$_N$'s for the induced, complex and triggered seismic responses in the LaRonde mine case study exhibit non-normal distributions. Seismic source parameters, such as energy and moment, commonly exhibit log-normal distributions, as discussed in Section 8.3. However, SRP$_N$ distributions vary significantly between types of seismicity. All SRP$_N$ and SRR distributions fail the Shapiro-Wilk W (Shapiro and Wilk, 1965) and Anderson-Darling (Anderson and Darling, 1954) test for normality. Table 40 depicts the Normal Probability Plots of SRP$_N$'s and SRR for induced, complex and triggered seismic responses to mining at LaRonde. These plots represent the inverse of the normal cumulative versus the ordered observations. In other words, if the data is normally distributed, the points will fall along a straight line (shown in red). Deviations from this line are indications of non-normality. All SRP$_N$ and SRR distributions deviate sufficiently as to be considered non-normal. More information surrounding distributions of SRP$_N$'s can be found throughout the individual case studies presented in Chapter 7.

Table 40: Summary table of normal probability plots for SRP_N's and SRR values of induced, complex and triggered seismic events contained within the case studies presented in Chapter 7. Table continued on subsequent page.

	Induced	Complex	Triggered
DTB_N	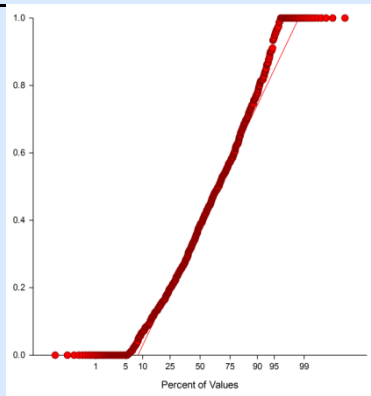	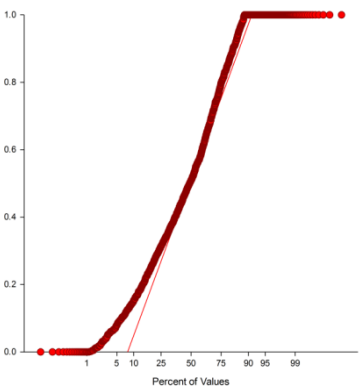	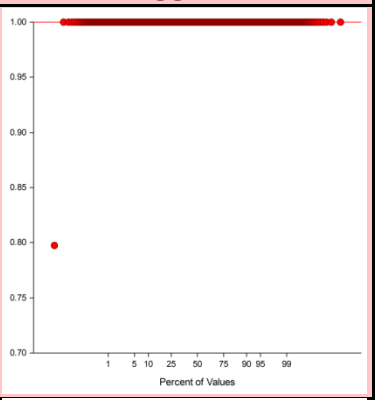
TAB_N	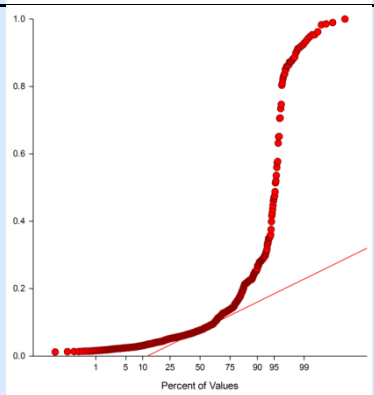	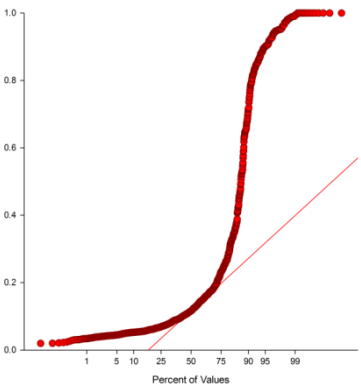	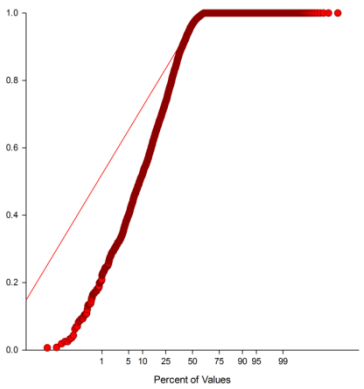
DTC_N	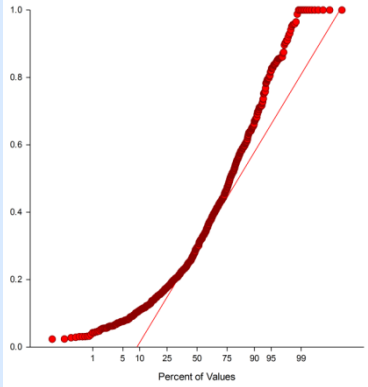	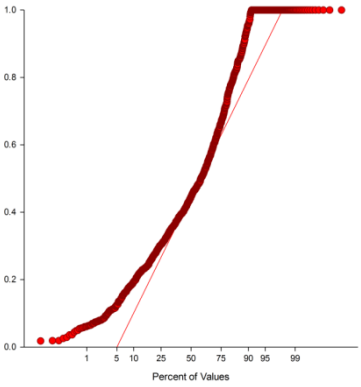	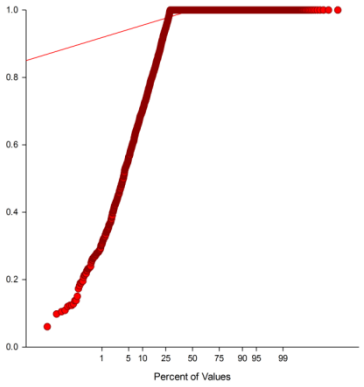
TBE_N	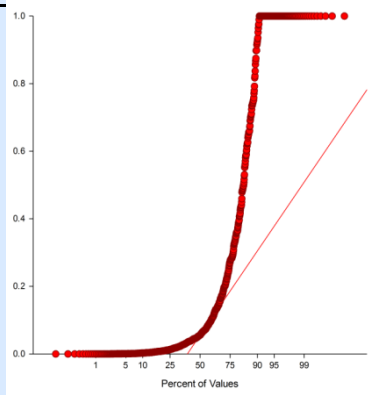	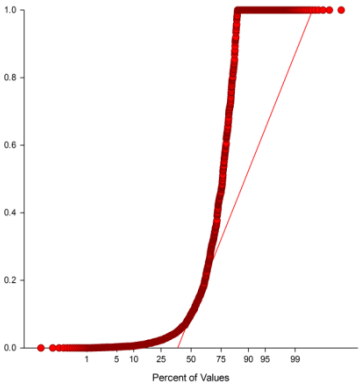	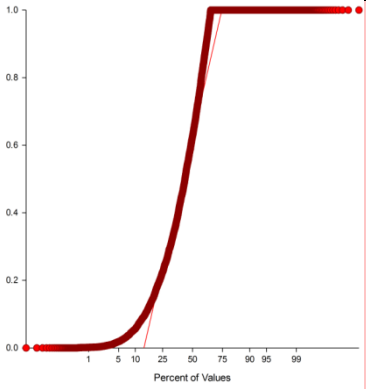

	Induced	Complex	Triggered
SRR	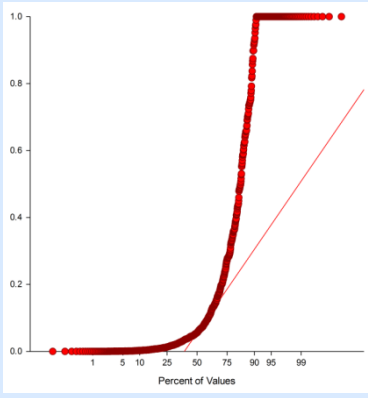	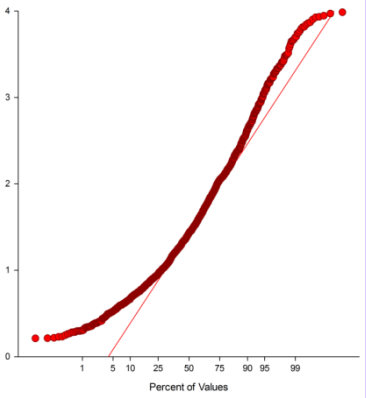	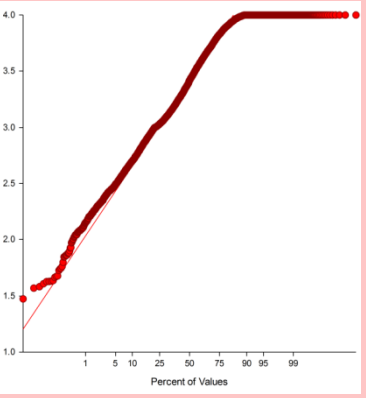

7.4.3.1 Internal Consistency

Internal consistency can provide insight into how well data are inter-correlated or vary together, and indicates the extent to which a set of data, or group of items, measures the same construct. With reference to SRP_N's, data reliability may serve as an indicator of how well different SRP_N's (e.g. TAB' and DTC'), measure the same seismicity classification. Table 41 summarizes the Cronbach Alpha and Average R (Average Inter-item Correlation) analysis results for induced, complex and triggered seismic events contained within the LaRonde mine case study presented in detail in Chapter 7. Criteria for a good scale of internal consistency are also shown (BrckaLorenz, A. *et al.*, 2013; Clark and Watson, 1995).

Cronbach Alpha measures the homogeneity of a group of items to assess internal consistency. It is an indication of how well different items complement each other in their measures of different aspects of the same quality. Values closer to one indicate a higher internal consistency, with values greater than 0.7 commonly accepted as good (BrckaLorenz, A. *et al.*, 2013). For the LaRonde mine case study, only the triggered seismic responses to mining exhibit Cronbach Alpha values less than 0.7. Although McMillan and Schumarcher (2001) suggest caution be used for data with Cronbach Alpha values less than 0.7, the triggered seismic response case study is arguably the most well-behaved, and the low value is likely a reflection of the high concentrations of SRP_N' values equal to one.

Inter-item Correlation, or Average R, can also serve as a measure of internal consistency. If a group of items measures the same underlying construct, it can be assumed that each item correlates well with the scale overall. Furthermore, it can be assumed that items within each scale are positively correlated. Clark and Watson (1995) suggest average inter-item correlations should fall between 0.15 and 0.50. Below this range items are not well correlated, and above this range items may be redundant. Average R values are indicative of good internal consistency for

induced, complex and triggered seismic responses to mining considered in the LaRonde mine Case Study, as shown in Table 41.

Table 41: Cronback Alpha and Average R (Average Inter-item Correlation) analysis results for the induced, complex and triggered seismic events contained within the case studies presented in Chapter 7. Results produced using the statistical software provided by Wessa (2008).

	Cronbach Alpha		Average R	
	*Criteria for Good Scale**	*Value*	*Criteria for Good Scale***	*Value*
Induced	Greater than or equal to 0.70	0.73	Between 0.15 and 0.50	0.37
Complex		0.75		0.40
Triggered		0.67		0.22

*BrckaLorenz, A. *et al*., 2013 **Clark and Watson, 1995

7.5 LaRonde Mine Case Study Summary

The primary objective of this case study, which was presented in three parts, was to demonstrate the applicability of SRP's to real mine seismic data. Throughout Chapters 4 and 5, observation guidelines were provided for induced, triggered and complex seismic responses to mining. These guidelines are generalizations based on the established spatial and temporal relations between mine blasts and variations in mine seismicity. Within a mining environment however, there can be considerable variability, and all seismic responses to mining are not likely to conform to theoretically perfect results. Table 42 summarizes the proposed observation guidelines and observed results for the three independent LaRonde mine case studies presented in this chapter. Few outliers were observed within the case studies, and no noteworthy outliers were present.

Case Study I focused on induced seismic responses to mining, considering development and production blast induced responses separately. The induced seismicity occurred in close spatial and temporal proximity to mine blasting, and both types of seismic responses exhibited similar SRR and SRP_N distributions, as shown in Table 42.

Case Study II focused on triggered seismic responses to mining, considering triggered and shutdown period responses separately. All triggered seismicity occurred spatially distant and temporally independent of mine blasting, and both types of seismic responses exhibited similar SRR and SRP_N distributions, as shown in Table 42.

Case Study III focused on complex seismic responses to mining, considering predominantly induced and triggered complex responses separately. The characteristics of complex seismicity depend largely on the relative proportions of included induced and triggered seismic events. As a result, when the two are combined they cover nearly the entire transitional zone between induced and triggered seismicity for SRR and SRP_N distributions, as shown in Table 42.

Median SRP_N values were used in the interpretation of seismic responses throughout this work. These values have been successfully used to interpret seismic responses, however it can be challenging to classify 100% of seismic responses observed in complex mining environments. Due to the rock mass uncertainty, there will undoubtedly always be a few unexplainable outliers in space and/or time.

Table 42: Summary of SRR and SRP_N expected general observation guidelines and median distributions for the LaRonde mine case study, for induced (blue), complex (purple) and triggered (red) seismic responses. 'O' symbols refer to Induced: Production, Complex: Triggered and Shutdown period responses to mining. 'X' symbols refer to Induced: Development, Complex: Induced and Triggered responses to mining. Table continued on subsequent page.

	Observation Guidelines		Median Distributions for LaRonde Case Study
SRR	I	Small SRR [$0 \leq SRR \leq 1.5$]	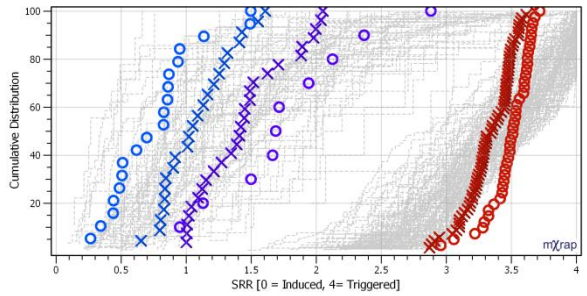
	C	Medium SRR [$1 \leq SRR \leq 3$]	
	T	Large SRR [$2.5 \leq SRR \leq 4$]	
DTB_N	I	Approaching Zero [$DTB_N < 1$]	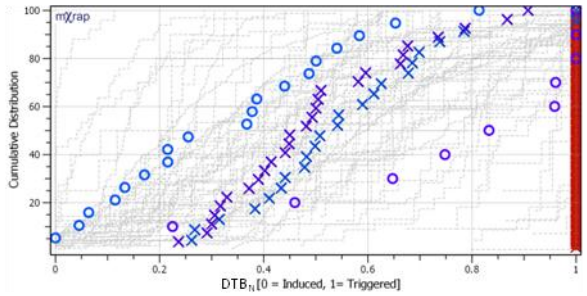
	C	Typically Less Than One [$0 \leq DTB_N \leq 1$]	
	T	Equal to One [$DTB_N = 1$]	
TAB_N	I	Approaching Zero [$TAB_N \approx 0$]	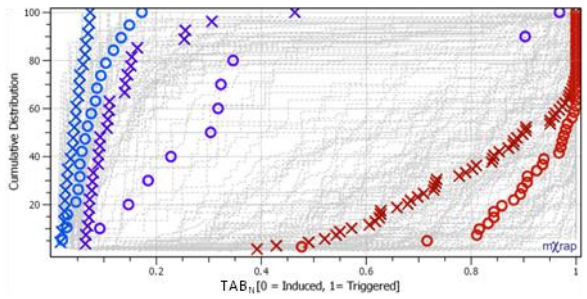
	C	Variable [$0 \leq TAB_N \leq 1$]	
	T	Approaching One [$0.5 \leq TAB_N \leq 1$]	
DTC_N	I	Approaching Zero [$0 \leq DTB_N < 1$]	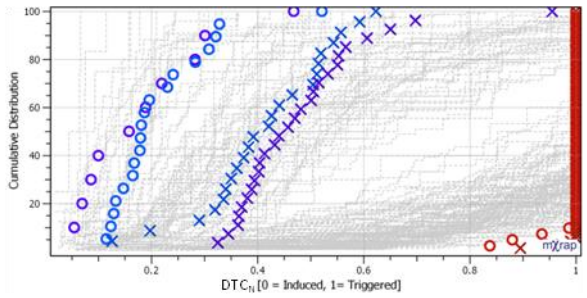
	C	Typically Less Than One [$0 \leq DTC_N \leq 1$]	
	T	Approaching One [$DTC_N \approx 1$]	

	Observation Guidelines		Median Distributions for LaRonde Case Study
TBE_N	I	Approaching Zero $[TBE_N \approx 0]$	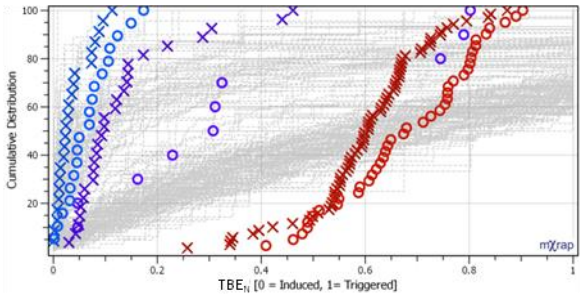
	C	Variable $[0 \leq TBE_N \leq 1]$	
	T	Approaching One $[0.5 \leq TBE_N \leq 1]$	

Chapter 8

8 Discussion

This chapter discusses the following topics:

- Underlying Assumptions of this Work
- Spatial vs. Temporal $SRP_{(N)}$'s
- SRR vs. Traditional Seismic Analysis
- Relation Between Triggered Seismicity and Background Seismicity
- Complex Seismic Responses to Mining and Seismic Hazard Evaluation

Discussion specific to SRP's and variations in induced, triggered and complex seismic responses to mining was provided in Sections 7.1, 7.2 and 7.3, respectively.

8.1 Underlying Assumptions of this Work

Due to the significant degree of unknowns in complex mining environments, some assumptions are required in order to qualitatively and quantitatively describe seismic responses to mining.

The following types of assumptions will be discussed within this section:

- Assumptions to Simplify the Complex Mining Environment
- Response Identification Assumptions

8.1.1 Assumptions to Simplify the Complex Mining Environment

8.1.1.1 Relating Discrete Mine Blasts to Changes in Rock Mass Stress

The ability to relate changes in rock mass stress to discrete mine blasts is a primary underlying assumption of this work (i.e. the assumed mining-induced stress change zone). This assumption is supported by previous work (Brady and Brown, 1985; Hoek and Brown, 1980; Hoek *et al.*, 1995; Kuzyk and Martino, 2008), which suggests that stress changes surrounding mine openings are not measurable beyond 5 excavation radii - discussed in more detail in Section 3.1. In order to account for any seismic monitoring limitations specific to seismic event location accuracy, the addition of a Location Error Factor is suggested when determining an appropriate assumed mining-induced stress change zone - discussed in more detail in Section 8.2.

The radius of the assumed mining-induced stress change zone directly impacts Seismic Response Parameters - specifically Normalized Seismic Response Parameters. Normalized SRP's are calculated assuming all seismic events occurring beyond the assumed mining-induced stress

change zone are not directly induced by the discrete mine blast considered. The LaRonde mine case study, presented in Chapters 6 and 7 of this work, suggests it may be beneficial to increase the assumed mining-induced stress change zone for certain cases in highly complex mining environments. This practice may account for aspects such as stress shedding and the presence of significant voids/fill.

Due to the long history and significant orebody extraction at LaRonde mine, it is not uncommon for seismic events to locate beyond the immediate rock mass area adjacent to newly blasted excavations. Figure 153 depicts the seismic response to a typical secondary stope production blast (shown as a blue star). Using single-link clustering with a d-value of 20 metres, two seismic response populations are identified surrounding the blast location: one in the hanging wall (black triangles), and one in the footwall (grey circles). A significant spatial offset is evident between the blast location and the location of the induced seismic events, particularly for the hanging wall events. The hanging wall event locations are likely a product of a number of factors, including: hanging wall rock mass relaxation towards the orebody, induced stress magnitude and orientation change around the new void, and potentially local microseismic monitoring limitations.

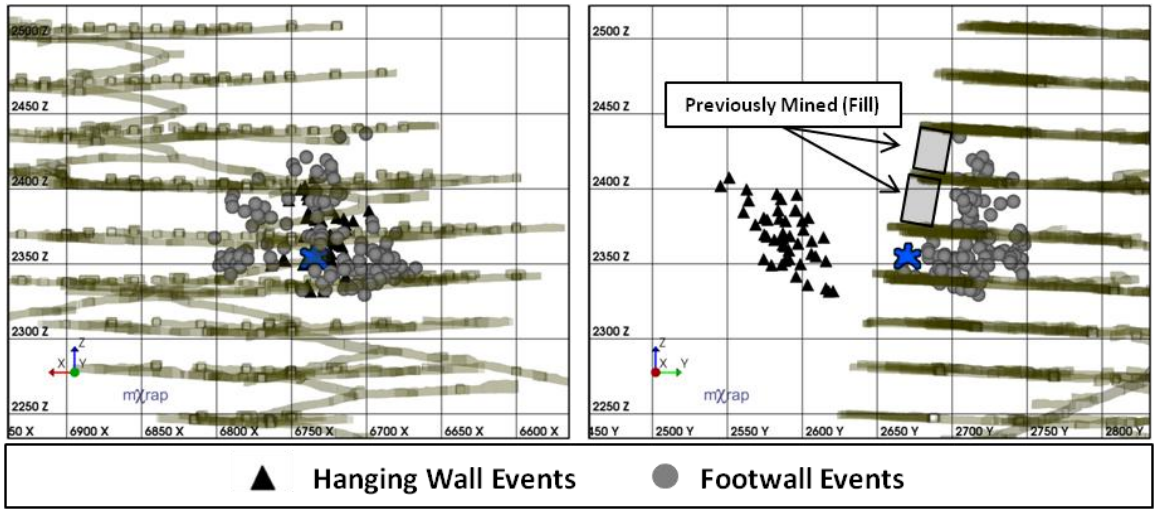

Figure 153: Longitudinal and cross-sectional projections of LaRonde mine showing a hanging wall (black triangles) and footwall (grey circles) induced seismic responses to mining, and the associated mine production blast (blue stars). The location of previously mined and fill stopes adjacent to seismic events is approximated by grey rectangles.

Due to the relatively large scale of production blasting, the spatial migration of seismic events (as shown in Figure 153), is accounted for by the large mining-induced stress change zone used in the calculation of DTB_N and DTC_N parameters. Parameter distributions, shown in Figure 154, for both the hanging wall and footwall response populations are indicative of a Complex: Induced seismic response to mining. More than 80% of events exhibit SRR values less than 2.5, and when the temporal parameters (TAB_N and TBE_N) are considered independently, it is very evident that these responses contain a significant induced component.

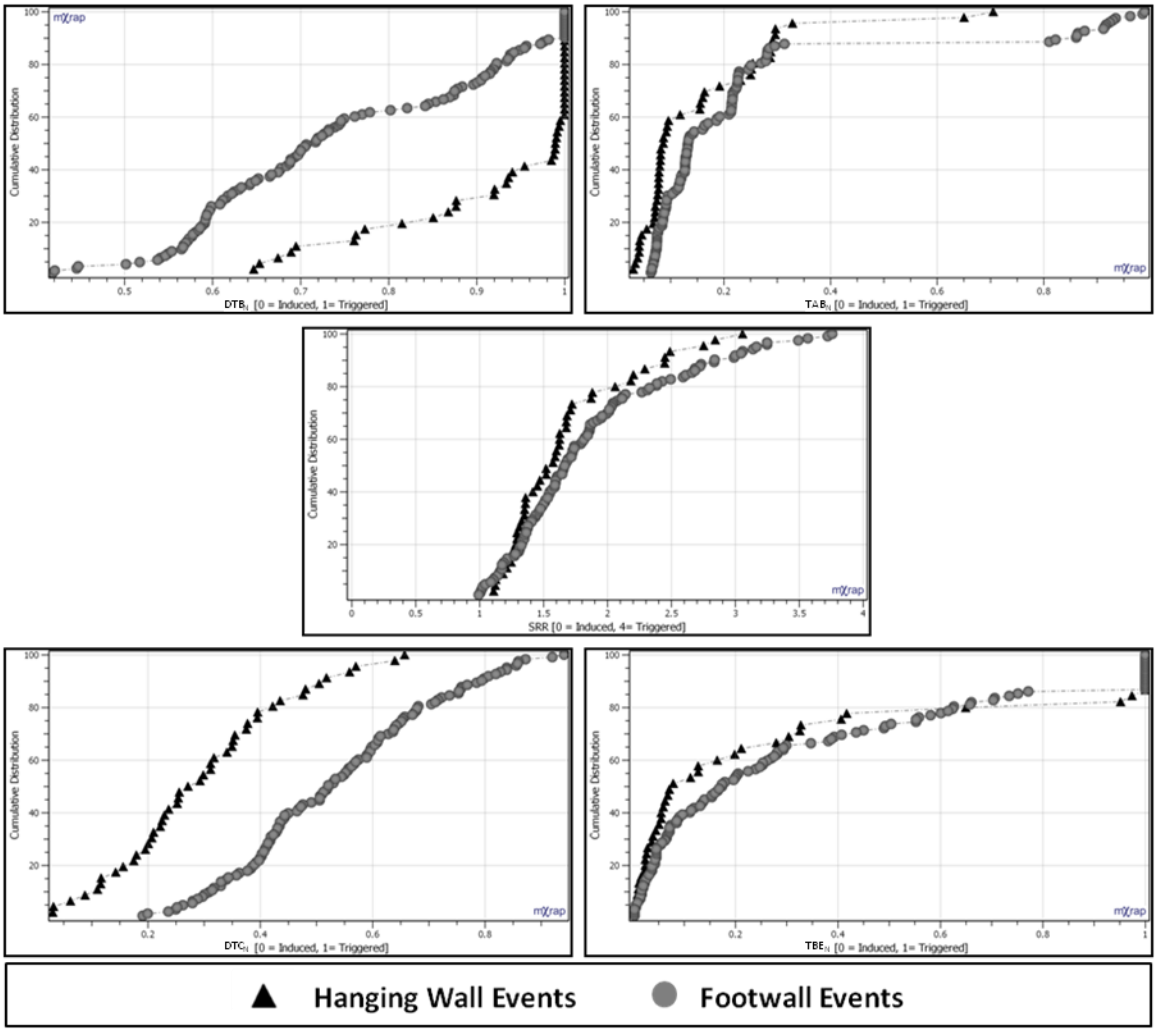

Figure 154: Cumulative distributions of DTB_N, TAB_N, SRR, DTC_N and TBE_N for the hanging wall and footwall seismic responses to production mining shown in Figure 153.

The relatively small scale of development blasting however, means that factors such as stress shedding and significant volumes of void/fill in the rock mass can have a significant impact on spatial $SRP_{(N)}$'s. A study focusing on mining-induced stress change measurements at Beiminghe mine (Ouyang *et al.*, 2009), concluded the maximum mining-induced stress change occurred 15 to 20 metres beyond the face. Furthermore, the total stress increasing area was measured as 3 to 55 metres beyond the working face. With standard drift dimensions of 4.2 metres wide by 3.9 metres high (Chadwick, 2007), the maximum mining-induced stress change appears to occur beyond 5 excavation radii in the case of Beiminghe mine.

Within a complex mining environment there are many unknowns with the potential to lead to significant stress shedding beyond 5 excavation radii. Arbitrarily increasing the assumed mining-induced stress change zone however, increases the likelihood of complex and/or triggered seismic responses to mining being wrongfully interpreted as induced. This must be considered when interpreting seismic responses to mining. An assumed mining-induced stress change zone

of 5 excavation radii, plus a Location Error Factor, produced consistent and meaningful results for both development and production scale mine blasting in this thesis. Within the LaRonde mine induced seismic responses to mining case study, presented in Section 7.1, there was evidence to suggest a larger mining-induced stress change zone may be warranted in some cases related to development blasting. This was particularly the case for blasts in close spatial proximity to the orebody, and other areas of the mine with relatively high local extraction ratios.

8.1.1.2 Other Seismic Response Stimuli in Complex Mining Environments

Natural earthquakes are commonly associated with the occurrence of aftershocks (Harris, 1998; Omori, 1894). When a significant rock mass failure occurs within a mining environment, it is not uncommon for the resulting local stress redistribution to generate subsequent seismic events (i.e. aftershocks). An underlying assumption of this work is that the only seismic response stimuli within the mining environment are mine blasts. As such, any seismic response that is not directly induced by a stress change resulting from a discrete mine blast is assumed to be triggered.

This assumption, regarding the inducing mechanism, is fundamental to blast related SRP_N's (DTB_N and TAB_N), but is not fundamental to response related SRP_N's (DTC_N and TBE_N). Consequently, when response related SRP_N's are indicative of an induced source mechanism, but blast related SRP_N's are not, it indicates that the mine blast associated with the response may not be the correct stimulus. For example, the correct stimulus may be a different blast within the mining environment, or a rock mass stress redistribution following a large magnitude seismic event.

Figure 155 depicts the location (a, b) and timing (c), of a seismic response following a large magnitude seismic event at LaRonde mine. The time of occurrence for the first large event is taken as the mine blast, or stimulus, time in the calculation of SRP_N's, shown in Figure 156. Approximately 70% of seismic events in Figure 156 exhibit TAB_N and TBE_N values less than 0.2 (typical of an induced response). Although this response is not related to mine blasting, individual event SRR values are indicative of induced or complex seismicity. Only three individual seismic events have SRR values indicative of triggered seismicity. This suggests that in certain cases, additional considerations may be required to account for seismic response stimuli (other than mine blasting), particularly in complex mining environments.

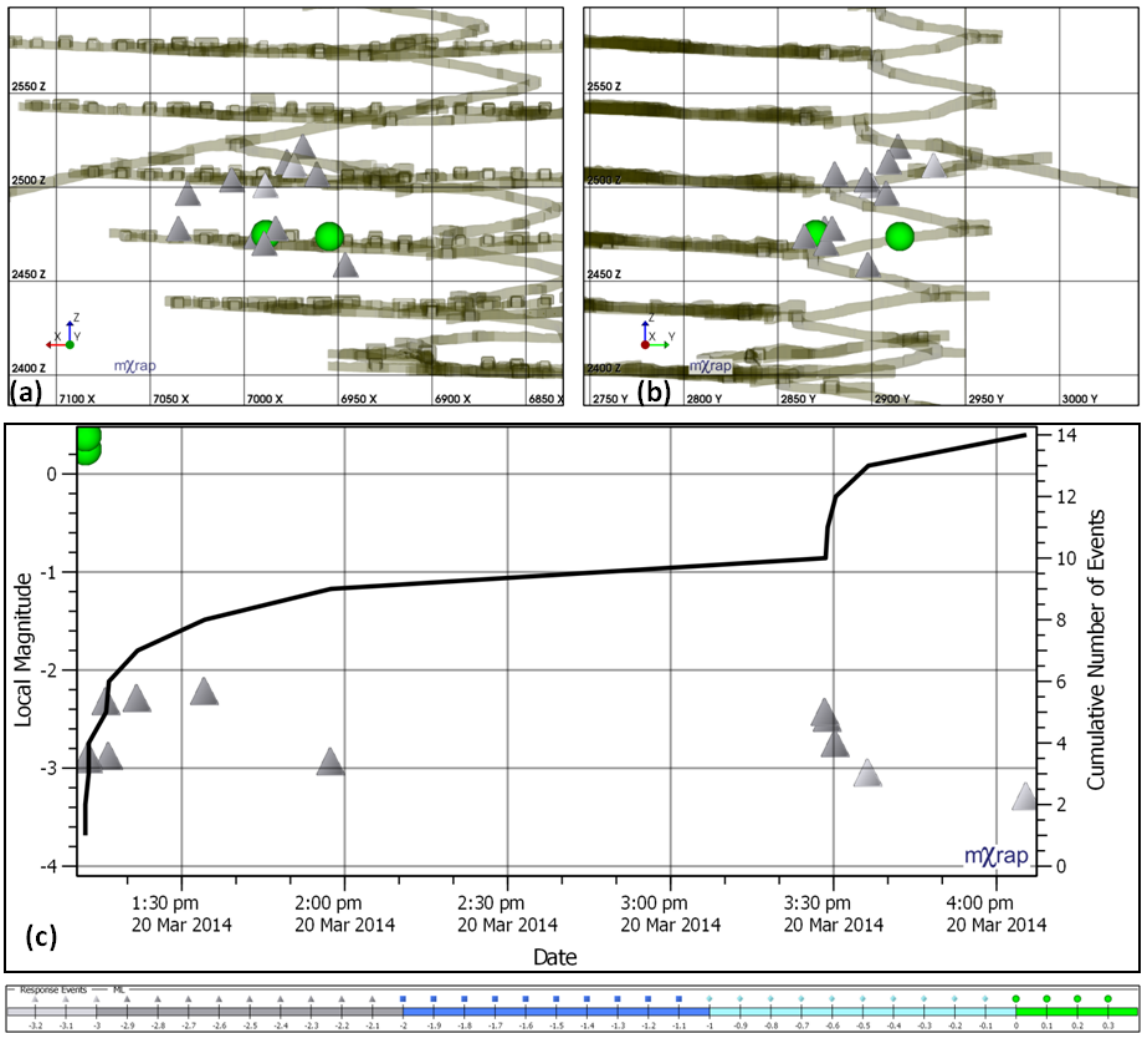

Figure 155: Longitudinal (a) and cross-sectional (b) projections of LaRonde mine showing a seismic response to a large magnitude seismic event. A Magnitude-Time History chart for the events shown in (a) and (b) is shown in (c). The seismic response is identified using single-link clustering with a d-value of 40 metres.

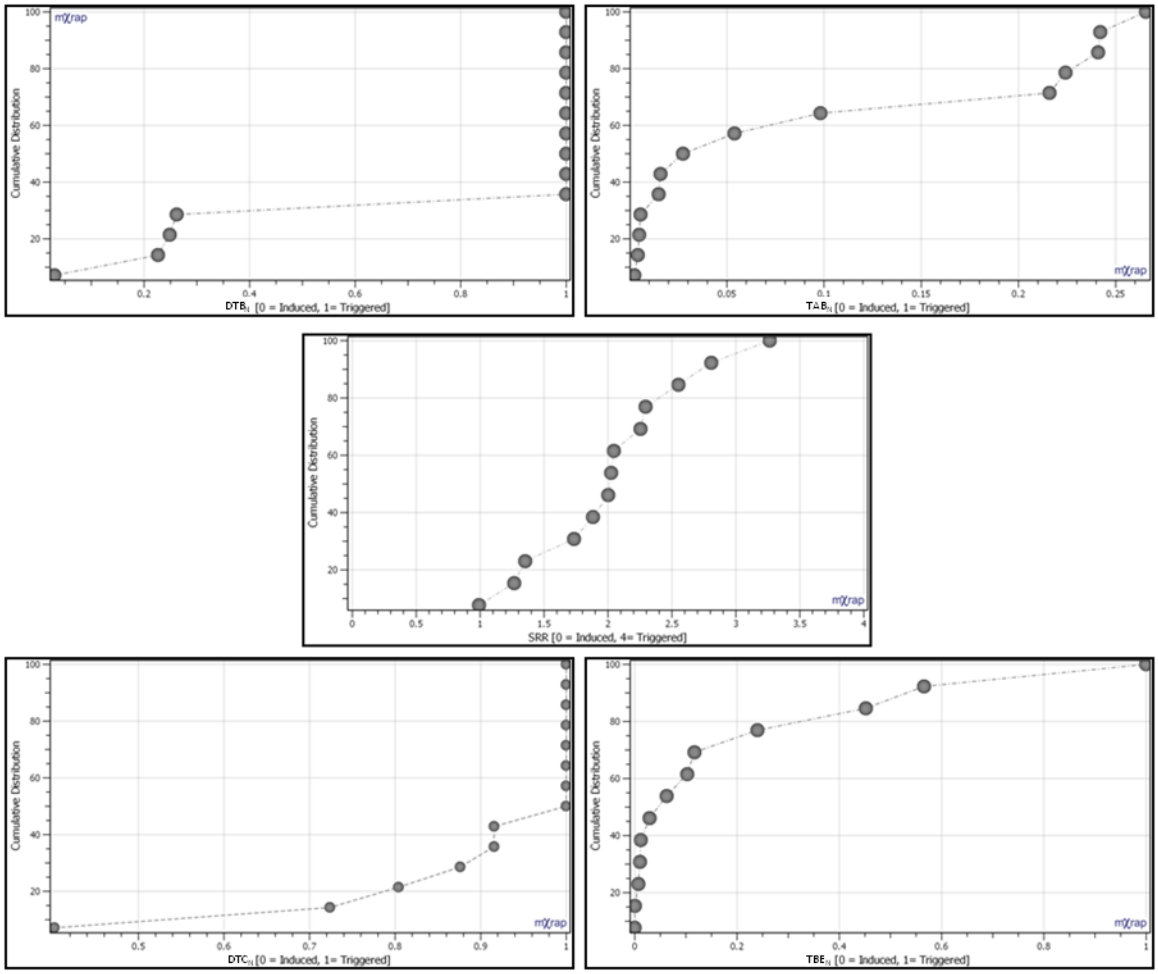

Figure 156: Cumulative distributions of DTB_N, TAB_N, SRR, DTC_N and TBE_N for the seismic responses to a large magnitude seismic event shown in Figure 155. The source radius of the large magnitude seismic event is taken as the radius of the assumed mining-induced stress change zone.

When using SRP_N's to interpret seismic responses to mining, it is critical to understand the underlying impact of the assumed mining-induced stress change zone and seismic response stimulus (i.e. mine blast). Both of these assumptions can have a significant impact on SRP_N's and SRR values. When spatial (DTB_N and DTC_N) and temporal (TAB_N and TBE_N) SRP_N's produce contradictory results, it likely indicates that an underlying assumption has been violated, or the seismic response itself has been identified poorly - as discussed in the subsequent section.

8.1.2 Response Identification Assumptions

For Seismic Response Parameters to provide meaningful insight into a seismic response to mining, the response itself most be identified with certain considerations. This has previously been discussed briefly in Section 6.3.

8.1.2.1 Spatial Considerations in Response Identification

In order to apply SRP's to seismic data, considerations are required surrounding how responses are identified in both space and time. Spatial considerations focus on ensuring that individual responses represent only a single source mechanism. For example, Figure 157 depicts seismic responses to a development blast at LaRonde mine using single-link clustering with a d-value of 20 metres (a), and a d-value of 30 metres (b). In (a), using the smaller d-value of 20 metres, two distinct response are identified, A and B. In (b), using the marginally larger d-value of 30 metres, the increased d-value joins all seismic events into a single response, C. While it may be visually obvious in Figure 157 that a spatial separation exists between responses A and B, likely reflecting two different source mechanisms, a simple automated clustering algorithm with a set d-value of 30 metres would produce only the single response C.

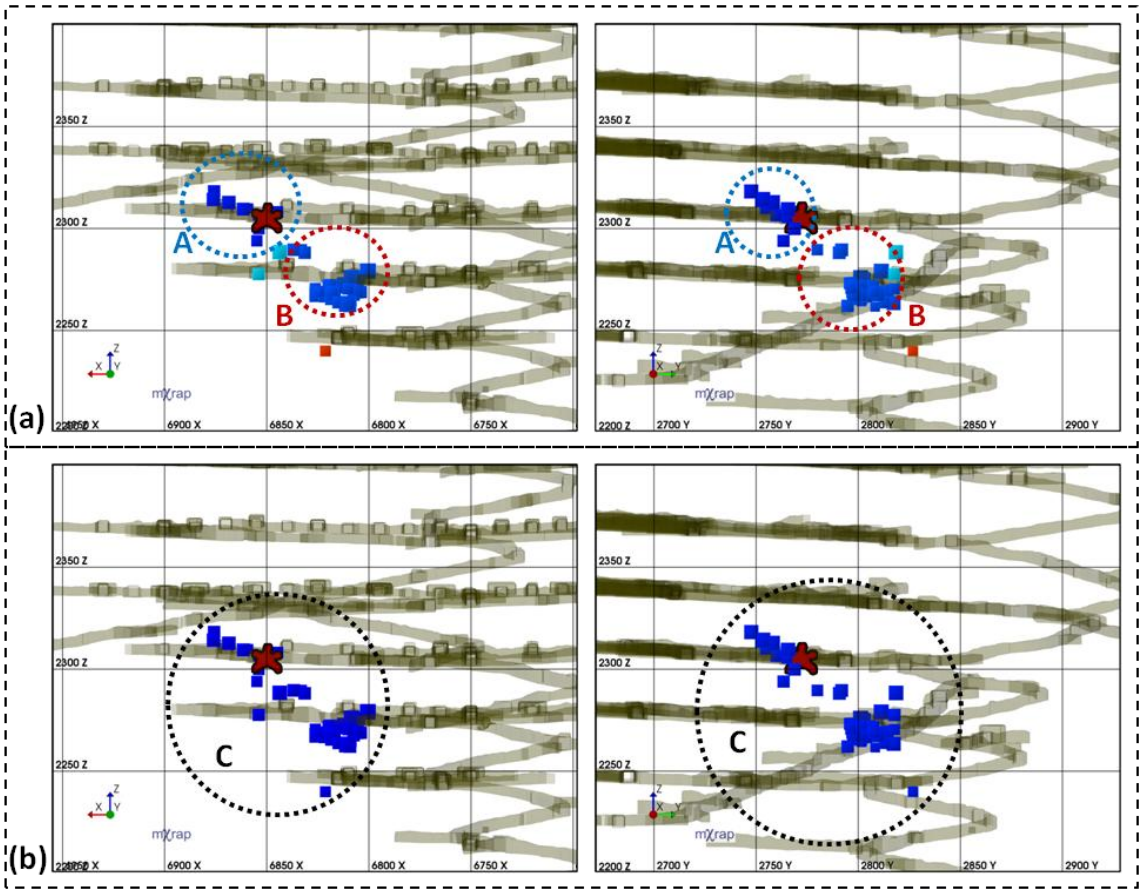

Figure 157: Longitudinal and cross-sectional projections of LaRonde mine showing the seismic response to a development blast (red star). Parts (a) and (b) depict the single-link clustering results using a d-value of 20 metres and 30 metres respectively.

The SRR values for seismic responses A, B and C (as shown in Figure 157), are shown in Figure 158. Response A is most likely induced, with 60% of the response exhibiting SRR values less than 1.5, and only a single event with a SRR value greater than 2.5. Response B is most likely

triggered, with all events exhibiting SRR values greater than 2, and 60% of SRR values greater than 2.5. Of particular interest is the relative change in SRR values of the individual seismic events when they are combined together in response C. When induced and triggered seismic responses to mining are joined together, it is common for the triggered response to dominate the population. For example, the induced response (A) contains SRR values less than 1.7, but there are no such SRR values when the two responses are joined together (forming C). This change is primarily driven by the DTC_N parameter. When the SRR values for events in responses A and B are calculated independently, the individual events in both responses are located much closer to their respective response centroids. When all events are combined however, the response centroid location changes significantly, and the individual events are located much further from the centroid.

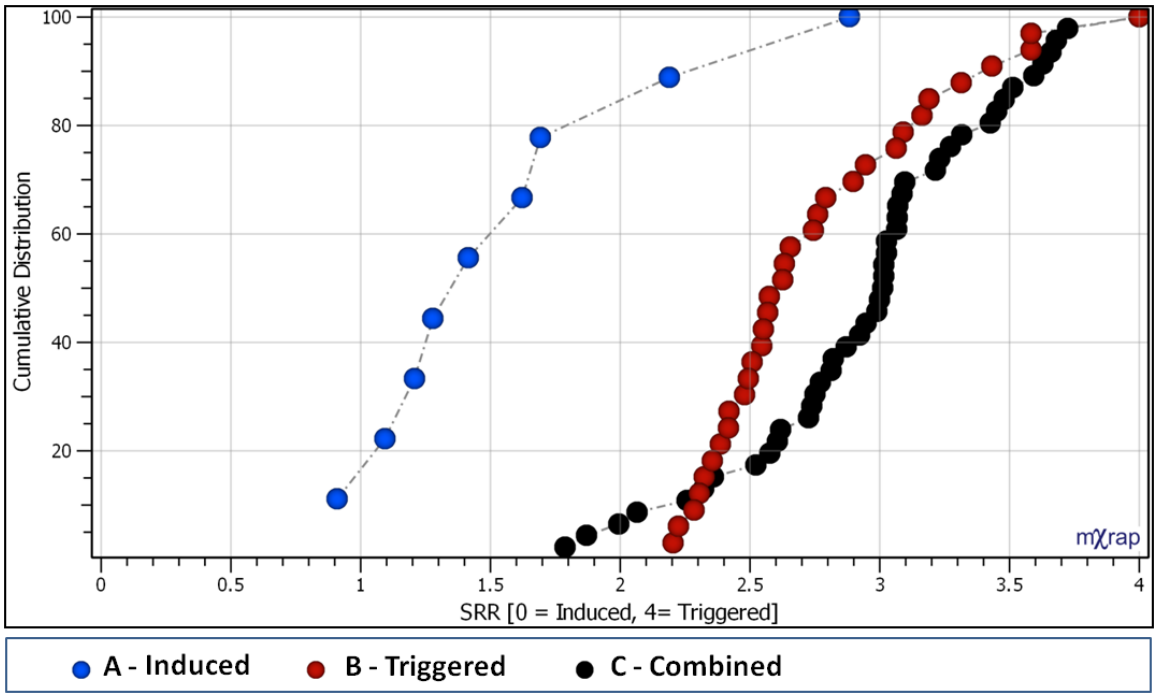

Figure 158: Cumulative distributions of SRR for the seismic responses A, B and C shown in Figure 157.

The selection of an optimal d-value (for single-link clustering), is critical for seismic analysis of individual responses. In this work, all seismic responses to mining were manually reviewed to ensure multiple responses were not arbitrarily combined into a single response (e.g. Figure 157 (b)). When this is not possible, it may be beneficial to perform a sensitivity analysis of d-value (and/or other variables), to ensure seismic responses to mining are optimally identified in space.

8.1.2.2 Temporal Considerations in Response Identification

Temporal response identification considerations focus on ensuring that the time window for response identification is as long as possible, and begins at blast time (t_0 = Blast Time). When

time windows are shortened, it may cause temporal parameters (TAB_N and TBE_N) to become less meaningful. In terms of SRP_N's, the absence of seismicity is of significant importance, as it implies a lack of triggered source mechanisms. The occurrence of seismic events in close temporal proximity to mine blasting is indicative of induced seismicity, but so is a lack of seismicity temporally distant to blasting. Time windows for response identification should aim to be as long as possible while ensuring adjacent mine blasting periods do not overlap within the same time window. Meaningful analysis of SRP_N's is negatively impacted when time windows are insufficiently long.

Small deviations in the beginning of the temporal window from the blast time have a minimal impact on SRP_N's; for example, if the temporal window is 12 hours and blast time deviates by a matter of minutes. As the degree of deviation increases however, it can have a considerable impact on temporal parameters (TAB_N and TBE_N). Figure 159 depicts Magnitude-Time History charts for a theoretical induced (a) and triggered (b) seismic response to mining. Time windows are denoted as TW_x, and consistently align with mine blasting. The distributions of temporal parameters are shown below each Magnitude-Time History chart respectively. As expected, the temporal parameters of the induced seismic responses are very small, with the triggered temporal response parameters being orders of magnitude larger.

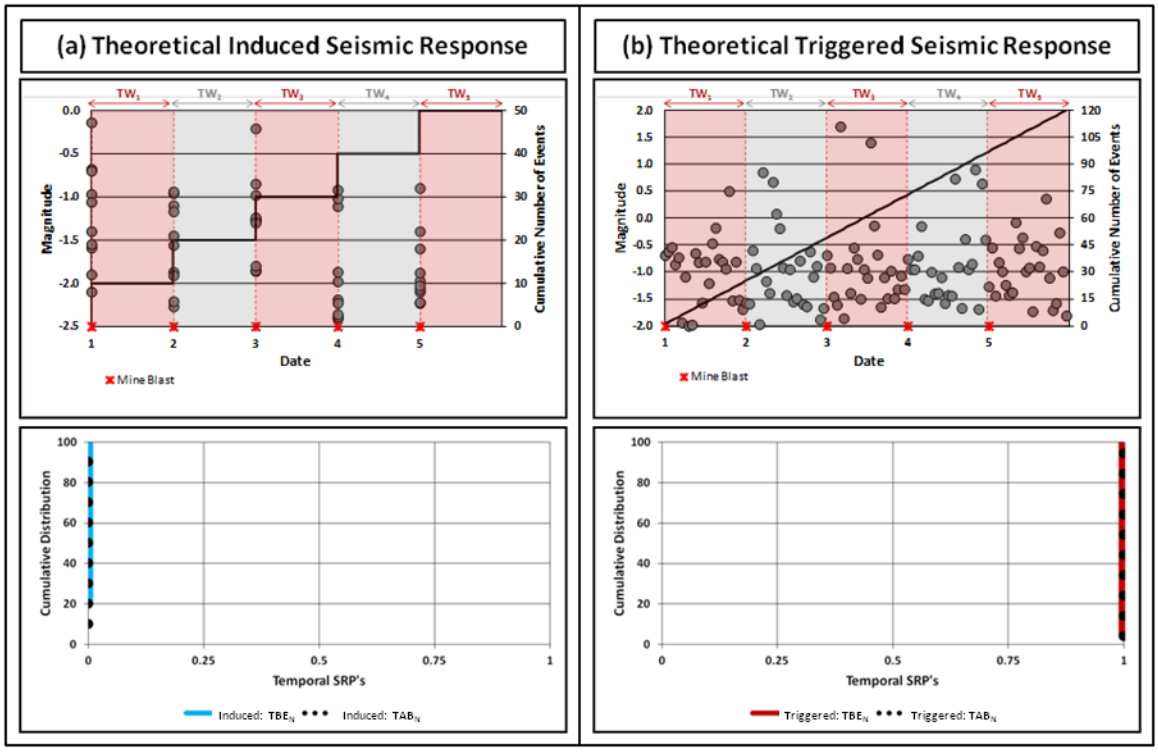

Figure 159:Magnitude-Time History charts and temporal parameter (TAB_N and TBE_N) distribution charts for a theoretical induced (a) and triggered (b) seismic response to mining. Time Window (TW) align directly with mine blast times.

Figure 160 depicts Magnitude-Time History charts for the same theoretical induced (c) and triggered (d) responses shown in Figure 159. The time windows however, have been arbitrarily moved by six hours, beginning halfway between consecutive mine blasts (as denoted by TW_x). Comparing the distributions of temporal parameters between Figure 159 and Figure 160, there is no impact on the triggered seismic responses to mining, as triggered seismicity occurs independent of mine blasting. There is also no impact on the TBE_N parameter of the induced responses, as the temporal window does not affect the relative position in time of the events to one another. The only notable change is in the TAB_N parameter of the induced seismic response. This change is significant, as it results in a direct increase to SRR values - moving away from induced and towards triggered. In order to accurately represent induced seismic responses to mining, it is critical that seismic identification time windows align as closely as possible with mine blast times, regardless of what spatial clustering algorithm is employed. A more detailed discussion surrounding spatial and temporal Seismic Response Parameters is provided in the subsequent section.

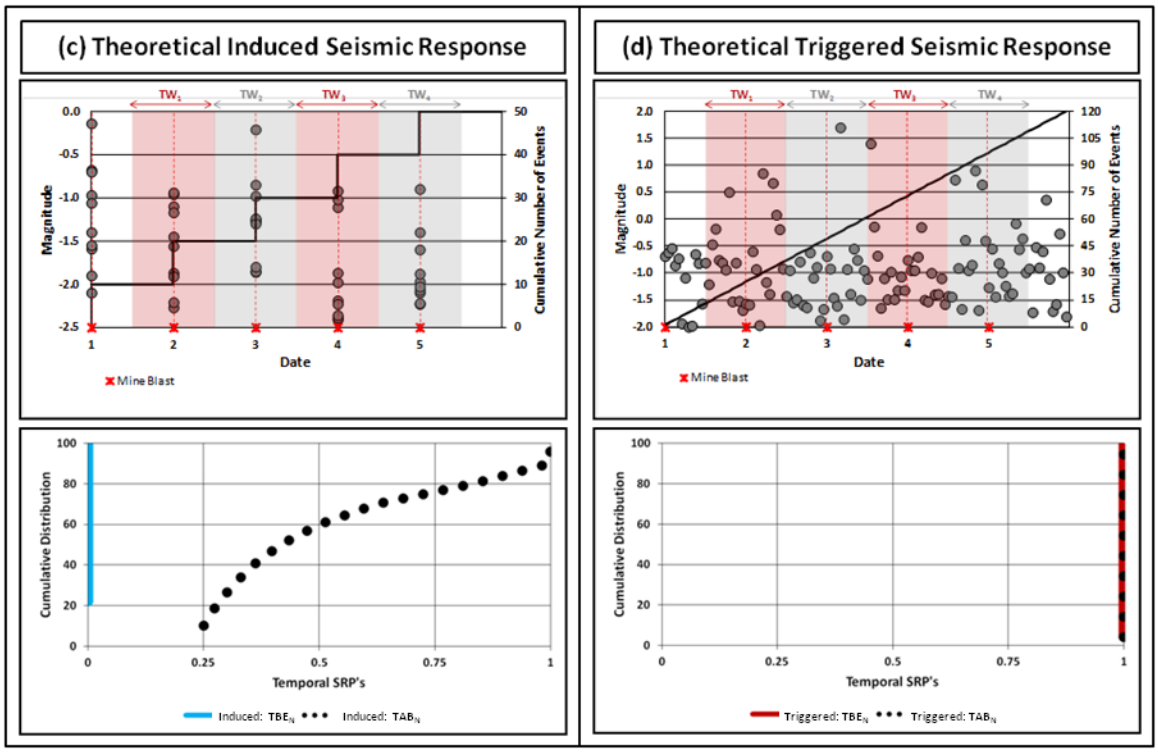

Figure 160: Magnitude-Time History charts and temporal parameter (TAB_N and TBE_N) distribution charts for a theoretical induced (c) and triggered (d) seismic response to mining. These are the same theoretical responses shown in Figure 159. Time Window (TW) have been arbitrarily moved by 6 hours, and do not align directly with mine blast times.

8.2 Spatial vs. Temporal Seismic Response Parameters

Space and time are the two primary considerations of SRP_N's. These two types of parameters however, spatial (DTB_N and DTC_N) and temporal (TAB_N and TBE_N), are associated with very different degrees of error.

8.2.1 Spatial Error

The error associated with seismic event location is largely dependent on any site specific underground microseismic monitoring system limitations (hardware and software), and consequently varies in space and time throughout the mining environment. Monitoring systems are designed to surround the area of interest, the orebody, and sensors are not often optimally placed to monitor triggered source mechanisms throughout the rock mass. Furthermore, the installation of seismic monitoring sensors requires underground access to areas of interest. As these areas are initially approached, new development headings will likely have relatively poor microseismic monitoring due to suboptimal sensor coverage. These factors, among others, can lead to significant seismic event location errors.

The location error values that are calculated and associated with individual seismic events are commonly the time residuals between measured and theoretical wave arrivals. These values are therefore largely dependent on the underlying assumptions of the monitoring system software, such as: correct identification of p-wave and s-wave arrivals, point-source locations and the velocity model. These assumptions generate a secondary degree of error, associated with the calculation of location error values, that can vary significantly for any given event.

The significance of location error of individual seismic events for Seismic Response Parameters depends primarily on the methodology employed to identify the individual seismic responses to mining. In this work, seismic responses were identified following a simple single-link clustering methodology. Inter-event clustering distances, or d-values, used in response identification ranged from 20 metres to 100 metres. Much larger d-values were required to identify triggered responses located in the deep footwall, due to both the nature of the failure mechanism and the seismic monitoring system limitations in this area of the mining environment. Depending on the methodology used, the location error of individual seismic events may have an increased or decreased significance in terms of $SRP_{(N)}$'s and seismic response interpretations.

8.2.2 Temporal Error

There is little to no error associated with seismic event time. All measures of time are synched within a seismic monitoring system, resulting in any deviation from an absolute time being constant across the system, and therefore arguably negligible for analysis purposes. This advantage of little to no error is unique to time among all of the independent seismic source parameters (time, location, energy, moment, size).

8.2.3 Relative Significance of Spatial vs. Temporal Seismic Response Parameters

Both spatial and temporal Seismic Response Parameters provide meaningful insight into seismic responses to mining. When a seismic response is spatially distant from a blast location, or is spatially diffuse relative to itself, it is most likely triggered. Distance to Blast values (DTB), are essentially infinite, as triggered responses can occur at any significant distance from the blast location (within the mining environment). To account for this infinite boundary, DTB_N values equal one when seismic events/responses occur at any distance beyond the assumed mining-induced stress change zone - regardless of relative distance from the stress change zone. In other words, all triggered seismicity should exhibit DTB_N values of 1.

Only the temporal component is bound on both ends - from the blast time to the end of the temporal response identification window. As a seismic events within a response becomes increasingly equally spaced in time, the response is more likely to be triggered. In practice however, triggered seismicity is not usually spaced exactly equidistance in time, and consequently TAB_N values should approach 1, but will vary.

Throughout the case study presented in this work (Chapters 6 and 7), both spatial (DTB_N and DTC_N) and temporal (TAB_N and TBE_N) SRP_N's have been analyzed. Temporal parameters have consistently shown to be the more meaningful and reliable of the two parameter types. Where this knowledge is most useful, is in interpreting complex seismic responses to mining. Because a complex seismic response occurs within the assumed mining-induced stress change zone, spatial parameters may not discriminate well between induced and complex seismicity.

Figure 161 depicts the cumulative distributions of median Spatial SRR (DTB_N + DTC_N) and Temporal SRR (TAB_N + TBE_N) values for all seismic responses considered in the LaRonde mine case study (Chapters 6 and 7). The Spatial SRR values (a) of the Induced: Development, Complex: Induced and Complex: Triggered response populations are overlapped such that there is virtually no distinguishable difference. Comparatively, the Temporal SRR values (b), exhibit strong offsets between all types of seismic responses. It is primarily though analyzing temporal parameters, and SRR values inclusive of temporal parameters, that distinctions can be made between induced and complex seismic responses to mining.

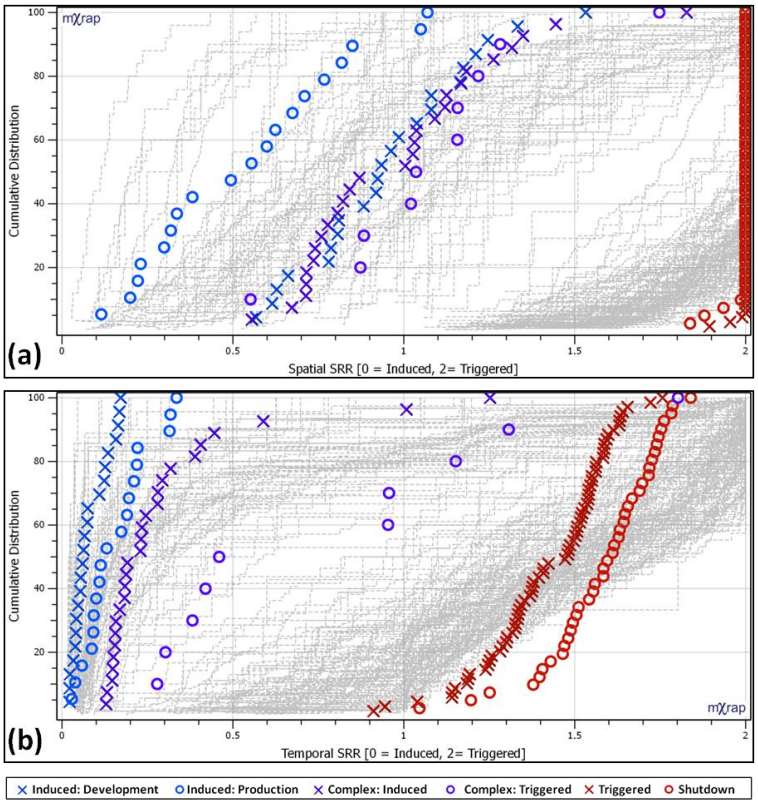

Figure 161: Cumulative distributions of (a) Spatial SRR (DTB_N + DTC_N) and (b)Temporal SRR (TAB_N + TBE_N) values for all seismic responses considered in the LaRonde mine case study.

8.3 SRR vs. Traditional Seismic Analysis

Traditional seismic analysis typically focuses on seismic populations comprised of many discrete seismic responses to mining. For example, a seismic population may consists of all seismic events occurring within a given rock mass volume for a month. This is very different from the analysis techniques employed in this work (e.g. SRR), which focus on relatively small seismic populations consisting of only one discrete seismic response to mining. Depending on the seismic analysis objectives, one technique may be more beneficial, or practically applicable, than the other.

8.3.1 Gutenberg-Richter Frequency-Magnitude Relation

One of the most fundamental traditional seismic analysis techniques is the Gutenberg-Richter Frequency-Magnitude relation (Gutenberg and Richter, 1944). Frequency-Magnitude relations are meant to be an indicative tool, and are somewhat dependent on the seismic monitoring system. Just as SRP_N's provide insight into source mechanism of a seismic response, the b-value or slope of a frequency-magnitude relation can serve as an indicator of source mechanism for a given seismic population. A low b-value (less than 0.8) is indicative of a fault-slip (triggered)

mechanism driving seismicity, while a high b-value (1.2 – 1.5) is indicative of a primarily volumetric and stress fracturing (induced) source mechanism (Hudyma, 2008).

Frequency-Magnitude relation charts, for each of the response type seismic populations examined in the LaRonde mine case study (Chapter 7), are shown in Figure 162. As a general rule, the larger a seismic population is, the more reliably frequency-magnitude relations can be applied (Hudyma, 2008). In order to generate populations of sufficient size, all same type seismic events are grouped together. The resulting linear relations are generally poor and significantly deviate from the true quantities of events. The b-values are unrepresentative and 'a/b' values are frequently exceeded by Mmax (largest magnitude event). Seismic analysis of this type would suggest poorly behaved seismic populations, and is unlikely to lead to meaningful conclusions. However, these same seismic responses to mining have been used throughout the LaRonde mine case study presented in this thesis to draw meaningful conclusions regarding seismic classification, and consequently, seismic source mechanism and seismic hazard. This is significant, as it further suggests there is inherent value in analyzing the space-time relation of seismic responses to mining, in reference to discrete mine blasts, using SRP_N's and SRR.

It is expected that the induced seismic response populations, shown in Figure 162 as parts (a) and (b), exhibit b-values greater than one. This is true for the Induced: Production population, but not for the Induced: Development population. With a b-value of 0.94, the Induced: Development population exhibits the lowest b-value of all the seismic response groups. It is expected that the triggered, shutdown and complex seismic response groups, shown in Figure 162 as parts (e), (f), and (c)/(d), respectively, exhibit b-values less than one. This is not the case, as all b-values for these seismic populations approximate one - indicating no presence of significant triggered source mechanisms in the local rock mass. It can be inferred however, from the large magnitude seismic events contained within these populations (Mmax), and the lack of blasting associated with the shutdown population, that there are triggered source mechanisms driving the occurrence of seismicity in these populations.

Beyond the b-values, 'a/b' values on a frequency-magnitude relation (commonly referred to as the largest expected event), can provide insight into seismic hazard. Generally, well-behaved seismic data is expected to exhibit an 'a/b' value greater than Mmax. The Mmax value is the magnitude of the largest seismic event contained within the seismic population. For four of the six response groups, notably one induced, both complex and one triggered, the Mmax has already exceeded the 'a/b' value. This has significant implications for seismic hazard evaluation, particularly in reference to complex seismic responses to mining.

A significant advantage of $SRP_{(N)}$'s is the ability to identify abnormal seismic responses, or the presence of triggered source mechanisms, prior to the occurrence of large and potentially damaging seismic events. If the individual responses containing large magnitude seismic events ($M_L \geq 0$) were removed from the complex seismic response groups, shown in Figure 162 as parts (c) and (d), a standard frequency-magnitude relation analysis would indicate relatively low

seismic hazard. Seismic analysis of the same responses using $SRP_{(N)}$'s however, strongly indicates the presence of a triggered source mechanism in the local rock mass and elevated seismic hazard. The significance of this is discussed in more detail in Section 8.5.

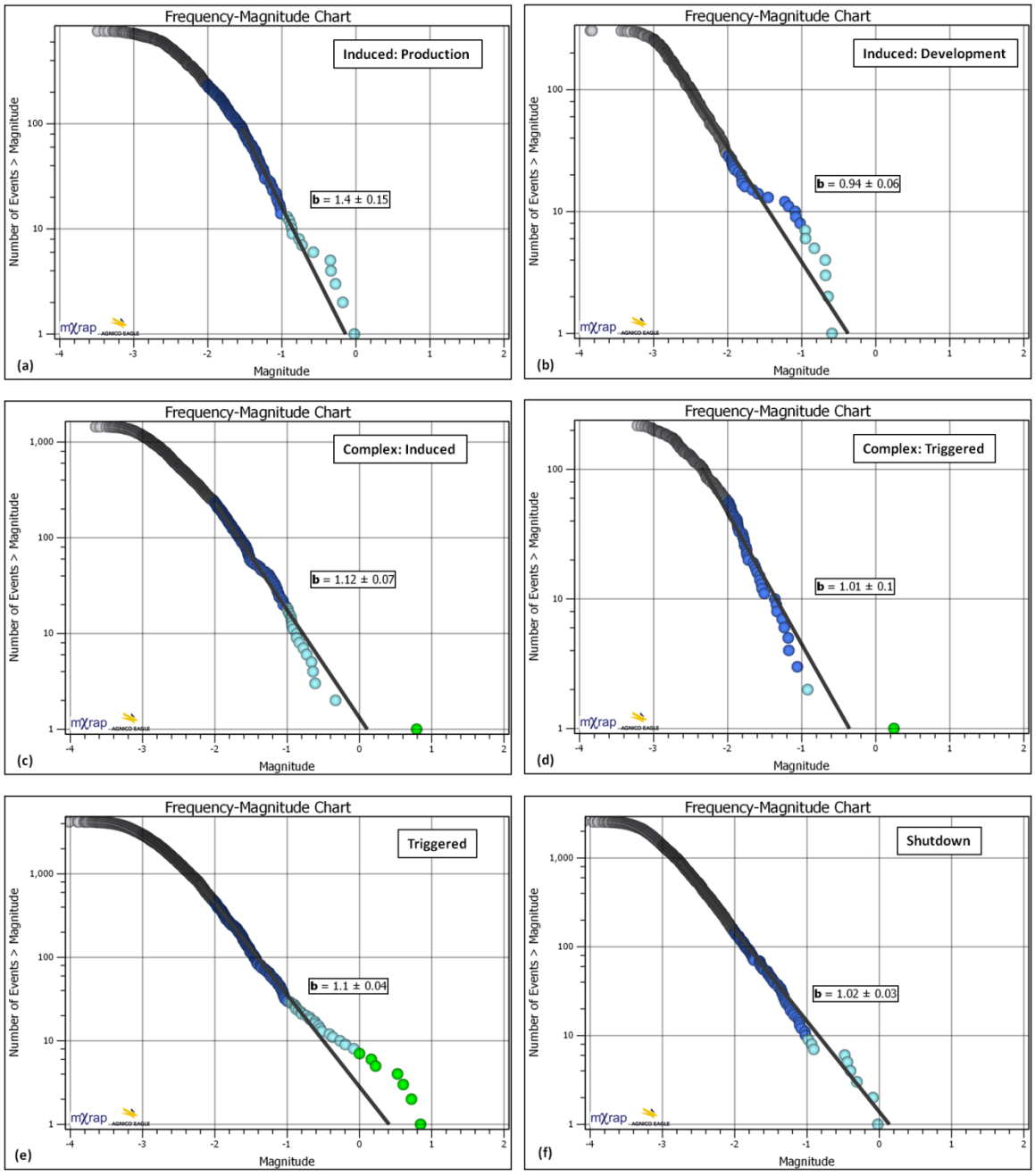

Figure 162: Gutenberg-Richter Frequency-Magnitude relations for all seismic response populations included in the LaRonde mine case study presented in Chapters 6 and 7.

As previously stated, a critical limitation of the Gutenberg-Richter Frequency-Magnitude relation analysis technique is the need for relatively large quantities of seismic events. In order to consistently draw meaningful relations and conclusions, populations often require hundreds to

thousands of individual events (Hudyma, 2008). The LaRonde mine case study, presented in Chapters 6 and 7, has demonstrated that individual seismic responses to mining, particularly induced responses, can be quite small - often less than 10 events. Seismic analysis using $SRP_{(N)}$'s enables meaningful conclusions to be drawn regarding source mechanism, and consequently seismic hazard, for very small populations of seismic events. This has significant implications for early stage and isolated mining, where extensive seismic monitoring records may not exist.

For the Frequency-Magnitude relations shown in Figure 162, there were few differentiating factors between the different types of response groups (induced, complex and triggered) - particularly in terms of b-values, which should provide the most insight into seismic source mechanism. Figure 163 depicts the relative frequency distributions of SRR for the same seismic response populations previously shown in Figure 162. Visual distinctions in the relative frequency distributions are present for the different response groups, most notably between the induced responses (a and b) and triggered responses (e and f). As expected, induced seismic responses exhibit relatively high frequencies of low SRR values, and triggered seismic responses exhibit relatively high frequencies of high SRR values. Complex seismic populations exhibit SRR values over a wide range, with increased quantities of low or high SRR values depending on if the population is predominantly induced or triggered.

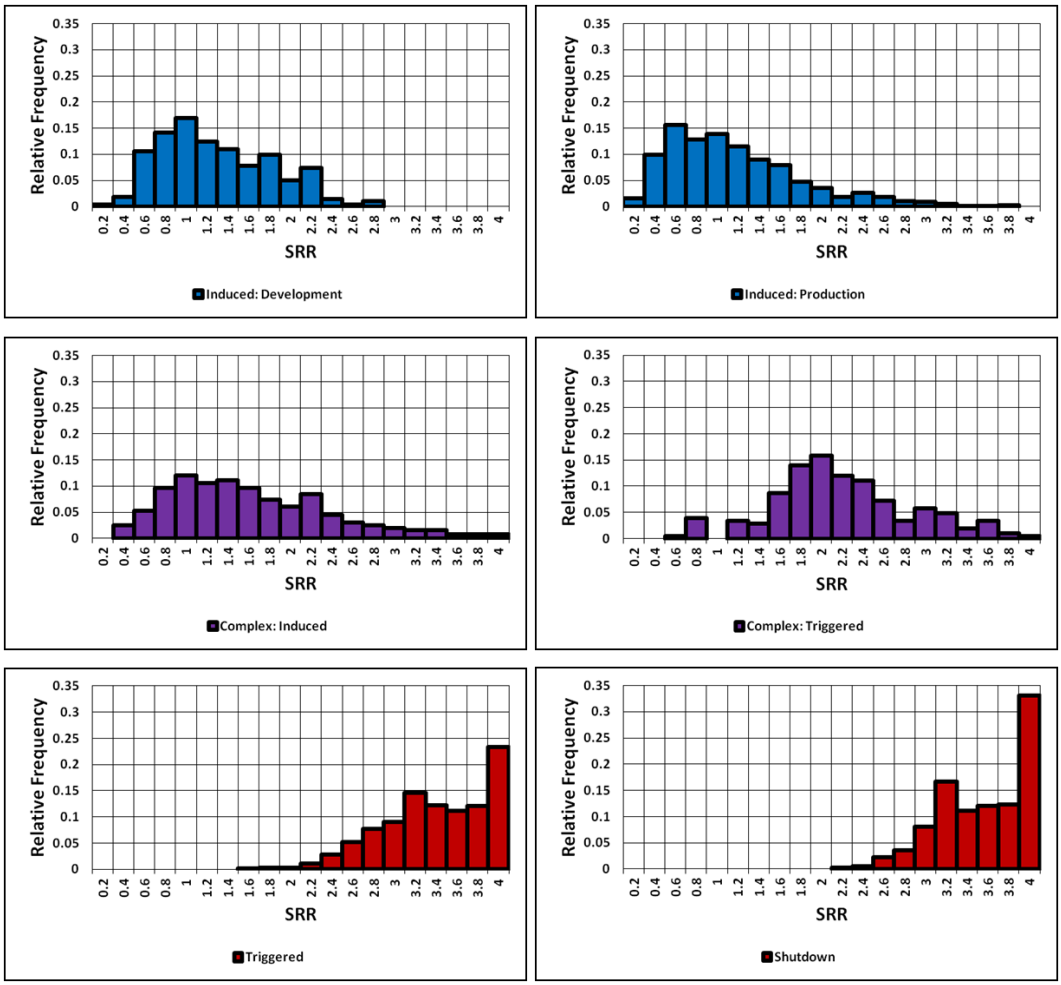

Figure 163: Relative frequency distributions of SRR for all seismic response populations previously identified and analyzed in the LaRonde mine case study (Chapters 6 and 7).

8.3.2 Seismic Source Parameters

The differences in relative frequency distributions of SRR values for varying types of seismic responses can be effectively quantified by the skewness of the distribution. Skewness describes the symmetry, or lack of symmetry, of a distribution; with normal distributions characterized by a skewness of zero. In Figure 163, induced and triggered SRR distributions exhibit characteristically different skews. Skewness is calculated as:

$$Skewness = \frac{n}{(n-1)(n-2)} \sum \left(\frac{x_i - \bar{x}}{s} \right)^3 \quad (21)$$

where,

n = Sample Size

x = Variable (e.g. SRR, Energy, Moment)

s = Sample Standard Deviation

Figure 164 depicts the cumulative distributions of SRR skewness for each individual seismic response analyzed in the LaRonde mine case study (Chapters 6 and 7). Triggered seismic responses are the most isolated, commonly exhibiting skewness values less than zero. As skewness values increase, typically to greater than zero, SRR values indicate responses are more likely to be induced. This pattern is mirrored in the relative frequency distributions for the LaRonde data SRP_N's, as was shown in Sections 7.1, 7.2 and 7.3, for induced, triggered and complex seismic responses to mining respectively. This suggests that skewness of SRP_N's and SRR values may be a good single value indicator of source mechanism - similar to how b-values are used for Frequency-Magnitude relations.

Figure 164 also depicts the skewness of the independent seismic source parameters not considered in the calculation of SRP_N's and SRR (i.e. total radiated seismic energy, average seismic moment and source size). Because all of these parameters exhibit log-normal distributions, nearly all skewness values for responses, regardless of the type of response or source mechanism, are greater than zero. The distinction of negative and positive skewness values being attributed to triggered and induced seismic responses, respectively, is unique to SRR and SRP_N's. This is significant, as a single value indicator regarding the nature of SRR distributions for seismic responses to mining, such as skewness, may be useful when interpreting seismic responses and performing seismic analysis. An example of this is provided in Section 8.5.

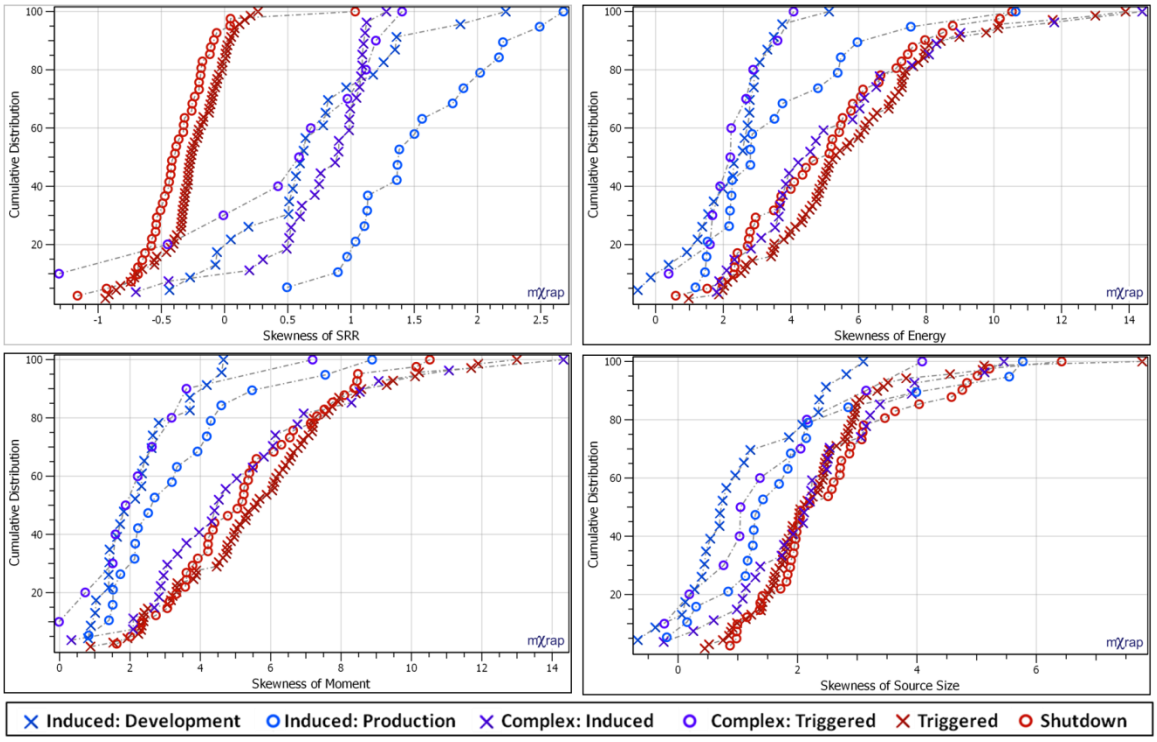

Figure 164: Cumulative distributions of skewness of SRR, Energy, Moment and Source Size for each individual seismic response considered in the LaRonde mine case study (Chapters 6 and 7).

As previously discussed, SRP_N's and SRR's focus on the independent seismic source parameters time and location. Other independent seismic source parameters however, i.e. energy, moment and size, are also traditionally examined in seismic analysis. Normalized Seismic Response Parameters have a distinct advantages over these source parameters, as they have finite bounds - from zero to one for SRP_N's and zero to four for SRR values. As such, value ranges indicative of specific types of seismic responses should be similar for varying mining environments. In other words, induced seismic responses should always exhibit SRR and SRP_N's values approaching zero, while triggered seismic responses should always exhibit SRR and SRP_N's values approaching four and one respectively. The site-specific considerations, in response identification and Seismic Response Parameter normalization, work to ensure SRP_N and SRR value ranges remain relatively constant irrespective of variations in individual mining environments.

Figure 165 depicts the cumulative distributions of SRR, Energy, Moment and Source Size for all events contained within the seismic responses previously identified in the LaRonde mine case study (Chapters 6 and 7). Strong offsets are visible in the SRR distributions, with similar response types located adjacent to one another. In other words, as SRR values increase, the distributions change from induced, to complex, to triggered. While SRR values range from zero to four, the ranges for energy, moment and source size are exponentially larger - spanning many orders of magnitude.

Unlike $SRP_{(N)}$'s, seismic source parameters describe the rock mass conditions at the time of failure and not necessarily the causative source mechanism. As a result, adjacent distributions, indicating similar parameter values, do not necessarily represents the same type of response (i.e. source mechanism), but instead the same relative rock mass conditions. For the seismic source parameter distributions shown in Figure 165, particularly energy and moment, two groupings are evident: Group 1 (Induced: Development, Complex: Induced and Shutdown), and Group 2 (Induced: Production and Complex: Triggered). As these groups do not represent similar source mechanisms, but instead rock mass conditions, it is expected that seismic events in the same group be found in relatively close spatial proximity.

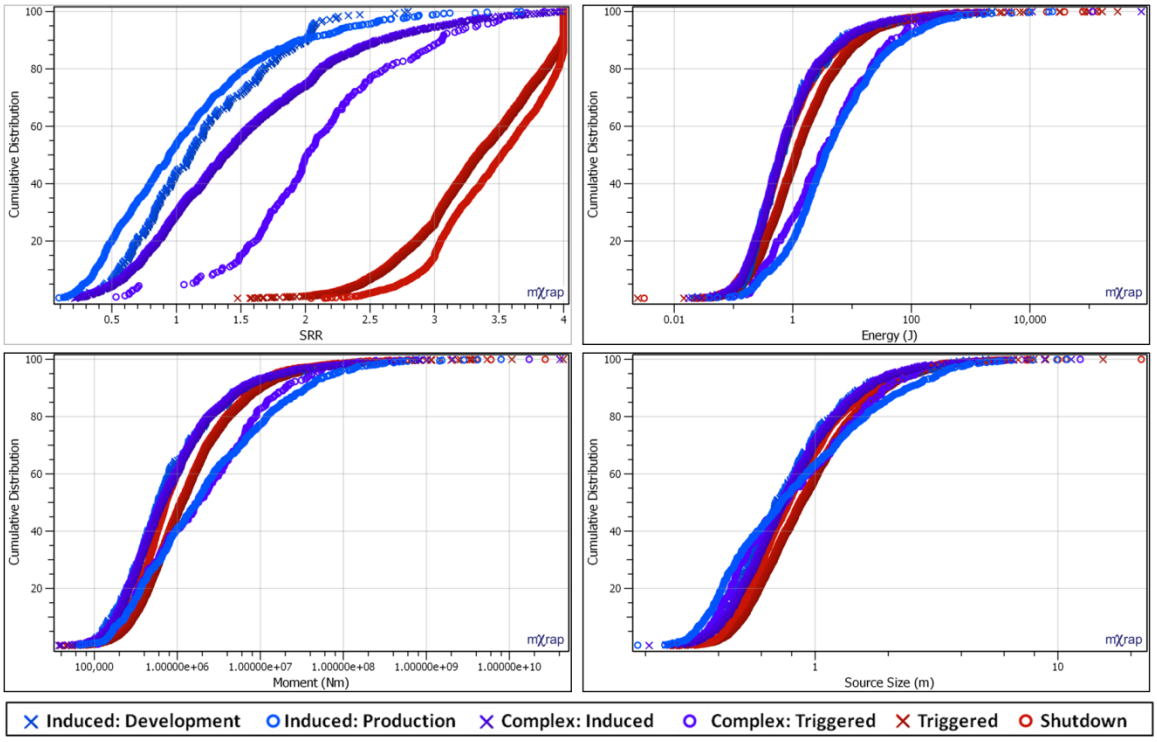

Figure 165: Cumulative distributions of SRR, Energy, Moment and Source Size for each individual seismic event considered in the LaRonde mine case study (Chapters 6 and 7).

Figure 166 depicts the response centroid locations for the events represented in Figure 165. As expected, centroids for responses exhibiting similar seismic source parameter distributions overlap in space. In (a), the centroids for Group 1 (Induced: Development, Complex: Induced and Shutdown) are shown. There is considerable overlap of the response centroids, particularly for the Induced: Development and Complex: Induced responses. In (b), the centroids for Group 2 (Induced: Production and Complex: Triggered) are shown. There is considerable overlap of the response centroids, particularly for secondary stope production blasts in the upper levels. These observations further support that SRR and $SRP_{(N)}$'s have a distinct advantage over traditional seismic source parameters in determining the nature of seismic responses to mining, and consequently, the types of source mechanisms driving rock mass failure.

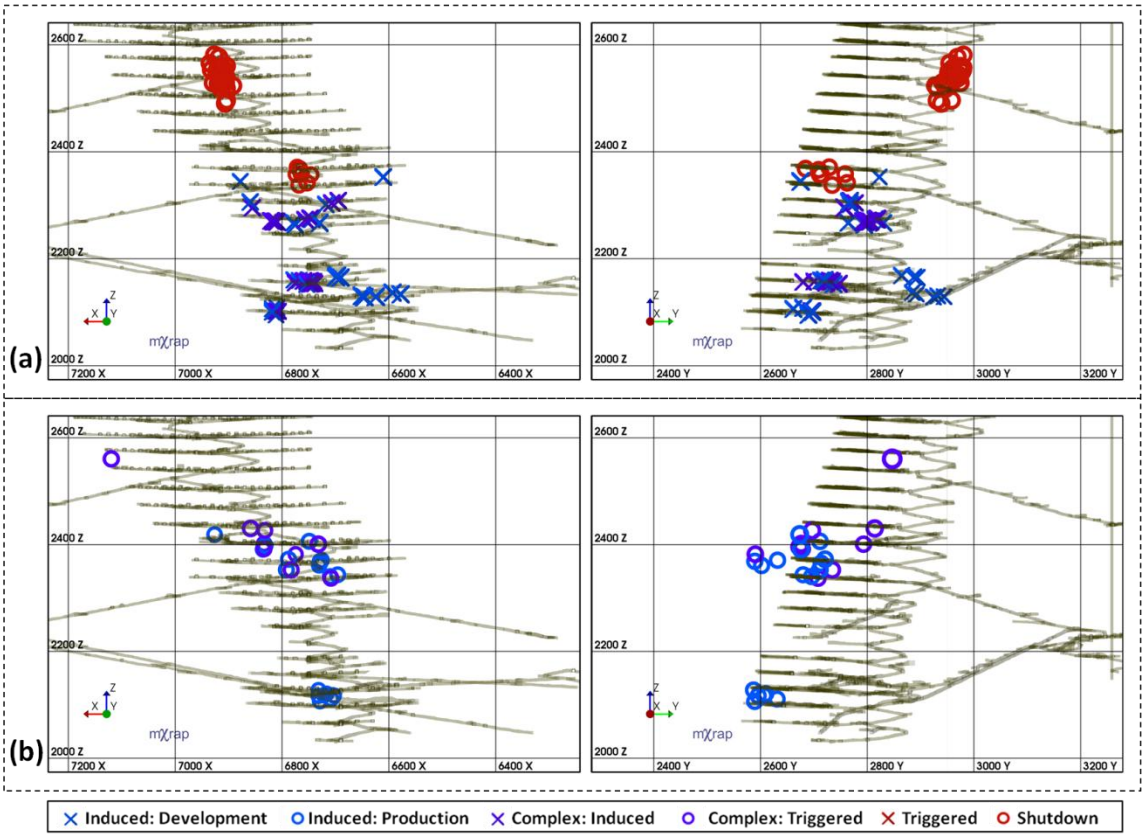

Figure 166: Longitudinal and cross-sectional projections of LaRonde mine showing the seismic response centroid locations for two groups: (a) Group 1 [Induced: Development, Complex: Induced and Shutdown], and (b) Group 2 [Induced: Production and Complex: Triggered].

8.4 Relation Between Triggered Seismicity and Background Seismicity

Previous work, completed by Mollison *et al.* (2003), reviewed seismic activity surrounding known sources before and during a care and maintenance period in an Australian mine. The authors conclude that the frequency of seismic events decreased at varying rates for different known source mechanisms following the cessation of mining activities and onset of the shutdown. Most notably, it was found that for some seismic populations, the energy release of seismic events increased during the shutdown. Possible reasons for this, as stated by the authors, include traditional triggered source mechanisms: natural tectonic movements and regional transfers of stress.

The time period for the case study included in this work, presented in Chapters 6 and 7, was selected to optimize the use of a mine shutdown period in July of 2014. Seismic responses to mining were quantified, using $SRP_{(N)}$'s, directly prior to the shutdown and throughout the shutdown. The results of this analysis indicate that seismic responses during the shutdown exhibit the same fundamental characteristics (in space and time), as triggered seismic responses during regular mining activities. This conclusion, further supported by the work of Mollison *et al.* (2003), has significant implications for the concept of background seismicity in mines.

Seismicity that is not directly induced by mine blasting is colloquially referred to as background seismicity. This type of seismicity is often considered of little consequence to mining operations, as common re-entry protocols aim for seismic rates to return to background prior to workforce re-entry (Vallejos and McKinnon, 2010). Kranz and Estey (1996), discuss how background seismicity is superimposed on seismic events directly resulting from active mining, and attempt to quantify a true rate of background seismicity in the absence of mine blasting - similar to the use of shutdown responses in the LaRonde mine case study of this work.

Throughout this thesis, no distinction is made between background and triggered seismicity. In simple terms, this work considers only two broad categories for seismic source mechanisms, induced and triggered. There is no tertiary category of 'background', which is a term with no associated source mechanism. Historically, background seismicity is primarily distinguished from triggered seismicity based solely on size (magnitude). Consequently, a seismic event remote from mine blasting is considered triggered only if it is of sufficient size, otherwise it is considered background. This distinction is made irrespective of the fact that both triggered and background seismicity have the same space/time characteristics relative to mine blasting - as was demonstrated in the LaRonde mine case study. In conclusion, this work strongly suggests that background seismicity is synonymous with triggered seismicity.

8.5 Complex Seismic Responses to Mining and Seismic Hazard Evaluation

Progression from qualitative to quantitative evaluation of seismic responses is critical to effective seismic hazard analysis in mines (Woodward, 2015). Seismic hazard refers to the likelihood of occurrence of a seismic event of a certain size. Elevated seismic hazard typically refers to an increased likelihood of occurrence of seismic events with the potential to generate visible rock mass damage (i.e. rockbursting). Events of this size radiate energy that is typically disproportionate to the energy expected from mine blasting - indicative of triggered seismicity. As previously discussed, while large seismic events are a strong indicator of triggered seismicity, any size seismic event occurring beyond the mining-induced stress change zone of mine blasting may represent a disproportionate energy release.

The ability to identify source mechanisms capable of producing rockbursts, prior to the occurrence of large and potentially damaging seismic events, is of significant value to mining operations. Because both small and large triggered seismic events exhibit the same space/time characteristics, as quantified by $SRP_{(N)}$'s, seismic analysis employing SRR and SRP_N's can potentially identify triggered source mechanisms prior to the occurrence of large events and rockbursts.

To demonstrate this concept, a relatively isolated area of LaRonde mine will be used, as shown in Figure 167. This area extends out to the west of the main LaRonde orebody, and is located in excess of 200 metres from any mine production blasting. As mining progresses to the west

(negative 'x' direction), the nature of the seismic response appears to change in both the quantity and size of seismic events. From Figure 167, it is evident that a distinct change in seismicity occurs between 6,400x and 6,350x. Beyond this point, as 'x' decreases, the mine blasts become increasingly obscured by the dense cluster of local seismic events.

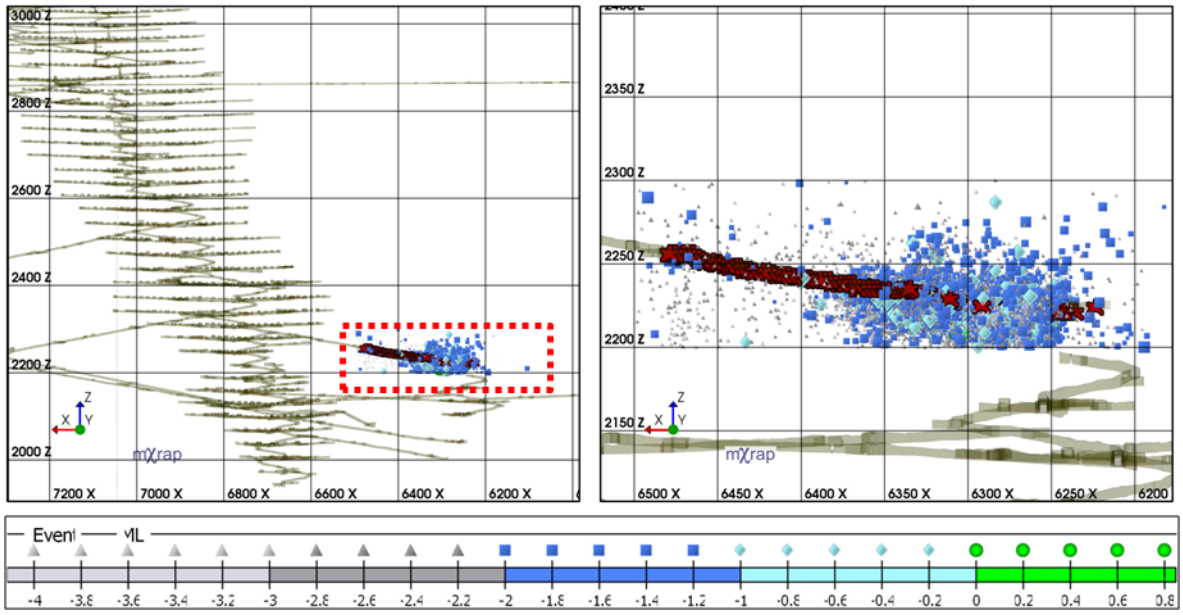

Figure 167: Longitudinal projection of LaRonde mine highlighting an area of interest. Development blasts (red stars) and seismic events occurring between 01/01/2015 and 01/01/2017 are shown.

Local magnitude zero events are considered large and potentially damaging for LaRonde mine. Figure 168 depicts only the large seismic events for the seismic population shown in Figure 167. Over the course of two years, six large magnitude seismic events occur in the area shown. With only local development blasting injecting energy into the rock mass, and significant isolation from the other areas of LaRonde mine, the size of these events is disproportionate to the development mine blasting, and indicative of triggered seismicity.

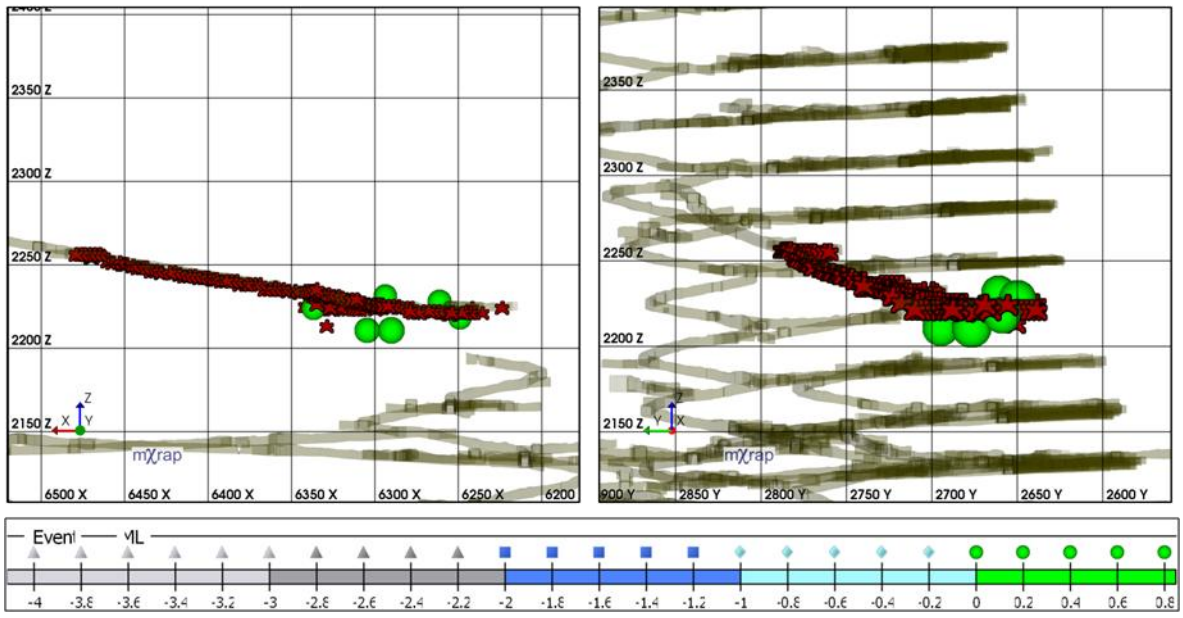

Figure 168: Longitudinal and cross-sectional projections of an area of interest at LaRonde mine. Development blasts (red stars) and large magnitude seismic events occurring between 01/01/2015 and 01/01/2017 are shown.

The same trend of a significant change in seismic response as 'x' decreases beyond 6,350x is observed for both the small magnitude events (Figure 167) and the large magnitude events (Figure 168). This suggests that any triggered source mechanisms, and consequently areas of elevated seismic hazard, are isolated to the rock mass west of 6,350x. These variations in seismic hazard should be reflected in the analysis of discrete seismic responses to mining over time. In other words, $SRP_{(N)}$'s of development blast responses prior to the occurrence of large magnitude seismic events should indicate the presence of triggered source mechanisms in the local rock mass.

Figure 169 is a Magnitude-Time History chart for the seismic events previously shown in Figure 167. Elements of both induced and triggered seismicity are evident, indicating an overall complex seismic response to development blasting (shown along the x-axis as red stars). This is most evident for periods of decreased local blasting, such as August 2015 and December 2016. During these time periods, no local blasting occurs to induce a seismic response, however seismic events continue to occur within the local rock mass. This failure is unlikely to be driven by local and discrete mining-induced stress changes, but rather local triggered source mechanisms.

In early 2015, when mine blasting is isolated to the east of 6,350x, there are relatively few seismic events, and no large seismic events. The month of March (2015) will be examined in more detail to further exemplify this, and is highlighted by a red rectangle in Figure 169. It is expected that seismic responses to mining in March 2015 will be induced.

In approximately July (2015), mine blasting progresses west of 6,350x. At this time, an increase in the quantity of seismic events, specifically events $M_L \geq -1$, is evident. Although no large

magnitude seismic events occur at this time, there is a distinct change in the nature of the seismic response. The month of July (2015) will be examined in more detail to further exemplify this and is highlighted by a red rectangle in Figure 169. It is expected that seismic responses to mining in July 2015 will be complex.

One year later, in July 2016, the seismic responses begin to exhibit large and potentially damaging seismic events ($M_L \geq 0$). The month of July (2016) will be examined in more detail to further exemplify this, and is highlighted by a red rectangle in Figure 169. It is expected that seismic responses to mining in July 2016 will be complex with a significant triggered component.

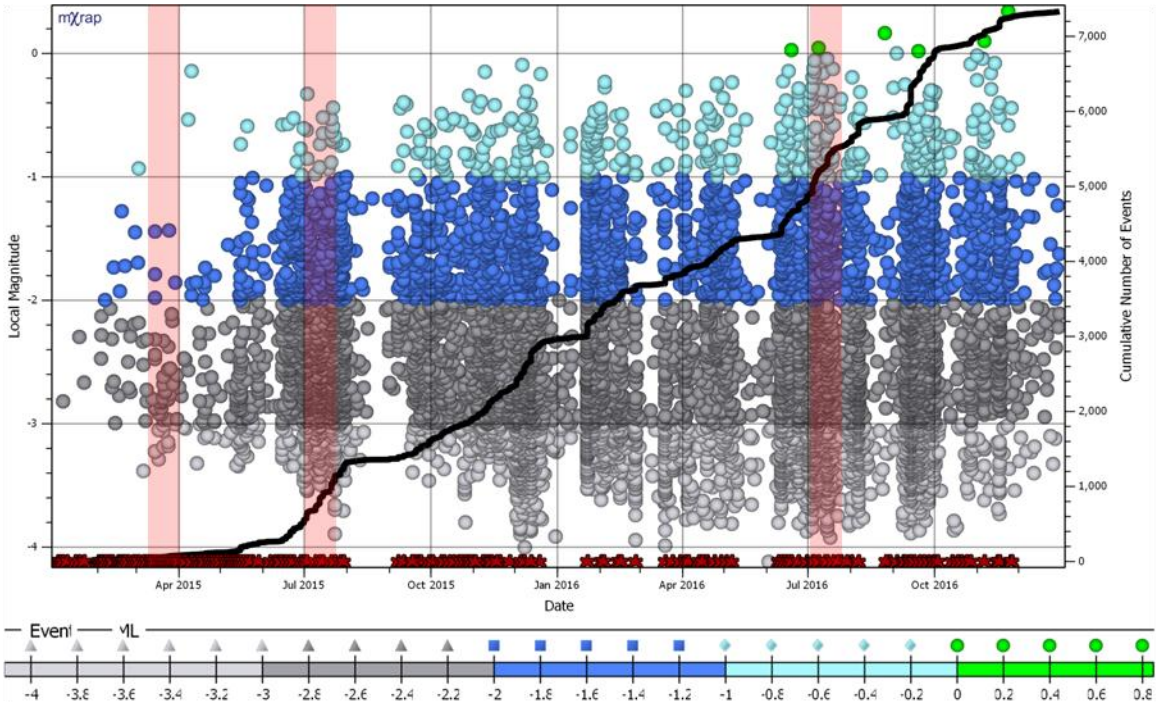

Figure 169: Magnitude-Time History chart for seismic data shown in Figure 167. Local mine development blasts are represented along the x-axis as red stars.

8.5.1 Evaluating Seismic Hazard using SRP_N's and SRR

Individual seismic responses are identified using the same single-link clustering methodology described in the LaRonde mine case study (Chapters 6 and 7). The d-value used in response identification is 50 metres - to account for higher event location errors associated with the reduced seismic array coverage in this isolated area of the mine. All response identification parameters are summarized in Table 43.

Table 43: Summary of parameters used to identify all seismic responses to mining at LaRonde and the common factors used in SRP and SRP_N calculation.

		Development Mining Response
Response Identification	**Single-Link Clustering d-value**	50 metres
	Temporal Window	Variable (Hours to Subsequent Blast)
	Time Period	03/2015; 07/2015; 07/2016
SRP/SRP_N Calculation	**Excavation Radius**	2.5 metres
	Location Error Factor	10 metres
	Potential Mining-Induced Stress Change Zone	22.5 metres from Excavation Boundary

Individual mine blast locations, and the associated seismic events are shown in parts (a) and (b) of Figure 170, respectively. As previously described, seismic responses to blasts in March 2015 are spatially isolated to the rock mass area east of 3,650x. Mine blasts in July 2015 and July 2016 are located to the west of 3,650x. It is this area of the rock mass that subsequently experiences large and disproportionate seismic events, and consequently is expected to contain triggered source mechanisms.

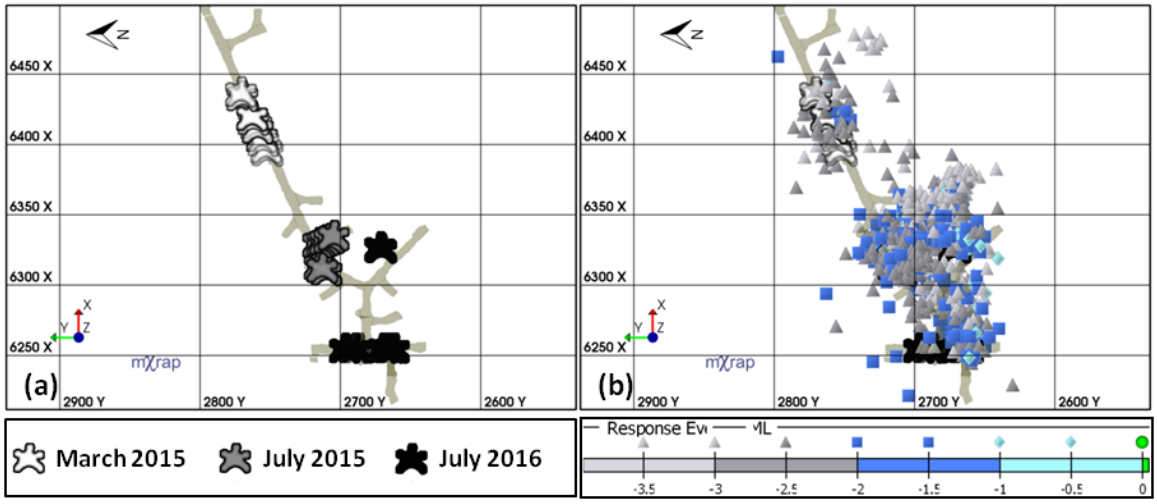

Figure 170: Plan views of mine blast locations (a) and associated seismic events (b) for the three time periods previously highlighted in Figure 169.

Figure 171 depicts the relative frequency distributions of SRR for each of the seismic response populations identified: March 2015 (a), July 2015 (b) and July 2016 (c). Part (d) indicates the measures of skewness for each of the three distributions shown. As previously discussed in Section 8.3.2, increasing skewness values indicate an increased likelihood of induced seismicity, while decreasing values, particularly negative values, indicate triggered seismicity. As expected, skewness values significantly decrease over time. A distinct change is evident from response population (a) to (b). It is this change in SRR, and skewness of the SRR distribution, that indicates the presence of triggered source mechanisms in the local rock mass, and elevated seismic hazard, prior to the occurrence of large events. The final response group, occurring in

July 2016 and containing large events, is characterized by a negative skewness value and is strongly indicative of triggered seismic source mechanisms.

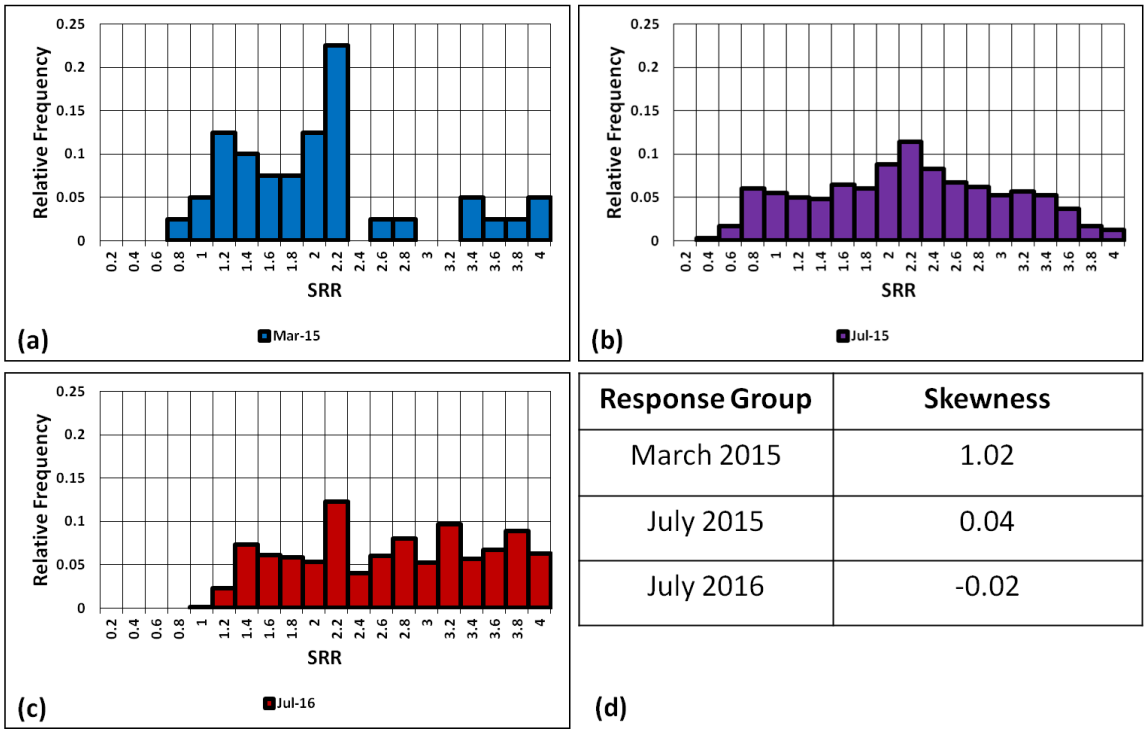

Response Group	Skewness
March 2015	1.02
July 2015	0.04
July 2016	-0.02

Figure 171: Relative frequency distributions of SRR for the seismic response populations in March 2015 (a), July 2015 (b) and July 2016 (c), as discussed in Figure 170. Part (d) indicates the measures of skewness for each distribution shown.

As previously discussed in Section 8.2.3, relative to spatial parameters, temporal parameters can be a more reliable indicator of the type of seismic response. Figure 172 depicts plan views of the individual seismic events used to identify the seismic response populations shown in Figure 171. Events are coloured according to SRR, and are successively shown for SRR value ranges: (a) $0 \leq SRR \leq 1$, (b) $0 \leq SRR \leq 2$, (c) $0 \leq SRR \leq 3$ and (d) $0 \leq SRR \leq 4$. In Figure 172, a strong relation is evident between increasing SRR values, and increasing distances from mine excavations and blast locations.

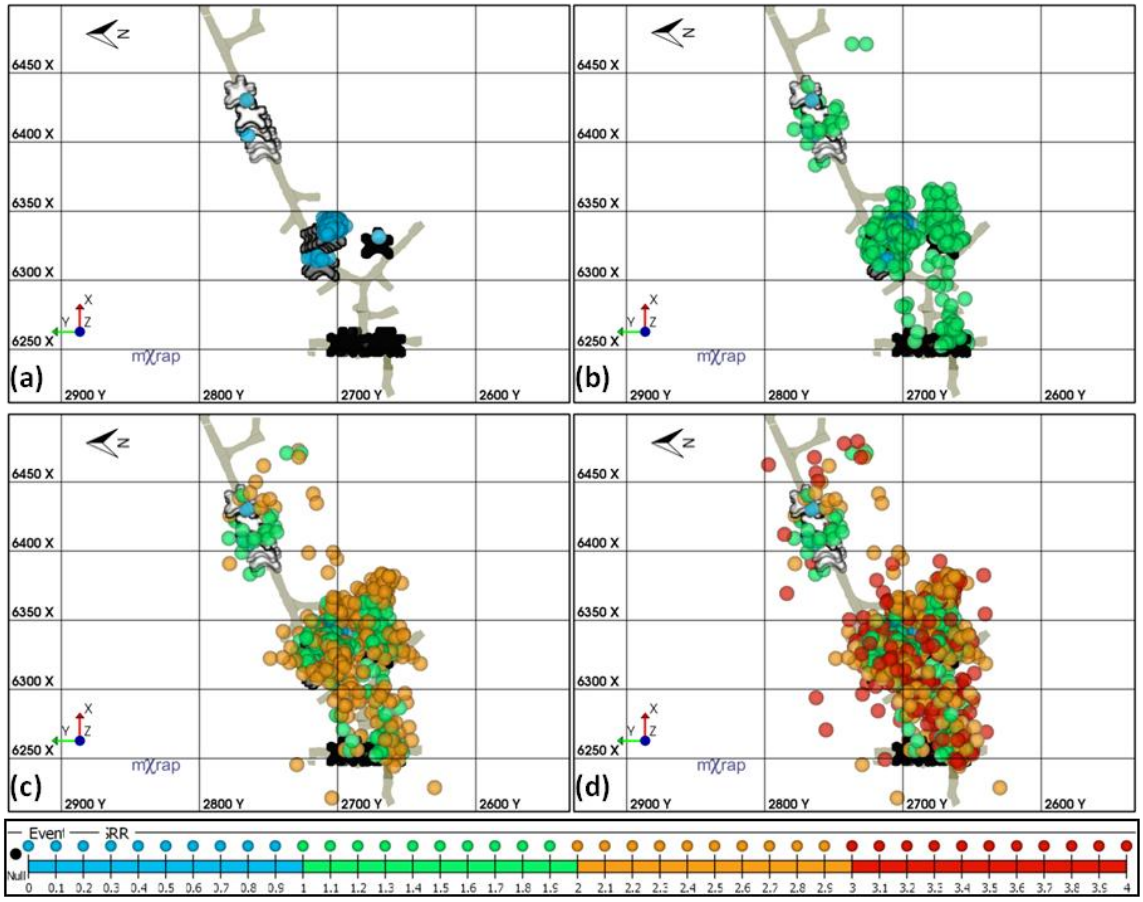

Figure 172: Plan views of an area of interest at LaRonde mine showing seismic response events coloured according to SRR. Mine blasts are shown as stars coloured to varying time periods consistent with Figure 170. Each subsequent plan view, (a) to (d), shows cumulative plots of SRR values from one to four.

Figure 173 further demonstrates the relative advantage of temporal to spatial SRP_N's. In part (a), the cumulative distributions of regular SRR values are shown for each of the seismic response populations. The individual populations align as expected, with relatively small to large SRR values being exhibited by the March 2015 to July 2016 populations respectively. The degree of separation between the populations is even more pronounced in part (b) however, where only temporal parameters (TAB_N and TBE_N) are summed in the calculation of SRR. Complete distributions for all Normalized Seismic Response Parameters can be found in Appendix H.

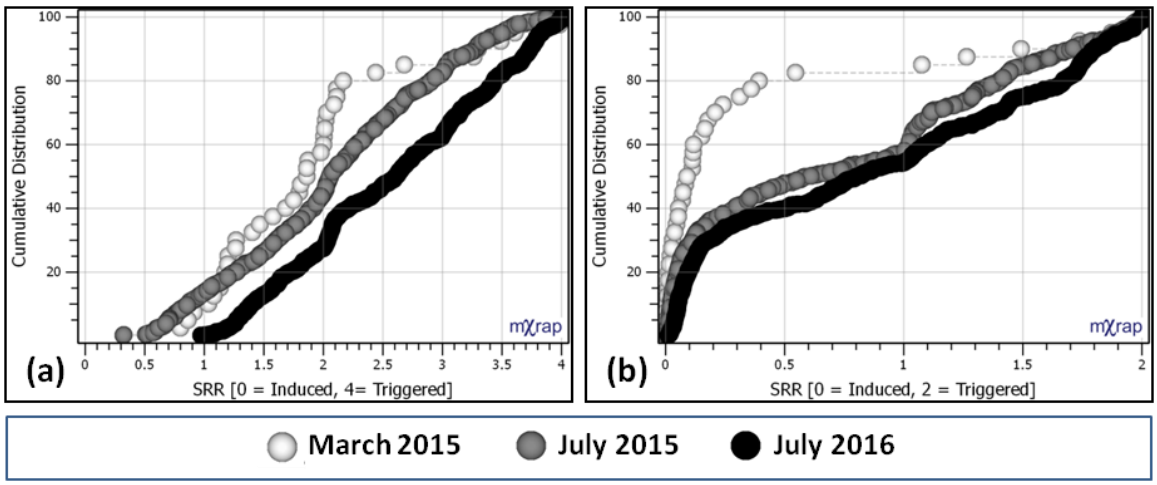

Figure 173: Cumulative distributions of SRR (a) and temporal SRR (b) for the three seismic response groups shown in Figure 171.

The conceptualization of complex seismic responses to mining from this work, and their implications surrounding triggered source mechanisms, is significant. For the example shown, active monitoring of the individual seismic responses to development mining indicate the presence of triggered source mechanisms, and elevated seismic hazard, well in advance of the occurrence of large and potentially damaging seismic events. Regular monitoring of seismic responses to development mining using SRP_N's has considerable potential and is the most significant contribution of this work to the field of mine seismicity.

Chapter 9

9 Conclusions

There are three classifications of seismic responses to mining discussed in this thesis:

- Induced: close spatial and temporal proximity to mine blasting.
- Complex: close spatial proximity and both close and remote temporal proximity to mine blasting. Contains both induced and triggered seismicity.
- Triggered: remote spatial and temporal proximity to mine blasting.

A means of differentiating between classifications of seismic responses to mining is desirable, as it may lead to meaningful insight surrounding seismic source mechanism, and consequently seismic hazard, in mining environments. Of particular concern to mining operations are triggered source mechanisms, with the potential to generate large magnitude seismic events at times independent of mine blasting. $SRP_{(N)}$'s, as presented in this work, quantify the space-time characteristics of seismic responses to mining, facilitating response interpretation and classification. A comprehensive case study from Agnico Eagle's LaRonde mine of induced, complex and triggered seismic responses to mining strongly supports the response parameters and observation guidelines proposed in this work. Within this thesis, an example from LaRonde mine demonstrates how variations in Seismic Response Rating may be used to indicate the potential of triggered source mechanisms in a mine prior to the occurrence of large and potentially damaging seismic events.

9.1 Contributions of this Thesis

The primary contributions of this thesis are explicitly stated in this section, followed by a discussion of the significance of these contributions to the broad field of mine seismicity.

9.1.1 Characterization of Complex Seismic Responses to Mining

Seismic responses to mining are typically discussed in terms of induced and triggered seismicity. This work further defines these types of responses, particularly the space-time relation between discrete seismic responses and mine blasting, along with introducing a novel concept of complex seismicity.

> A complex seismic response to mining, as characterized by this work, is defined as spatially occurring within the assumed mining-induced stress change zone of a discrete mine blast. Temporally, complex responses contain both events in close temporal

proximity to mine blasting, and events occurring throughout the response identification time window. Complex seismicity is indicative of mixed seismic source mechanisms, and commonly includes significant triggered mechanisms with the potential to produce large and possibly damaging seismic events. This possibility of disproportionate energy release is associated with moderate to high seismic hazard.

9.1.2 Seismic Response Parameters ($SRP_{(N)}$'s)

Four novel Seismic Response Parameters, and Normalized Seismic Response Parameters, constitute the bulk of this thesis. Seismic Response Parameters are a means of quantitatively describing seismic responses to mining. Normalized Seismic Response Parameters are a means of quantitatively assessing if a seismic event/response is more likely to be induced, complex, or triggered. More details regarding individual $SRP_{(N)}$'s are provided in the subsequent sections.

9.1.2.1 Distance to Blast (DTB and DTB_N)

The Distance to Blast parameter (DTB), quantitatively describes the spatial relation between mine blasting and seismic events/responses in mines. In this thesis, the DTB values from the LaRonde mine case study varied from zero metres to over 700 metres.

The Normalized Distant to Blast parameter (DTB_N), is an indicative measure of how likely a seismic event/response is to be induced or triggered by a discrete mine blast. The theoretical bounds of DTB_N are zero to one. A DTB_N value of zero to one indicates the seismic event/response occurs within the assumed mining induced stress zone, and is likely induced or possibly complex. A DTB_N value of one indicates the seismic event/response occurs beyond the assumed mining induced stress zone, and is likely triggered.

9.1.2.2 Time After Blast (TAB and TAB_N)

The Time After Blast parameter (TAB), quantitatively describes the temporal relation between blasting and seismic events/responses in mines. In this thesis, the TAB values from the LaRonde mine case study varied from zero hours to more than 11 hours.

The Normalized Time After Blast parameter (TAB_N), is an indicative measure of how likely a seismic event/response is to be induced or triggered by a discrete mine blast. The theoretical bounds of TAB_N are zero to one. TAB_N values of zero reflect the occurrence of seismic events at the same time as the mine blast. A TAB_N value approaching zero indicates the seismic event/response is more likely induced. A TAB_N value approaching one indicates the seismic event/response is more likely triggered.

9.1.2.3 Distance to Centroid (DTC and DTC_N)

The Distance to Centroid parameter (DTC), quantitatively describes the spatial relation of individual seismic events relative to an entire seismic response. It is indicative of the spatial concentration (density) of a seismic response. In this thesis, the DTC values from the LaRonde mine case study varied from less than one metre to over 415 metres.

The Normalized Distant to Centroid parameter (DTC_N), is an indicative measure of how likely a seismic event/response is to be induced or triggered by a discrete mining-induced stress change. The theoretical bounds of DTC_N are zero to one. A DTC_N value of zero to one indicates the seismic event/response occurs within a volume equivalent to the assumed mining induced stress zone, and is likely a relatively dense induced or possibly complex seismic response. A DTC_N value of one indicates the seismic event/response occurs beyond a volume equivalent to the assumed mining induced stress zone, and is likely a relatively sparse triggered seismic response.

9.1.2.4 Time Between Events (TBE and TBE_N)

Unlike the other $SRP_{(N)}$'s, Time Between Events has previously been formally defined for seismic populations (Beneteau, 2012). The definition of the normalized parameter, TBE_N, is novel.

The Time Between Events parameter (TBE), quantitatively describes the temporal relation between a seismic event in a response and the preceding seismic event. There is no TBE value calculated for the first event occurring in a seismic population or response. In this thesis, the TBE values from the LaRonde mine case study varied from zero hours to more than 10 hours.

The Normalized Time Between Events parameter (TBE_N), is an indicative measure of how likely a seismic event/response is to be induced or triggered. The theoretical bounds of TAB_N are zero to one. A TBE_N value of zero indicates the occurrence of a seismic event at the same time as the preceding event. A TBE_N value approaching zero indicates the seismic event/response is more likely to be induced. As a TBE_N value moves towards one, it reflects a more constant rate of seismic event occurrence over time, and indicates a seismic response is more likely triggered.

9.1.2.5 SRP_N Charts

SRP_N charts are a means of visually communicating SRP_N's using a radar chart. The simultaneous communication of all four Normalized Seismic Response Parameters facilities the interpretation and comparison of seismic responses to mining. Figure 174 is a SRP_N chart for a theoretically perfect induced and theoretically perfect triggered seismic response to mining.

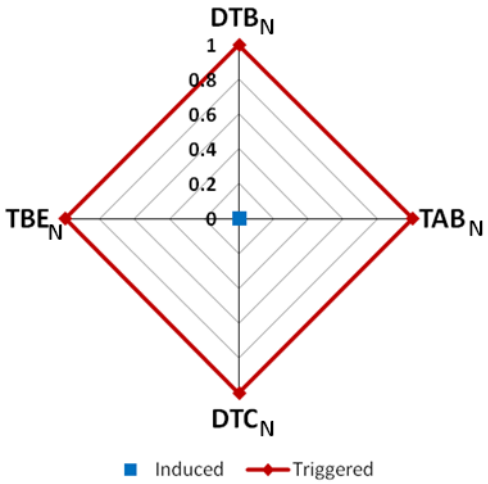

Figure 174: SRP_N chart for a theoretically perfect induced and theoretically perfect triggered seismic response to mining shown in blue and red respectively. Redrawn from Figure 48.

9.1.3 Seismic Response Rating (SRR)

Seismic response rating (SRR) is a quantitative measure of the space-time relation of a seismic response to mining. SRR is the summation of all Normalized Seismic Response Parameters for a given seismic event.

The contribution of SRR to mine seismicity is of particular significance, as it is the first quantitative means of describing the space-time characteristics of a seismic response to mining using a single numerical value. SRR is an indicative measure of how likely a seismic event or response is of being induced, complex, or triggered. The theoretical bounds of SRR are zero to four. A SRR approaching zero indicates the seismic event/response is more likely induced. A SRR value approaching four indicates the seismic event/response is more likely triggered. Middle SRR values, ranging from approximately one to three, are indicative of complex seismicity. As SRR values for complex seismic responses to mining decrease (approaching one) and increase (approaching three), they are classified as predominantly induced and triggered, respectively.

9.1.3.1 SRR Charts

SRR charts visually communicate Seismic Response Rating values through the use of stacked SRP_N bars, as shown in Figure 175. SRR values are shown along the y-axis. Individual bars on SRR charts can be used to represent entire responses or individual events contained within seismic responses.

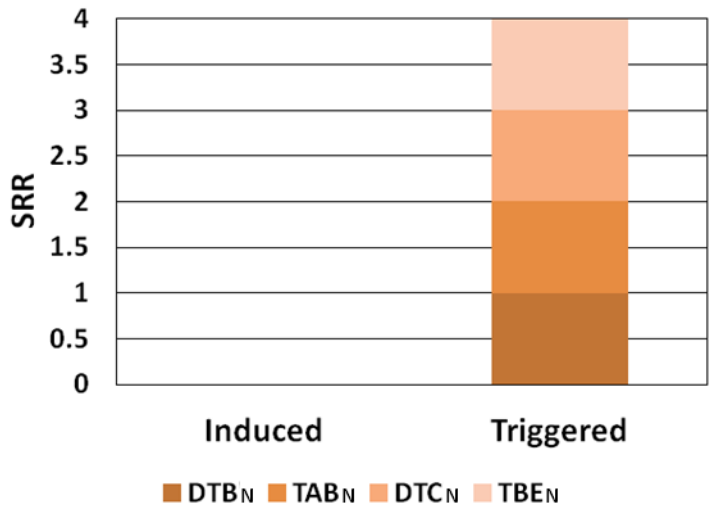

Figure 175: SRR chart for a theoretically perfect induced (SRR = 0) and a theoretically perfect triggered (SRR = 4) seismic response to mining. Colour variations correspond to individual SRP_N values used to calculate SRR. redrawn from Figure 54.

9.1.4 Discussion of Contribution Significance

While $SRP_{(N)}$'s themselves are a significant contribution of this work, this section aims to discuss the contributions of this thesis in terms of their relative significance to the broad field of mine seismicity.

The following topics are discussed:

- Ability to draw meaningful conclusions regarding seismic source mechanism, and consequently seismic hazard, from very limited quantities of seismic data.
- Introduction of normalized parameters, which promote consistent quantitative assessment of seismic responses across varying mining environments.
- Significant advancements in quantitatively relating seismic responses in mines to mine blasting.

9.1.4.1 Meaningful Conclusions from Limited Quantities of Seismic Data

The ability of $SRP_{(N)}$'s and SRR values to provide meaningful insight into seismic source mechanism from very limited quantities of seismic data was previously discussed in Section 8.3. In summary, other seismic analysis techniques which provide insight into source mechanism, such as Gutenberg-Richter Frequency-Magnitude Relations, are consistently reliable for large seismic populations (hundreds to thousands of individual events), but rarely reliable for small seismic populations (tens to hundreds of individual events). SRP analysis is unique, as both the occurrence and lack of occurrence of seismic events throughout a mining environment in space

and time are of significant value. As a result, meaningful conclusions can be formed using very small seismic populations. This was demonstrated in the LaRonde mine case study, as 26 seismic responses (mostly induced) were composed of ten seismic events or less.

9.1.4.2 Normalized Parameters

The introduction of normalized parameters for analysis of mine seismic events is novel. As previously discussed in Section 8.3, the main advantage of normalization is the potential for consistent quantitative assessment of seismic responses across varying mining environments. Seismic Response Parameters that are not normalized, (DTB, TAB, DTC and TBE), can be any numerical value, with the potential to vary significantly between mining practices and environments. Normalized parameters however, (DTB_N, TAB_N, DTC_N and TBE_N) which are used in the calculation of SRR, have clearly defined numerical limits based on the theoretical bounds defined in Chapter 4. As a result, SRR values and normalized parameter values for seismic responses to mining should be comparable across varying mining environments. This is an area of potential future work related to $SRP_{(N)}$'s.

9.1.4.3 Relating Seismic Responses to Mine Blasting

Many of the advantages attributed to $SRP_{(N)}$'s would not be possible without the underlying relations drawn between the occurrence of seismic responses and the causative activity or stimulus (mine blasting). As stated in the literature review (Chapter 2), many authors have acknowledged the significant potential in relating mine seismicity to discrete mining activities, yet this research is rarely undertaken. Within this thesis, a clear methodology has been laid out for relating individual seismic responses to discrete mine blasts. The application of this methodology to a case study of seismic data from LaRonde mine, as outlined in Chapters 6 and 7, demonstrates the value of this work, and the significant implications for source mechanism evaluation of seismic populations. This is further demonstrated by the development mining example discussed in Section 8.5.

9.2 Recommendations for Future Work

This work introduces, defines and demonstrates the application of Seismic Response Parameters for quantitatively describing seismic responses to mining. There are a number of opportunities for future work surrounding $SRP_{(N)}$'s.

9.2.1 Application of $SRP_{(N)}$'s to Varying Mining Environments

In this work, $SRP_{(N)}$'s were successfully applied to a variety of seismic response to mining at LaRonde mine - a very deep and complex mining environment. It is recommended that future work investigate the applicability of $SRP_{(N)}$'s to seismic response in other mining environments; particularly environments associated with varying degrees of seismic hazard.

9.2.2 Response Identification

There is no significant focus placed on response identification in this work, but rather the quantification of seismic responses once they have been identified. Many methodologies exist for response identification beyond the single-link clustering method employed in this work. The application of $SRP_{(N)}$'s to seismic responses identified using alternative methodologies, or the optimal development of a methodology for the specific application of $SRP_{(N)}$'s, are both potential areas of interest for future work.

9.2.3 Further Delineation of Triggered Seismic Responses to Mining

This work primarily considers triggered seismic responses that are spatially diffuse relative to themselves (as characterized by DTC). Dense spatial clusters of triggered seismicity, spatially concentrated around smaller scale triggered source mechanisms, are relatively underrepresented in this work. The application of $SRP_{(N)}$'s to these types of triggered seismic responses in mines may be an area of interest for future work.

9.2.4 Use of Mine Shutdown Data

This work demonstrated significant value in using mine shutdown data towards a better understanding of triggered and complex seismic responses to mining. Shutdown data is typically underutilized in mine seismicity. Further investigation of seismic responses to mining in the absence of mine blasting (i.e. during shutdown periods), may be an area of interest for future work.

9.2.5 Seismic Hazard Assessment Using $SRP_{(N)}$'s

As previously discussed in Section 8.5, the use of $SRP_{(N)}$'s to infer the location of triggered source mechanisms, prior to the occurrence of large and potentially damaging seismic events, is significant for seismic hazard assessment in mines. The development of methodologies to best utilize this contribution to mine seismicity is an area of interest for future work.

9.2.6 Seismic Response Analysis with Source Parameter Considerations

The research presented in this work focuses on two of the five independent seismic source parameters: time and location. Other independent parameters however, primarily radiated seismic energy and seismic moment, have historically been fundamental to seismic hazard evaluation. The investigation of Seismic Response Parameters in association with seismic source parameters, focusing on discrete seismic response hazard evaluation, may be an area of interest for future work.

References

Agnico Eagle Mines Limited (2017) LaRonde. Retrieved July 2017 from: https://www.agnicoeagle.com/English/operations-and-development-projects/operations/laronde/default.aspx

Anderson, T.W. and Darling, D.A. (1954) A test of goodness-of-fit. *Journal of the American Statistical Association*, Vol. 49, pp. 765-769.

Baig, A., Urbancic, T.I. and Bosman, K. (2017) Connecting hydraulic fracture deformation to microseismicity. *Proceedings of Seventy-Ninth EAGE Conference and Exhibition*, Paris, France, 5p.

Barton, N.R., Lien, R. and Lunde, J. (1974) Engineering classification of rock masses for the design of tunnel support. *Rock Mechanics*, Vol. 6, No. 4, pp. 189-239.

Beneteau, D.L. (2012) A study in relating time-between-event to seismic source mechanisms in hardrock mining. MASc Thesis, Laurentian University, 269 p.

Beneteau, D. and Hudyma, M. (2012) Time-between-events, a tool for understanding seismic source mechanisms in hard rock mining applications. *Proceedings of Rock Engineering and Technology for Sustainable Underground Construction*, Stockholm, Sweden, 14 p.

Bieniawski, Z.T. (1976) Rock mass classification in rock engineering. *Proceedings of Exploration for rock engineering*, (Editor: ZT Bieniawski), Cape Town: Balkema, pp. 97-106.

Bieniawski, Z.T. (1989) Engineering rock mass classifications. New York: Wiley.

Brady, B.H.G. and Brown E.T. (1985) Rock mechanics for underground mining. George Allen and Unwin Ltd, London, 527 p.

BrckaLorenz, A., Chaing, Y. and Nelson Laird, T. (2013) Internal consistency. *FSSE Psychometric Portfolio*. Retrieved June 2018 from: fsse.indiana.edu

Brown, L.G. (2015) Seismic hazard evaluation using apparent stress ratio for mining-induced seismic events. MASc Thesis, Laurentian University, 223 p.

Brown, L. and Hudyma, M. (2017) Identification of stress change within a rock mass through apparent stress of local seismic events. *Rock Mechanics and Rock Engineering*, Vol. 50, No. 1, pp. 81-88.

Brown L.G. and Hudyma M.R. (2018a) Mining induced seismicity in Canada: A 2017 Update. *Proceedings of Fifty-Second Rock Mechanics/Geomechanics Symposium,* Seattle, Washington, 8 p.

Brown L.G. and Hudyma M.R. (2018b) Observed variations in seismic response during a mine shutdown. *Proceedings of Fifty-Second Rock Mechanics/Geomechanics Symposium,* Seattle, Washington, 8 p.

Butler, A.G. (1997) Space-time clustering of potentially damaging seismic events and seismic viscosity in Western Deep Levels East and West Mines. *Proceedings of Rockbursts and Seismicity in Mines,* (Editors: S Gibowicz and S Lasocki), Krakow, pp. 89-93.

Chadwick, J. (2007) Beiminghe. *Operation Focus: International Mining Magazine,* pp. 10-11.

Clark, L.A. and Watson, D. (1995) Constructing validity: Basic issues in objective scale development. *Psychological Assessment*, Vol. 7, pp. 309-319.

Collins D.S., Toya, T., Pinnock, I., Shumila, V., and Hosseini, Z. (2014) 3D velocity model with complex geology and voids for microseismic location and mechanism. *Proceedings of the Seventh International Conference on Deep and High Stress Mining*, (Editors: M Hudyma and Y Potvin), Australian Centre for Geomechanics, Sudbury, pp. 681-688.

Cook, N.G.W. (1976) Seismicity associated with mining. *Engineering Geology,* Vol. 10, pp. 99-122.

Delgado, J. and Mercer, R. (2006) Microseismic monitoring and rockbursting activity at the Campbell mine, Ontario, Canada. *Proceedings of the Forty-First U.S. Symposium on Rock Mechanics: "50 Years of Rock Mechanics - Landmarks and Future Challenges".* Golden, Colorado. 11 p.

Disley, N.V. (2014) Seismic risk and hazard management at Kidd Mine. *Proceedings of the Seventh International Conference on Deep and High Stress Mining*, (Editors: M Hudyma and Y Potvin), Australian Centre for Geomechanics, Sudbury, pp. 107-121.

Dodge D.A. and Sprenke, K.F. (1992) Improvements in mining induced microseismic source locations at the Lucky Friday mine using an automated whole-waveform analysis system. *Pure and Applied Geophysics*, Vol. 139, No. 3/4, pp. 609-626.

Duplancic, P. (2001) Characterisation of caving mechanisms through analysis of stress and seismicity. PhD Thesis, University of Western Australia, Perth, Australia, 157 p.

Ecobichon, D., Hudyma, M. and Laplante, B. (1992) Understanding geomechanics problems through microseismic monitoring at Lac Shortt. *Proceedings of Ninety-Forth Annual General Meeting of the CIM: Rock Mechanics and Strata Control Sessions,* Montreal, 13 p.

Eremenko, V.A., Eremenko, A.A., Rasheva, S.V. and Turuntaev, S.B. (2009) Blasting and the man-made seismicity in the Tashtagol mining area. *Mining Science*, Vol. 45, No. 5, pp. 468-474.

Frohlich, C. and Davis, S.D. (1990) Single-link cluster analysis as a method to evaluate spatial and temporal properties of earthquake catalogues. *Geophysical Journal International*, Vol. 100, No. 1, pp. 19-32.

Gay, N.C. and Ortlepp, W.D. (1979) The anatomy of a mining-induced fault zone. *Bulletin of the Seismological Society of America*, Vol. 90, pp. 47-58.

Gibowicz, S.J. (1990) The mechanism of seismic events induced by mining - A review. *Proceedings of Rockbursts and Seismicity in Mines*, (Editor: C Fairhurst), Rotterdam, A.A. Balkema, pp. 3-27.

Gibowicz, S.J. and Kijko, A. (1994) An introduction to mining seismology. 1st edition. San Diego, Academic Press, 396 p.

Gibowicz, S.J. and Lasocki, S. (2001) Seismicity induced by mining: Ten years later. *Advances in Geophysics*, Vol. 44, pp. 39-181.

Gutenberg, B. and Richter, C.F. (1944) Frequency of earthquakes in California. *Bulletin of the Seismological Society of America*, Vol. 34, pp. 185-188.

Harris, R.A. (1998) Introduction to special section: Stress triggers, stress shadows, and implications for seismic hazard. *Journal of Geophysical Research*, Vol. 103, No. B10, pp. 24347-24358.

Harris, P.C. and Wesseloo J. (2015) mXrap, version 5, Australian Centre for Geomechanics, Perth, http://www.mxrap.com/

Hasegawa, H.S., Wetmiller, R.J. and Gendzwill, D.J. (1989) Induced seismicity in mines in Canada - an overview. *Pure and Applied Geophysics,* Vol. 129, pp. 432-453.

Hedley, D.G.F. (1992) Rockburst handbook for Ontario hardrock mines. CANMET Special Report SP92-1E, 305 p.

Herget, G. (1988) Stresses in rock. A.A Balkema, Rotterdam, Netherlands, 179 p.

Herget, G. (1974) Ground stress determinations in Canada. *Rock Mechanics*, Volume 6, pp. 53-64.

Hoek, E. and Brown, E.T. (1980) Underground excavations in rock. London: The Institution of Mining and Metallurgy, 527 p.

Hoek, E., Kaiser, P.K. and Bawden, W.F. (1995) Support of underground excavations in hard rock. Rotterdam, Netherlands: Balkema, 215 p.

Hudyma, M.R. (2004) Mining-induced seismicity in underground, mechanized, hardrock mines. Unpublished Report. Australian Centre for Geomechanics, Perth, 138 p.

Hudyma, M.R. (2008) Analysis and interpretation of clusters of seismic events in mines. PhD Thesis, University of Western Australia, 408 p.

Hudyma, M.R., Heal, D. and Mikula, P. (2003) Seismic monitoring in mines - old technology - new applications. *Proceedings First Australasian Ground Control in Mining Conference*, Sydney, Australia, pp. 201-218.

Hudyma, M.R., Potvin, Y., Grant, D.R., Milne, D., Brummer, R.K. and Board, M. (1994) Geomechanics of sill pillar mining. *Proceedings of the First North American Rock Mechanics Symposium*, (Editors: P.P. Nelson and S.E. Laubach), A.A. Balkema, Rotterdam, pp. 969-976.

Kaiser, P.K., McCreath, D.R. and Tannant D.D. (1996) Canadian rockburst support handbook. Geomechanics Research Centre, Laurentian University, Sudbury, 303 p.

Kijko, A. and Funk, C.W. (1996) Space-time interaction amongst clusters of mining induced seismicity. *Pure and Applied Geophysics*, Vol. 147, No. 2, pp. 277-288.

Kijko, A., Funk, C.W. and Brink, A.v.Z. (1993) Identification of anomalous patterns in time-dependent mine seismicity. *Proceedings of Rockbursts and Seismicity in Mines,* (Editor: RP Young), Rotterdam: Balkema, Kingston, Ontario, pp. 205-210.

Kgarume, T.E., Spottiswoode, S.M. and Durrheim, R.J. (2010) Deterministic properties of mine tremor aftershocks. *Proceedings of Deep and High Stress Mining*, (Editors: M Van Sint Jan and Y Potvin), Australian Centre for Geomechanics, Santiago, Chile, pp. 227-237.

Kranz, R.L. and L.H. Estey (1996) Listening to a mine relax for over a year at 10 to 1000 meter scale. *Proceedings of the Second North American Rock Mechanics Symposium,* Rotterdam, Balkema, pp. 491–498.

Kuzyk, G.W. and Martino, J.B. (2008) Development of excavation technologies at the Canadian underground research laboratory. *Proceedings of the International Conference of Underground Disposal Unit Design & Emplacement Processes for a Deep Geological Repository*, Prague, 13 p.

Lechner, V. and Weidmann, K.H. (2015) Visualizing database-performance through shape, reflecting the development opportunities of radar charts. *Proceedings of HCI International 2015 Conference*, Springer, Los Angeles.

Leslie, I. and Vezina, F. (2001) Seismic data analysis in underground mining operations using ESG's Hyperion systems, *Proceedings of the 16th Quebec Mining Association Ground Control Colloque*, Val D'Or.

McGarr, A. (1971) Violent deformation of rock near deep-level, tabular excavations - seismic events. *Bulletin of the Seismological Society of America*, Vol. 61, No. 5, pp. 1456-1466.

McGarr, A. and Simpson, D. (1997) Keynote lecture: a broad look at induced and triggered seismicity. *Proceedings of Rockbursts and Seismicity in Mines*, (Editors: SJ Gibowicz and S Lasocki), Poland, A.A. Balkema, pp. 385-396.

McGarr, A., Simpson, D. and Seeber, L. (2002) Case histories of induced and triggered seismicity. *International Handbook of Earthquake and Engineering Seismology Part A (International Geophysics)* (Editors: HK Williams, H Kanamori, PC Jennings and C Kisslinger), Academic Press, International Geophysics, Vol. 81 A, pp. 647-661.

McKinnon, S.D. (2006) Triggering of seismicity remote from active mining excavations. *Rock Mechanics and Rock Engineering*, Vol. 39, No. 3, pp. 255-279.

McMillan, J.H. and Schumacher, S. (2001) Research in education: A conceptual introduction. 5th edition. New York, Longman, 660 p.

Mendecki, A.J. (2001) Keynote address: data-driven understanding of seismic rock mass response to mining. *Proceedings of the Fifth International Symposium on Rockbursts and Seismicity in Mines*, (Editors: G van Aswegen, RJ Durrheim and WD Ortlepp), South African Institute of Mining and Metallurgy, Johannesburg, pp. 1-9.

Mendecki, A.J. and Lynch, R.A. (2004) GAP601a: Experimental and theoretical investigations of fundamental processes in mining induced fracturing and rock instability close to excavations. ISS International Limited, Johannesburg.

Mendecki, A.J., van Aswegen, G. and Mountfort, P. (1999) A guide to routine seismic monitoring in mines. *A Handbook on Rock Engineering Practices for Tabular Hard Rock Mines,* (Editors: AJ Jager and JA Ryder), Creda Communications, Cape Town, 371 p.

Mercier-Langevin, F. (2010) LaRonde Extension – mine design at three kilometres. *Proceedings of the Fifth International Conference on Deep and High Stress Mining*, (Editors: M. Van Sint Jan and Y. Potvin), Australian Centre for Geomechanics, Santiago, pp. 3-15.

Mollison, L., Sweby, G., and Potvin, Y. (2001) Changes in mine seismicity following a mine shutdown. *Proceedings First Australasian Ground Control in Mining Conference*, Sydney, pp. 187-197.

Omori, F. (1894) On after-shocks. *Seismological Journal of Japan*, Vol. 19, pp. 71-80.

Ortlecka-Sikora, B. (2010) The role of static stress transfer in mining induced seismic events occurrence, a case study of the Rudna mine in the Legnica-Glogow Copper District in Poland. *Geophysical Journal International*, Vol. 182, No. 2, pp. 1087-1095.

Ortlepp, W.D. (1997) Rock fracturing and rockbursts: an illustrated study. Monograph Series M9, South African Institute of Mining and Metallurgy, Johannesburg, 98 p.

Ouyang, Z., Li, C., Xu, W. and Li, H. (2009) Measurements of in situ stress and mining-induced stress in Beiminghe iron mine of China. *Journal of Central South University of Technology*, Vol. 16, No. 1, pp. 85-90.

Owen, M., Hudyma, M.R. and Potvin, Y. (2002) Risk Analysis of Mine Seismicity. *Proceedings of the Fifth North American Rock Mechanics Symposium, Toronto,* (Editors: R. Hammah, W.F. Bawden, J. Curran, M. Telesnicki), University of Toronto Press, pp. 1079-1086.

Plenkers, K., Kwiatek, G., Nakatani, M. and Dresen, G. (2010) Observation of seismic events with frequencies F > 25 kHz at Mponeng Deep Gold Mine, South Africa. *Seismological Research Letters*, Vol. 81, No. 3, pp. 467-479.

Potvin, Y. and Hudyma, M.R. (2001) Seismic monitoring in highly mechanised hardrock mines in Canada and Australia. *Proceedings of Rockbursts and Seismicity in Mines – RaSiM 5*, Johannesburg, (Editors: G. van Aswegen, RJ Durrheim and WD Ortlepp), Johannesburg: South African Institute of Mining and Metallurgy, pp. 267-280.

Rebuli, D.B. and Kohler, S.J. (2014) Using clustering algorithms to assist short-term seismic hazard analysis in deep South African mines. *Proceedings of the Seventh International Conference on Deep and High Stress Mining*, (Editors: M Hudyma and Y Potvin), Australian Centre for Geomechanics, Sudbury, pp. 107-121.

Richardson, E. and Jordan, T.H. (2002) Seismicity in deep gold mines of south Africa: implications for tectonic earthquakes. *Bulletin of the Seismological Society of America*, Vol. 92, pp. 1766-1782.

Richter, C.F. (1935) An instrumental earthquake magnitude scale. *Bulletin of the Seismological Society of America,* Vol. 25, pp. 1-32.

Shapiro, S.S. and Wilk, M.B. (1965) An analysis of variance test for normality. *Biometrika,* Vol. 52, pp. 591-611.

Slade, J. and Ascott, B. (2002) Impact of rockburst damage upon a narrow vein gold deposit in the Eastern Goldfields, Western Australia. *Proceedings of International Seminar on Deep and High Stress Mining*, Australian Centre for Geomechanics, Perth, Australia, 19 p.

Spottiswoode, S.M. (1989) Perspectives on seismic and rockburst research in the South African gold mining industry: 1983-1987. *Pure and Applied Geophysics*, Vol. 129, No. 3/4, pp. 673-680.

Steacy, S., Gomberg, J. and Cocco, M. (2005) Introduction to special section: stress transfer, earthquake triggering, and time-dependent seismic hazard. *Journal of Geophysical Research*, Vol. 110, B05S01.

Swan, G. and Semadeni, T. (1992) Rockbursts in a development drift: field observations. *Workshop on Induced Seismicity*, (Editor: C Ramseyer), Santa Fe, 12 p.

Turcotte, P. (2014) Practical applications of a rockburst database to ground support design at LaRonde mine. *Proceedings of the Seventh International Conference on Deep and High Stress Mining*, (Editors: M Hudyma and Y Potvin), Australian Centre for Geomechanics, Sudbury, pp. 79-92.

Urbancic, T.I., Young, R.P., Bird, S. and Bawden, W. (1992) Microseismic source parameters and their use in characterizing rock mass behaviour: considerations from Strathcona mine. *CIM Annual General Meeting*, Montreal, pp. 36-47.

Utsu, T. (1961) A statistical study of the occurrence of aftershocks. *Geophysical Magazine*, Vol. 30, No. 4, pp. 521-605.

Vallejos, J.A. and McKinnon, S.D. (2010) Omori's law applied to mining-induced seismicity and re-entry protocol development. *Pure and Applied Geophysics*, Vol. 167, No. 1-2, pp. 91-106.

Wessa, P. (2018) Chronbach alpa (v1.0.5). *Free Statistics Software (v1.2.1)*, Office for Research Development and Education, URL https://www.wessa.net/rwasp_cronbach.wasp/

Whyatt, J., Blake, W., Williams, T. and White, B. (2002) 60 years of rockbursting in the Coeur d'Alene district of Northern Idaho, USA: lessons learned and remaining issues. *Presentation at One Hundred and Ninth Annual Exhibit and Meeting, Society for Mining, Metallurgy, and Exploration*, Phoenix, Arizona, preprint 02-164, 8 p.

Woodward, K.R. (2015) Identification and delineation of mining induced seismic responses. PhD Thesis, University of Western Australia, 326 p.

Woodward K. and Wesseloo, J. (2015) Observed spatial and temporal behaviour of seismic rock mass response to blasting. *Journal of the South African Institute of Mining and Metallurgy*, Vol. 115, No. 11, pp. 1045-1056.

Woodward, K., Wesseloo, J. and Potvin, Y. (2017) The spatial and temporal assessment of clustered and time-dependent seismic responses to mining. *Proceedings of the Eighth International Conference on Deep and High Stress Mining*, (Editor: J Wesseloo), Australian Centre for Geomechanics, Perth, pp. 157-171.

Appendices

Appendix A: Summary table of observation guidelines for Normalized Seismic Response Parameters (DTB_N, TAB_N, DTC_N, and TBE_N) as they pertain to induced, complex and triggered seismic responses to mining. Stimulus commonly refers to a mine blast. Table continued on subsequent page.

	Induced	**Complex**	**Triggered**
Normalized Distance To Blast [DTB_N]	Within the assumed mining-induced stress change zone *All Events:* $DTB_N < 1$	Within the assumed mining-induced stress change zone and potentially beyond *Significant No. Events:* $DTB_N < 1$ *&* *All Events:* $0 \leq DTB_N \leq 1$	Beyond the assumed mining-induced stress change zone *All Events:* $DTB_N = 1$
Normalized Time After Blast [TAB_N]	Within the first few hours of mine blasting *Significant No. Events:* $TAB_N \approx 0$ *Typically,* $TAB_N \leq 0.2$	Significant number of events within the first few hours of mine blasting and events independent of mine blasting *Significant No. Events:* $0 \leq TAB_N \leq 0.2$ *&* *All Events:* $0 \leq TAB_N \leq 1$	Independent of mine blasting *Significant No. Events:* $TAB_N \geq 0.5$ *&* *All Events:* $0 \leq TAB_N \leq 1$
Normalized Distance To Centroid [DTC_N]	Within a volume equivalent to the assumed mining-induced stress change zone *All Events:* $DTC_N < 1$	Within a volume equivalent to the assumed mining-induced stress change zone and potentially beyond *Significant No. Events:* $DTC_N < 1$ *&* *All Events:* $0 \leq DTC_N \leq 1$	Approaching and beyond a volume equivalent to the assumed mining-induced stress change zone *Significant No. Events:* $DTC_N = 1$ *&* *All Events:* $0 \leq DTC_N \leq 1$

	Induced	**Complex**	**Triggered**
Normalized Time Between Events [TBE_N]	Temporally close together (typically within seconds to minutes) *Significant No. Events:* $TBE_N \approx 0$ *Typically,* $TBE_N \leq 0.2$	Significant number of events temporally close together and events over time *Significant No. Events:* $0 \leq TBE_N \leq 0.2$ *&* *All Events:* $0 \leq TBE_N \leq 1$	Relatively constant rate of events over time *Significant No. Events:* $TBE_N \geq 0.5$ & *All Events:* $0 \leq TBE_N \leq 1$

Appendix B: SRR charts for all production blast induced seismic responses to mining considered in the LaRonde Case Study.

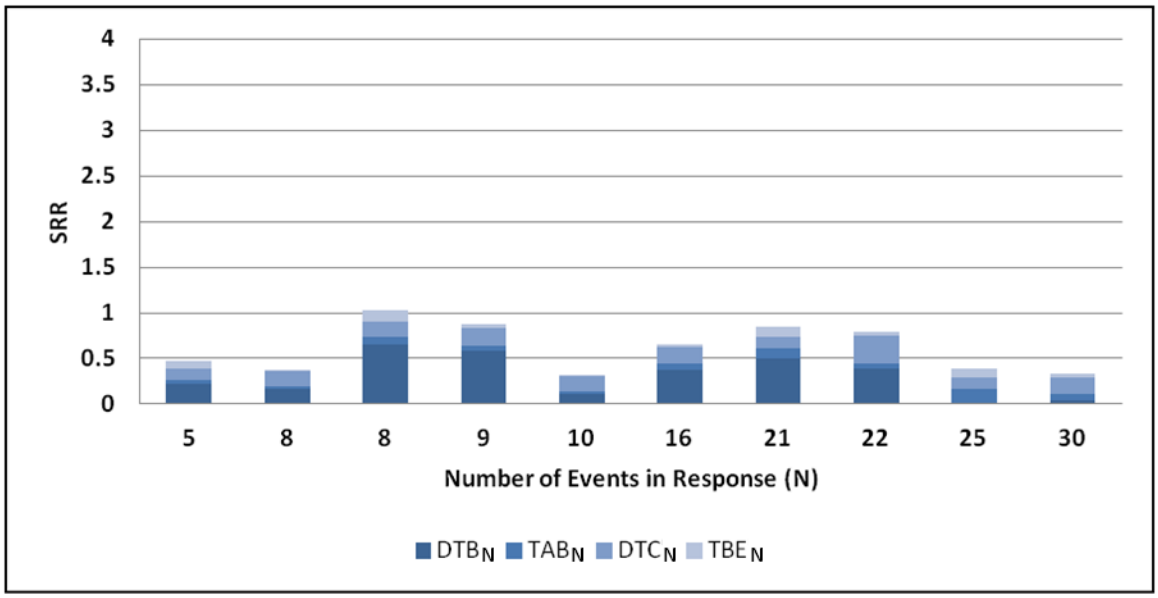

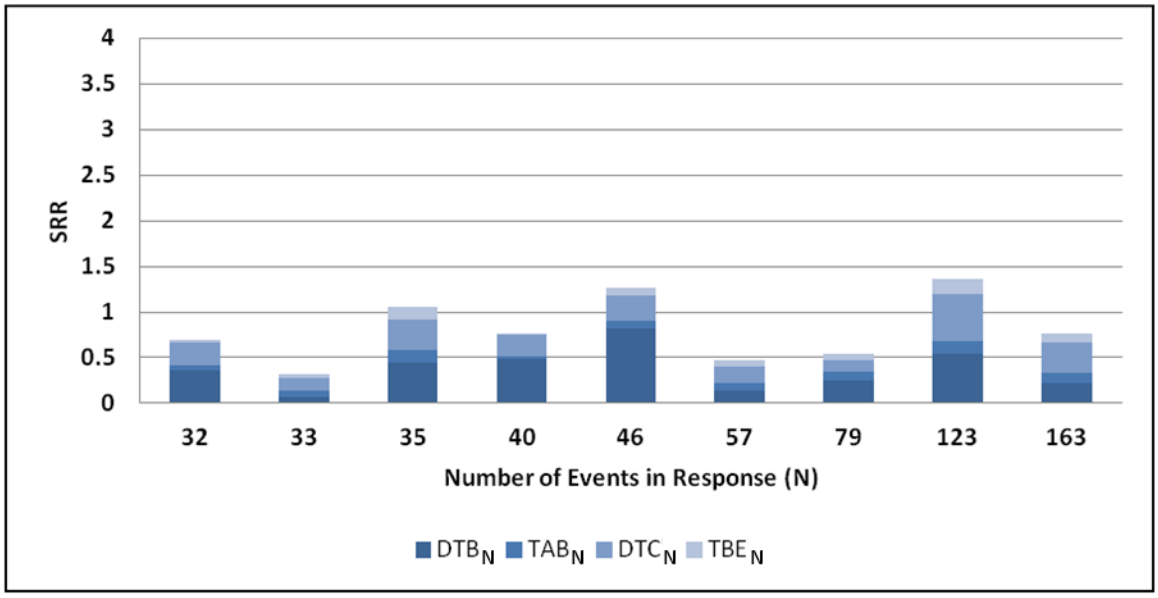

Appendix C: SRR charts for all development blast induced seismic responses to mining considered in the LaRonde Case Study.

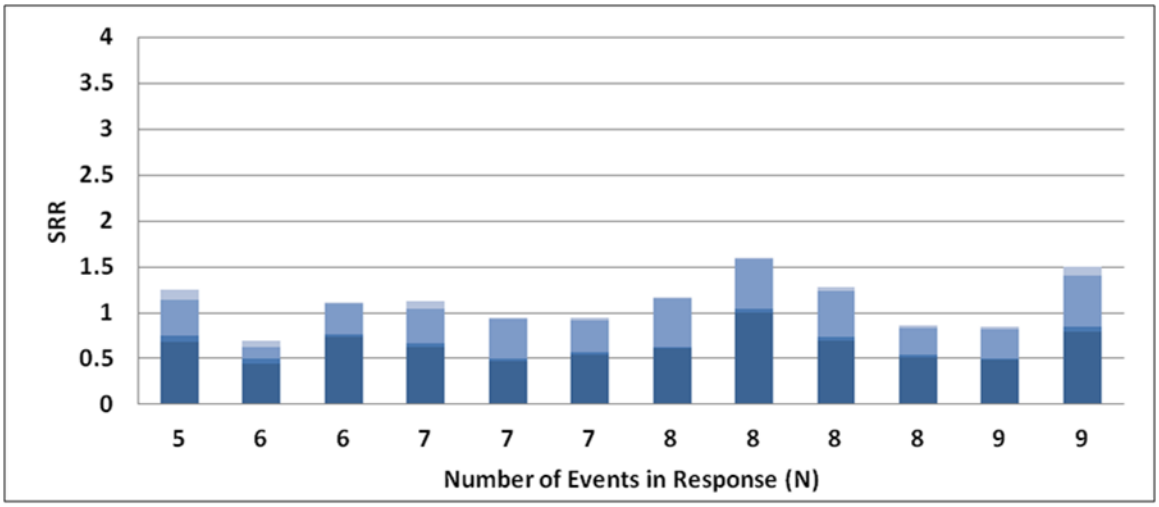

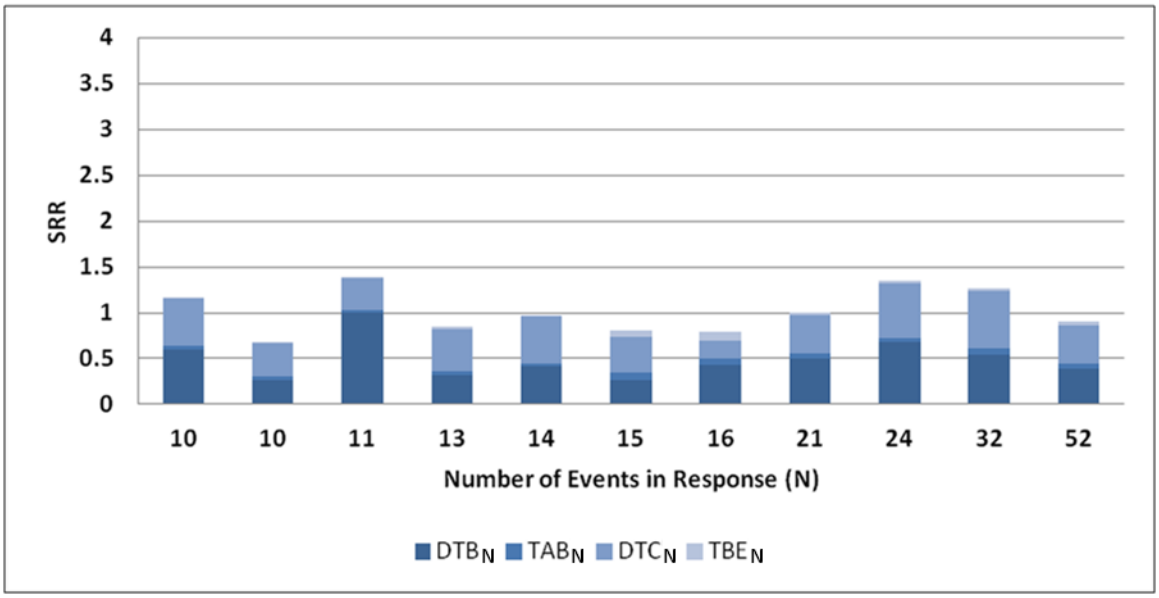

Appendix D: SRR charts for all triggered seismic responses to mining considered in the LaRonde mine case study.

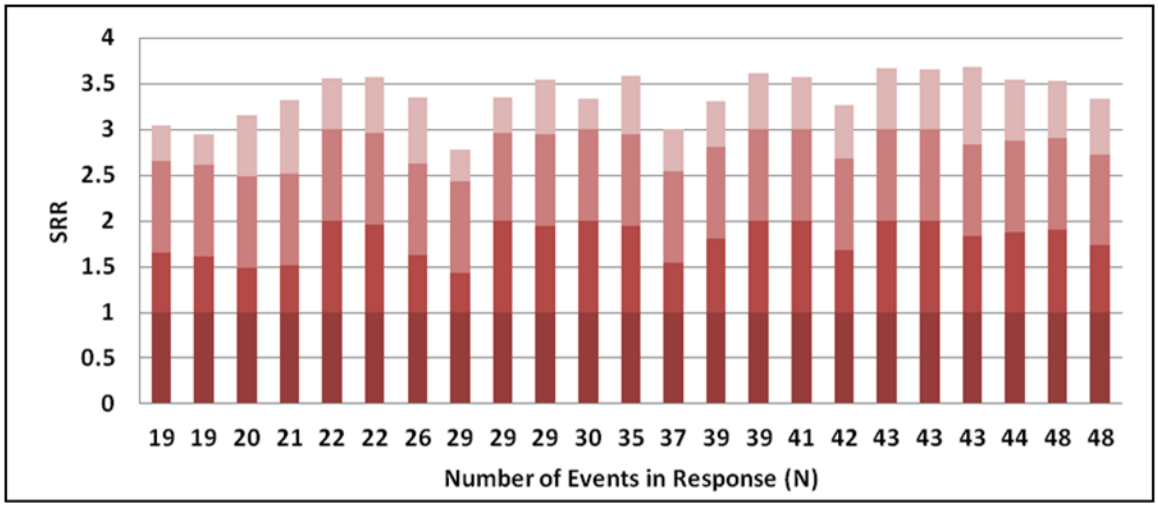

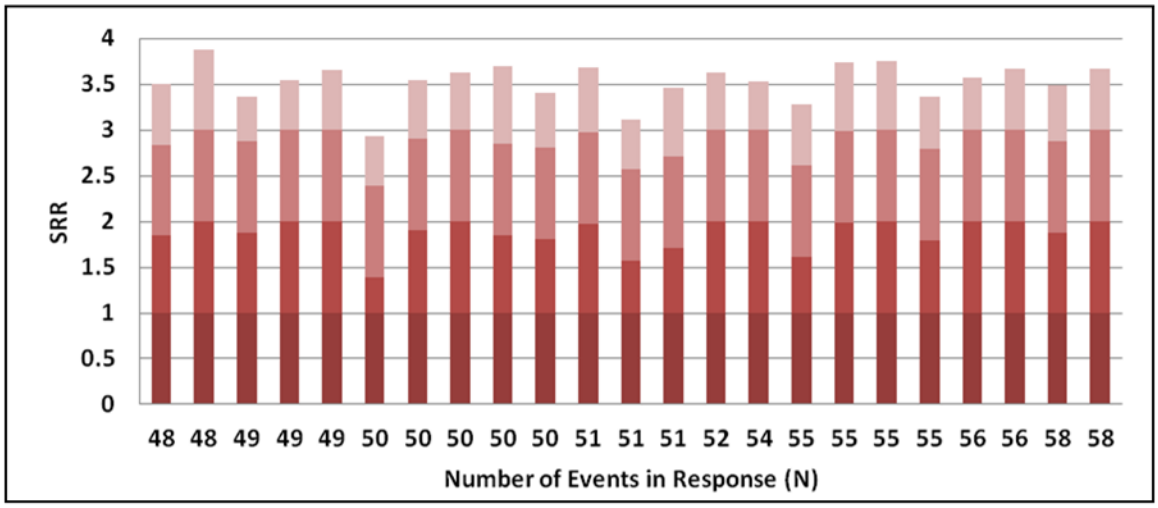

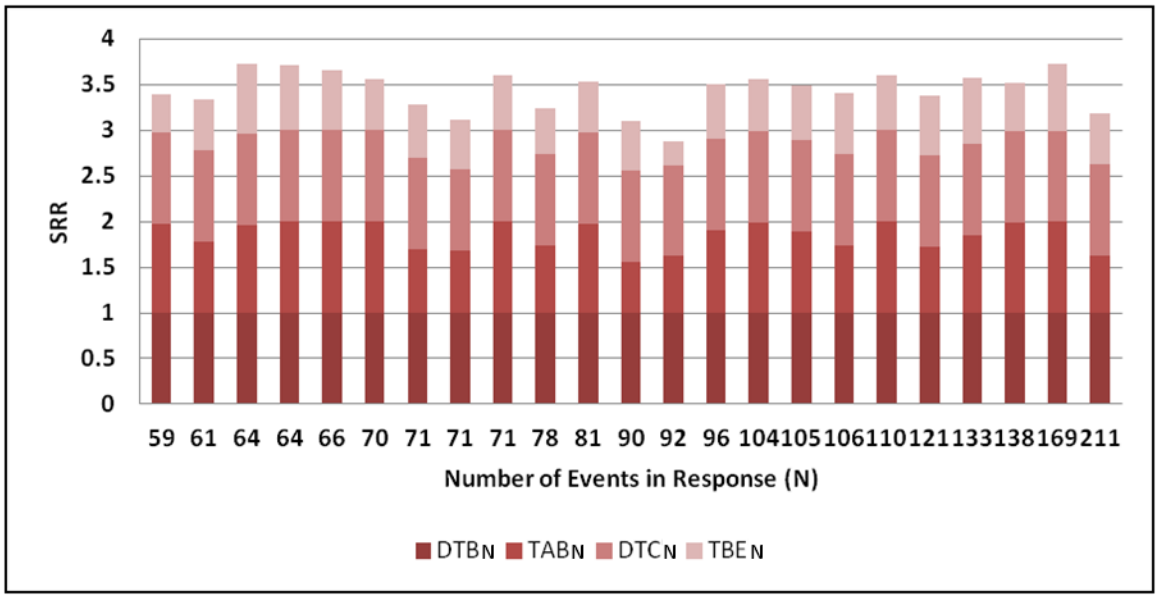

Appendix E: SRR charts for all shutdown period seismic responses to mining considered in the LaRonde mine case study.

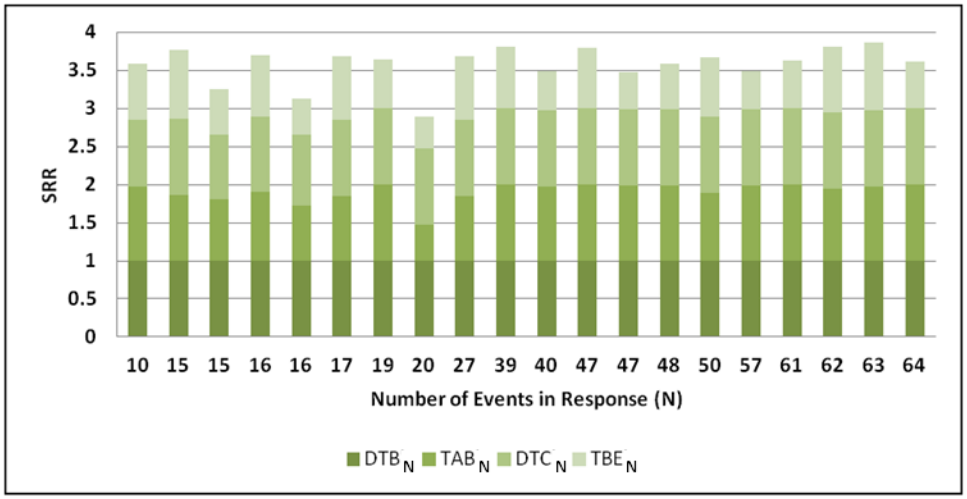

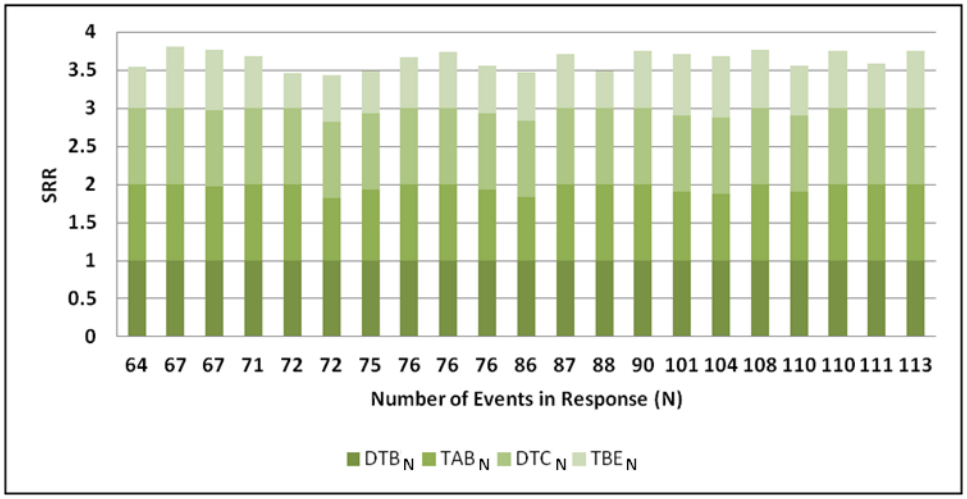

Appendix F: SRR charts for all Complex: Induced seismic responses to mining considered in the LaRonde Case Study.

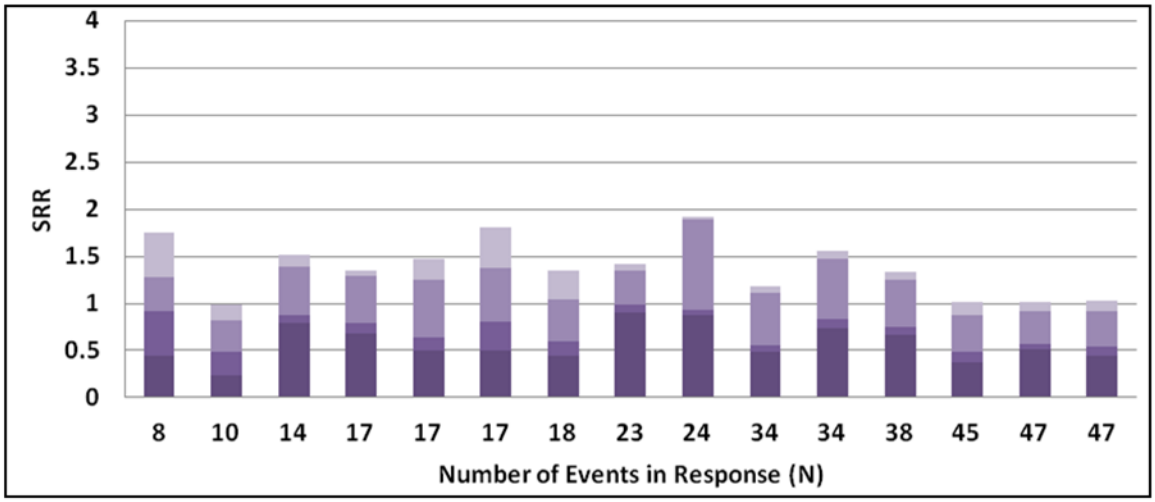

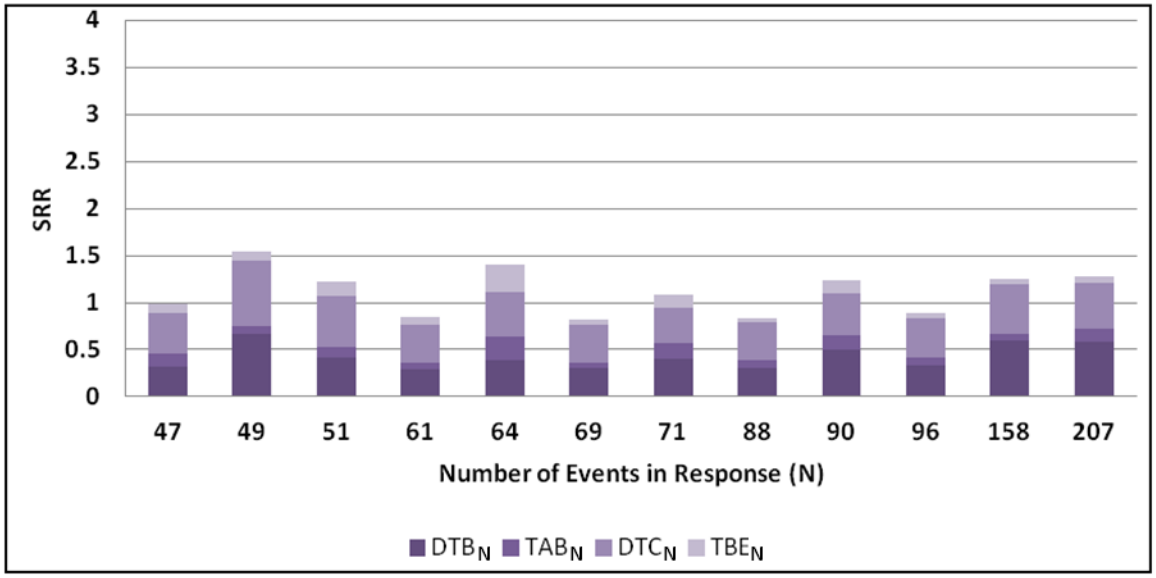

Appendix G: SRR charts for all Complex: Triggered seismic responses to mining considered in the LaRonde Case Study.

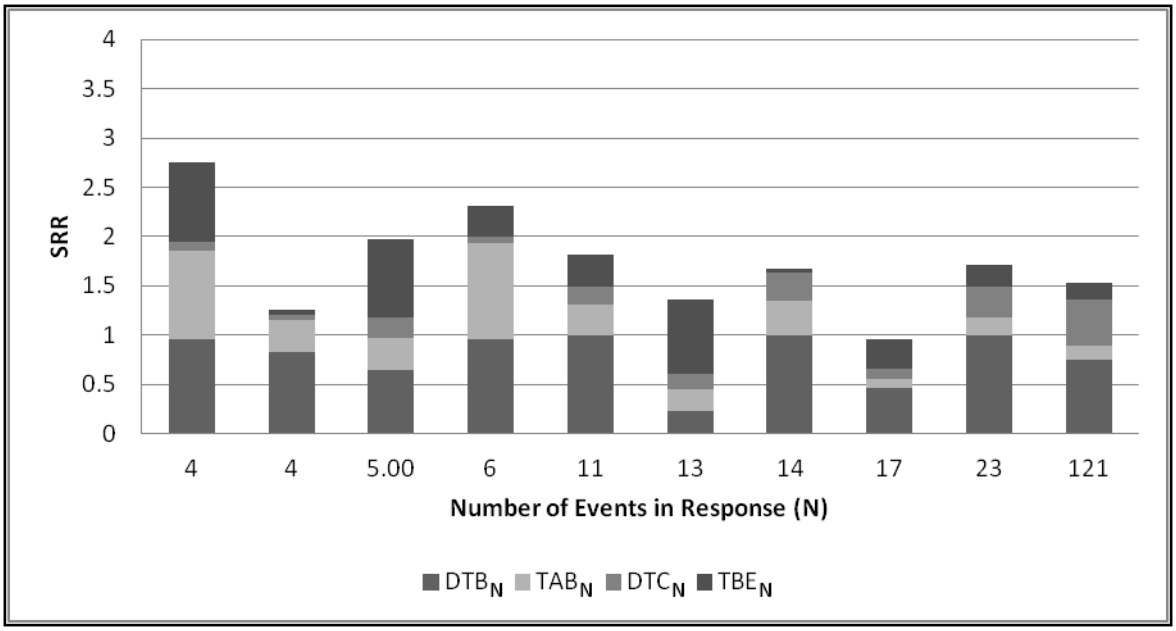

Appendix H: Normalized Seismic Response Parameter cumulative distribution charts for seismic response populations described in Section 8.5.